

**IN VITRO MODULATION OF CLASS II MHC ANTIGEN EXPRESSION BY  
HUMAN CEREBRAL ENDOTHELIUM AND ENDOTHELIAL CELL -  
LYMPHOCYTE INTERACTIONS BY INTERFERONS  $\gamma$  AND  $\beta$**

by

HANH KIM HUYNH

M.Sc., Cell Biology, The University of British Columbia, 1989

A THESIS SUBMITTED IN PARTIAL FULFILLMENT OF  
THE REQUIREMENTS FOR THE DEGREE OF  
INTERDISCIPLINARY DOCTOR OF PHILOSOPHY

in

THE FACULTY OF GRADUATE STUDIES  
(Departments of Neuroscience and Pathology)

We accept this thesis as conforming  
to the required standard

THE UNIVERSITY OF BRITISH COLUMBIA

April 1994

© Hanh Kim Huynh, 1994

In presenting this thesis in partial fulfilment of the requirements for an advanced degree at the University of British Columbia, I agree that the Library shall make it freely available for reference and study. I further agree that permission for extensive copying of this thesis for scholarly purposes may be granted by the head of my department or by his or her representatives. It is understood that copying or publication of this thesis for financial gain shall not be allowed without my written permission.

Departments of NEUROSCIENCE and PATHOLOGY

The University of British Columbia  
Vancouver, Canada

Date April 15<sup>th</sup> / 94

## ABSTRACT

In autoimmune demyelinating disorders of the central nervous system (CNS), the blood-brain-barrier (BBB) becomes permeable to plasma proteins and circulating leukocytes. Studies on Multiple Sclerosis (MS) suggest the involvement of T4<sup>+</sup> lymphocytes and Ia<sup>+</sup> macrophages in lesion extension and demyelination. Circulating lymphocytes recognize antigen only when it is complexed with Ia molecules on the surface of antigen presenting cells. Recent studies aiming at defining cell populations in the CNS capable of expressing Ia antigen (Ia Ag) indicate Ia Ag expression by EC, astrocytes, microglia and macrophages in MS lesions, while in experimental allergic encephalomyelitis, Ia Ag expression by brain endothelium has been reported by some, but not other investigators. The role of cerebral endothelium in CNS inflammation, therefore, remains ill defined and rather controversial.

The objective of this thesis was to investigate the: 1) Induction of Ia Ag on human brain microvessel endothelial cells (HBMEC) treated with interferons (IFN)  $\gamma$  and  $\beta$ , and 2) modulation of T-lymphocyte adhesion and migration across HBMEC monolayers by IFN- $\gamma$  and  $\beta$ . To address these issues, an in vitro model of the human BBB was utilized. The results indicate that HBMEC do not constitutively express Ia Ag. Treatment with IFN- $\gamma$ , not  $\beta$ , results in de novo, polarized expression of Ia Ag. Co-incubation with IFN- $\beta$  downregulates the IFN- $\gamma$ -induced Ia Ag expression. Treatment with IFN- $\gamma$ , not  $\beta$ , induces morphological and functional changes of HBMEC associated with increased permeability to macromolecules. IFN- $\gamma$  induced changes do not appear in cultures incubated with both cytokines.

Treatment of HBMEC with IFN- $\gamma$  upregulates the adhesion and migration of resting and activated T lymphocytes across the monolayers. T-lymphocyte activation alone greatly augments both processes. Treatment with IFN- $\beta$  has no effect on lymphocyte adhesion/migration, however, the IFN- $\gamma$ -mediated increase in adhesion/migration is

suppressed by IFN- $\beta$ . MAb blocking studies suggest a direct role of Ia molecules in adhesion/migration.

These studies indicate a potentially important role of HBMEC in CNS inflammation and increase our understanding of some of the factors involved in the recruitment of lymphocytes into chronic inflammatory sites in the CNS. Therapeutic interventions utilizing mAbs against HLA-DR molecules as well as the use of cytokines, such as IFN- $\beta$ , that can suppress IFN- $\gamma$ -mediated responses, may have considerable therapeutic potential.

## TABLE OF CONTENTS

Abstract . . . . .	ii
Table of Contents . . . . .	.iv
List of Table . . . . .	.viii
List of Figures . . . . .	.ix
List of Abbreviations . . . . .	.xiii
Acknowledgements . . . . .	.xvi
Dedication . . . . .	.xvii

### CHAPTER ONE INTRODUCTION

1.1 Inflammation . . . . .	1
1.1.1 Definition . . . . .	1
1.1.2 General aspects . . . . .	2
1.1.3 Role of EC . . . . .	4
1.2 Interferons . . . . .	7
1.2.1 IFN- $\gamma$ . . . . .	8
1.2.2 IFN- $\beta$ . . . . .	9
1.3 Major histocompatibility molecules . . . . .	9
1.3.1 Definition . . . . .	9
1.3.2 Class I MHC . . . . .	10
1.3.3 Class II MHC . . . . .	10
a) Role in autoimmune disorder . . . . .	11
b) Expression by EC . . . . .	12
1.4 Central nervous system inflammation and autoimmunity . . . . .	15
1.4.1 Permeability of the Blood-Brain-Barrier . . . . .	15
1.4.2 Lymphocyte infiltration . . . . .	17
a) Ia Ag association . . . . .	17
b) Lymphocyte-EC adhesion . . . . .	18
c) Transendothelial migration of lymphocytes . . . . .	20
1.4.3 FVRIIR:Ag in primary cultures of HBMEC . . . . .	21
1.5 Summary and objectives . . . . .	24

### CHAPTER TWO MATERIALS AND METHODS

2.1 Isolation and culture of HBMEC . . . . .	27
2.2 Antibodies . . . . .	28
2.3 Induction of Ia Ag expression on HBMEC by IFN- $\gamma$ and $\beta$ . . . . .	29
2.3.1 Treatment of primary HBMEC cultures . . . . .	29

2.3.2	Light microscopic immunocytochemical localization of Ia Ag . . . . .	30
2.3.3	Immunoelectron microscopy . . . . .	31
2.3.4	Enzyme linked immunosorbent assay (ELISA) . . . . .	32
2.3.5	Quantitation of Ia Ag expression by HBMEC . . . . .	32
2.4	Scanning electron microscopy . . . . .	33
2.5	Permeability studies . . . . .	33
2.6	Growth studies . . . . .	34
2.7	Preparation of T lymphocytes . . . . .	35
2.8	Activation of T cells . . . . .	36
2.9	HBMEC-lymphocyte adhesion assay . . . . .	37
2.10	HBMEC-lymphocyte migration assay . . . . .	38
2.11	Monoclonal antibody-blocking studies . . . . .	39
2.12	Quantitation of lymphocyte adhesion and migration . . . . .	40
2.13	Transmission electron microscopy . . . . .	40
2.14	Localization of FVIII:Ag in HBMEC . . . . .	41
2.14.1	In vitro drug treatment of EC . . . . .	41
2.14.2	Immunoelectron microscopy for FVIII:Ag . . . . .	41
2.15	Statistical analysis . . . . .	42

## CHAPTER THREE RESULTS

3.1	Human brain microvessel endothelial cell . . . . .	43
3.2	Immunocytochemical localization of FVIII:Ag . . . . .	44
3.3	Induction of Ia Ag expression on primary cultures of HBMEC	45
3.3.1	Effects of recombinant human IFN- $\gamma$ . . . . .	45
3.3.2	Effects of recombinant human IFN- $\beta$ . . . . .	46
3.4	Kinetics of the downregulation of Ia Ag expression by IFN- $\beta$ .	47
3.5	Effects of IFN- $\gamma$ and IFN- $\beta$ on cell morphology, organization and growth . . . . .	49
3.5.1	IFN- $\gamma$ . . . . .	49
3.5.2	IFN- $\beta$ . . . . .	50
3.6	Permeability of HBMEC monolayers . . . . .	50

3.7	Lymphocyte characterization . . . . .	51
3.8	Human T lymphocyte adhesion to untreated and cytokine-stimulated HBMEC . . . . .	52
3.9	Adhesion of activated T-lymphocytes to untreated and cytokine-stimulated HBMEC . . . . .	53
3.10	Effects of blocking antibodies on lymphocyte adhesion . . . . .	55
3.11	Transendothelial migration of resting T lymphocytes . . . . .	55
3.12	Migration of activated T-lymphocytes across untreated and cytokine treated HBMEC monolayers . . . . .	57
3.13	Effects of blocking antibodies on lymphocyte migration . . . . .	58
3.14	Effects of calcium ionophore A23187, EGTA and IFN- $\gamma$ on the constitutive pathway of factor VIII:Ag release . . . . .	58

#### CHAPTER FOUR DISCUSSION

4.1	Influence of cytokines on Ia Ag expression on HBMEC . . . . .	60
4.1.1	Human brain microvessel EC . . . . .	60
4.1.2	Induction of Ia Ag expression on primary cultures of HBMEC . . . . .	60
4.1.3	Surface localization of Ia Ag on HBMEC . . . . .	62
4.1.4	Effects of IFN- $\beta$ on Ia Ag expression by HBMEC . . . . .	63
4.1.5	Regulatory mechanism of Ia Ag expression . . . . .	64
4.1.6	Kinetic studies on the modulation of Ia Ag expression by interferons $\gamma$ and $\beta$ . . . . .	64
4.2	Effects of interferons $\gamma$ and $\beta$ on the morphological phenotype and growth of HBMEC, organization of the monolayers and permeability to macromolecules . . . . .	66
4.2.1	Effects of IFN- $\gamma$ and IFN- $\beta$ on HBMEC growth . . . . .	67
4.2.2	Effects of interferons $\gamma$ and $\beta$ on HBMEC morphology and organization of the EC monolayers . . . . .	67
4.2.3	Permeability of IFN- $\gamma$ treated HBMEC monolayers to macromolecules . . . . .	69
4.3	Significance of Ia Ag expression on HBMEC . . . . .	70
4.4	Adhesion of resting and anti-CD3 stimulated lymphocytes to untreated, IFN- $\gamma$ and/or IFN- $\beta$ treated HBMEC . . . . .	72
4.4.1	Activation of lymphocytes . . . . .	72
4.4.2	Adhesion of resting lymphocytes to untreated, IFN- $\gamma$ and/or IFN- $\beta$ treated HBMEC . . . . .	73
4.4.3	Adhesion of activated lymphocytes to untreated, IFN- $\gamma$ and/or IFN- $\beta$ treated HBMEC . . . . .	78

4.5	Migration of resting and anti-CD3 stimulated lymphocytes across untreated and cytokine treated HBMEC . . . . .	.84
4.5.1	Migration of resting lymphocytes across untreated, IFN- $\gamma$ and/or IFN- $\beta$ treated HBMEC monolayers . . . . .	84
4.5.2	Migration of anti-CD3 stimulated lymphocytes across untreated, IFN- $\gamma$ and/or IFN- $\beta$ treated HBMEC monolayers . . . . .	.86
4.6	Effects of IFN- $\gamma$ on the storage and release of FVIII:Ag from HBMEC in primary culture . . . . .	91
4.6.1	Immunocytochemical localization of FVIII:Ag in HBMEC . . . . .	.91
4.6.2	Effects of IFN- $\gamma$ on the storage and/or release of FVIII:Ag from HBMEC . . . . .	93

## CHAPTER FIVE

## CONCLUSIONS

5.1	Summary and conclusions . . . . .	.95
5.2	Future prospects . . . . .	.98
5.3	Significance of this thesis . . . . .	101
	TABLE . . . . .	.103
	FIGURES . . . . .	.104
	REFERENCES . . . . .	.214

**LIST OF TABLE**

Table 1.	Permeability of HBMEC Monolayers to HRP: Quantitation of endocytosis and tight junction permeability of untreated and IFN- $\gamma$ -treated HBMEC . . . .	103
----------	--	-----

## LIST OF FIGURES

Figure 1.	Diagram of the longitudinal section of the double chemotactic culturing chamber . . . . .	104
Figure 2.	Primary cultures of HBMEC grown on plastic wells or collagen discs form confluent monolayers . . . . .	106
Figure 3.	Immunoperoxidase staining for FVIII:Ag and UEA I confirming the endothelial origin of primary cultures of HBMEC . . . . .	108
Figure 4.	Ultrastructural studies demonstrating the elongated morphology of EC with their overlapping processes. . . . .	110
Figure 5.	Ultrastructural demonstration of the pentalaminar configuration characteristic of the tight junctions that are present in areas of cell to cell contact (a-d) . . . . .	112
Figure 6.	Cytoplasmic morphology of an untreated HBMEC (a, b) . . . . .	117
Figure 7.	Immunocytochemical localization of FVIII:Ag in untreated EC (a-d) . . . . .	120
Figure 8.	Time course of Ia Ag induction on HBMEC by IFN- $\gamma$ . . . . .	122
Figure 9.	Dose - response of Ia Ag induction by IFN- $\gamma$ on HBMEC . . . . .	124
Figure 10.	Ia antigen expression by HBMEC detected by immunogold silver staining in untreated/IFN- $\gamma$ treated EC at various times and also in cultures coincubated with anti-IFN- $\gamma$ antibody . . . . .	126
Figure 11.	Immunogold staining of HBMEC for the demonstration of Ia antigen in untreated/IFN- $\gamma$ treated EC . . . . .	128
Figure 12.	Ia antigen expression by HBMEC detected by immunogold silver staining in cells treated with IFN- $\beta$ alone or a combination of IFN- $\beta$ and $\gamma$ . . . . .	130
Figure 13.	Dose-response of Ia Ag expression by HBMEC treated with IFN- $\gamma$ and/or IFN- $\beta$ . . . . .	132

Figure 14.	Effects of different treatments of IFN- $\gamma$ and $\beta$ on Ia Ag expression by HBMEC . . . . .	134
Figure 15.	Quantitation by ELISA of Ia Ag expression by HBMEC treated with IFN- $\gamma$ and/or IFN- $\beta$ . . . . .	136
Figure 16.	Phase contrast microscopic demonstration of morphological alteration induced by IFN- $\gamma$ treatment of confluent cultures of HBMEC . . . . .	138
Figure 17.	SEM demonstration of morphological alteration induced by IFN- $\gamma$ treatment of confluent cultures of HBMEC . . . . .	140
Figure 18.	Effects of IFN- $\gamma$ and $\beta$ upon the growth of primary cultures of HBMEC . . . . .	142
Figure 19.	SEM of HBMEC grown in the presence of IFN- $\beta$ alone (a) or a combination of IFN- $\beta$ and $\gamma$ (b) . . . . .	144
Figure 20.	HRP localization in untreated (A) and (B) and IFN- $\gamma$ -treated (C-F) confluent HBMEC monolayers . . . . .	147
Figure 21.	Expression of IL-2R on resting and anti-CD3 stimulated T lymphocytes . . . . .	151
Figure 22.	Immunoperoxidase staining for the demonstration of resting T lymphocyte and untreated HBMEC adhesion . . . . .	153
Figure 23.	Adhesion of resting lymphocytes to IFN- $\gamma$ treated HBMEC . . . . .	155
Figure 24.	Adhesion of resting lymphocytes to IFN- $\beta$ treated HBMEC . . . . .	157
Figure 25.	Adhesion of resting lymphocytes to untreated and cytokine-treated HBMEC . . . . .	159
Figure 26.	SEM of adhesion of resting T lymphocytes to untreated HBMEC . . . . .	161
Figure 27.	SEM of adhesion of resting T lymphocytes to IFN- $\gamma$ treated HBMEC . . . . .	166
Figure 28.	Adhesion of anti-CD3 stimulated T lymphocytes to untreated HBMEC . . . . .	169

Figure 29.	Adhesion of anti-CD3 stimulated T lymphocytes to IFN- $\gamma$ treated HBMEC . . .	171
Figure 30.	Adhesion of anti-CD3 stimulated T lymphocytes to IFN- $\gamma$ and $\beta$ treated HBMEC . . . . .	173
Figure 31.	Summary bar graph of adhesion of anti-CD3 activated lymphocytes to untreated and cytokine-treated HBMEC . . . . .	175
Figure 32.	SEM demonstration of adhesion of anti-CD3 activated lymphocytes to untreated and cytokine-treated HBMEC . . . . .	177
Figure 33.	Adhesion of stimulated lymphocytes to untreated HBMEC . . . . .	181
Figure 34.	Adhesion of stimulated T cells to untreated HBMEC . . . . .	183
Figure 35.	Light micrograph of adhesion of resting lymphocytes to IFN- $\gamma$ and anti-human HLA-DR treated HBMEC . . . . .	185
Figure 36.	Light micrograph of adhesion of anti-CD3 stimulated lymphocytes to IFN- $\gamma$ and anti-human HLA-DR treated HBMEC . . . . .	187
Figure 37.	Migration of resting lymphocytes across untreated and cytokine-treated HBMEC . . . . .	189
Figure 38.	Summary bar graph of migration of resting and anti-CD3 activated T cells across untreated and IFN- $\gamma$ and/or IFN- $\beta$ treated HBMEC . . . . .	191
Figure 39.	TEM examination of migration of resting T lymphocytes across untreated HBMEC . . . . .	193
Figure 40.	TEM examination of transendothelial migration of resting T lymphocytes across untreated HBMEC . . . . .	198
Figure 41.	TEM examination of the integrity of the EC monolayers at the end of migration of resting lymphocytes across IFN- $\gamma$ treated HBMEC . . . . .	200
Figure 42.	Light microscopic examination of migration of activated lymphocytes across untreated HBMEC . . . . .	203

Figure 43.	TEM examination of migration of anti-CD3 stimulated lymphocytes across untreated and IFN- $\gamma$ treated HBMEC . . . . .	205
Figure 44.	TEM examination of migration of anti-CD3 stimulated lymphocytes across IFN- $\gamma$ treated HBMEC . . . . .	208
Figure 45.	Immunocytochemical localization of FVIII:Ag in chemical, cytokine-treated HBMEC . . . . .	210
Figure 46.	Summary bar graph of the immunocytochemical localization of FVIII:Ag in HBMEC . . . . .	212

**LIST OF ABBREVIATIONS**

AD	Autoimmune Disorder
BBB	Blood-brain-barrier
BSA	Bovine Serum Albumin
cAMP	Cyclic Adenosine Monophosphate
CD3	Cluster of Differentiation 3
CNS	Central Nervous System
con A	Concanavalin A
CSF	Cerebrospinal Fluid
EAE	Experimental Allergic/Autoimmune Encephalomyelitis
EAN	Experimental Autoimmune Neuritis
EAU	Experimental Autoimmune Uveoretinitis
EC	Endothelial Cell
EGTA	Ethyleneglycol-tetraacetic acid
ELISA	Enzyme Linked Immunosorbent Assay
FACS	Fluorescence Activated Cell Sorter
FCS	Fetal Calf Serum
FVIII:Ag	Factor VIII related antigen
GAMiG	Goat anti-mouse immunoglobulin G
HBMEC	Human Brain Microvessel Endothelial Cell

HBSS	Hanks' Balanced Salt Solution
HDMEC	Human Dermal Microvessel Endothelial Cell
HLA	Human Leucocyte Antigen
HRP	Horseradish peroxidase
HS	Horse Serum
HUVEC	Human Umbilical Vein Endothelial Cell
Ia Ag	Immune associated antigen
ICAM-1	Intercellular adhesion molecule-1
IFN- $\beta$	Human recombinant interferon-beta
IFN- $\gamma$	Human recombinant interferon-gamma
IFNs	Interferons
IgG	Immunoglobulin G isotype
IL-1	Interleukin-1
IL-2	Interleukin-2
IL-2R	Interleukin-2 receptor
LCA	Leucocyte common antigen
LFA-1	Lymphocyte Function-associated Antigen-1
mAb	monoclonal antibody
MHC	Major Histocompatibility complex
mRNA	messenger ribonucleic acid
MS	Multiple Sclerosis

NGS	Normal Goat Serum
PBS	Phosphate buffered saline
PECAM-1	Platelet/endothelial cell adhesion molecule-1
RNA	Ribonucleic acid
SEM	Scanning Electron Microscopy
TCR	T cell receptor
TEM	Transmission Electron Microscopy
TNF- $\alpha$	Tumor necrosis factor-alpha
UEA-I	Ulex Europaeus type I
VCAM-1	Vascular cell adhesion molecule-1
VLA-4	Very late antigen-4

## ACKNOWLEDGEMENTS

I would like to thank my supervisor Dr. K. Dorovini-Zis for her guidance, support and interest in my thesis, Mrs. R. Prameya for plating the EC, Donald Wong for his computer advice, Ms. Vivian Wu and Yolanda Bouwman for helping with the lymphocyte characterization. Thank you all very much.

## DEDICATION

I would like to dedicate this thesis to my supervisor, my mentor, DR. **K. DOROVINI-ZIS**, for her guidance, supervision, encouragement and patience during my Ph.D. training in Neuropathology Research, and to my very dear **Mom** (Huynh Thi Ngoc Suong), **Dad** (Huynh Van Tu), **Brother** (Huynh Kim Huu and family) and **Sisters** (Huynh Thi Kim Lien, Huynh Thi Tuyet Mai, Huynh Thi My Dung, Huynh Thi Hoang Yen, Huynh Thi Hoang Anh and their family members) for their sacrifice, their support and their belief in me, and most importantly, to my loving **Mom** and **Dad** who always believe that education is the best gift that any parents can give to their children, and last but not least to **God** for all of the blessings that I have been given. Thank you all for helping me through this.

## INTRODUCTION

### 1.1 INFLAMMATION

#### 1.1.1 Definition

Inflammation is a localized protective response which occurs as a defensive mechanism against the invasion of the host by foreign material, frequently microbial in nature. Responses to toxins, neoplasms, and mechanical trauma may also result in inflammatory reactions. Inflammation serves to destroy, dilute, or wall-off both the injurious agent and the injured tissue. The symptoms of inflammation include redness (rubor), swelling (tumor), pain (dolor), heat (calor), and loss of function (functio laesa).

According to Julius Friedrich Cohnheim, a pathologist in the late 1800's, the first four symptoms (redness, swelling, pain and heat) represent the cardinal signs of acute inflammation, while the functional loss (functio laesa) is in reality a resulting condition. He described "redness" as the overloading of all blood vessels, "swelling" due to the increased vascular fulness, especially the great increase of transudation, "pain" due to the pressure on, and dragging of, the nerves of sensation by the overfilled vessels and abundant transudation, and finally "heat" resulting from a more than normal amount of heat supplied to the site from within by the increased blood supply (1).

Inflammatory processes play a central role in mediating immune host defense and wound healing, but unfortunately, they also participate in the pathogenesis of many diseases, e.g. allograft rejection. Information concerning the mechanisms whereby inflammatory cells

accumulate in tissues, as well as the mechanisms whereby such cells are stimulated to damage tissues, should provide better insight into the pathogenesis of human diseases and should also provide clues for developing more rational forms of therapy (2, 3).

### 1.1.2 General aspects

As first witnessed by Cohnheim (1), and later by Clark in 1935 (4), using intravital microscopy, the initial event in leukocyte localization to sites of inflammation is called "margination", whereby leukocytes leave the central stream of blood flow in post-capillary venules. These leukocytes then interact with the endothelium lining the vessel wall by "rolling" along the luminal surface, a process which occurs within minutes of the inflammatory stimulus. As inflammation progresses, the number of rolling leukocytes increases along with a decrease in their velocity, and the process finally comes to a halt. Consequently, "diapedesis" will take place, a process whereby the leukocytes migrate through the endothelial cell (EC) junctions along the vessel wall and into the tissues. The accumulation and subsequent activation of leukocytes are central events in the pathogenesis of virtually all forms of inflammation. The recruitment of humoral and cellular components of the immune system leads to the amplification and propagation of most forms of inflammation.

Immunologically-mediated elimination of foreign material proceeds through a series of steps. **Firstly**, the material to be eliminated (i.e. antigen) is recognized as being "foreign" by either specific or non-specific means: a) Specific recognition is mediated by immunoglobulins (i.e. antibodies) or by T cell receptors which bind to specific determinants

(i.e. epitopes) on the antigen. b) Non-specific forms of recognition, such as recognition of denatured proteins or endotoxins, can be mediated directly by the alternative complement pathway or by phagocytes. **Secondly**, the binding of a recognition component of the immune system to an antigen generally leads to activation of an amplification system, initiating production of proinflammatory substances. These mediators then, in turn, will alter the blood flow, increase vascular permeability, augment adherence of circulating leukocytes to vascular endothelium, promote migration of leukocytes into the tissues, and stimulate leukocytes to destroy the inciting agent. The production of inflammatory mediators which leads to alterations of the normal function of the blood vessels had been suggested by Cohnheim more than one hundred years ago based on his research in inflammation. He speculated that in inflammation, a chemical change must occur in the vessels to induce the characteristic circulatory disturbances that he observed (1).

The actual destruction of antigens by immune mechanisms is mediated by phagocytic cells. These cells may migrate freely or may exist at the fixed tissue sites as components of the mononuclear phagocytic system. Macrophages and related cells (e.g. Kupffer cells, type-A synovial lining cells) are the central components of this system. Destruction of antigens outside of the mononuclear phagocytic system generally takes place in tissue spaces and is mediated by polymorphonuclear leukocytes (neutrophils) or monocytes, which are recruited from blood.

### 1.1.3 Role of endothelial cells

Endothelial cells (EC) are strategically located between the intravascular elements and the parenchyma of every organ. Therefore, it appears reasonable to assume that, in addition to forming this crucial boundary, EC may participate in a number of important physiologic roles. However, in the past, the role of EC in inflammatory processes had primarily been considered to be passive. It was not until a series of breakthroughs occurred which allowed for the isolation and subsequent culture of EC in vitro that substantive questions could be addressed in a stepwise manner. Most of the information about the structure and function of human EC comes from studies of human umbilical vein EC (HUVEC) because these cells are relatively easy to obtain, isolate and culture. These studies have provided convincing evidence that EC not only provide a nonthrombogenic surface to the intravascular compartment but also perform a host of other functions. These include wound healing, angiogenesis, production of clotting factors, tumor metastasis, cytokine production, leukocyte trafficking, vascular tone, and many others. Consequently, far from being either passive elements in physiologic processes or non-participants in pathologic processes, it is now realized that EC are intimately involved in inflammation and help to create, modulate, and terminate inflammation. In vitro studies of cytokine effects on EC have provided much of the information regarding the role of EC in inflammation (5).

It is interesting to note that the observation made by Cohnheim (1) more than one hundred years ago led to his remark, "we have here to deal with a molecular change of the vessel walls", and it took almost a century to establish the molecular basis for leukocyte

interaction with endothelium. An early event in inflammation involves the adhesion of polymorphonuclear leukocytes (i.e. neutrophils) to the blood vessel wall (i.e. EC) which is a crucial step leading to leukocyte accumulation within the inflammatory site. EC exposed to agents such as histamine or thrombin can express signals (e.g. granule membrane protein-140 and platelet activating factor) which attract neutrophils and other blood leukocytes to leave the main vascular stream and marginate along the vessel wall (6). Within minutes of this triggering, a phenomenon called "rolling" which involves leucocytic attachment to, and detachment from endothelium is initiated. During the initial stages of adhesion, the neutrophils come in close contact with the endothelium and extend pseudopodia that attach to the endothelial surface or are directed toward interendothelial junctions. The dynamic interaction between different adhesion molecules expressed by endothelium and blood leukocytes plays an important role in leucocytic entry into tissues. The migration process starts by insertion of a portion of the cytoplasm between two adjacent EC, followed by the movement of the entire cell across the monolayer (7). It is still unclear how exactly the neutrophils force the interendothelial junctions apart and what molecular mechanisms are responsible for the disassembly and resealing of the tight junctions. It has been shown that various cytokines participate in this process, and interleukin-1 (IL-1), tumor necrosis factor- $\alpha$  (TNF- $\alpha$ ), and interferon- $\gamma$  (IFN- $\gamma$ ) are among the most potent inflammatory agents (8).

Interleukin-1 and tumor necrosis factor appear to play pivotal roles in leukocyte-endothelial adhesion. They act on neutrophils, rendering them more "sticky" than normal. Through separate sets of mechanisms, interleukin-1 and tumor necrosis factor also act on EC,

rendering these cells more adhesive for neutrophils, monocytes and lymphocytes (9 - 11). The effects of IL-1 and TNF- $\alpha$  on EC can be blocked by RNA and protein synthesis inhibitors (10, 11).

Interleukin-1 is synthesized by macrophages, microglia and astrocytes. Its effects include chemotaxis, induction of increased adherence, enhanced vascular permeability, stimulation of the release of platelet-activating factor and prostacyclin by EC (12, 13). Tumor necrosis factor- $\alpha$  is synthesized predominantly by macrophages, but also by T cells, astrocytes and microglia cells. This cytokine has been linked to the inflammatory demyelinating process of experimental autoimmune neuritis (EAN), experimental autoimmune encephalomyelitis (EAE), and multiple sclerosis (MS) (8). MS is a chronic inflammatory disease involving demyelination of the central nervous system, while EAE is an animal model for MS. Interferon- $\gamma$ , predominantly produced by CD4<sup>+</sup> T lymphocytes of the T helper inflammatory phenotype, also exerts a multitude of inflammatory effects. This cytokine is the most potent inducer or upmodulator of the major histocompatibility class II molecules (MHC Class II), and it also enhances vascular permeability. The most convincing evidence that IFN- $\gamma$  plays an important role in inflammatory demyelination arises from a clinical trial in which the systemic administration of IFN- $\gamma$  to MS patients resulted in clinical exacerbations. These exacerbations were accompanied by increased numbers of monocytes expressing Human Leucocyte Antigen (HLA), especially HLA-DR subtype, enhanced proliferative responses of peripheral blood T cells and natural killer cell activity (15).

Although many valuable observations have been made during in vitro studies of

human large-vessel EC, most physiologic and pathophysiologic events take place at the level of the microvasculature. Furthermore, emerging evidence suggests that selected differences exist between EC of the microvasculature and those that line the large blood vessels as well as between EC from different vascular beds. These include differences in morphology, in secreted products, in expression of cell adhesion molecules, in cytokine-induced regulation of commonly expressed cell adhesion molecules, and in response to EC injury (5, 16 - 19). Subsequently, it is uncertain whether the observations on large vessel EC of other organs also apply to the human brain microvascular EC (HBMEC), so that the results should not be extrapolated from one system to the other.

## 1.2 INTERFERONS

The interferons (IFNs) represent a group of glycoproteins discovered in 1957 as biological agents interfering with the replication of viruses, hence the name "Interferon" (20). The IFNs can be produced by all nucleated cells and can be classified as cytokines. They are multifunctional and are components of the host defenses against viral and parasitic infections (e.g. chronic infection with hepatitis B and C viruses), and also certain tumors (e.g. hairy cell leukemia, Kaposi's sarcoma, non-Hodgkin's lymphoma). They influence the functioning of the immune system in various ways and also affect cell proliferation and differentiation. The IFNs exert their multiple activities primarily by inducing the synthesis of many proteins (21). The IFNs were originally classified by their sources as leucocyte, fibroblast and immune IFNs. Leucocyte and fibroblast IFNs, together, were also categorized as type 1 IFNs and immune

IFN as type 2 IFN. For the time being, the nomenclature is based on sequencing data. Leucocyte IFNs as IFN- $\alpha$  and  $\omega$ , fibroblast IFN as IFN- $\beta$ , and immune IFN as IFN- $\gamma$ .

IFN- $\gamma$  will be examined in this study because of its role in inducing Ia Ag expression (22), activating EC to bind T lymphocytes (23) and in enhancing the migration of lymphocytes across EC monolayers (24). The effects of IFN- $\beta$  will also be determined because of its role in downregulating the effects seen with IFN- $\gamma$  (25 - 27) and more importantly, because of its potential therapeutic application in treating autoimmune disorders of the CNS such as MS (28, 282).

### 1.2.1 IFN- $\gamma$

The gene coding for IFN- $\gamma$  has been located on chromosome 12, and the mature IFN- $\gamma$  is made of 166 amino acids (29). IFN- $\gamma$  was initially considered to be a secreted product exclusively of T lymphocytes, especially of the T helper subset. However, this interpretation was later recognized to be too restrictive. Many cytolytic T cells also release IFN- $\gamma$  upon contact with the specific target, such as virally infected syngeneic cells (30, 31). Natural killer cells have also been shown to be another source of IFN- $\gamma$  when they are exposed to target cells, interleukin-2 (IL-2) (32), or hydrogen peroxide (33).

It is now recognized that the most important immunomodulatory IFN is IFN- $\gamma$ . The proteins induced by IFN- $\gamma$  comprise those encoded by the major histocompatibility complex class I and especially class II regions. These proteins are involved mainly in the processing, transport, and cell surface presentation of antigens, and also in cell to cell recognition (21).

### 1.2.2 IFN- $\beta$

The gene coding for this cytokine has been located on the short arm of chromosome 9, and mature IFN- $\beta$  is comprised of approximately 165 - 172 amino acids long (29). IFN- $\beta$  is expressed exclusively by fibroblasts and it is induced essentially by viruses or double-stranded RNAs (34). As mentioned previously, the IFNs (i.e. IFN- $\alpha$ ,  $\beta$ , and  $\gamma$ ) were originally identified as antiviral proteins. Accumulating evidence, however, indicates that IFN- $\beta$  also plays an important role in the control of cell growth and differentiation (35, 36). Together with IFN- $\gamma$ , IFN- $\beta$  produces synergistic and antiproliferative activities (37). In contrast, the immunomodulatory effects of IFN- $\beta$  include its capability to inhibit or down-regulate IFN- $\gamma$  production in MS (38, 39), to antagonize the Ia-inducing effect of IFN- $\gamma$  in vitro (40, 41) and to augment suppressor cell function in MS patients (42).

## 1.3 MAJOR HISTOCOMPATIBILITY MOLECULES

### 1.3.1 Definition

The major histocompatibility complex (MHC) molecules are proteins discovered by the British geneticist Peter Gorer and by George D. Snell of Jackson Laboratory in Bar Harbor, ME, as the cause of graft rejection. Their long-winded names are derived from the Greek word for tissues (histo) and the ability to get along (compatibility). These MHC molecules can be categorized into two classes: class I and class II MHC molecules (43).

### 1.3.2 Class I MHC

These molecules can be found in almost all types of body cells. They are transporting proteins which are synthesized in the endoplasmic reticulum, and each MHC molecule has a deep groove into which a short peptide, or protein fragment, can bind. Class I MHC molecules bind to peptides that originate from proteins in the cytosolic compartment of the cell, however, they can only hold short peptides because their binding site is closed off. This class I-peptide complex is then transported to the cell surface, and if the peptide is foreign to the cell, it will be recognized by the passing T cells. These immune cells will release lymphotoxins or other structurally related molecules that destroy the cell presenting the peptide. These T cells are referred to as killer T cells (43).

### 1.3.3 Class II MHC

Class II MHC or human leucocyte antigens (e.g. HLA-DR, HLA-DQ, HLA-DP) are distributed on the cell surface as  $\alpha\beta$  heterodimers which can be found primarily on specialized antigen presenting cells such as macrophages, dendritic cells and B lymphocytes (44). They play an important role in the initiation of immune responses because the activation of T helper lymphocytes by an antigen is restricted to the presentation of the processed antigen together with the homologous class II MHC molecule on macrophages and other accessory cells (45). It is now realized that class II MHC molecules, HLA-DR antigen in particular (commonly referred to as Ia Ag), are actually peptide transport proteins which bind, transport to, and display at the cell membrane peptides that are derived from extracellular proteins. In contrast

to class I MHC molecules, class II MHC can bind to peptides of different lengths, because the binding site is open at both ends. They present these peptides to helper T cells as part of the mechanism for identifying foreign antigens and producing an immune response (46 - 48).

a) Role in autoimmune disorder

Autoimmune disorders (AD) affect 5% to 7% of the population. The AD are produced by autoimmunization secondary to a disruption of the normal self-tolerance which Erlich referred to as "Horror autotoxicus" (49). The autoimmune process may be initiated by an erroneous antigen presentation by the MHC molecules. It is important to realize that AD is not the result of a unique mutation of the HLA alleles exclusively found among the patients. Instead, the same sequence found among these patients can also be found in the healthy controls, although with a different frequency.

With the recent development of biochemical and molecular biological methods, it appears that HLA class II molecules are important for at least some diseases because: i) the HLA class II specific associations are maintained in different ethnic groups (50), and ii) in some animal models, the induction of AD may be blocked by monoclonal antibodies directed against the alleged antigen, and the comparison of specific sequences between diseased and control groups has shown extremely strong associations with specific class II alleles (51).

The immune recognition of normal self components which leads to tissue destruction and pathological abnormalities underlies a group of disparate diseases such as insulin-dependent-diabetes mellitus, rheumatoid arthritis, myasthenia gravis, and multiple sclerosis,

collectively known as autoimmune disorders. It has been shown that the susceptibility to these diseases is strongly associated with particular class II alleles, suggesting that the class II MHC-restricted binding and presentation of specific autoantigens may be involved in the disease process (51 - 59). Class II MHC are also associated with a heterogeneous group of leukoencephalopathy including cerebrovascular disease, Alzheimer disease and mixed dementia of Alzheimer type (60), IgA nephropathy (61), anterior uveitis (62), and lupus erythematosus disseminatus (63).

b) Expression by EC

Due to the strategic location of the endothelium of blood vessels, i.e. as the first cell layer that interacts with the blood constituents, the role of EC as active participants in immune regulation has been extensively investigated in recent years. Thus, it has been shown that EC of extracerebral blood vessels can be induced to express class II molecules and that the immunogenic capacity of the EC is directly proportional to the extent of class II MHC antigen expression on the cell surface (64). There are conflicting reports as to whether the capillary endothelium in brain expresses the HLA-DR antigen in normal or diseased states, e.g. the antigen could not be detected in rat brain microvessels in both control or EAE rats (65). In contrast, the antigen is found in approximately 10% of guinea pig brain microvessels in the control state and in 35% of guinea pig brain microvessels in EAE (66). In humans, the microvascular DR-antigen has been reported to be rarely detectable in normal brain (67), but discontinuous vascular immunoreactivity for the antigen can be found in multiple sclerosis

(68). However, Pardridge et al. have demonstrated that the DR-antigen can be detected in the brain microvasculature of both normal subjects and subjects with neurologic disease (69). In vitro studies have shown that untreated primary cultures of rat brain endothelium are absolutely negative for class II staining, but these EC can be induced to express Ia Ag in vitro when they are treated with IFN- $\gamma$  (70).

The ability of IFN- $\gamma$  to induce Ia Ag expression has been well documented in many different cell types including human and murine epithelial cells (71, 72), rat glomerular mesangial cells (73), murine macrophages, mast cells and myelomonocytic lines (74 - 77), human melanoma cells (78), monocytes (78, 79), dermal fibroblasts (80), human myoblasts (81) and myotubes (82) in vitro. Moreover, IFN- $\gamma$  can induce class II MHC expression on extracerebral EC such as HUVEC (22, 83), and human dermal microvascular EC (HDMEC) (84) in cultures. These cells do not express class II MHC constitutively under standard culture conditions. The effects of IFN- $\gamma$  on the aberrant expression of Ia Ag on cell types that do not normally function as antigen presenting cells may lead to the presentation of cellular proteins to the immune system which can then contribute to the induction of autoimmune diseases (85, 86) or graft rejection (87). It has been reported that IFN- $\gamma$  upregulates class II MHC expression on heart EC which plays a role in the organ allograft rejection (64). Subsequently, many studies have focussed on determining the mechanisms by which Ia Ag expression can be downregulated, especially in situations involving IFN- $\gamma$  upregulation.

The IFNs have been suggested to have therapeutic potential in MS because of the hypothesis that a viral infection, an immunoregulatory defect, or both, may be implicated in

the disease process (88 - 90). Reports of deficient IFN- $\gamma$  production in MS patients (91, 92) further suggested the possibility of using IFN- $\gamma$  for therapeutic trial. In contrast, later studies using a sensitive solid phase radioimmunoassay to test for IFN- $\gamma$  levels reported that the lymphocytes isolated from untreated MS patients actually produced more IFN- $\gamma$  than the normal controls (93, 94). Moreover, a small increase in cerebrospinal fluid IFN- $\gamma$  was also observed in active MS patients (95).

In the early 1980's, when highly purified IFN preparations became available, it was possible to demonstrate for the first time the specific binding of IFN to cellular binding sites. The binding studies established that IFN- $\gamma$  binds to a receptor different from that for IFN- $\beta$  (96 - 100). However, several different groups have also reported that there is some cross-reactivity with IFN- $\beta$  for the binding site for IFN- $\gamma$  (101 - 104). IFN- $\beta$  has been shown to be one of the substances that can antagonize the induction of Ia Ag expression by IFN- $\gamma$ . The antagonistic effects of IFN- $\beta$  have been demonstrated in cultured adult human astrocytes (25), human glioma cells (26), murine macrophages (27, 36), blood monocytes isolated from MS patients (28), astrocytoma cell lines (37) and also in other EC systems (105, 106).

The ability of IFN- $\gamma$  and IFN- $\beta$  to induce and suppress Ia Ag expression on HBMEC, respectively, was examined in this study in an effort to provide better understanding of the potential role of HBMEC as antigen presenting cells and to provide an in vitro system for screening drug therapies which may show promising value in MS.

## 1.4 CENTRAL NERVOUS SYSTEM INFLAMMATION AND AUTOIMMUNITY

### 1.4.1 Permeability of the Blood-Brain-Barrier

The presence of tight junctions between adjacent EC, the absence of vesicular transport system and the paucity of cytoplasmic vesicles are unique characteristics of brain microvascular EC, forming the basis of the blood-brain barrier (BBB) (107, 108). Under normal physiological conditions, cerebral EC restrict the paracellular movement of proteins, ions, large lipid-insoluble nonelectrolytes, and the access of antibodies, complement molecules and white blood cells from the blood to the brain parenchyma. Subsequently, the BBB controls the lymphocyte traffic into the CNS which is normally very limited.

A variety of clinical and experimental conditions may modify or damage the BBB, leading to enhanced permeability to plasma proteins, ions, water and circulating white blood cells (108, 109). The cerebrospinal fluid (CSF): serum albumin ratio indicates the level of vascular permeability in the CNS. As long as the BBB is intact, the ratio between the two remains relatively constant (110). Several studies have focussed on the mechanisms of opening of the BBB under different experimental and clinical conditions. Transmission electron microscopic examination using horseradish peroxidase and lanthanum as electron dense tracers have demonstrated that these molecules may traverse the endothelial barrier via opened tight junctions (111 - 114) or by means of accelerated vesicular transport (115 - 118). Moreover, the tight junctions between the EC also become permeable to the electron dense tracers if a hyperosmotic solution is administered into the rat via intracarotid injection (113). It has been reported that in EAE, the experimental autoimmune demyelination of the CNS

mediated by T cells, increase in the BBB permeability to small molecules occurs early in the disease process (119 - 124). Alterations in BBB permeability in MS have also been detected using gadolinium contrast enhancement (125). The mechanisms responsible for the increased BBB permeability in disease are still unknown. MS is a demyelinating disorder of the CNS where some inflammation exists. It is thought to be immune mediated. The presence of lymphocytes on brain slides suggests that they have egressed from the vessels. The reason why they accumulate in the cerebral parenchyma is probably due to an increased exit from the circulation (i.e. by an increase in the permeability of the BBB). Interestingly, IFN- $\gamma$  has been shown to induce alterations in the morphology and permeability properties of cultured EC (84, 126 - 128). Studies on the effects of different combinations of cytokines, e.g. IFN- $\gamma$ , tumor necrosis factor- $\alpha$  (TNF- $\alpha$ ), and interleukin-1  $\alpha/\beta$  (IL-1  $\alpha/\beta$ ), on HUVEC monolayer permeability have indicated that IFN- $\gamma$  plays a central role in increasing the permeability of EC monolayer (128). These results support previous *in vitro* observations on IFN- $\gamma$  effects on HBMEC permeability (127). Moreover, an increase in vascular permeability was detected when Wistar rats were injected intradermally with IFN- $\gamma$  (129). The effects of IFN- $\gamma$  on EC permeability are further confirmed by studies demonstrating augmentation of lymphocyte migration across HUVEC monolayers by IFN- $\gamma$ , and the effect has been shown to be due to a selective action on EC (24). Furthermore, direct interaction between memory T cells and vascular EC in a noncytolytic manner augments the EC permeability to macromolecules. It is suggested that modulation of endothelial permeability may be a critical factor contributing to the preferential migration and accumulation of lymphocytes at chronic inflammatory sites

(130).

#### 1.4.2 Lymphocyte infiltration

Autoimmune demyelinating disorders of the CNS such as MS are characterized by demyelination and migration of acute and chronic inflammatory cells from the blood into the brain parenchyma through the cerebral vasculature that normally excludes circulating leukocytes from entering the brain. MS is a recurrent and progressive inflammation of the CNS, and it has been reported that the number of lymphocytes circulating through the cerebral microvasculature is always many folds higher than the disease-free control (110). The mechanism(s) leading to the migration of these cells from blood to brain through the highly specialized BBB are largely unknown.

##### a) Ia Ag association

Epidemiological studies suggest that common viral-like infections, primarily respiratory infections, are temporally associated with exacerbations in MS (131). More recent studies also show a close relationship between common febrile events and new MS disease activity (132). Poser has suggested that a systemic viral infection may play a role in the disease process of MS whereby activated T cells can secrete IFN- $\gamma$  in response to a viral infection (133). As mentioned previously, IFN- $\gamma$  is the most potent inducer of class II MHC molecules (Ia Ag), and its induction has been reported in extracerebral endothelium (22, 84, 134) as well as cerebral endothelium (70, 127, 135, 136). The expression of Ia Ag may subsequently allow EC to present antigen to T cells (137) with the consequent release of

cytokines leading to the amplification of the immune response. Immunohistochemical studies in EAE and brain sections of MS lesions have demonstrated Ia Ag expression on EC, astrocytes and macrophages, while the antigen is not detected in the normal brain tissue (66, 68, 138 - 141). Class II MHC (Ia Ag) expression appears 12 to 48 hours after exposure of EC to IFN- $\gamma$  in vitro, reaches a plateau by 4 to 6 days and is associated with the expression of all known class II antigens (80, 142). The mechanism of action of IFN- $\gamma$  is by increasing mRNA levels for class II molecules (80, 143). Moreover, untreated human EC have no detectable mRNA for class II antigen (80, 144).

b) Lymphocyte - EC adhesion

Adhesion of T lymphocytes to vascular endothelium is a necessary prerequisite to migration of lymphocytes from the blood into chronic inflammatory sites. Studies of lymphocyte-EC adhesive mechanisms have shown that IFN- $\gamma$  plays an important role in augmenting lymphocyte-EC adhesion (23, 24, 134, 135, 145). IFN- $\gamma$ -mediated increase in adhesion occurred when EC were preincubated with this cytokine. In contrast, preincubation of lymphocytes with IFN- $\gamma$  did not affect the adhesion, indicating that the action of cytokine was mainly on the EC (23). Moreover, lymphocyte adhesion to EC and expression of HLA-DR antigens on EC are well correlated in terms of both kinetics and the dose-response pattern of IFN- $\gamma$  (134). The extent of lymphocyte adhesion to EC appears to depend on the density of HLA-DR antigens expressed on the EC. Blocking studies with monoclonal antibodies directed against HLA-DR or CD4 molecules significantly inhibit lymphocyte-EC adhesion in both autologous and non-autologous syngeneic combinations, suggesting that in IFN- $\gamma$ -

enhanced binding, Ia Ag plays a central role in the increased adhesion of T cells to HUVEC (134, 145). CD4 molecules are expressed in a subpopulation of lymphocytes, mainly T-helper cells, and are known to have an affinity for class II molecules (146, 147), providing strong suggestion for the involvement of IFN- $\gamma$ -induced class II MHC as the corresponding endothelial adhesion molecule. To further support the above statements, *in vivo* studies on EAE mice injected with mAb against Ia molecules show a decrease in lymphocyte accumulation in the CNS (148). Subsequently, it is speculated that the anti-Ia antibody must have blocked the adhesion of Ia-reactive T cells to Ia-expressing EC, leading to inhibition of T cell migration from blood into the CNS. Masuyama et al. (134) have suggested that T cell recognition of HLA-DR antigen may represent the signal for the initiation of a subsequent adhesive processes whereby complementary adhesion surface molecules become engaged. These observations indicate that the release of IFN- $\gamma$  by activated lymphocytes in chronic inflammatory sites can upregulate the adhesion of circulating lymphocytes to the local EC. Since lymphocyte-EC adhesion represents the initial step of lymphocyte migration through the microvessels (149), the IFN- $\gamma$ -mediated increase in lymphocyte adhesion on the surface of microvessels may lead to further influx of lymphocytes into the site of chronic inflammation.

*In vitro* studies have demonstrated that lymphocyte-EC adhesion can be significantly upregulated by stimulating the T cells with phorbol esters (150 - 153), con A (154 - 156), or IL-2 (157, 158). Significant increase in T-cell adhesion to purified ICAM-1 substrates has also been reported when T cells were pretreated with anti-CD3 IgG and anti-IgG (159). Preincubation studies with phorbol esters have shown that enhancement of the lymphocyte-EC

binding is entirely attributable to an effect on T cells, with no action on EC (150). Moreover, additive enhancement of adhesion can be detected when both lymphocyte and EC are activated (150, 154). More recent studies have demonstrated that IFN- $\gamma$  treatment of passaged cultures of human cerebral EC further enhances the lymphocyte-EC adhesion. The activated lymphocytes were isolated from peripheral blood of acute relapsing MS patients during exacerbations (160).

c) Transendothelial migration of lymphocytes

In vivo observations on T-lymphocyte entry into the CNS have determined that lymphocyte activation enhances their ability to cross the BBB and rapidly appear in the CNS tissue, irrespective of their antigen specificity, MHC compatibility, T-cell phenotype, and T-cell receptor gene usage (161). Moreover, the level of lymphocyte infiltration into the tissue is significantly upregulated in chronic inflammatory disorders, a process that may be modulated by the enhancement of interactions between different adhesion molecules expressed on both lymphocytes and vascular EC (150, 162). Studies of lymphocyte traffic through various organs (e.g. lungs, liver, lymph nodes) have reported differences in the migratory patterns of resting and activated lymphocytes. Generally, resting lymphocytes move rapidly while peripherally activated lymphocytes move much more slowly through the organs. T-lymphoblasts can readily leave the circulation and migrate into an inflammatory site (163). Migration of activated T cells from the peripheral blood to the CNS has been demonstrated in EAE (164) along with a significant decrease in their activated T-cell levels in the peripheral blood during exacerbations (165). A decreased proportion of activated T cells in the

peripheral blood of MS patients has also been reported (166, 167). Exacerbations in MS were usually accompanied by further decreases in activated T cells in the peripheral blood (167). Moreover, lower percentages of activated T cells were consistently found in the CSF of MS patients (168), suggesting that these cells may accumulate in the MS plaques. In vivo treatment of EAE rats with a monoclonal antibody specific for activated rat T cells has demonstrated significant reduction in inflammation (169).

Subsequently, these observations suggest that activation of both lymphocytes and EC plays a central role in upregulating the adhesive and migratory interactions between lymphocytes and EC. It is notable that studies of lymphocyte migration across cultured rat retinal microvessel EC have shown that con A activation of T-cells did not augment the migratory process. Furthermore, IFN- $\gamma$  treatment of EC resulted in a slight, but not significant, increase in migration (170). The insignificant increase in migration of lymphocytes across rat retinal EC when both systems are activated supports the concept of immune privileged site of the eye due to the presence of the blood-retinal barrier. These results further confirm the heterogeneity that exists among EC isolated from vascular beds of different organs and species with regard to immunological responses to cytokine treatment (19, 155).

#### 1.4.3 FVIII:Ag in primary cultures of HBMEC

Factor VIII-related antigen (FVIII:Ag) is a large multimeric glycoprotein synthesized and released by EC of large and small blood vessels, and it is widely considered as the most

specific marker for cells of endothelial origin (171, 172). The protein has also been shown to be synthesized in primary cultures of HBMEC as demonstrated by immunofluorescence and immunoperoxidase techniques at the light microscopic level (107). When vascular injury occurs, FVIII:Ag facilitates the adhesion of platelets to the subendothelial matrix (173). Biochemical and immunohistochemical studies indicate that FVIII:Ag is generally stored in rod-shaped, membrane-bound cytoplasmic organelles called Weibel-Palade bodies (named after the investigators who first described them) which are found exclusively in EC (174 - 177). However, these organelles are rarely found in EC lining the cerebral capillaries, and they are absent in primary cultures of HBMEC when examined ultrastructurally (107). Weibel-Palade bodies are also absent in primary cultures of microvessel EC derived from mouse (178) and rat (179 - 181) brain. It has been recently reported that IFN- $\gamma$  treatment of HUVEC causes a decrease in the release of FVIII:Ag from these EC (182). The mechanism of IFN- $\gamma$ -suppressed release of FVIII:Ag is still unknown at the present time. Tannenbaum and Gralnick speculated that IFN- $\gamma$ -mediated depression of FVIII:Ag release from the EC may assist in maintaining blood fluidity during immune activation (182). Subsequently, this study examined the distribution and fine structural localization of FVIII:Ag in primary cultures of HBMEC and also investigated the influence of IFN- $\gamma$  on the storage and release of this glycoprotein by HBMEC, considering the important role of IFN- $\gamma$  in autoimmune disorders of the CNS.

Consequently, the effects of IFN- $\gamma$  and IFN- $\beta$  as potential factors regulating lymphocyte entry into the CNS will be examined in this study. Their influences on Ia Ag

expression, cell proliferation, alteration of the morphology and permeability characteristics of HBMEC in cultures will be investigated. Furthermore, using primary cultures of HBMEC as a model of the BBB, these cytokines will also be tested for their effects on the adhesion and migration of peripheral blood lymphocytes across HBMEC monolayers which may be relevant in understanding the in vivo immune reactions including increased vascular permeability and cell shape changes. Blocking experiments with mAbs directed against human HLA-DR molecules will further determine the role of Ia Ag in the adhesive and migratory processes. The results of this study will emphasize the potentially critical role of HBMEC in the initiation of the immune reaction in autoimmune disorders of the CNS. Elucidation of the factors modulating the adhesion and migration of lymphocytes across microvascular EC can have great therapeutic potential. The information may assist in designing protocols that can prevent further amplification of the unwanted inflammation or immune responses such as that in MS.

In conclusion, understanding of the pathobiology of HBMEC, such as their responses to IFN- $\gamma$  and IFN- $\beta$  treatments and their ability to mediate lymphocyte traffic into the CNS, is central to the understanding of CNS inflammation.

## 1.5 SUMMARY AND OBJECTIVES

In summary, a large body of evidence indicates that Ia Ag expression can be induced by IFN- $\gamma$  in many different cell types including EC. It has also been reported that IFN- $\beta$  is capable of suppressing the IFN- $\gamma$ -induced Ia Ag expression. Furthermore, it has been demonstrated that lymphocyte-EC adhesion and migration can be augmented by IFN- $\gamma$ . Monoclonal antibody blocking studies indicate that Ia Ag might play a critical role in the adhesive and migratory processes. Finally, IFN- $\gamma$  has been shown to alter the morphology and permeability characteristics of the EC monolayers which may facilitate the influx of lymphocytes into chronic inflammatory sites. It is uncertain at the present time whether the observations on EC of other organs and species also apply to the HBMEC. It is now well accepted that great heterogeneity exists among different types of EC with regard to antigenic determinants, cell surface molecules, metabolic properties, permeability functions and immunological responses to cytokines. Cerebral EC are characterized by unique features responsible for the formation of the BBB. How this barrier is breached in inflammation and autoimmune disorders of the CNS is still poorly understood.

The main objective of this thesis is to determine the effects of IFN- $\gamma$  and IFN- $\beta$  on Ia Ag expression, proliferation, and alteration of the morphology and permeability characteristics of HBMEC monolayers. Furthermore, the effects of these cytokines on the adhesion and migration of resting/anti-CD3 stimulated T lymphocytes across the EC monolayers will be investigated. Finally, the effects of IFN- $\gamma$  on the storage and release of FVIII:Ag by HBMEC will be examined.

My working hypothesis is that, in a chronic inflammatory site, some activated T lymphocytes, mainly T helper/inducer phenotypes, release IFN- $\gamma$  locally. This cytokine can then activate the local capillary EC by inducing Ia Ag expression and morphological alterations on the EC, and by increasing the vascular permeability. These changes will augment the adhesion and migration of the lymphocytes across the EC, leading to an influx of lymphocytes into the chronic inflammatory sites. The administration of IFN- $\beta$  will play an antagonistic role on the IFN- $\gamma$ -mediated immunological responses. IFN- $\beta$  will suppress the IFN- $\gamma$ -induced Ia Ag expression and morphological alteration on EC and the IFN- $\gamma$ -mediated increase in adhesion and migration, resulting in the reduction of lymphocyte numbers in the chronic inflammatory sites. Finally, the ability of IFN- $\gamma$  to affect the storage and release of FVIII:Ag in HBMEC may have some important implications in maintaining blood fluidity during immune activation, considering the important role of IFN- $\gamma$  in autoimmune disorders of the CNS.

The method of approach used in this study involved the successful application of immunogold labeling with silver enhancement technique for the detection of Ia Ag expression at the light microscopic level. ELISA was further applied to confirm the IFN- $\beta$  effects in suppressing the IFN- $\gamma$ -induced Ia Ag expression. Kinetic studies of the cytokine effects on Ia Ag expression on HBMEC were also carried out in this study. Ultrastructural localization of Ia molecules on the surface of EC was determined using mAbs conjugated with colloidal gold markers. Electron dense tracer studies were applied in order to assess the permeability of confluent untreated or IFN- $\gamma$  treated HBMEC monolayers. Immunoperoxidase techniques

were used to study the IFN- $\gamma$  and IFN- $\beta$  effects on lymphocyte-EC adhesion and migration. Scanning and transmission EM studies further showed the effects of the cytokines on the morphological phenotype of HBMEC, and on lymphocyte-EC adhesion and migration. Finally, immunoelectron microscopy was performed for the ultrastructural localization of FVIIIIR:Ag in HBMEC, and the effect of IFN- $\gamma$  on its storage and release.

The Specific Aims of this thesis are:

- 1) **To determine, in vitro, whether primary cultures of HBMEC constitutively express Ia antigen, and whether the expression can be modulated by inflammatory cytokines such as IFN- $\gamma$  and IFN- $\beta$ .**
- 2) **To determine whether IFN- $\gamma$  and IFN- $\beta$  exert antiproliferative effects on primary cultures of HBMEC, whether these cytokines can induce alterations in the morphology and organization of the EC monolayers, and whether IFN- $\gamma$  can influence the permeability and endocytotic characteristics of HBMEC that would be relevant to the in situ immune reaction.**
- 3) **To determine whether IFN- $\gamma$  and IFN- $\beta$  treatment of HBMEC can affect the adhesion of resting/activated lymphocytes to these untreated/cytokine-treated EC.**
- 4) **To determine whether IFN- $\gamma$  and IFN- $\beta$  treatment of HBMEC can influence the migration of resting/activated lymphocytes across untreated/cytokine-treated EC.**
- 5) **To determine the influence of IFN- $\gamma$  on the storage and release of FVIIIIR:Ag in primary cultures of HBMEC which may reflect the maintenance of blood fluidity during immune reactions in vivo.**

## MATERIALS and METHODS

### 2.1 Isolation and culture of HBMEC

HBMEC were isolated from normal brains obtained at autopsy and from temporal lobectomy specimens removed for intractable seizure disorders and cultured according to methods previously described (107). The time interval between death and removal of brain ranged from 3.5 hours to 15 hours. Pathologic abnormalities were not detected in any of the brains used for isolation of cerebral microvessels. Large vessels and the leptomeninges were removed from the cerebral cortex with fine forceps, and the tissue was cut into 1 to 2 mm cubes. The tissue was then incubated for 3 hours at 37 °C in medium M199 (Gibco, Burlington, Ontario) containing 0.5% dispase (Boehringer Mannheim, Indianapolis, Indiana). Following centrifugation at 1000 x g for 10 minutes, the pellets were resuspended in media containing 15% Dextran (Sigma, St. Louis, Missouri; average molecular weight, 70,000 daltons) and centrifuged at 5,800 x g for 10 minutes in order to separate the microvessels from other brain components. The isolated microvessels were then incubated in M199 containing 1 mg/ml of collagenase/dispase (Boehringer Mannheim) for 12 to 16 hours at 37 °C. Following incubation, the microvessels were resuspended in M199 containing 5% horse serum (HS) (Hyclone Laboratories, Logan, Utah), layered over Percoll (Sigma) gradients prepared as described by Bowman et al. (183) and centrifuged at 1,000 x g for 10 minutes in order to separate the EC from red blood cells, pericytes and cellular debris. The layer containing the EC was washed in 10% HS in M199, and collected by centrifugation for 10 minutes at 1,000

x g. Cell numbers were counted with a hemocytometer. Cell viability, as determined by the trypan blue exclusion test, ranged between 85 and 90%.

The isolated clumps of EC were seeded onto plastic wells (Corning Plastics, Corning, NY) previously coated with fibronectin (Sigma). The cultures were maintained in M199 supplemented with 10% HS, 25 mM HEPES, 10 mM sodium bicarbonate, EC growth supplement (20 µg/ml), heparin (100 µg/ml) (all from Sigma), and penicillin (100 µg/ml), streptomycin (100 µg/ml), and amphotericin B (2.5 µg/ml) (Gibco) at 37 °C in a humidified 2.5% CO<sub>2</sub>/97.5% air atmosphere. The culture media were changed every second or third day. The endothelial origin of the cells was confirmed by their intense, granular perinuclear staining for Factor VIII-related antigen (FVIIIIR:Ag) and their binding of Ulex Europaeus-I lectin as previously reported (107). Confluent, contact-inhibiting monolayers were obtained 7 to 9 days after plating. The monolayers were used once they reached confluency.

## 2.2 Antibodies

Mouse monoclonal antibody (mAb) against human recombinant interferon- $\gamma$  (KM48, IgG<sub>1</sub>) and mouse anti-human HLA-DR IgG (DK22, IgG<sub>2a</sub>, kappa) were obtained from Dimension Laboratories Inc., Mississauga, ONT. Goat anti-mouse IgG (GAMIgG) coupled to 5nm gold particles (Auroprobe LMGAM IgG) was obtained from Janssen/Cedarlane Labs Ltd., (Hornby, ONT), GAMIgG coupled to peroxidase from Jackson Immunoresearch Lab Inc., PA, and mouse anti-human pituitary follicle-stimulating hormone IgG from Biogenex Laboratories, CA. Mouse anti-human Leu-4 (CD3) mAb was purchased from Becton-Dickinson, and mouse

mAb to human Leukocyte common Ag (CD45) from Dimension Lab, Inc., Mississauga, ONT. For the ultrastructural localization of FVIII:Ag, mouse mAb raised against human factor VIII antigen (Cedarlane Laboratories, Hornby, ONT) was used as the primary antibody and goat anti-mouse IgG coupled to 5nm gold particles (Janssen / Cedarlane) as the secondary antibody. For the light microscopy immunoperoxidase staining, a rabbit antiserum to factor VIII antigen (Dakopatts, Santa Barbara, CA) was used as the primary antibody and goat anti-rabbit IgG conjugated with HRP (Jackson Immunoresearch Laboratories, West Grove, PA) as the secondary antibody.

### 2.3 Induction of Ia Ag expression on HBMEC by human recombinant Interferon-gamma and beta

#### 2.3.1 **Treatment of primary HBMEC cultures**

Human recombinant interferon- $\gamma$  (IFN- $\gamma$ ; Collaborative Research Inc., Bedford, MA) was diluted in complete media to a final concentration of 10, 20, 50, 100, 150 and 200 U/ml. Confluent monolayers of HBMEC, grown in replicate wells were incubated with different concentrations of IFN- $\gamma$  for 4 days and with 200 U/ml for 12 hours to 4 days at 37 °C. Cultures used for these experiments were derived from EC isolated from several different autopsy brains. The specificity of Ia Ag induction by IFN- $\gamma$  was tested in cultures co-incubated with IFN- $\gamma$  (200 U/ml) and anti-IFN- $\gamma$  mAb (optimal concentration, 10  $\mu$ g/ml) for 4 days. In order to study the reversibility of Ia Ag expression, monolayers previously treated with IFN- $\gamma$

(200 U/ml) for 4 days were thoroughly washed with M199 to remove the cytokine, then placed in complete media and returned to the incubator for another 4 days prior to Ia Ag detection.

For the IFN- $\beta$  studies, recombinant human interferon- $\beta_{\text{ser}}$  (Triton Biosciences Inc., Alameda, CA) was used at 100, 250, 500, 1,000, 2,000 and 6,000 U/ml. These units were determined by the National Institutes of Health reference standard. This IFN- $\beta$  is the same cytokine that is used for MS therapeutical trial, and it is now available for patient use. Confluent cultures of HBMEC grown in replicate wells were incubated with 100 U/ml IFN- $\gamma$  with or without various concentrations of IFN- $\beta$  for 4 days. In separate experiments, replicate wells were preincubated with IFN- $\beta$  (6,000 U/ml) or IFN- $\gamma$  (100 U/ml) for 2 days prior to coincubation with IFN- $\beta$  and  $\gamma$  for another 4 days.

All experiments were performed in duplicate or triplicate wells.

### **2.3.2 Light microscopic immunocytochemical localization of Ia Ag**

Following cytokine treatment, the monolayers were washed 3 times with buffer containing phosphate buffered saline (PBS - 10 mM, pH 7.2), 1% bovine serum albumin (BSA) and 1% normal goat serum (PBS/BSA/NGS) and incubated for 40 minutes at room temperature with mouse anti-human HLA-DR mAb at 1:30 dilution in carrier buffer containing PBS, 5% BSA and 4% NGS. Following brief washing with PBS/BSA/NGS, the monolayers were incubated with the secondary antibody (Auroprobe LMGAM IgG coupled to 5 nm gold particles) diluted 1:40 in carrier buffer for 60 minutes at room temperature. At the end of the incubation period, the cells were washed with PBS/BSA/NGS, fixed in freshly prepared buffered formaldehyde-

acetone fixative (20 mg  $\text{Na}_2\text{HPO}_4$ , 100 mg  $\text{KH}_2\text{PO}_4$ , 30 ml distilled  $\text{H}_2\text{O}$ , 25 ml 37% formaldehyde and 45 ml acetone) for 30 seconds, washed with distilled  $\text{H}_2\text{O}$ , and incubated in silver enhancing solution (IntenseM, Janssen/ Cedarlane) for 25 - 35 minutes. After washing with distilled  $\text{H}_2\text{O}$ , the monolayers were counterstained with Giemsa and coverslipped using JB-4 plus (Polysciences/Analychem, Markham, ONT) as mounting medium.

Controls included untreated monolayers grown in the absence of IFN- $\gamma$  and IFN- $\beta$  and IFN- $\gamma$  treated cultures incubated with 1) normal mouse IgG at the same concentration as the primary antibody (5.9  $\mu\text{g}/\text{ml}$  IgG), or 2) carrier buffer or 3) an irrelevant antibody (anti-human pituitary follicle-stimulating hormone IgG) instead of the primary antibody.

### 2.3.3 Immunoelectron microscopy

HBMEC monolayers treated with 200 U/ml IFN- $\gamma$  for 4 days were washed with buffer containing PBS, 1% BSA and 0.2%  $\text{NaN}_3$  (PBS/BSA) and incubated with mouse anti-human HLA-DR mAb at 1:30 dilution in carrier buffer containing PBS, 5% BSA and 4% NGS for 30 minutes at room temperature. After washing with PBS/BSA, the cells were incubated with 5 nm gold particle-conjugated secondary antibody (Auroprobe LMGAMIgG) at 1:40 dilution in carrier buffer for 45 minutes, washed, and fixed in periodate-lysine-paraformaldehyde fixative (184) overnight at 4 °C. Following fixation, the cells were washed in PBS, post fixed in 1% buffered  $\text{OsO}_4$ , stained en bloc with uranyl magnesium acetate overnight at 4 °C, dehydrated in graded series of methanol, and embedded in Epon-Araldite. Blocks cut out from the

embedded cultures were re-embedded for cross-sectioning. Thin sections were examined in a Philips EM400 without heavy metal staining. Controls consisted of cells maintained in IFN- $\gamma$  free growth media and monolayers incubated with normal mouse IgG or carrier buffer instead of the primary antibody.

#### **2.3.4 Enzyme linked immunosorbent assay (ELISA)**

Following incubation with IFN- $\gamma$  and/or IFN- $\beta$ , the cells were washed 3 times with PBS and fixed with 0.025% glutaraldehyde in PBS for 10 minutes at room temperature. The monolayers were thoroughly rinsed with PBS, washed 3 times with PBS/BSA/NGS and incubated with mouse anti-human HLA-DR mAb at 1:30 dilution in carrier buffer containing PBS, 5% BSA and 4% NGS for 60 minutes at room temperature. After brief washing with PBS/BSA/NGS, the cells were incubated with horseradish peroxidase-conjugated goat anti-mouse IgG diluted 1:5,000 in carrier buffer for 60 minutes at room temperature. Following washing in PBS, the cultures were incubated with o-Phenylenediamine (OPD) dihydrochloride (Sigma) (2 mg/ml) diluted in 0.1 M PBS containing 0.015% H<sub>2</sub>O<sub>2</sub> for 45 minutes at room temperature. The reaction was stopped by the addition of 2 M H<sub>2</sub>SO<sub>4</sub>. Absorbance was measured at 490 nm on a Elisa Microtiter Plate Reader (Molecular Devices, CA). All experiments were performed in triplicate.

#### **2.3.5 Quantitation of Ia Ag expression by HBMEC**

HBMEC monolayers stained for the light microscopic localization of Ia Ag were examined

under a Nikon Labophot light microscope. Quantitation of Ia Ag expression was performed by counting one central and four peripheral randomly selected fields of each culture well with an ocular grid under X200 magnification. All counts were performed blindly. Data are expressed as the mean  $\pm$  standard error of the mean.

#### 2.4 Scanning electron microscopy (SEM)

Confluent HBMEC monolayers treated with 200 U/ml IFN- $\gamma$ , 6,000 U/ml IFN- $\beta$  or a combination of IFN- $\gamma$  (200 U/ml) and  $\beta$  (6,000 U/ml) for 3 to 4 days, monolayers coincubated with 200 U/ml IFN- $\gamma$  and 10 $\mu$ g/ml anti-IFN- $\gamma$  monoclonal antibody for the same period of time, as well as untreated control cultures were processed for SEM as described by Schroeter et al. (185). Briefly, the cultures were washed in Hank's balanced salt solution and fixed in 2.5% glutaraldehyde in 0.05 M sodium cacodylate buffer (pH 7.2) for 1 hour at 4 °C. Following washing in cacodylate buffer, the cells were post fixed in buffered 1% OsO<sub>4</sub> for 1 hour, washed in buffer and treated with 1% Tannic acid for 1 hour. After further washing in cacodylate buffer, the monolayers were dehydrated in graded series of methanol up to 70%, and block stained with 4% uranyl acetate overnight at 4 °C. The cells were then dehydrated with methanol up to 100%, critical point dried, gold coated and viewed with a Cambridge Stereoscan 250T scanning electron microscope.

#### 2.5 Permeability studies

Confluent HBMEC monolayers treated with IFN- $\gamma$  (200 U/ml) for 4 days were washed with

serum-free  $\alpha$ MEM and incubated in  $\alpha$ MEM containing 1 mg/ml horseradish peroxidase (HRP; Sigma Type VI) for 5 - 10 minutes at 37 °C as previously described (186). At the end of the incubation period, the cells were fixed in 2.5% glutaraldehyde and 2% paraformaldehyde in 0.1 M sodium cacodylate buffer (pH 7.4) for 1 hour at 4 °C. Following washing with buffer, the monolayers were incubated with 3,3' - diaminobenzidine (Sigma) for 1 hour at 4 °C, washed with cacodylate buffer, post-fixed in 1% buffered OsO<sub>4</sub>, stained en bloc with uranyl magnesium acetate, dehydrated with graded series of methanol, and embedded in Epon-Araldite. Thin plastic sections were examined in a Philips EM400 without heavy metal staining. Controls consisted of identical age-matched primary cultures grown to confluence in IFN- $\gamma$  free media.

Quantitation of the junctional permeability and pinocytotic activity of EC was performed by counting the number of permeable and impermeable intercellular contacts and the number of HRP labeled and unlabeled cytoplasmic vesicles in 100 IFN- $\gamma$  treated and 100 untreated cells photographed at standard EM magnification.

## 2.6 Growth Studies

Freshly isolated EC were plated in replicate wells of Corning 24 - well plates at a density of  $1 \times 10^5$  cells/cm<sup>2</sup> on day 0. On day 1, all experimental wells were refed with complete medium containing IFN- $\gamma$  (150 U/ml), IFN- $\beta$  (1,000 U/ml) or a combination of IFN- $\gamma$  and  $\beta$  (150 U/ml and 1,000 U/ml, respectively). All experiments were carried out in duplicate and media were changed every other day. Control cultures were maintained in growth media in the absence of

the interferons. The cells were viewed with a Nikon Diaphot TMD inverted microscope and photographs of one central and four peripheral fields of each well were taken daily at 10X magnification. The number of cells in each photograph were counted and the data are expressed as the mean  $\pm$  standard error of the mean.

## 2.7 Preparation of T lymphocytes

Human peripheral blood lymphocytes (PBL) were prepared from heparinized venous blood of normal adult volunteers by Ficoll-Hypaque density gradient centrifugation (Histopaque - 1077, Sigma, St. Louis, MO, USA) at 500 x g for 30 minutes. The PBL were washed three times in PBS and resuspended in RPMI 1640 (Gibco) containing 10% fetal calf serum (FCS) (Gibco), 2 mM Glutamine, 100 U/ml penicillin, 100  $\mu$ g/ml streptomycin, 0.25  $\mu$ g/ml Amphotericin B, and 125  $\mu$ g/ml gentamicin. By this procedure cell fractions containing 85 - 89% lymphocytes were obtained. Viability was 95 - 98% by the Trypan Blue exclusion test. T lymphocytes were prepared by the nylon-wool separation technique (187). Sterile nylon-wool (Robbins Scientific Corporation, Sunnyvale, CA) was packed into 6 ml syringes at 500 mg/syringe. The columns were washed 10 times alternately with distilled H<sub>2</sub>O and 0.02 N HCl and then with 15 ml of 1X Hank's balanced salt solution (with Ca<sup>2+</sup> and Mg<sup>2+</sup>), followed by 15 ml of 10% Fetal Calf Serum in RPMI 1640 media (10% FCS/RPMI) per column. The columns were used immediately or kept frozen at -20 °C for up to 2 months. Frozen columns were thawed for 30 minutes at room temperature, followed by another 30 minutes at 37 °C. They were then washed with 10 ml of 10% FCS/RPMI, and compressed to 1ml volume prior

to cell incubation. One ml suspension of isolated PBL ( $1 \times 10^7$  cells/ml) was placed over each column dropwise and the columns were incubated for 45 minutes at 37 °C. Non-adherent T lymphocytes were eluted with 12 ml 10% FCS/RPMI. By this method, we routinely obtained 5 to 6 X  $10^6$  cells/ml. Phenotypic characterization of the lymphocytes in the eluate was carried out according to the following protocol: aliquots of lymphocyte suspension (200  $\mu$ l containing 2 X  $10^6$  cells/ml) were incubated for 30 min at 4 °C with the following mouse mAbs: anti CD2 (for T and Natural killer (NK) cells), anti CD4 (for T helper phenotype), anti CD8 (for T cytotoxic phenotype), anti CD16 and anti CD 56 (for resting NK cells), anti CD20 (for B cells), and anti-CD56 (for resting and activated NK cells) (Phycoerythrin-conjugated anti CD2, CD8 and CD56 from Coulter Corporation, Hialeah, Fl., Fluorescein-conjugated anti CD4 and CD20 from Becton Dickinson, Mississauga, ONT). The tubes were then filled with 2% FCS in TC 199 (Gibco) and centrifuged at 500 x g for 10 minutes. The supernatant was discarded and 0.5 ml of 1% paraformaldehyde solution was slowly added while vortexing the tubes. Fluorescence was read on the Epic Profile I (Coulter Corporation, Hialeah, Fl.). The quadrant was set by using isotypic control, and dead cells were gated out. CD4<sup>+</sup> cells comprised 57% of the eluate while CD8<sup>+</sup> cells constituted 22% of the cell suspension. There was a small number of NK cells (<10%), and B cells (4%).

## 2.8 Activation of T cells

Freshly isolated lymphocytes were cultured for 72 hours at 37 °C with mouse mAb to human Leu 4 (CD3) (10 ng/ml; Becton Dickinson, Mississauga, ONT). Before their use, lymphocytes

were washed extensively and resuspended in 10% FCS/RPMI. Lymphocyte activation was determined by the following protocol: aliquots of lymphocyte suspension (200  $\mu$ l containing  $2 \times 10^6$  cells/ml) were incubated for 30 min at 4 °C with fluorescein-conjugated mouse monoclonal anti CD25 antibody (for IL-2R, p55) (Becton Dickenson, Mississauga, ONT.). The cells were washed in PBS and centrifuged at 300 x g for 5 minutes. The pellet was resuspended and fixed in 1% paraformaldehyde diluted in PBS for 30 min at room temperature. Fluorescence was read at 580 nm. Approximately 2 fold increase in IL-2R expression was detected in anti CD3 stimulated lymphocytes in comparison to resting lymphocytes.

## 2.9 HBMEC-lymphocyte adhesion assay

Confluent monolayers of HBMEC were treated with recombinant human IFN- $\gamma$  (150 U/ml), or IFN- $\beta$  (2,000 U/ml) or a combination of IFN- $\beta$  (2,000 U/ml) and  $\gamma$  (150 U/ml) for 3 days. Prior to use, the cultures were washed extensively. 500  $\mu$ l of freshly isolated resting T cells or activated lymphocytes containing  $2 \times 10^6$  cells/ml were incubated with the EC monolayers for 1 hour at 37 °C. Following incubation, the monolayers were washed thoroughly with warmed Hanks' balanced salt solution (HBSS) and PBS (pH 7.2, 10mM) containing  $\text{Ca}^{2+}$  and  $\text{Mg}^{2+}$  to remove non adherent lymphocytes, fixed in Acetone: Ethanol (1:1 ratio) for 7 minutes at 4 °C, air dried and washed with Tris buffer. Blocking of the endogenous peroxidase was carried out by incubation with  $\text{H}_2\text{O}_2$  and Methanol (1:4 ratio) for 30 minutes at room temperature. After several washes with Tris buffer, the cells were incubated for 90 minutes with mouse

monoclonal anti human leucocyte common antigen (LCA) (Dimension Laboratories Inc., Mississauga, ONT.) at 1:100 dilution, and then with horseradish peroxidase conjugated goat anti mouse IgG at 1:200 dilution (Jackson Immunoresearch Laboratories Inc., West Grove, PA) for 120 minutes at room temperature. After washing with Tris buffer, the cells were treated with 3,3'-diaminobenzidine (0.5 mg/ml; Sigma) and 0.01% H<sub>2</sub>O<sub>2</sub> in Tris buffer (pH 7.6) for 20 minutes at 4 °C, washed with H<sub>2</sub>O, and counterstained with haematoxylin. Subsequently, the monolayers with adherent lymphocytes were covered with JB4 mounting medium and the walls of the wells cut out with a hot scalpel blade prior to counting. Controls consisted of untreated HBMEC cultures incubated with resting or activated lymphocytes.

For scanning EM studies of lymphocyte-EC adhesion, HBMEC were grown to confluency on collagen discs (section 2.10) and then incubated with IFN- $\gamma$  (150 U/ml, 3 days) or left untreated (controls), followed by incubation with either resting or anti CD3 stimulated T cells for 2 hours at 37 °C. The cells were then processed for scanning EM as described above (section 2.4).

#### 2.10 HBMEC-lymphocyte migration assay

For the migration studies, HBMEC were grown on permeable collagen membranes made of highly purified, pyrogen-free, pepsin-solubilized collagen forming the floor of 14 mm diameter wells (Cellagen Discs, ICN Biomedicals, Inc., Cleveland, OH) (Fig. 1). Immediately before seeding the cells, collagen discs were placed inside 24-well culture plates and immersed in M199. This double chemotactic chamber has been previously demonstrated to be

suitable for studying the adhesion and migration of human polymorphonuclear leukocytes across cultured bovine brain microvessel EC (7). Plating of EC on collagen discs did not require prior coating with fibronectin. Isolated clumps of HBMEC were plated at 50,000 cells/cm<sup>2</sup>. Media were changed every other day. Confluent monolayers of FVIIIIR:Ag positive EC were obtained by six to eight days in culture. Confluent cultures of HBMEC were treated either with IFN- $\gamma$  (150 U/ml), IFN- $\beta$  (2,000 U/ml) or a combination of IFN- $\beta$  (2,000 U/ml) and  $\gamma$  (150 U/ml) for 3 days at 37°C. Before their use, HBMEC were rinsed three times and the last wash was replaced by 200  $\mu$ l of lymphocyte suspension containing  $2 \times 10^6$  cells/ml. Resting or activated lymphocytes were incubated with EC for 3 hours at 37 °C. Following incubation, the monolayers were washed with warm M199 and then PBS to remove non-adherent lymphocytes and processed for transmission electron microscopy (section 2.16). One  $\mu$ m thick and ultrathin sections were cut with an Ultracut E ultramicrotome (Reichert-Jung, Austria). One  $\mu$ m thick sections were stained with toluidine blue, coverslipped and used for quantitation of lymphocyte transendothelial migration by light microscopy (section 2.12). Thin sections were stained with uranyl acetate and lead citrate.

#### 2.11 Monoclonal antibody-blocking studies

The effects of mAbs to IFN- $\gamma$  and HLA-DR on the adhesion and migration of resting T cells and activated lymphocytes across HBMEC monolayers were examined in separate experiments. Monolayers were coincubated with IFN- $\gamma$  (150 U/ml) and mouse monoclonal anti human IFN- $\gamma$  IgG (10  $\mu$ g/ml) for 3 days at 37°C, or with IFN- $\gamma$  (150 U/ml) for 3 days at

37°C followed by incubation with mouse monoclonal anti human HLA-DR IgG (6 µg/ml) for 2 hours prior to incubation with lymphocytes. Monolayers were thoroughly washed three times with M199 to remove the IFN-γ and mAbs before the adhesion and migration assays. Both antibodies were purchased from Dimension Laboratories Inc., Mississauga, ONT.

### 2.12 Quantitation of lymphocyte adhesion and migration

Lymphocyte-EC adhesion was quantitated by counting the number of adherent lymphocytes to EC monolayers in one central and four peripheral randomly selected fields of each culture well using a bright field microscope equipped with a 1 cm<sup>2</sup> ocular grid under X 200 magnification. Adhesion index is expressed as the number of adherent T cells per mm<sup>2</sup> of the monolayer. Transendothelial migration was quantitated by counting the number of lymphocytes that migrated across the monolayers by light microscopy in 1 µm thick plastic sections stained with toluidine blue. For each treatment, 200 sections (40 µm apart), were counted.

### 2.13 Transmission electron microscopy

EC monolayers were washed three times in serum-free media and fixed in 2.5% glutaraldehyde and 2% paraformaldehyde in 0.1M sodium cacodylate buffer (pH 7.35) for 1 hour at 4°C. After washing with 0.2M cacodylate buffer for 30 minutes, the cells were post-fixed in 1% OsO<sub>4</sub> in 0.1M sodium cacodylate buffer for 1 hour at 4°C, block-stained with uranyl magnesium acetate overnight at 4°C, dehydrated and embedded in Epon-Araldite.

Ultrathin sections were stained with uranyl acetate and lead citrate and examined in a Philips EM 400.

## 2.14 Localization of FVIII:Ag in untreated, cytokine/chemical-treated HBMEC

### 2.14.1 **In vitro drug treatment of EC**

The effects of calcium ionophore A23187, ethyleneglycol-tetraacetic acid (EGTA) and interferon- $\gamma$  (IFN- $\gamma$ ) on the release of FVIII:Ag were studied in confluent 8 day old cultures. The cells were incubated with growth medium containing: a) 10 $\mu$ M Ca<sup>2+</sup> ionophore A23187 (Sigma), diluted from a 10mM stock dissolved in dimethylsulfoxide, for 10 minutes; b) 1mM EGTA (Sigma) for 10 minutes and c) 200U/ml IFN- $\gamma$  (Collaborative Research Incorporation, Bedford, MA) for 24 hours. At the end of the incubation period the cultures were washed with PBS and processed for immunoelectron microscopy.

### 2.14.2 **Immunoelectron microscopy for FVIII:Ag**

Endothelial monolayers were washed with phosphate buffered saline (PBS) with 0.1g/l CaCl<sub>2</sub> and fixed in freshly prepared periodate-lysine-paraformaldehyde (PLP) fixative (184) overnight at 4°C. After fixation the cultures were washed with PBS for 30 minutes and incubated in cold 10% sucrose solution in PBS for 4 hours, 15% sucrose for 4 hrs and 20% sucrose overnight. The cells were permeabilized by incubation in 0.01% to 0.05% Triton X-100 (Sigma) in freshly prepared PLP for 10 minutes at room temperature, washed with PLP for 20 minutes and then with 0.1M glycine in PBS for 30 minutes. The monolayers were

incubated with 5% normal goat serum (NGS) in 0.1% BSA-Tris buffer (BSA-Tris) for 20 minutes and then with the primary antibody (mouse anti-human FVIII antigen) at 1:50 dilution with 1% NGS in BSA-Tris for 2.5 hours at room temperature. Following washing in BSA-Tris, the cells were incubated with the secondary antibody (goat antimouse IgG) at 1:20 dilution in BSA-Tris for 1.5 hours at room temperature. Cultures were further fixed in 1% glutaraldehyde in PBS containing 0.2% tannic acid for 40 minutes at room temperature, washed in PBS and post-fixed in 0.5% osmium tetroxide ( $\text{OsO}_4$ ) in PBS for 15 minutes. Following post-fixation, the cells were washed in acetate buffer, block stained in uranyl magnesium acetate overnight at 4°C, dehydrated through graded series of methanol and embedded in Epon-Araldite. Blocks cut from the embedded cultures were re-embedded for cross-sectioning. Thin sections were examined in a Philips EM400 without heavy metal staining.

### 2.15 Statistical analysis

Student's t-test, a procedure designed to test for differences in two groups, was used for statistical evaluation of the data.

Sigmastat program was used for this analysis.

## RESULTS

### 3.1 Human brain microvessel endothelial cell

HBMEC grown on plastic wells or collagen membranes formed confluent monolayers by 7 to 10 days in culture. EC were elongated and grew in close association with each other. Upon reaching confluency, HBMEC exhibited density-dependent growth inhibition with significant decrease in mitotic activity and cellular proliferation. There was no difference in the growth pattern between cells grown on plastic wells and those cultivated on collagen discs (Fig. 2 a, b).

Immunofluorescence and immunoperoxidase staining for Factor VIII related antigen (FVIII:R:Ag) revealed strongly positive, perinuclear, granular staining of cells, thus confirming their endothelial origin (Fig. 3a). Binding of *Ulex europaeus* type I (UEA I) lectin, a marker for normal and neoplastic human endothelium (188, 189), by HBMEC, was demonstrated by their strongly positive immunoperoxidase staining for UEA-1 as previously described (Fig. 3b) (107). There were no other contaminating cells in any of the cultures used for these experiments.

Ultrastructurally, EC were elongated with overlapping processes (Fig. 4). Junctional complexes with the characteristic pentalaminar configuration of tight junctions were present in areas of cell to cell contact (Fig. 5 a, b, c, d). The cytoplasm was dense and contained prominent rough endoplasmic reticulum, frequent mitochondria and scattered 8 to 10nm intermediate filaments (Fig. 6a). Pinocytotic vesicles were infrequently seen. Rod-shaped,

membrane bound cytoplasmic organelles with parallel arrays of tubular structures (Weibel-Palade bodies) were not observed in the cytoplasm of HBMEC. A constant finding in all cells examined was the presence of dilated cytoplasmic vesicles or vacuoles bound by a single smooth limiting membrane. These vesicular structures were invariably located in the vicinity of the nucleus, in close association with the cisternae of the rough endoplasmic reticulum and were absent from the most peripheral portions of the cytoplasm and the cell processes. They varied in size from 0.15 to 1.1 $\mu$ m and they appeared empty or contained small amounts of amorphous material (Fig. 6b).

### 3.2 Immunocytochemical Localization of FVIII:Ag

In cultures stained for FVIII:Ag with the immunogold technique, 5nm gold particles were distinctly localized within the vesicular profiles immediately adjacent to the rough endoplasmic reticulum (Fig. 7a) and close to Golgi cisternae in sections where the Golgi apparatus was present (Fig. 7b) as previously mentioned. The endoplasmic reticulum was largely unstained with the rare exception of single isolated particles within its cisternae. Occasionally, labeled vesicles communicated directly with cisternae containing gold particles (Fig. 7c). The number of labeled vesicles and the degree of labeling (number of gold particles per vesicle) varied among different cells. This is largely attributed to variable leakage of intracellular proteins following permeabilization or to insufficient permeabilization and penetration of individual EC by the antibodies. Low (0.01%) and high (0.05%) concentrations of Triton X-100 resulted in poor labeling while a concentration of 0.03% was associated with

frequent and denser labeling. There was no staining of the cytoplasmic membrane or the discontinuous basement membrane-like material underlying the basal cell surface. The specific staining was eliminated in control cultures incubated with normal mouse IgG or carrier buffer (Fig. 7d).

### 3.3 Induction of Ia Ag expression on Primary cultures of HBMEC

#### 3.3.1 Effects of recombinant human IFN- $\gamma$

Treatment of cultures with IFN- $\gamma$  induced expression of Ia Ag by EC, which was dependent upon the concentration and length of exposure to IFN- $\gamma$ . Surface labeling was observed as early as 12 hours following incubation with 200 U/ml in a small cell population ( $9.24 \pm 0.99\%$ ), increased up to  $88.35 \pm 0.18\%$  after 24 hours and reached 100% after 48 hours (Fig. 8). Ia Ag expression reached plateau levels after 2 days and persisted for 4 days in the continuous presence of the cytokine. Expression was maximal with 100 - 200 U/ml IFN- $\gamma$  (100% of cells) and minimal with 10 U/ml ( $25.76 \pm 7\%$ ) (Fig. 9). Incubation with 20 U/ml of IFN- $\gamma$  induced Ia Ag expression in  $68.73 \pm 18.5\%$  of cells, while  $90.85 \pm 5.5\%$  of cells were labeled after treatment with 50 U/ml. EC expressing Ia Ag showed diffuse surface staining in the form of dark brown-black, granular deposits (Fig. 10A). In marked contrast, untreated EC invariably lacked Ia Ag expression as indicated by their consistently negative staining with immunogold (Fig. 10B). The staining intensity varied with the concentration and length of incubation with IFN- $\gamma$ . Thus, labeling was less intense in cells incubated with 10 to 20 U/ml for 4 days or with 200 U/ml for 12 to 24 hours (Fig. 10C), and most dense in cultures treated

with higher concentrations for 3 to 4 days (Fig. 10A). Within the same culture, the larger cells were usually stained most intensely. There were no differences in Ia Ag expression among HBMEC monolayers originating from different individuals and subjected to identical culture conditions and IFN- $\gamma$  treatment. Staining was not observed in control cultures incubated with normal mouse IgG, carrier buffer or irrelevant antibody.

In monolayers co-incubated with IFN- $\gamma$  and anti-IFN- $\gamma$  mAb for 4 days, induction of Ia Ag was completely abolished (Fig. 10D) indicating that IFN- $\gamma$  specifically induces expression of Class II MHC molecules on human brain EC. Treatment of cells with 200 U/ml IFN- $\gamma$  followed by withdrawal and culture in regular growth media resulted in complete reversal of Ia Ag expression and negative staining of the cultures.

Ultrastructural examination following immunogold labeling showed that Ia Ag was readily detectable on the apical surface of EC. Gold particles were found at the cell membrane with a tendency to localize on or near thin cytoplasmic processes (Fig. 11a). The basal cell surface was not labeled. No labeling was seen in untreated control cultures (Fig. 11b).

### 3.3.2 Effects of recombinant human IFN- $\beta$

Treatment of primary HBMEC cultures with IFN- $\beta$  for 4 days at concentrations of 100 - 6,000 U/ml failed to induce surface expression of Ia Ag as indicated by the negative staining of EC (Fig. 12a). Coincubation of EC with IFN- $\gamma$  and  $\beta$  resulted in downregulation of Ia Ag expression in a dose-dependent fashion. Thus, expression was decreased by approximately 40% in monolayers treated with 100 U/ml IFN- $\beta$  and 100 U/ml IFN- $\gamma$  for 4 days. Increase of

the IFN- $\beta$  concentration to 250 U/ml and 500 U/ml resulted in 62% and 79% suppression, respectively (Fig. 12b). Downregulation of Ia Ag expression was maximal (89%) following coincubation with 100 U/ml IFN- $\gamma$  and 2,000 U/ml IFN- $\beta$ ; however, complete inhibition of Ia Ag expression was not observed even with IFN- $\beta$  concentrations as high as 6,000 U/ml (Fig. 13).

### 3.4 Kinetics of the downregulation of Ia Ag expression by IFN- $\beta$

In order to obtain greater insight into the temporal effects of IFN- $\beta$  on the induced Ia Ag expression by HBMEC, several treatment protocols were applied. Treatment of HBMEC with 100 U/ml IFN- $\gamma$  for 4 days induced Ia Ag expression in 86% of the EC. Incubation of the monolayers with a combination of IFN- $\beta$  and IFN- $\gamma$  (6,000 U/ml and 100 U/ml, respectively) for 4 days, significantly downregulated Ia Ag expression with positive immunogold staining limited to <20% of EC (Fig. 14). Similar levels of downregulation were also achieved when EC were pretreated with IFN- $\beta$  (6,000 U/ml) for 2 days, followed by a combination of IFN- $\beta$  and IFN- $\gamma$  (6,000 U/ml and 100 U/ml respectively) for another 4 days (Fig. 14).

Interestingly, a much less significant decrease in Ia Ag expression was noted when cultures were pretreated for 2 days with IFN- $\gamma$  (100 U/ml), followed by a combination of IFN- $\beta$  and  $\gamma$  (6,000 U/ml and 100 U/ml respectively) for another 4 days. However, when cultures were pretreated for 2 days with a combination of IFN- $\beta$  (6,000 U/ml) and  $\gamma$  (100 U/ml), followed by a 4 day incubation with 100 U/ml IFN- $\gamma$ , no suppression of Ia Ag expression was detected (Fig. 14).

These results indicate that downregulation of Ia Ag expression by IFN- $\beta$  is most effective when HBMEC monolayers are coincubated with both cytokines with or without pretreatment with IFN- $\beta$  alone. However, IFN- $\gamma$ -induced Ia Ag expression is not suppressed when treatment with IFN- $\beta$  and  $\gamma$  is preceded or followed by incubation with IFN- $\gamma$ .

The effects of IFN- $\beta$  on the IFN- $\gamma$  induced Ia Ag expression by HBMEC was further determined by Enzyme linked Immunosorbent Assay (ELISA) performed on primary confluent HBMEC cultures. Various concentrations of IFN- $\beta$  (100 to 6,000 U/ml) were used in combination with an optimal concentration of IFN- $\gamma$  (100 U/ml) and different treatment protocols, similar to the ones used for immunohistochemistry were applied. The results were similar to those obtained by immunohistochemistry. Thus, treatment with IFN- $\beta$  failed to induce expression of Ia Ag. Coincubation with IFN- $\beta$  and  $\gamma$  resulted in significant downregulation of Ia Ag expression that was dependent upon the IFN- $\beta$  concentration (Fig. 15). Significant reduction in Ia Ag expression was noted in cultures treated with 100 U/ml IFN- $\gamma$  in combination with 100 U/ml IFN- $\beta$  for 4 days (Fig. 15). Further suppression of Ia Ag expression was observed with higher concentrations of INF- $\beta$  (500 U/ml to 6,000 U/ml), however, complete inhibition of Ia Ag expression by IFN- $\beta$  was never achieved (Fig. 15). Downregulation of Ia Ag expression was maximal when EC were pretreated with IFN- $\beta$  for 2 days, followed by coincubation with IFN- $\beta$  and  $\gamma$  for another 4 days. In monolayers incubated with IFN- $\gamma$  for 2 days followed by a combined treatment with IFN- $\gamma$  and  $\beta$  for 4 days, a similarly significant suppression of Ia Ag expression was obtained.

### 3.5 Effects of IFN- $\gamma$ and IFN- $\beta$ on cell morphology, organization and growth

#### 3.5.1 IFN- $\gamma$

Primary cultures of HBMEC grown in regular medium in the absence of IFN- $\gamma$  formed highly ordered confluent monolayers of elongated, closely associated, contact inhibiting cells (Fig. 16a). EC treated with 200 U/ml IFN- $\gamma$  for 3 to 4 days acquired a spindle-like shape and long attenuated processes. These markedly elongated cells frequently arranged themselves in ill-defined whorls and exhibited prominent overlapping, thus contributing to a unique appearance of the monolayers (Fig. 16b).

These changes were most conspicuous under SEM examination. Under normal culture conditions, elongated HBMEC grow in close contact to each other and display distinct marginal folds in areas of cell-to-cell contact (Fig. 17a). In contrast, EC treated with IFN- $\gamma$  became attenuated and their long, thin processes often extended over and covered adjacent cells (Fig. 17b). As a result of this rearrangement, intercellular contacts and marginal folds became less prominent and the monolayers lost their highly organized appearance. The above morphological changes were reversed 4 days following withdrawal of the cytokine from the culture medium and were not observed in cultures co-incubated with IFN- $\gamma$  and anti-IFN- $\gamma$  antibody.

The effect of IFN- $\gamma$  on the growth of HBMEC was less profound. Thus, the number of cells in primary HBMEC cultures treated with 150 U/ml IFN- $\gamma$  from day 1, was slightly less than that in control cultures (Fig. 18). This slight inhibitory growth effect of IFN- $\gamma$  provides further support to the observation that re-arrangement and overlapping of HBMEC is the direct

effect of the cytokine and not the result of cell overgrowth.

### 3.5.2 IFN- $\beta$

Primary cultures of HBMEC grown in media containing IFN- $\beta$  (6,000 U/ml) for 4 days showed no changes in cell morphology and organization and were morphologically identical to untreated cultures (Fig. 19a). When monolayers were coincubated with IFN- $\beta$  and IFN- $\gamma$  (6,000 U/ml and 200 U/ml, respectively) for 4 days, changes in cell shape and organization of the monolayers induced by IFN- $\gamma$ , were not detected (Fig. 19b). Similarly, scanning EM studies of EC treated with IFN- $\beta$  alone, or a combination of IFN- $\beta$  and IFN- $\gamma$ , confirmed the normal morphology and growth pattern of HBMEC and the absence of the morphological phenotype and overlapping induced by IFN- $\gamma$  (Fig. 19, arrows).

On the other hand, the effect of IFN- $\beta$  on the growth of HBMEC was profound: inhibition of growth was observed when HBMEC were treated from day 1 with IFN- $\beta$  alone (1,000 U/ml) or a combination of IFN- $\beta$  and IFN- $\gamma$  (1,000 U/ml and 100 U/ml, respectively) when compared to untreated cultures (Fig. 18).

## 3.6 **Permeability of HBMEC monolayers**

In order to examine if IFN- $\gamma$ , in parallel to morphological changes, also induced changes in the permeability of the monolayers to macromolecules, confluent treated and untreated cultures were incubated with HRP and the labeling of intercellular contacts and cytoplasmic vesicles was assessed ultrastructurally. Intercellular contacts that impeded the

tracer entirely or were penetrated only for a short distance from either the apical or basal cell surface by HRP, were considered impermeable. In untreated cultures, 75.2% of interendothelial junctions prevented the passage of HRP, in contrast with 36.6% in cultures incubated with the cytokine for 4 days (Table 1). In untreated monolayers, EC formed a single cell layer and were bound together by junctions, most of which were not labeled with the tracer (Fig. 20a). Focally, HRP penetrated an intercellular contact for a short distance from the basal aspect of the monolayer before being arrested at a junctional complex of an otherwise intact cleft (Fig. 20b). In treated cultures, interendothelial clefts were often penetrated by the tracer throughout their entire length (Fig. 20c). Overlapping of EC resulted in the formation of 2 or more layers. Horseradish peroxidase often penetrated the intercellular clefts between EC at the top layer, and extensive deposits were found between adjacent cells at the lower layers (Fig. 20d). The number of cytoplasmic vesicles labeled with HRP was equally low in control and experimental cultures (Table 1), indicating that, contrary to the prominent conformational and organizational changes, the pinocytotic activity of HBMEC is not affected by IFN- $\gamma$  treatment.

### 3.7 Lymphocyte characterization

The different subsets of lymphocytes obtained by the nylon-wool separation technique were characterized by using mouse mAbs directed against human T cell surface molecules of interest. The results were determined by Coulter cytometry with the Epics Profile Analyzer. Greater than 90% of cells ( $91.3 \pm 2.8\%$ ) recovered after nylon-wool separation were T cells.

When peripheral blood lymphocytes were activated by incubation with mouse anti-human Leu-4 (CD3) monoclonal antibody for 3 days at 37 °C, up to  $91.5 \pm 6\%$  of cells were T lymphocytes. Stimulation with anti-CD3 resulted in more than 2 fold increase in Interleukin-2 receptor (IL-2R) expression as compared to resting T lymphocytes (Fig. 21). Scanning and transmission EM studies showed that the surface membrane of activated T cells appeared ruffled with numerous folds on the cell surface. In contrast, resting lymphocytes exhibited a smooth surface membrane. Subsequently, anti-CD3 treated T cells provided morphological and functional evidence of activation.

### 3.8 Human T-lymphocyte adhesion to untreated and cytokine-stimulated HBMEC

Confluent cultures of HBMEC grown on plastic wells for 7 days were treated with IFN- $\gamma$  (150 U/ml) or IFN- $\beta$  (2,000 U/ml), or a combination of IFN- $\gamma$  (150 U/ml) and  $\beta$  (2,000 U/ml) for 3 days. Controls consisted of monolayers grown to confluency in the absence of cytokines.

By light microscopy, following immunoperoxidase staining for leukocyte common antigen, a small number of resting lymphocytes adhered to untreated HBMEC ( $50 \pm 10$  T cells per  $\text{mm}^2$  of EC monolayers) (Fig. 22, 25). Treatment of HBMEC with IFN- $\gamma$  for 3 days resulted in more than 3 fold increase in adhesion over control values ( $165 \pm 13$  T cells per  $\text{mm}^2$  of EC monolayers) (Figs 23, 25). Treatment of the monolayers with IFN- $\beta$  had no effect on the basal adhesion of lymphocytes to endothelium ( $p = 0.953$ ) (Figs. 24, 25). In cultures incubated with both cytokines, adhesion was not significantly different from that observed in

control cultures ( $p = 0.004$ ) (Fig. 25).

Examination by SEM revealed that untreated HBMEC monolayers consisted of closely associated cells with marginal folds in areas of cell to cell contact. A similar morphology and growth pattern was observed in EC cultures treated with IFN- $\beta$  or with a combination of IFN- $\gamma$  and  $\beta$ . Resting T lymphocytes first adhered to the endothelium by extending pseudopodia that contacted the endothelial surface (Fig. 26a). Eventually they positioned themselves between adjacent EC (Fig. 26b), and began migrating across the monolayer (Fig. 26c). Less frequently, lymphocytes were seen penetrating the apical EC plasma membrane and moving through the endothelial cytoplasm (Fig. 26d). Monolayers treated with IFN- $\gamma$  exhibited elongation and overlapping of EC. A large number of lymphocytes established contact with the endothelium via pseudopodia (Fig. 27a), and singly or in small aggregates aligned themselves preferentially along the borders between adjacent EC in preparation for crossing the monolayers (Fig. 27b). Adhesion and penetration of EC cytoplasm by lymphocytes was encountered much less frequently. Ultrastructurally, lymphocytes first established contact with intact or cytokine treated EC by extending finger-like cytoplasmic processes to the surface of the endothelium. The two cell membranes became closely apposed.

### **3.9 Adhesion of activated T-lymphocytes to untreated and cytokine stimulated HBMEC**

Activation of T-lymphocytes with anti-CD3 resulted in a three fold increase in adhesion to untreated EC over control values ( $202 \pm 36$  activated T cells per  $\text{mm}^2$  of EC

monolayers) ( $p = 0.010$ ) (Figs. 28, 31). Following pretreatment of EC with IFN- $\gamma$ , adhesion of activated T cells to endothelium was 2 fold greater than adhesion to untreated EC ( $403 \pm 29$  activated T cells per  $\text{mm}^2$  of EC monolayers) (Figs. 29, 31) ( $p = 0.012$ ). Pretreatment of HBMEC with IFN- $\beta$  had no effect on the adhesion of activated T cells to the endothelium. Preincubation of EC with a combination of IFN- $\gamma$  and  $\beta$ , however, resulted in levels of adhesion comparable to those obtained when activated T cells were incubated with untreated EC (Fig. 30, 31), indicating that IFN- $\beta$  downregulates the IFN- $\gamma$ -mediated increase in adhesion ( $218 \pm 44$  activated T cells per  $\text{mm}^2$  of EC monolayers) ( $p = 0.788$ ) (Fig. 31). Examination by SEM revealed prominent changes in the morphology of activated T lymphocytes which appeared larger and exhibited a ruffled cell membrane with numerous folds. Activated lymphocytes adhered to the endothelium in large numbers (Fig. 32a-c). They appeared considerably larger than resting T cells and their surface was decorated with numerous folds and cytoplasmic projections. As observed with resting T cells, activated lymphocytes established close contacts with EC by means of cytoplasmic projections and usually positioned themselves along the borders between adjacent EC in both untreated and cytokine-treated cultures in preparation for migration. Direct penetration of the endothelial cytoplasm by adherent lymphocytes was rarely observed. In such instances, a protuberance on the apical surface of the endothelium, having the size and shape of an activated T cell, indicated movement through the EC cytoplasm (Fig. 32, arrows). Ultrastructurally, activated lymphocytes displayed abundant cytoplasm, increased numbers of mitochondria and variable numbers of cytoplasmic vacuoles containing amorphous, flocculent material (Fig. 33). The

cell surface was extremely irregular due to the presence of numerous thin, finger-like, variably undulating, cytoplasmic processes. Several points of close cell-to-cell contact between endothelium and processes of adherent lymphocytes were present (Figs. 33, 34).

### **3.10 Effects of blocking antibodies on lymphocyte adhesion**

The ability of mAbs to IFN- $\gamma$  and human HLA-DR to block the adhesion of resting and anti-CD3 activated T cells to HBMEC was examined. In monolayers coincubated with IFN- $\gamma$  and mAb to IFN- $\gamma$  for 3 days, adhesion of resting and activated T-lymphocytes was significantly decreased ( $p = 0.002$  and  $p = 0.001$ , respectively) (Figs. 25, 31). When EC cultures were treated with IFN- $\gamma$  for 3 days, followed by incubation with mAb to human HLA-DR for 2 hours prior to incubation of T cells with EC, marked suppression of IFN- $\gamma$ -induced adhesion of resting and activated T-cells was observed ( $p = 0.012$  and  $p = 0.014$ , respectively) (Figs. 25, 31, 35, 36).

### **3.11 Transendothelial migration of resting T lymphocytes**

Transendothelial migration of resting T lymphocytes across untreated HBMEC monolayers was minimal (Figs. 37a, 38). Significant increase in migration, up to 3 fold, was observed when cerebral EC were pretreated with an optimal concentration of IFN- $\gamma$  (150 U/ml), known to induce maximal Ia Ag expression, for 3 days prior to incubation with the lymphocytes ( $p < 0.001$ ) (Figs. 37b, 38). In contrast, IFN- $\beta$  treatment had no effect on migration as the numbers of T cells detected underneath the EC monolayers were comparable

to those that migrated across untreated HBMEC ( $p = 0.304$ ) (Fig. 38). Moreover, the INF- $\gamma$ -mediated increase in migration was markedly suppressed when EC were preincubated for 3 days with a combination of INF- $\gamma$  and INF- $\beta$  and then allowed to interact with the resting lymphocytes for 3 hours (Figs. 37c, 38). Adhesion of lymphocytes directly to collagen membranes in the absence of EC was not observed. The results indicate that INF- $\beta$  significantly downregulated the INF- $\gamma$ -induced increase in transendothelial migration ( $p < 0.001$ ).

One  $\mu\text{m}$  thick, toluidine blue stained cross sections of the monolayers revealed that T cells initially attached and subsequently moved across the endothelium. At the end of their migration, lymphocytes positioned themselves underneath the monolayer between EC and the collagen membrane and assumed a flattened, elongated shape. The endothelial monolayers overlying the migrated lymphocytes appeared to retain their continuity (Fig. 37a to c).

Examination by TEM revealed that resting T-lymphocytes initiated their migration across the EC monolayers by directing one or more cytoplasmic processes between two adjacent EC (Fig. 39a). Eventually, a small segment of the cytoplasm, without the nucleus, was inserted between the two EC and was followed by the remaining cytoplasm and nucleus (39 b, c). After passing between the EC, the lymphocytes became elongated and flattened and remained between the overlying EC and the underlying collagen membrane (39d). Throughout the migratory process, lymphocytes remained in close contact with the EC, the adjacent plasma membranes of the two cell types being tightly apposed (Figs. 39a to d). Infrequently, lymphocytes migrated by moving through the cytoplasm of EC. A lymphocyte

was considered moving through rather than between adjacent EC only when the cytoplasm of the EC completely surrounded the lymphocyte (Fig. 40). At the end of the migration period, EC monolayers rapidly assumed their continuity and appeared structurally intact. Cultures treated with IFN- $\gamma$  showed variable overlapping of EC. Lymphocytes that had completed their migration across adjacent EC of the top layer, would then proceed to migrate across the second layer of EC. The integrity of the monolayers was reestablished once resting T cells completely migrated across the untreated/cytokine treated EC (Fig. 41 a, b).

### **3.12 Migration of activated T lymphocytes across untreated and cytokine treated HBMEC monolayers**

To determine whether nonspecific activation of T lymphocytes had any effect on migration, peripheral blood lymphocytes treated with anti-CD3 antibody for 3 days were incubated with HBMEC for 3 hrs.

Activation of T cells resulted in a four fold increase in the number of cells that migrated across untreated monolayers of HBMEC as compared with the migration of resting lymphocytes across untreated brain endothelium ( $p < 0.001$ ) (Figs. 38, 42). Pretreatment of EC with IFN- $\gamma$  further increased the migratory response by approximately 30% ( $p < 0.001$ ) (Fig. 38). In contrast, IFN- $\beta$  had no effect on the basal level of migration of activated T cells ( $p = 0.341$ ). Moreover, when HBMEC were preincubated with a combination of IFN- $\gamma$  and IFN- $\beta$ , the level of migration was not different from that obtained when activated T lymphocytes migrated across untreated EC monolayers ( $p = 0.268$ ), indicating that IFN- $\beta$

downregulated the IFN- $\gamma$ -mediated increase in migration (Fig. 38).

Ultrastructurally, large numbers of activated lymphocytes migrated across the endothelial monolayers. Although migration proceeded in a fashion similar to the one observed during migration of resting T cells (Figs. 43 a, b), crossing of the monolayers by means of moving through the cytoplasm of EC, was not observed in any of the material examined. Migration of activated lymphocytes was not associated with any apparent disruption of the monolayers (Fig. 43b). Lymphocytes that had completed their migration across adjacent EC of the top layer, would then proceed to migrate across the next layer of EC (Fig. 44).

### **3.13 Effects of blocking antibodies on lymphocyte migration**

T lymphocyte migration across IFN- $\gamma$ -treated HBMEC monolayers was significantly blocked by preincubation of EC with a mAb to human HLA-DR ( $p < 0.001$ ) regardless of the activation status of lymphocytes. The level of suppression approximated that obtained by treating EC with a combination of IFN- $\gamma$  and IFN- $\beta$  (Fig. 38). These results suggest that class II MHC molecules (Ia Ag) play a central role in the IFN- $\gamma$ -induced upregulation of T lymphocyte migration across HBMEC, irrespective of the activation status of the lymphocytes.

### **3.14 Effects of calcium ionophore A23187, EGTA and IFN- $\gamma$ on the constitutive pathway of factor VIII:Ag release**

Treatment of the monolayers with 10 $\mu$ M Ca<sup>2+</sup> ionophore A23187 for 10 minutes

resulted in almost complete loss of staining (Fig. 45a), while incubation with 1mM EGTA for 10 minutes was associated with slightly increased numbers of labeled vesicles (Fig. 45b). When the monolayers were preincubated with 200U/ml IFN- $\gamma$  for 24 hours, there was a significant increase in the number of immunostained vesicles over the untreated cultures (Fig. 45c). In order to quantitate these findings, the number of labeled and unlabeled vesicles was counted in 100 cells in each group of treated and in untreated cultures. Fig. 46 summarizes these results. The differences reflect variations in the percentage of immunostained vesicles. There was no appreciable difference in the number of gold particles per vesicle between treated and untreated cells. The difference in the number of labeled vesicles between controls and IFN- $\gamma$  treated EC was statistically significant ( $p = 0.000$ ), while no significant difference was found between controls and EGTA treated cultures ( $p = 0.21$ ).

## DISCUSSION

### 4.1 INFLUENCE OF CYTOKINES ON Ia Ag EXPRESSION ON HBMEC

**The first specific aim of this thesis was to determine whether Ia Ag is constitutively expressed in primary cultures of HBMEC and whether its expression can be induced and modulated in vitro by the cytokines IFN- $\gamma$  and IFN- $\beta$ .**

#### 4.1.1 Human brain microvessel EC

Human brain microvessel EC in primary culture form confluent contact-inhibiting monolayers composed of elongated, closely associated cells. EC are uniformly positive for Factor VIII R:Antigen, the most specific marker for cells of endothelial origin, and bind the lectin *Ulex europaeus*, a marker for human EC. Cultured HBMEC contain few pinocytotic vesicles and are bound together by tight junctional complexes that restrict the paracellular movement of macromolecules. Primary cultures of HBMEC retain their human EC properties, exhibit morphological and permeability characteristics similar to cerebral endothelium in vivo and, therefore, provide a useful in vitro model for studying the biology and immunopathology of these cells.

#### 4.1.2 Induction of Ia Ag expression on primary cultures of HBMEC

The present studies demonstrate that human recombinant IFN- $\gamma$  induces de novo

expression of class II MHC antigen (Ia Ag) by HBMEC in primary culture in a time and concentration - dependent manner. Unstimulated HBMEC grown under standard culture conditions do not constitutively express Ia Ag as indicated by lack of immunogold staining on light and electron microscopy. Previous *in vivo* immunohistochemical studies have demonstrated absence of Ia Ag expression by EC within the normal human CNS with low levels of reactivity detected in blood vessels of patients with brain neoplasms, abscesses, autoimmune connective tissue disease, cerebral infarcts and in older patients without identifiable CNS lesions (68, 190 - 192). Although the EC used in our studies were isolated from normal brains of several donors with a wide age distribution, expression of Ia Ag was not observed in any of the untreated cultures. A similar lack of constitutive expression of class II molecules has been observed in primary cultures of rat brain endothelium (70), in freshly isolated human umbilical vein EC (HUVEC) (22, 193), in serially passaged cultures of human cerebral vascular EC (136) and HUVEC (194), as well as in human glioblastoma multiforme cells (195), and cultured adult human astrocytes (25) maintained under normal culture conditions. Contrary to these reports, EC of normal guinea pig CNS display surface MHC *in vivo* and *in vitro* (196) and minimal basal expression has been reported in primary cultures of rhesus monkey cerebral endothelium (197), while cultured rat heart vascular EC constitutively express considerably higher levels of Ia Ag (64). It is apparent, from the above studies, that the presence of Ia Ag on normal, unstimulated vascular endothelium may vary among different species and vascular beds.

Previous studies on Ia Ag induction by IFN- $\gamma$  on HUVEC report a rapid increase of

MHC class II mRNA that precedes surface expression by 1 - 2 days and rapidly declines to almost undetectable levels following withdrawal of the cytokine, while surface expression declines slowly after 4 days (80). In HBMEC, removal of IFN- $\gamma$  from the media results in uniform loss, rather than decrease to lower levels, of class II MHC surface expression after 4 days. Rat heart endothelium, however, behaves in a much different way, since withdrawal of IFN- $\gamma$  is not followed by return of the Ia Ag expression to basal levels after 3 days (64).

#### 4.1.3 Surface localization of Ia Ag on HBMEC

Previous immunohistochemical studies on MS and EAE have demonstrated that surface expression of Ia Ag on EC is discontinuous along the microvessel lumen, so that Ia<sup>+</sup> cells are interposed between EC lacking Ia Ag expression (68, 139). A similarly variable expression of Ia Ag was observed in vitro when HBMEC were treated with low concentrations of IFN- $\gamma$  or with higher concentrations for less than 2 days. Taken together with the in vivo studies, these observations may indicate individual cell variation in the regulation of class II MHC molecule expression.

Induction of Ia Ag expression on HBMEC was restricted to the apical portion of the cell membrane. Immunogold particles were not identified on the lateral or basal cell surfaces. Our findings correlate with previous immunohistochemical studies in acute EAE demonstrating Ia expression on the luminal but not abluminal surface of cerebral microvessel EC (139) and with similar observations in a variety of epithelial cells in mice treated with IFN- $\gamma$  (72). Although the mechanisms responsible for the asymmetrical presentation of Ia Ag

on the cell membrane are not known, polarization of expression is probably of functional significance since it would enable circulating T lymphocytes to recognize antigen in association with class II MHC molecules on the luminal surface of the cerebral endothelium and then migrate to sites of inflammation.

#### 4.1.4 Effects of IFN- $\beta$ on Ia Ag expression by HBMEC

Human recombinant IFN- $\beta$  failed to induce expression of Ia Ag on HBMEC at all concentrations tested. A similar lack of Ia Ag expression has been previously reported in cultured adult human astrocytes (25), human dermal microvascular EC (84), and human glioblastoma multiforme cells (26) treated with IFN- $\beta$ . In our studies, the results obtained from the immunocytochemical staining and ELISA indicate that IFN- $\beta$  downregulates the IFN- $\gamma$ -induced Ia Ag expression in a concentration-dependent manner. Immunocytochemical labeling indicates the total number of Ia-positive cells in the cultures, but provides no information on the membrane density of HLA-DR molecules per cell. ELISA provides relative measurement of the total density of HLA-DR molecules within the culture but with no indication of the number of cells expressing Ia Ag. The suppressive effect of IFN- $\beta$  on Ia Ag expression has been previously observed in other EC systems (105, 106). Downregulation of the IFN- $\gamma$  induced Ia Ag expression by IFN- $\beta$  has also been reported in cultured adult human astrocytes (25), human glioma cells (26), murine macrophages (27, 40), blood monocytes isolated from MS patients (28), and in an astrocytoma cell line (41).

#### 4.1.5 Regulatory mechanism of Ia Ag expression

It has been shown that the induction of Ia Ag on macrophages by IFN- $\gamma$  operates at the level of transcription and requires de novo synthesis of a new protein(s) (198). It has been reported that the plateau values of HLA-DR mRNA content in HUVEC and human dermal fibroblasts treated with IFN- $\gamma$  precede maximal surface expression by 1 to 2 days (80). This could explain the lag period of 12 to 24 hours between addition of IFN- $\gamma$  to the media and detection of Ia Ag surface expression by immunohistochemistry on HBMEC (127). Interferons- $\beta$  and  $\gamma$  bind to different receptors on the cell surface (21) and the inhibitory effect of IFN- $\beta$  on IFN- $\gamma$  induction of the Ia Ag genes is exerted at the transcriptional level (41, 75). It has been suggested that there is a complex interplay of trans-acting factors involved in modulating the expression of the Ia genes product and the subsequent expression of their peptide products on the cell surface (41, 75). The fact that IFN- $\beta$  failed to completely inhibit the induction of Ia Ag by IFN- $\gamma$  is not fully understood at the present time; further studies are required in order to elucidate the exact mechanism(s).

#### 4.1.6 Kinetic studies on the modulation of Ia Ag expression by interferons $\gamma$ and $\beta$

In our studies, the most significant downregulation of the IFN- $\gamma$  induced Ia Ag expression was found when HBMEC were either coincubated with the two cytokines for 4 days or pretreated with IFN- $\beta$  for 2 days and then treated with a combination of IFN- $\beta$  and  $\gamma$  for 4 days (approximately 80% reduction). In contrast, significant decrease in Ia Ag expression was not observed (0% to 15% suppression) when EC were pretreated with IFN- $\beta$

and  $\gamma$  for 2 days, followed by another 4 day treatment with IFN- $\gamma$ , or pretreated for 2 days with IFN- $\gamma$  followed by coincubation with IFN- $\beta$  and  $\gamma$  for another 4 days. Similar observations have been reported in cultured adult human astrocytes. The addition of IFN- $\alpha$  or  $\beta$  24 hours after incubation of astrocytic cultures with IFN- $\gamma$  did not significantly alter HLA-DR expression, while IFN- $\alpha$  or  $\beta$  added 24 hours before or at the initiation of incubation with suboptimal concentrations of IFN- $\gamma$  reduced the extent of HLA-DR expression (25). Further work using human astrocytoma cell lines demonstrated that the suppressive effect of IFN- $\beta$  on the HLA-DR induction by IFN- $\gamma$  was relatively gene-specific since IFN- $\beta$  could not impair the induction of intercellular adhesion molecule-1 (ICAM-1) expression by IFN- $\gamma$  in these cell lines (41). Similar results were observed in HDMEC, and the authors speculated that the effect of IFN- $\gamma$  on HDMEC may be mediated through multiple distinct pathways which can be independently regulated (106). Consequently, the results could not be explained by IFN- $\beta$  downregulation of IFN- $\gamma$  receptors or defective receptor-linked signal transduction. The inhibition was also suggested to be tissue-specific because IFN- $\beta$  did not antagonize IFN- $\gamma$  induction of HLA-DR expression in human monocytes (41). The results of the present studies indicate that in order to effectively suppress the induction of Ia Ag by IFN- $\gamma$  in vitro, IFN- $\beta$  must be present continuously in the culture media. It is also shown that once the cells have been activated by IFN- $\gamma$ , downregulation of Ia Ag expression does not occur in the continued presence of IFN- $\beta$  in the culture media. Taking into consideration that increased levels of Ia Ag have been associated with induction of autoimmune disorders of the CNS such as MS (68, 199), and that antibody blocking directed against class II MHC determinants can prevent the

induction of experimental autoimmune disease (200), these findings may partly explain the significant therapeutic potential of IFN- $\beta$  in MS (281). Inaba et al. have shown that there is a correlation between downregulation of Ia Ag expression and reduced levels of antigen presentation by macrophages in vitro (27). Together with the finding that IFN- $\gamma$  is unsuitable for use as a therapeutic agent in MS (15), Joseph et al. suggested that administration of IFN- $\beta$  in patients with MS could have beneficial effects if reduced Ia Ag expression occurs, and there is reduced antigen presentation in the CNS (26). The expected results would be longer remission periods or fewer relapses in MS patients. Therapeutic application of recombinant interferon beta-1b for the treatment of MS has recently reported that the cytokine is well tolerated and has a beneficial effect on the course of relapsing-remitting MS (281). Based on the results obtained from our studies on HBMEC and others (26 - 28, 40), a repetitive dosing with IFN- $\beta$  may be essential to effectively downregulate Ia Ag expression.

#### 4.2 EFFECTS OF INTERFERONS $\gamma$ AND $\beta$ ON THE MORPHOLOGICAL PHENOTYPE AND GROWTH OF HBMEC, ORGANIZATION OF THE MONOLAYERS AND PERMEABILITY TO MACROMOLECULES

**The second specific aim of this thesis was to determine whether IFN- $\gamma$  and IFN- $\beta$  exert antiproliferative effects on HBMEC and whether treatment with these cytokines can modulate the morphological phenotype and organization of the EC cultures, and alter the permeability of the monolayers to macromolecules.**

#### 4.2.1 Effects of IFN- $\gamma$ and IFN- $\beta$ on HBMEC growth

The anti-proliferative effect of IFN- $\gamma$  on primary cultures of HBMEC correlates with previous studies demonstrating inhibition of cell growth by IFN- $\gamma$  induced on extracerebral large and small vessel endothelial cultures in a dose-dependent manner (84, 126, 201, 202) and possibly through modulation of the EC growth factor receptors (202). Lower concentrations of IFN- $\gamma$  (10 - 100 U/ml), however, appear to have a stimulating effect on cultured HUVEC both in the absence and presence of EC growth factor (203). In addition, IFN- $\gamma$  significantly inhibits formation of endothelial tubular structures in in vitro models of angiogenesis (204, 205).

When the cells were treated with IFN- $\beta$  or a combination of IFN- $\beta$  and  $\gamma$ , significant growth inhibition was detected. The antiproliferative effects of IFN- $\gamma$  and especially of IFN- $\beta$  on primary cultures of HBMEC correlate with previous studies demonstrating inhibition of cell growth by these cytokines induced on human dermal microvascular EC (HDMEC) (84), human glioblastoma multiforme cells (195), cultured human brain tumors (206), and human vascular smooth muscle cells in vitro (207).

#### 4.2.2 Effects of interferons $\gamma$ and $\beta$ on HBMEC morphology and organization of the EC monolayers

IFN- $\gamma$ -treated EC undergo unique changes in their morphology and organization, which are associated with a considerable increase in the permeability of confluent cultures to macromolecules. Treatment of HBMEC with IFN- $\gamma$  induces marked elongation of EC, prominent overlapping and frequent arrangement in a whorled pattern. A similar alteration of

the morphological phenotype and monolayer organization has been previously reported in cultures of HUVEC (126, 202) and HDMEC (84) treated with IFN- $\gamma$  for 3 to 4 days and has been shown to be associated with reorganization of the cytoskeletal filaments and considerable loss of the fibronectin matrix (126).

It has been previously demonstrated that IFN- $\beta$  alters the morphology of cultured HDMEC. IFN- $\beta$  treated cells become spindle - shaped, an alteration which was also observed in cultures treated with IFN- $\gamma$  in comparison to untreated cells that showed the typical morphology of human EC (84). In contrast, morphologic changes were not observed in HUVEC treated with IFN- $\beta$  (126). Furthermore, treatment of HBMEC with IFN- $\beta$  failed to induce structural or organizational alterations on the monolayers; in fact, it inhibited the morphological changes induced by IFN- $\gamma$  when the cells were incubated simultaneously with a combination of IFN- $\beta$  and  $\gamma$ . These observations further emphasize the heterogeneity which exists between EC derived from different organs or species (19).

Our studies, therefore, demonstrate that IFN- $\beta$  downregulates the expression of Ia Ag induced by IFN- $\gamma$  on HBMEC and alone or in combination with IFN- $\gamma$  has greater antiproliferative effect on these cells than IFN- $\gamma$ . In addition, IFN- $\beta$  downmodulates the IFN- $\gamma$ -mediated changes in cell morphology and organization of the EC monolayer which may be relevant to the in vivo immune response. These findings and the work of other investigators would indicate that in situ vascular changes take place in response to cytokines generated at the inflammatory site. Thus, IFN- $\gamma$  alone or in combination with other locally generated cytokines, induces changes that may mimick immune regulatory events which signal

endothelial preparation for inflammatory cells to adhere and transmigrate, while IFN- $\beta$  may play a negative regulatory role in inflammation or disorders upmodulated by enhanced IFN- $\gamma$  secretion. In fact, it has been reported that systemic administration of IFN- $\beta$  to MS patients inhibits endogenous IFN- $\gamma$  synthesis in their peripheral blood mononuclear cells (38). At the present time, it is not known whether cerebral EC in vivo undergo the same or a similar spectrum of changes in response to cytokines in inflammatory foci of the human CNS.

#### 4.2.3 Permeability of IFN- $\gamma$ treated HBMEC monolayers to macromolecules

Human cerebral microvessel EC in primary culture are bound together by tight junctions and have a paucity of cytoplasmic vesicles, two important morphological characteristics of their in vivo counterparts (107, 186). Under standard culture conditions, the great majority of interendothelial junctions restrict the passage of HRP. In cultures incubated with IFN- $\gamma$ , an increase in the permeability of the monolayers was observed that coincided temporally with changes in morphology and rearrangement of the cells. The number of labeled cytoplasmic vesicles was not increased in IFN- $\gamma$  treated monolayers indicating that increased junctional permeability is primarily responsible for the permeability changes of the monolayers. The mechanism(s) responsible for the increased junctional permeability are not known at present. Recent in vitro studies have demonstrated that tumor necrosis factor (TNF)-treated aortic EC cultures undergo prominent cytoskeletal changes similar to those induced by IFN- $\gamma$  alone or in combination with TNF, which are temporally related to increase in the permeability of the monolayers to macromolecules and are regulated by G protein (208). The

fact that leakiness of intercellular contacts appears concomitantly with the morphological changes of the endothelium following IFN- $\gamma$  treatment may indicate that physiologically "tight" tight junctional complexes fail to form during the extensive rearrangement of the cells and their cytoskeleton. However, other mechanisms, such as modulation of regulatory proteins or cell surface molecules by IFN- $\gamma$  cannot be excluded. Disruption of the BBB has been previously described as an early and critical event in the evolution of EAE (119, 120, 209, 210). Recent electron microscopic studies indicate that increased junctional permeability as well as increased interendothelial space and migration of inflammatory cells are primarily responsible for the increased permeability of the BBB to macromolecules in this disease (211). The functional significance of the in vitro morphological and permeability changes of HBMEC, observed in this study, is presently unknown. If, however, similar changes are induced in situ on cerebral EC by cytokines released locally by activated T-lymphocytes, they would provide an additional mechanism for the opening of the BBB and could facilitate the transmigration of inflammatory cells from blood into brain across the endothelial barrier.

#### **4.3 SIGNIFICANCE OF Ia Ag EXPRESSION BY HBMEC**

Expression of Ia Ag in situ by cerebral vascular endothelium has been previously demonstrated in autoimmune demyelinating CNS disorders. Thus, class II MHC molecules have been localized on the surface of EC lining microvessels at the edge of demyelinating plaques as well as within the adjacent white matter in acute, active and silent chronic MS lesions (68, 138). The presence of Ia positive EC has also been documented in acute EAE

(139, 140), while expression of Ia Ag by cerebral endothelium in chronic relapsing EAE appears to coincide with the appearance of inflammatory cell infiltrates and diminishes when inflammation subsides (141). In addition, murine cerebral EC isolated from SJL mice with EAE are able to present antigen to sensitized syngeneic lymph node cells following incubation with IFN- $\gamma$  in vitro (137). Contrary to these observations, cultured rat brain EC are not effective at stimulating T-cell division and therefore, have not been considered important as antigen presenting cells (212). Recent studies using murine endothelial and fibroblast cell lines to determine their capabilities in presenting antigen to helper T cells have reported the necessary requirements for costimulatory signals (213 - 216). The lack of signals such as B7, CTLA4 molecules on the surface of the potential antigen presenting cells can result in the inability of T helper cells to proliferate in response to a specific antigen. Consequently, the conclusions drawn by Pryce et al. (212) that rat brain EC are not important antigen presenting cells, prior to the realization that costimulatory signals may be required for the efficient function of antigen presenting cells, deserve further investigation. The present work demonstrates that class II MHC molecules are not detectable on intact HBMEC isolated and cultured from normal human brain microvessels by the methods employed in our study, but can be specifically induced in vitro by human recombinant IFN- $\gamma$  in association with prominent alterations in the morphology, organization and permeability of the monolayers to macromolecules. Although the ability to present antigen by HBMEC has yet to be unequivocally proven, our findings indicate a possibly important role of the human cerebral endothelium in lymphocyte-endothelial interactions, lymphocyte recruitment and alteration of

blood-brain barrier permeability in immune - mediated CNS inflammation.

#### 4.4 **ADHESION OF RESTING AND ANTI-CD3 STIMULATED LYMPHOCYTES TO UNTREATED, IFN- $\gamma$ and/or IFN- $\beta$ TREATED HBMEC**

**The third specific aim of this thesis was to examine the effects of cytokine treatment of HBMEC on the adhesion of resting and anti-CD3 stimulated lymphocytes to the endothelium.**

##### 4.4.1 Activation of lymphocytes

The CD3-molecular complex is comprised of a series of noncovalently linked polypeptides (217). Monoclonal antibodies directed against the CD3 molecules have been widely used to study T cell activation (218, 219). The binding of anti-CD3 antibodies to T cells leads to the rapid hydrolysis of phosphatidylinositols and results in an increase in free intracellular calcium concentration, in generation of diacylglycerol, and activation of protein kinase C (220, 221). It is notable that binding of mAbs to CD3 molecules clearly results in the generation of activation signals (220), but this situation has been reported to be insufficient to initiate T cell proliferation (222). Moreover, Ledbetter et al. (223) have demonstrated that binding of anti-CD3 antibody to T cells results in a rapid rise (4 to 6 fold) in cyclic adenosine monophosphate (cAMP), and high levels of cAMP are known to inhibit T cell growth. It has also been shown that other cAMP-elevating agents such as prostaglandin E<sub>2</sub>, cholera toxin,

and the cell-permeable analog 8-bromo-cAMP can inhibit nuclear IL-2 transcription and decrease the stability of IL-2 mRNA (224, 225). Interestingly, other studies have shown that T cells proliferate in response to soluble anti-CD3 mAb in the presence of IL-2, a lymphokine central to the mediation of antigen-activated T cell proliferation. IL-2 is produced by activated T cells, and binds to the IL-2 receptor of secreting T cells and other antigen-stimulated cells (226). Since the expression of IL-2 receptor is reported to be increased when T lymphocytes are treated with anti-CD3 antibody (227, 228), activation of peripheral blood lymphocytes with anti-CD3 mAb was confirmed in this study by the upregulation of IL-2 receptor rather than by the conventional tritiated thymidine uptake assay. The results obtained by Fluorocytometry demonstrated more than 2 fold increase in IL-2R expression. By SEM, lymphocytes treated with CD3 mAb appeared larger than resting T cells and their surface membranes exhibited a ruffled appearance in contrast to the smooth membrane of resting T cells, confirming their activated state. Moreover, transmission EM studies showed numerous cytoplasmic folds and finger-like projections at the surface of activated lymphocytes along with a significant number of vacuoles in the cell cytoplasm. Subsequently, anti-CD3 activated T cells are functionally and morphologically different from resting T lymphocytes.

#### 4.4.2 Adhesion of resting lymphocytes to untreated, IFN- $\gamma$ and/or IFN- $\beta$ treated HBMEC

The present studies demonstrate that lymphocyte adhesion to cultured HBMEC can be modulated by treatment of the EC with IFN- $\gamma$  and/or IFN- $\beta$ . A low basal level of adhesion between resting T cells and untreated EC was detected. Pretreatment of EC with an optimal

concentration of IFN- $\gamma$  (150 U/ml) known to induce Ia Ag expression (127), significantly augmented lymphocyte-EC adhesion. Scanning EM studies demonstrated that a small number of resting lymphocytes, with relatively smooth surface membranes, adhered to confluent monolayers of untreated HBMEC. The lymphocytes lined up on the borders between adjacent EC, and occasionally adhered to the apical surface of the endothelium. Significant increase in adhesion of resting lymphocytes to IFN- $\gamma$ -treated EC was noted by light microscopy and SEM. By SEM, increased numbers of resting T cells were detected along the overlapping processes of IFN- $\gamma$ -treated EC. The results suggest that the changes in the organization of the monolayers induced by IFN- $\gamma$  may further facilitate lymphocyte migration across these EC. Previous studies on HUVEC (23, 134), rat retinal endothelium (156), and rat (229) and mouse brain EC (135) have also demonstrated IFN- $\gamma$ -mediated increase in lymphocyte-endothelial adhesion. Moreover, it has been shown that treatment of rat brain endothelium with cycloheximide, an inhibitor of protein synthesis, inhibits the IFN- $\gamma$ -mediated increase in adhesion, implying the requirement for new protein synthesis (154). It is notable that the optimal concentration of IFN- $\gamma$  required for maximal adhesive response varies with different species of EC. Our results, therefore, provide additional evidence for the existence of heterogeneity among EC of different organs or species with regard to cytokine responses. The adhesion of lymphocytes to mouse and rat brain EC has also been reported to increase with the length of IFN- $\gamma$  treatment (from 4 hours to 2 days) when compared with the controls (135, 154), suggesting that different adhesion molecules with different kinetics of induction may participate in the lymphocyte-EC adhesive mechanisms over different time periods.

HBMEC treated for 3 days with IFN- $\beta$  (2,000 U/ml) showed no increase in lymphocyte adhesion as compared with the baseline of adhesion in untreated control. Moreover, IFN- $\beta$  actually suppressed the increase in adhesion induced by IFN- $\gamma$  when brain EC were treated with a combination of IFN- $\gamma$  and IFN- $\beta$ . This observation indicates a potentially important role of IFN- $\beta$  in downregulating immune responses mediated, at least partly, by IFN- $\gamma$ .

The mAb blocking studies indicate that de novo expression of class II MHC Ag by HBMEC is largely responsible for the increased T lymphocyte-EC adhesion. Similar results have been reported in mouse brain EC (135). These investigators further confirmed their observations by transfecting a murine lung EC line with cDNA for the class II MHC molecules in order to demonstrate the role of Ia Ag in lymphocyte-EC adhesion. The adhesive role of EC is totally distinct from any antigen presenting function, as the lymphocytes are non-activated and there is no antigen present in either system (135). It is notable that complete suppression of IFN- $\gamma$ -enhanced adhesion by anti-human HLA-DR antibody was not achieved, indicating that other mechanisms, not related to DR antigens, operate during lymphocyte-EC binding. MAb blocking studies in HUVEC have also reported similar observations (134). Working with retinal capillary EC, Liversidge et al. (230) have suggested that, if several adhesion pathways are available for cellular interactions, then mAbs blocking one pathway may be ineffective in completely reducing the number of cells bound, since alternative ligands would be utilized. MAb blocking studies with anti-human IFN- $\gamma$  indicate that the increase in adhesion observed with resting T cells is specifically mediated by IFN- $\gamma$ .

The results of the present study provide evidence that IFN- $\beta$ , used at a concentration known to significantly suppress the IFN- $\gamma$ -induced Ia Ag expression (2,000 U/ml), can downregulate the increase in adhesion mediated by IFN- $\gamma$ . Taken with the IFN- $\beta$  effects on the IFN- $\gamma$  induced Ia Ag expression, these results suggest that the IFN- $\beta$  suppression of the IFN- $\gamma$ -mediated increase in adhesion may be largely due to the downregulation of Class II MHC molecules by IFN- $\beta$ .

The role of class II MHC molecules in antigen presentation has been well documented (137); however, the role of class II MHC molecules in lymphocyte-EC adhesion remains controversial. Curtis (231) was the first to suggest that class II MHC molecules may function in the adhesion of non-activated lymphocytes to endothelium and, together with Rooney (232), they state that these molecules may also participate in contact inhibition between epithelial cells, a process which partially involves cell adhesion. Doyle and Strominger report that B lymphocytes expressing class II MHC molecules could bind to CD4 transfected fibroblasts in vitro and speculate that the interaction between these two molecules would cause cell-cell adhesion independently of antigen presentation (147). They also suggest that at more physiological levels of expression, it is possible that CD4 molecules and class II antigens help to mediate low affinity, transient interactions among lymphocytes, and together with other specific and accessory adhesion molecules, functional cell-cell interactions can take place (147). Studies with HUVEC systems have also shown that HLA-DR molecules play an important role in IFN- $\gamma$ -mediated HUVEC-lymphocyte adhesion (134). Furthermore, mAb blocking experiments implicate CD4-class II MHC interaction in IFN- $\gamma$ -induced endothelial-

lymphocyte adhesion (145, 233). Interestingly, there is no significant difference in the adhesion between autologous and allogeneic assays which suggests that the interaction is not simply alloreactive, but may be part of a physiological mechanism for the adhesion, migration and accumulation of lymphocytes at sites of chronic inflammation (145). It has also been demonstrated that experimental allergic encephalomyelitis (EAE), a model disease for MS in vivo, can be prevented by administration of monoclonal antibodies to class II molecules (234). Alteration in the homing of lymphocytes to the brain in EAE has been implicated as the possible mechanism for the prevention of disease development in anti-Ia antibody treatment (235). Finally, Ia Ag expression on EC in EAE has been shown to precede lymphocyte infiltration (66). Taken together, these results suggest an important role for class II MHC molecules in the interactions between lymphocytes and cerebral EC and in the development of the disease process.

The adhesion of circulating lymphocytes to brain EC in vivo takes place in a dynamic rather than in a static system. Furthermore, the adhesive capacity of Ia Ag in situ would be of a much lower affinity than observed in vitro, since the concentration of IFN- $\gamma$  and the subsequent level of Ia Ag expression on individual EC and its distribution would probably be lower. Nevertheless, if under the influence of focally increased concentrations of IFN- $\gamma$  in the cerebral microvessel microenvironment, a minimal level of initial adhesion could take place via class II MHC molecules, followed by antigen presentation to specific T cells, leading to the production of more cytokines including IFN- $\gamma$ , class II MHC expression can then be elevated and subsequently, enhance lymphocyte-EC adhesion. Working with HUVEC,

Masuyama and his coworkers (134) have suggested that T cell recognition of HLA-DR molecules may be the signal for the initiation of subsequent adhesive processes in which complementary adhesion surface molecules become engaged. McCarron et al. (236) have further speculated that the CNS-immune cell interactions may be responsible for localized alterations in the BBB permeability, resulting in the subsequent influx of non-specific inflammatory cells. In addition, the IFN- $\gamma$ -induced changes in EC morphology and monolayer permeability, observed in our studies, may further facilitate the movement of lymphocytes across the BBB.

#### 4.4.3 Adhesion of activated lymphocytes to untreated, IFN- $\gamma$ and/or IFN- $\beta$ treated HBMEC

Lymphocyte activation results in great increase in adhesion of activated T cells to untreated HBMEC, indicating that the activation status of the lymphocytes plays an important role in lymphocyte-EC adhesion. The adhesive interaction is further augmented by treating the EC with IFN- $\gamma$ . Studies with HUVEC (150), human (230) and rat retinal EC (156), rat aortic and brain microvascular endothelia (154, 155) and activated lymphocytes have also reported significant increase in lymphocyte-EC adhesion. These studies have shown that the adhesion between lymphocytes and EC is dependent on the state of cell activation: maximal level of adhesion occurs when activated T cells interact with cytokine-stimulated EC. Scanning EM studies further confirm the light microscopic observations. Activated lymphocytes preferentially adhere at the borders between adjacent and overlapping EC. MAb blocking studies with anti-human IFN- $\gamma$  indicate that the enhanced adhesion of activated

lymphocytes to IFN- $\gamma$ -treated EC is specifically mediated by IFN- $\gamma$ . It has been reported that irrespective of the state of cell activation, the level of lymphocyte adhesion to CNS-derived endothelium is generally lower than that reported for extracerebral large and small vessel EC (154 - 156, 237, 238). Subsequently, this low level of adhesion may account for the limited lymphocyte traffic through the CNS of normal healthy individuals. Furthermore, it is notable that irrespective of the mode of lymphocyte activation (150, 154 - 158, 230) (i.e. ConA, Phorbol ester, Phytohaemagglutinin, anti-CD3 antibody), adhesion of activated lymphocytes to EC is significantly upregulated in comparison to that of resting T cells.

Significant increase in adhesion of anti-CD3 activated T cells to intercellular adhesion molecule-1 (ICAM-1) substrates has been previously reported (159). ICAM-1 is a member of the immunoglobulin gene superfamily; it is expressed constitutively by HBMEC and can be upregulated by various cytokines such as IFN- $\gamma$ , TNF- $\alpha$  and IL-1 $\beta$  (239). Its counter receptor is the lymphocyte function-associated antigen-1 (LFA-1) which belongs to the integrin family; LFA-1 is expressed on T lymphocytes, not EC, and comprised of heterodimeric, divalent cation-dependent adhesion molecules (162). MAb blocking experiments directed against ICAM-1 and the  $\alpha$  and  $\beta$  subunits of LFA-1 molecules completely block the anti-CD3 stimulated adhesion to purified ICAM-1 (159). Since there is no significant change in LFA-1 expression by T cells treated with anti-CD3 antibody versus resting lymphocytes, the authors conclude that the stimulated increase in T-cell adhesion seems to be due mainly to an increase in LFA-1 avidity (159). Fluorescence-activated cell sorter (FACS) studies with mAbs directed against both  $\alpha$  and  $\beta$  subunits of LFA-1 molecules on the adhesion of resting or stimulated T

cells to HUVEC have also shown that the increased adhesion of stimulated lymphocytes to EC is possibly due to the altered function, not increase in expression, of the LFA-1 molecules (240).

The binding of anti-CD3 antibodies to T cells triggers phosphatidylinositol turnover and elevates cytoplasmic  $\text{Ca}^{2+}$  (220, 221). It has been demonstrated in rat cerebral and aortic endothelia that the removal of  $\text{Ca}^{2+}$  from the media can effectively inhibit lymphocyte-EC adhesion (155). Interestingly, earlier work indicates that a  $\text{Ca}^{2+}$ -dependent epitope on LFA-1, termed L16, is a prerequisite for LFA-1 to mediate cell adhesion and may distinguish resting lymphocytes from activated lymphocytes (241). Subsequently, it has been shown that L16 epitope is expressed when the lymphocytes are stimulated by phorbol ester or T cell receptor/CD3 (TCR/CD3) complex. It has been suggested that there are possibly 3 distinct forms of LFA-1: a) an inactive form, partially exposed epitope, is present on resting T cells, b) an intermediate one can be found on mature or previously activated cells, and finally, c) an active epitope, capable of high affinity ligand binding, can be demonstrated after TCR/CD3 or phorbol ester activation (241). Studies with human retinal pigment epithelial cells have demonstrated that these cells constitutively express high levels of ICAM-1, and these molecules are functional in binding activated T lymphocytes but not resting T cells (230). LFA-1-dependent pathway has been implicated in the increased adhesion of activated lymphocytes to vascular endothelium such as high EC (HEC) and HUVEC (151, 158, 240). Therefore, these results suggest that LFA-1/ICAM-1 interactions may also play a significant role in the increased binding between anti-CD3 activated T cells and untreated HBMEC

observed in this study.

Total inhibition of binding by monoclonal antibodies directed against LFA-1 molecules has not been observed (151, 240). Approximately 20% to 40% of adhesion between several T cell leukemia cell lines and HUVEC can not be suppressed by blocking with anti-LFA-1 and anti-VLA-4 antibodies (242). In fact, these observations are in accordance with other studies indicating that there are at least three to four other mechanisms or pathways controlling lymphocyte-EC adhesion (243, 244). Studies on adhesion of activated T cell leukemia cell lines to HUVEC have suggested that the LFA-1 adhesive mechanism dominates the interaction; however, very late antigen-4 (VLA-4) is used by T lymphocytes to bind EC when LFA-1 is not expressed or not functional to mediate adhesion (242), pointing to a selective use of different adhesion receptors by the T cells. In contrast, resting lymphocytes use both LFA-1 and VLA-4 adhesion pathways (242). Like LFA-1, VLA-4 also belongs to the integrin family of cell surface heterodimers; it is expressed by lymphocytes and can interact with vascular cell adhesion molecule-1 (VCAM-1) (245). VCAM-1 is a member of the immunoglobulin superfamily like ICAM-1 (246); however, VCAM-1 is not expressed by peripheral blood lymphocytes (247, 248). Primary cultures of HBMEC have been shown to express low levels of VCAM-1 constitutively (249). Blocking experiments with mAbs directed against LFA-1, ICAM-1, VLA-4, and VCAM-1 molecules on the adhesion of resting T cells to untreated/activated HUVEC have demonstrated that the VLA-4/VCAM-1 adhesive mechanism is largely responsible for the adhesion of T lymphocytes to cytokine-treated EC, while LFA-1/ICAM-1 pathway mediates much of the binding of T cells to unstimulated EC.

Furthermore, the binding of activated lymphocytes is not blocked by antibodies to VLA-4 or VCAM-1, irrespective of the activation status of the EC. However, antibodies to LFA-1 or ICAM-1 can modestly inhibit the adhesion of activated T cells to HUVEC. It is notable that complete inhibition of T cell-EC interactions by these antibodies has never been detected (152). Other studies with high EC and rat cerebral EC have also indicated that VLA-4/VCAM-1 mechanisms do participate in lymphocyte-EC adhesion (158, 250). Finally, the participation of other pathways besides the LFA-1/ICAM-1 system in the T cell - EC binding has been examined using LFA-1-deficient T cell clones generated from a patient with leukocyte adhesion deficiency. The results of these experiments confirm previous observations by Dustin et al. (243) and Shimizu et al. (244) stating that there are other pathways mediating lymphocyte-EC adhesion in addition to LFA-1/ICAM-1 mechanism. In fact, VLA-4/VCAM-1 represent the alternate receptor/ligand pairs which mediate the binding of LFA-1-deficient T cells to HUVEC (153).

Treatment of HBMEC with IFN- $\gamma$  and IFN- $\beta$  further modulates the anti-CD3 stimulated T lymphocyte-EC interactions. Activation of HBMEC with an optimal concentration of IFN- $\gamma$  (150 U/ml), known to induce maximal Ia Ag expression and markedly upregulate the binding of resting T cells to EC, results in a 2 fold increase in adhesion of activated lymphocytes to cytokine treated brain EC. Further enhancement of lymphocyte-EC interactions when both systems are activated has been reported with rat retinal (156), aortic (155) and brain endothelia (154), and also HUVEC (150). Interestingly, the level of adhesion between activated T cells and IFN- $\beta$  treated HBMEC is comparable to that of untreated EC,

indicating that IFN- $\beta$  alone has no influence on adhesion. Moreover, a combined treatment of human brain EC with IFN- $\gamma$  and IFN- $\beta$  in the present studies, demonstrated that IFN- $\beta$  actually inhibits the IFN- $\gamma$ -mediated binding. These observations further support the negative regulatory role of IFN- $\beta$  on changes induced by IFN- $\gamma$ . The IFN- $\gamma$ -mediated increase in adhesion of activated lymphocytes to HBMEC can also be suppressed by mAbs directed against human HLA-DR. In addition, blocking studies with anti-human IFN- $\gamma$  indicate that IFN- $\gamma$  is responsible for the increased adhesion between activated T cells and IFN- $\gamma$ -treated HBMEC most likely through induction of class II molecule expression by HBMEC. These results indicate that class II MHC molecules play a central role in mediating the increased adhesion of activated T cells to IFN- $\gamma$ -treated HBMEC. The fact that IFN- $\beta$  suppresses the IFN- $\gamma$ -induced Ia Ag expression on HBMEC also suggests that IFN- $\beta$  downregulates the IFN- $\gamma$ -mediated binding via the Ia Ag mechanism, which is further supported by the results obtained from mAb blocking experiments. In this respect, IFN- $\beta$  downmodulates the IFN- $\gamma$  induced increased binding between T lymphocytes and HBMEC regardless of the activation status of the lymphocytes. Studies on lymphocyte-EC binding with mAbs directed against  $\alpha$  and  $\beta$  subunits of LFA-1 molecules have demonstrated significant inhibition of binding between resting or stimulated T cells to untreated HUVEC; however, these antibodies have no influence on the adhesion of lymphocytes to cytokine-treated EC (240). These authors have suggested that the mechanism of binding of T cells to unstimulated endothelia differs from that to stimulated endothelia, and the latter appears to be independent of LFA-1. Male et al. have also indicated in their work with rat cerebral EC that the control of basal binding and

binding to activated endothelia are regulated by different mechanisms. This system would allow brain endothelium to have low basal binding to minimize lymphocyte traffic into the brain normally, while permitting rapid increase in traffic if the cerebral EC are stimulated appropriately (155).

#### **4.5 MIGRATION OF RESTING and ANTI-CD3 STIMULATED LYMPHOCYTES ACROSS UNTREATED, and CYTOKINE TREATED HBMEC**

**The fourth specific aim of this thesis was to determine whether migration of resting and anti-CD3 stimulated lymphocytes across cerebral endothelium can be influenced by treatment of HBMEC with interferons  $\gamma$  and/or  $\beta$ .**

##### 4.5.1 Migration of resting lymphocytes across untreated, IFN- $\gamma$ and/or IFN- $\beta$ treated HBMEC monolayers

If the low basal level of migration of resting T lymphocytes across untreated HBMEC monolayers in vitro reflects the limited lymphocyte traffic into the CNS in vivo, it would contribute to the relative immunological isolation of the brain under normal physiological conditions. As observed with adhesion, migration of resting lymphocytes was also regulated by cytokine treatment of the cerebral endothelium in this study. Treatment of HBMEC with IFN- $\gamma$  results in a 3 fold increase in migration compared to that of untreated EC, suggesting that IFN- $\gamma$  enhances the migration of T cells across the EC monolayers possibly by a direct

action on the endothelium. Light microscopic and TEM studies demonstrate large numbers of migrated lymphocytes underneath the monolayers of HBMEC previously treated with IFN- $\gamma$ , while fewer lymphocytes crossed untreated EC. Migration of resting T cells is not associated with damage to the integrity of the monolayers in either untreated or IFN- $\gamma$  treated monolayer. Lymphocyte migration usually takes place between adjacent EC. Migration through the cytoplasm of EC is a less common route of migration across the monolayers. IFN- $\gamma$  has been previously reported to significantly upregulate the migration of lymphocytes across HUVEC (24) and rat retinal EC (170). Oppenheimer-Marks and Ziff (24) observed that the augmenting effect of IFN- $\gamma$  on lymphocyte transendothelial migration is not dependent on the presence of an exogenously added chemotactic factor below the EC monolayer. Using passaged cultures of rat cerebral EC, Male et al. (251) demonstrated that the activation status of the endothelium has no influence on the migration of activated T cells, however, they observed that the brain-specific surface phenotype of the cultured cells deteriorated after the first passage (251). Our studies, therefore, indicate that IFN- $\gamma$  upmodulates both adhesion and migration of resting T cells across the cerebral endothelial barrier. Whether the level of lymphocyte migration in the brain is a reflection of the level of lymphocyte-EC adhesion or the two events are pathophysiologically different and under the control of distinct influences by IFNs and/or other cytokines remains to be further investigated.

The level of migration of resting T cells across IFN- $\beta$  treated HBMEC is comparable to that of untreated endothelia, indicating that IFN- $\beta$  has no direct effect on lymphocyte migration. Treatment of HBMEC with a combination of IFN- $\gamma$  and IFN- $\beta$  results in significant

suppression of the IFN- $\gamma$ -mediated increased migration which further supports the downregulatory role of IFN- $\beta$ .

#### 4.5.2 Migration of anti-CD3 stimulated lymphocytes across untreated, IFN- $\gamma$ and/or IFN- $\beta$ treated HBMEC monolayers

In this study, nonspecific stimulation of T lymphocytes with anti-CD3 generates a significant increase in migration across untreated monolayers of HBMEC as compared to the migration of resting lymphocytes across untreated EC. In accordance with the observations on resting T cells, the level of stimulated lymphocyte traffic in the CNS most likely reflects the level of adhesion of activated T cells to HBMEC: the rate of increase of lymphocyte migration is comparable to that of adhesion. It has been previously demonstrated that lymphocyte activation induces three to four fold increase in migration across HUVEC in vitro when compared to resting T cells (151). MAb blocking studies directed against various adhesion molecules and their ligands including LFA-1, ICAM-1, VLA-4 and VCAM-1 have reported that the LFA-1/ICAM-1 interaction plays an important role in transendothelial migration of activated lymphocytes through HUVEC (151, 152). In contrast, VCAM-1 has thus far not been found to be utilized during the migration process, regardless of the activation status of the T cells or EC (152). Migration of activated T cells is not entirely blocked by mAbs to LFA-1 and ICAM-1, indicating that additional surface molecules are required for transendothelial migration (151, 152). Furthermore, studies on patients with LFA-1 deficient leukocytes have shown the presence of lymphocytes in inflammatory lesions of these patients, indicating that

lymphocyte migration into inflammatory foci is not entirely dependent upon the expression of LFA-1 molecules (252). The fact that migration of activated lymphocytes across untreated HBMEC is significantly greater than that of resting T cells through IFN- $\gamma$  treated cultures, indicates that antigen-nonspecific stimulation of lymphocytes plays a critical role in their emigration from the blood into the perivascular tissue. In vivo observations in the rat have reported that activated lymphocytes can rapidly enter into the CNS tissue once they are introduced into the circulation, irrespective of antigen specificity, MHC compatibility, T-cell phenotype or T-cell receptor gene usage (161). Furthermore, it has been shown that activated lymphocytes can increase the levels of the enzyme heparan sulfate endoglycosidase (253), and substances that inhibit this enzymatic activity can prevent the development of EAE which is dependent upon T-cell entry into the CNS (254). These features may play some role in the migration of activated T cells, however, other mechanisms may also participate in this migratory process.

Immunohistochemical studies on the migration of T cells across HUVEC cultures have shown the presence of ICAM-1 along the intercellular contacts between EC that are in contact with the migrating lymphocytes as well as on the basal membrane of the EC. The presence of ICAM-1 molecules at these sites as well as at sites of contact between the EC membrane and the leading edge of migrating T cells suggests a critical role of ICAM-1 in transendothelial migration of T cells. The authors conclude that, as the T cells migrate across the EC layer, migration proceeds by the successive formation of adhesive bonds between receptors on T lymphocytes and their counter-receptors on EC, like a "zipper" mechanism

(152). Recent studies have demonstrated that primary cultures of HBMEC express relatively high levels of ICAM-1 (up to 40%) constitutively (239). As discussed previously, activation of lymphocytes may lead to an increase in avidity of LFA-1 molecules present on the T cells (159) which can further enhance the interaction of LFA-1 to its counter receptor, ICAM-1. MAb blocking studies directed against LFA-1 molecules have found that migration of resting T cells across HUVEC is not inhibited, while migration of activated T lymphocytes can be suppressed to a comparable level with resting T cells (151). Subsequently, the LFA-1/ICAM-1 dependent pathway may play a central role in the marked increase in migration of anti-CD3 stimulated lymphocytes across untreated HBMEC.

Studies on platelet/EC adhesion molecule 1 (PECAM-1) have recently indicated that this molecule may also play an important role in transendothelial migration of leukocytes (255). PECAM-1 is a member of the immunoglobulin gene superfamily (256), appears to be concentrated at the junctions between EC (257) and is expressed on the surface of monocytes, neutrophils, and a small subset of lymphocytes (258 - 260). Muller et al. have suggested several possible roles of PECAM-1 in transendothelial migration of leukocytes. The most obvious role involves PECAM-1 as a direct adhesion molecule binding the leukocyte tightly to the HUVEC during its passage through the junctions (255), since PECAM-1 has been shown to be concentrated at the intercellular junctions, with approximately 15% exposed to the apical surface (257). These authors suggest that an apical-basal gradient of PECAM-1 may exist through the HUVEC junction which can act similarly to a surface-bound chemotactic gradient to produce directed migration of leukocytes through the junction. Another possible role is that

PECAM-1 may be ligated on the surface of leukocytes, which can then activate CD11/CD18 binding activity, and this mechanism could apply as well if an apical-basal gradient of PECAM-1 exists (255). Finally, induction of PECAM-1 has been reported on activated T cells (258), thus suggesting a possible role of this adhesion molecule in mediating migration of activated lymphocytes across untreated monolayers of HBMEC in addition to the LFA-1/ICAM-1 mechanism.

Migration of activated T lymphocytes across EC monolayers is further enhanced by IFN- $\gamma$  treatment of HBMEC. Similar observations have also been reported for the migration of resting or activated lymphocytes across untreated and cytokine treated HUVEC (24, 151). In contrast, treatment of rat retinal EC with IFN- $\gamma$  is associated with a small, but not significant, increase in the level of activated T-cell line lymphocyte migration (170). In addition, Male et al. have reported that migration of activated lymphocytes across rat brain endothelia does not appear to depend on the activation state of the EC (251). A possible explanation for these results could be the relatively low concentrations of IFN- $\gamma$  used. Alternatively, inherent differences in the culture systems used could account for these discrepancies.

Transmission EM studies show significant numbers of activated lymphocytes migrating across untreated as well as IFN- $\gamma$  treated HBMEC. Activated T cells display increased size and altered appearance. Finger-like projections decorate the cytoplasmic membrane and significant numbers of mitochondria and vacuoles occupy the cell cytoplasm. Migration of both resting and anti-CD3 stimulated lymphocytes across untreated and IFN- $\gamma$  treated HBMEC is not associated with disruption of the monolayers. The integrity of the

monolayers is reestablished once lymphocyte migration is completed. Similarly, migration of bovine peripheral blood lymphocytes across the endothelium of pulmonary artery intimal explants has been shown to cause no damage to the continuity of the vascular endothelium (261).

The optimal concentration of IFN- $\gamma$  used for the adhesion and migration assays has been shown to induce maximal Ia Ag expression on HBMEC in primary culture (127). We observed no significant change in the degree of activated T cell migration across IFN- $\beta$  treated EC as compared to controls, indicating that IFN- $\beta$  has no direct effect on the migration process. However, the IFN- $\gamma$ -mediated increase in migration is downregulated by IFN- $\beta$ , since migration of activated lymphocytes across EC coincubated with IFN- $\gamma$  and IFN- $\beta$  is comparable to that of controls. Blocking experiments with mAbs against human HLA-DR in IFN- $\gamma$  treated HBMEC show comparable levels of decrease in migration to those obtained by treating HBMEC with both cytokines.

Taken together, the results of our studies on the migration of resting and nonspecifically stimulated T lymphocytes across untreated and cytokine treated HBMEC monolayers, indicate that induction of class II molecules on the surface of HBMEC by IFN- $\gamma$  is, at least in part, responsible for the increased migration of T cells across the monolayers. IFN- $\beta$  has no direct effect on lymphocyte-EC binding, but downregulates the IFN- $\gamma$ -mediated increase in transendothelial migration most likely through downregulation of the IFN- $\gamma$  induced de novo expression of class II MHC molecules by HBMEC.

#### 4.6 EFFECTS OF IFN- $\gamma$ ON THE STORAGE AND RELEASE OF FVIII:Ag FROM HBMEC IN PRIMARY CULTURE

The fifth and final specific aim of this thesis was to investigate the effects of IFN- $\gamma$  on the storage and release of FVIII:Ag following its immunocytochemical localization in primary cultures of HBMEC.

##### 4.6.1 Immunocytochemical localization of FVIII:Ag in HBMEC

Human brain microvessel EC in primary culture synthesize FVIII:Ag as indicated by their positive, granular, perinuclear staining for FVIII:Ag with the immunoperoxidase technique. By immunoelectron microscopy FVIII:Ag is localized within cytoplasmic vesicles closely associated with the rough endoplasmic reticulum and Golgi apparatus in the perinuclear region. Treatment of EC with Ca<sup>2+</sup> ionophore A23187 results in marked reduction in labeled vesicles, while preincubation with IFN- $\gamma$  leads to increase of intracellular pools of FVIII:Ag.

EC lining large vessels and arterioles synthesize and secrete FVIII:Ag and store the newly synthesized glycoprotein within cytoplasmic organelles unique to these cells, known as Weibel-Palade bodies (174 - 176). These rod-shaped structures are absent in primary cultures of microvessel EC derived from rat (179 - 180), mouse (178) and bovine cerebral cortex (262) and bovine retina (263), but have been reported to be present in EC derived from rat and bovine brain white matter (264). Weibel-Palade bodies are extremely rare or absent in normal

human cerebral capillaries (265, 266). They have been observed in the orbital cortex of normal aged humans (267) and with increased frequency in certain brain tumors (266, 268). HBMEC in primary culture are similarly devoid of Weibel-Palade bodies. The perinuclear, granular staining for FVIII:Ag with the immunoperoxidase technique corresponds to variably dilated vesicular profiles within which deposits of colloidal gold were observed ultrastructurally. The single limiting membrane of these vesicles is not decorated with ribosomes and therefore, it is unlikely that they represent dilated cisternae of rough endoplasmic reticulum. Their constant presence near the Golgi apparatus and the rough endoplasmic reticulum suggests that the immunolabeled vesicles belong to the polymorphous vacuoles that form part of the transmost Golgi section (269). These trans Golgi elements have been found to be part of the pathway of newly synthesized molecules (270). It is, therefore, likely that, following synthesis in the endoplasmic reticulum and extensive modification in the Golgi apparatus (271), the newly synthesized FVIII:Ag is transported to the trans Golgi polymorphous vesicles where it is concentrated. In the absence of Weibel-Palade bodies in cerebral microvessel EC, these vesicular bodies most likely represent sites of short-term storage of FVIII:Ag prior to release. Previous *in vivo* studies on the localization of FVIII:Ag in vascular endothelium of normal human extracerebral tissues and one capillary hemangioma by immunoelectron microscopy demonstrated immunolabeling of endoplasmic reticulum and cytoplasmic vesicles and vacuoles in addition to Weibel-Palade bodies (176). These vesicular profiles strongly resemble the ones observed in the present study. A similar localization of FVIII:Ag within cytoplasmic vesicles has been reported in EC lining the saphenous vein (172).

#### 4.6.2 Effects of IFN- $\gamma$ on the storage and/or release of FVIII:Ag from HBMEC

Large vessel EC secrete the newly formed FVIII:Ag via two pathways (272, 273). The regulated pathway involves release of the large multimeric forms of the glycoprotein from the specific storage organelles, the Weibel-Palade bodies. In vitro studies on the secretion of von Willebrand factor by umbilical vein EC indicate that this pathway is highly polarized and dependent upon intact microtubular system, since microtubule-depolymerizing agents inhibit the regulated release (274). The majority of FVIII:Ag synthesized by EC is secreted constitutively in the form of small multimers. In contrast to the regulated pathway, constitutive release is not affected by microtubule-depolymerizing agents (275) and is not polarized. Since HBMEC do not store FVIII:Ag in Weibel-Palade bodies, it is quite possible that they secrete the newly synthesized protein through the constitutive pathway only, with the Golgi-associated cytoplasmic vesicles serving as temporary storage pools following multimerization and prior to release.

A variety of stimuli can lead to increased release of FVIII:Ag from EC in vitro. Most of these factors stimulate the regulated pathway of secretion. Thus, treatment of EC monolayers with calcium ionophore A23187, thrombin or phorbol-myristate-acetate results in release of the large multimeric forms of FVIII:Ag and a simultaneous disappearance of Weibel Palade bodies from EC (272 - 274, 276) in association with a rise in the concentration of intracellular calcium. The effect of calcium ionophore was inhibited by EGTA in a dose-dependent manner (276). The basal secretion was apparently not affected by these treatments. In the present study short preincubation of HBMEC with calcium ionophore led to rapid

reduction in the number of labeled cytoplasmic vesicles. In contrast, addition of the calcium chelating agent EGTA to the culture media resulted in slight increase in immunostained vacuoles, which was not statistically significant when compared to untreated cells. Loss of staining following calcium ionophore treatment may represent rapid release of FVIII:Ag from intracellular pools, although other mechanisms, such as antigen degradation following ionophore - mediated protease activation, cannot be ruled out. These findings indicate that at least some of the factors that stimulate the regulated pathway in large vessel EC, similarly influence the release of FVIII:Ag from microvessel endothelium in the absence of Weibel-Palade bodies. Whether the FVIII:Ag secreted by cerebral small vessel endothelium is in the form of small or large multimers, is presently unknown.

Incubation of HBMEC with IFN- $\gamma$  for 24 hours resulted in significant increase in the number of immunostained vesicles suggesting that IFN- $\gamma$  interferes with the release and/or storage of FVIII:Ag. Recent studies on the effect of cytokines on the release of von Willebrand factor indicate that IFN- $\gamma$  decreases the constitutive and regulated release from cultured HUVEC reversibly and in a time and dose-dependent manner (182). Although the exact mechanism of action is not presently known, it is possible that IFN- $\gamma$  exerts its effect by modifying the concentration of intracellular calcium. It has been recently demonstrated that IFN- $\gamma$  can activate the calcium-dependent pathway through activation of phospholipase C and induce, in addition, a significant outflux of calcium ions from EC (277). Inhibition of FVIII:Ag release by IFN- $\gamma$  may be important considering its pivotal role as mediator of the localized immune response in autoimmune diseases of the central nervous system.

## CONCLUSIONS

### 5.1 SUMMARY AND CONCLUSIONS

The main objective of this thesis was to examine the effects of IFN- $\gamma$  and IFN- $\beta$  on Ia Ag expression, cell proliferation, and alteration of the morphology and permeability properties of HBMEC using an in vitro model of the human BBB. In addition, the adhesion and migration of resting and anti-CD3 stimulated T cells across untreated and cytokine-treated HBMEC was studied. Finally, the effects of IFN- $\gamma$  on the storage and release of FVIII:Ag by HBMEC was determined.

The working hypothesis of this thesis was that in chronic inflammation, some activated T lymphocytes will release inflammatory cytokines including IFN- $\gamma$ . This cytokine can then induce the local brain endothelia to express Ia Ag on the cell surface, to alter their morphology and increase their permeability to macromolecules. These changes will facilitate the adhesion and migration of resting lymphocytes across the cerebral endothelial barrier. Lymphocyte activation will further augment adhesion and migration. Finally, IFN- $\gamma$  by inhibiting the release of FVIII:Ag from HBMEC will contribute to the maintenance of blood fluidity during the immune reaction.

In this study, IFN- $\gamma$  induces de novo expression of Ia Ag on HBMEC in a time and dose-dependent fashion. Primary cultures of HBMEC do not express Ia Ag constitutively. The expression of Ia molecules on HBMEC can be detected as early as 12 hours following incubation with IFN- $\gamma$  and reaches plateau levels by 48 hours. Surface labeling for Ia Ag is

maximal with 100 to 200 U/ml IFN- $\gamma$  and minimal with 10 U/ml. In contrast, treatment of HBMEC with IFN- $\beta$  has no influence on Ia Ag expression. Moreover, incubation of HBMEC with a combination of IFN- $\gamma$  and IFN- $\beta$  results in downregulation of Ia Ag expression. IFN- $\beta$  suppresses the IFN- $\gamma$ -induced expression in a dose-dependent manner, however, complete inhibition was not detected. Kinetic studies on the effects of IFN- $\gamma$  and IFN- $\beta$  on Ia Ag expression indicate that administration of IFN- $\beta$  prior to or simultaneously with IFN- $\gamma$  treatment generates the most significant downregulation of IFN- $\gamma$ -induced Ia Ag expression. These observations may partly explain the results of recent therapeutic trials with IFN- $\beta$  in MS.

Treatment of HBMEC with IFN- $\gamma$  results in changes in cell shape and organization of the EC monolayers. The IFN- $\gamma$ -treated endothelia acquire a spindle-like shape and long attenuated processes. Prominent overlapping and ill-defined whorls are unique features of IFN- $\gamma$ -treated EC monolayer. The IFN- $\gamma$ -induced phenotypic alterations on HBMEC are inhibited when EC are incubated simultaneously with IFN- $\gamma$  and IFN- $\beta$ ; the monolayers resume their highly organized growth pattern with prominent marginal folds in the areas of cell to cell contact. The morphological changes are associated with increased permeability of confluent monolayers to horseradish peroxidase as compared with untreated cultures. The number of HRP labeled vesicles was not increased in IFN- $\gamma$  treated EC as compared to untreated EC.

Lymphocyte-EC adhesion is significantly upregulated when HBMEC are pretreated with IFN- $\gamma$ , while IFN- $\beta$  inhibits the IFN- $\gamma$ -enhanced adhesion when the brain endothelia are

incubated with a combination of IFN- $\gamma$  and IFN- $\beta$ . IFN- $\beta$  alone has no effect on lymphocyte-EC interactions since the level of adhesion is comparable to that of untreated EC. Nonspecific activation of T lymphocyte causes a significant increase in lymphocyte-EC adhesion; in fact, the level of adhesion of activated lymphocytes to untreated EC is greater than that of resting T cells to IFN- $\gamma$  treated EC, suggesting that lymphocyte activation plays an important role in T cell-EC adhesion. Similar to the responses obtained with resting lymphocytes, IFN- $\beta$  inhibits the IFN- $\gamma$ -enhanced adhesion of activated T cells when EC are treated simultaneously with IFN- $\gamma$  and IFN- $\beta$ . However, IFN- $\beta$  treatment alone has no effect on the adhesion of activated T lymphocytes to EC. MAb blocking studies against IFN- $\gamma$  and human HLA-DR molecules indicate that the enhanced binding is specifically induced by IFN- $\gamma$  and HLA-DR molecules play a central role in the IFN- $\gamma$  upregulated adhesion.

Migration of resting lymphocytes is markedly augmented when HBMEC are treated with IFN- $\gamma$ , but not IFN- $\beta$ . Treatment of cerebral EC with a combination of IFN- $\gamma$  and IFN- $\beta$  significantly downmodulates the IFN- $\gamma$ -mediated migration. Activation of lymphocytes is associated with a dramatic increase in migration across untreated EC, and the level of migration is greater than that of resting T cells through IFN- $\gamma$  treated EC. IFN- $\gamma$ , but not IFN- $\beta$ , further augments the migration of activated T cells. The IFN- $\gamma$ -enhanced migration is suppressed by IFN- $\beta$  treatment. Blocking studies with mAbs against HLA-DR molecules indicate that Ia Ag plays a central role in the IFN- $\gamma$  mediated migration of both resting and anti-CD3 stimulated lymphocytes.

Finally, it has been determined that IFN- $\gamma$  suppresses the release of FVIII:Ag from

HBMEC which suggests that IFN- $\gamma$  may also play a role in maintaining blood fluidity during the immune reaction.

In conclusion, the results of these studies demonstrate the critical function of IFN- $\gamma$  in upregulating the immune response which plays an essential role in the host defense mechanism. Indeed, autoimmune disorders of the CNS such as MS may arise as the results of unwanted inflammatory or immunological responses. Subsequently, the ability of cytokines such as IFN- $\beta$  to reduce or suppress the IFN- $\gamma$ -enhanced reactions may explain their therapeutic effect. The facts that IFN- $\beta$  is able to inhibit the IFN- $\gamma$ -induced Ia Ag expression and to suppress the IFN- $\gamma$ -mediated increase in lymphocyte-EC adhesion and migration indicate that Ia Ag plays a central role in these immunological responses. This statement is further supported by results obtained from mAb blocking studies directed against human HLA-DR. Therefore, the results of this thesis demonstrate the important role of HBMEC in CNS inflammation and enhance our understanding of some of the factors involved in the recruitment of lymphocytes into chronic inflammatory sites in the CNS.

## 5.2 FUTURE PROSPECTS

The results obtained from this study indicate that class II MHC participates in the IFN- $\gamma$ -mediated increase in lymphocyte-HBMEC adhesion and migration. An avenue for immediate future research would be to determine the role of HBMEC as antigen presenting cells in CNS inflammation using this in vitro BBB model. HBMEC can be induced to express Ia Ag by IFN- $\gamma$  and allowed to endocytose and process myelin basic protein (MBP), a protein

component of the myelin sheath. At the appropriate time, MBP-specific lymphocytes are incubated with these HBMEC, and lymphocyte proliferation can be determined with tritiated thymidine assay.

Since it has been demonstrated in this thesis that antigen-nonspecific stimulation of peripheral blood lymphocytes plays a central role in markedly upregulating the lymphocyte-EC adhesion and migration, another avenue for future research would be to examine the molecular mechanisms that are responsible for augmenting the adhesion and migration of activated lymphocytes to HBMEC. The application of mAbs directed against specific adhesion molecules such as ICAM-1, LFA-1, VCAM-1, VLA-4, that are present on the surface of both lymphocyte and EC will help to determine the molecules responsible for upmodulating the immunological reactions.

Finally, a concern that also needs to be addressed in future research in CNS inflammation is the question: What is the significance of peripherally activated T lymphocytes in the development of immune reactions in the brain?

In one version of rat EAE, autoimmune demyelination can be induced by immunization with myelin basic protein, and systemic injection of a specific monoclonal antibody directed against myelin/oligodendrocyte glycoprotein can amplify demyelination. Immunotherapy of this antibody-induced demyelination is possible with another specific mAb directed to an antigen on activated rat T cells, suggesting an important role of T lymphocyte activation in the disease development (169). Studies on the migration of activated lymphocytes across rat brain endothelium lead Male and his coworkers (154) to speculate that lymphocyte activation in the

periphery may lead to increased traffic through the brain. This lymphocyte traffic can have serious consequences if antigen specific interaction develops between circulating T cells and antigen presenting cells in the CNS. Amplification of the immune reaction can result from cytokine release and local activation of the brain endothelium, causing further increases in cellular migration. As suggested, this scenario is possible in *Bordetella pertussis* vaccination in a small proportion of individuals. In accord with the above speculation, *in vivo* studies of T-lymphocyte entry into the rat CNS by Hickey and his coworkers (161) have reported that activated T cells appear to enter the CNS in a random manner, irrespective of their antigen specificity, MHC compatibility, T cell phenotype, and T-cell receptor gene usage. These authors also showed that only T-lymphocytes that are able to recognize a specific antigen in the CNS of the host remain beyond 72 hours in the target organ while non-specifically activated T-cells exit the CNS within 1 to 2 days.

The above observations raise question(s) about the "immunological privilege" status of the CNS because any T-cell that is activated in the tissues of the immune system can possibly gain access to the brain in a random manner once it enters the circulation. Transplantation of allogeneic tissue into the CNS is well accepted by the recipient; however, the graft is quickly rejected when the same alloantigen is exposed to the host periphery (278). In concordance with the results described by Hickey et al. (161), *in vivo* studies of mice EAE, Cross et al. (279) have shown that <sup>14</sup>C-labeled CNS antigen-specific T cells home to the CNS endothelia 24 hours prior to and during the initial clinical disease, but these cells always remain within the perivascular area. The antigen-specific lymphocytes only represent 1% to 4% of the

inflammatory cells that are present in the brain parenchyma during disease development. These investigators conclude that the inflammatory cells are predominantly of recipient derivation. More recently, Caspi et al. (280) have demonstrated that in experimental autoimmune uveoretinitis (EAU), a T cell-mediated autoimmune disease in rat serving as a model for a number of human blinding ocular diseases of a presumed autoimmune nature, only mild or essentially no disease can be induced by the CNS antigen-specific T cell lines in unreconstituted athymic rats. However, the situation can be significantly reversed by infusion of naive cell populations containing immunocompetent T cells. Subsequently, the recruitment of naive T cells constitutes an amplification mechanism that is central to the expression and pathogenesis of uveitis. The phenomenon of recruitment can magnify the effect of a tiny number of antigen-specific "pathogenic" T lymphocytes into a destructive inflammation.

Consequently, the results that are available hitherto do support the significant role that peripherally activated, antigen-nonspecific T cells can have in the development of immune reactions in the brain. The ability to suppress these activated lymphocytes, for example, with anti-LFA-1 monoclonal antibodies to block the LFA-1 dependent pathway of adhesion during an unfavorable inflammation of the CNS may have great therapeutic potential.

### **5.3 SIGNIFICANCE OF THIS THESIS**

Primary cultures of HBMEC provide a useful in vitro model for investigating the effects of cytokines on the morphology and function of the cerebral endothelium and on the complex processes of lymphocyte adhesion and migration across the cerebral endothelium

barrier. These studies indicate that interferons  $\gamma$  and  $\beta$  are important mediators of the localized immune response within the human CNS and that class II MHC molecules, induced de novo on HBMEC, play a pivotal role in lymphocyte-EC interactions in the CNS.

As pointed out by Wekerle et al. (14), the detailed analyses of the cellular and molecular mechanisms involved in the interaction between T cells and the BBB are of tremendous importance for various reasons: a) Such knowledge will give insight into the development of CNS disorders with putative autoimmune pathogenesis, e.g. multiple sclerosis. b) The information obtained will provide a better understanding of the mechanisms involved in physiological immune surveillance, as they are relevant in the prevention and the control of infectious diseases within the CNS. c) On the basis of such knowledge, it may be possible to design novel specific therapies of CNS (autoimmune) disease.

Table 1. *Permeability of HBMEC monolayers to HRP*

	No. of labeled cytoplasmic vesicles *	No. of interendothelial tight junctions**	
		Permeable	Impermeable
Control	2.0 $\pm$ 1.7 vesicles/cell	24.8 $\pm$ 2.7%	75.2 $\pm$ 2.7%
Experimental	2.4 $\pm$ 2.1 vesicles/cell	63.4 $\pm$ 5.2%	36.6 $\pm$ 5.2%

\* Numbers represent mean  $\pm$  SD of labeled vesicles in 100 control and 100 IFN- $\gamma$  treated cells from one experiment.  $P > 0.05$

\*\* Numbers represent mean  $\pm$  SD of 400 junctions (200 treated and 200 untreated) from two experiments using two different isolates.  $P < 0.05$

Figure 1: Diagram of the double chamber chemotaxis system used to study the migration of lymphocytes across confluent HBMEC monolayers. The collagen membrane is a firm membrane, made up of solubilized collagen, that forms the bottom of 14 mm diameter wells. These wells are placed inside larger wells of 24-well plates. Four support feet separated the inner from the outer chamber. HBMEC are seeded onto the collagen membranes and grown inside the inner chamber. Initial attachment of EC to the membranes does not require precoating with fibronectin. This system can be used to study the interactions between EC and inflammatory cells such as lymphocytes or polymorphonuclear leukocytes.

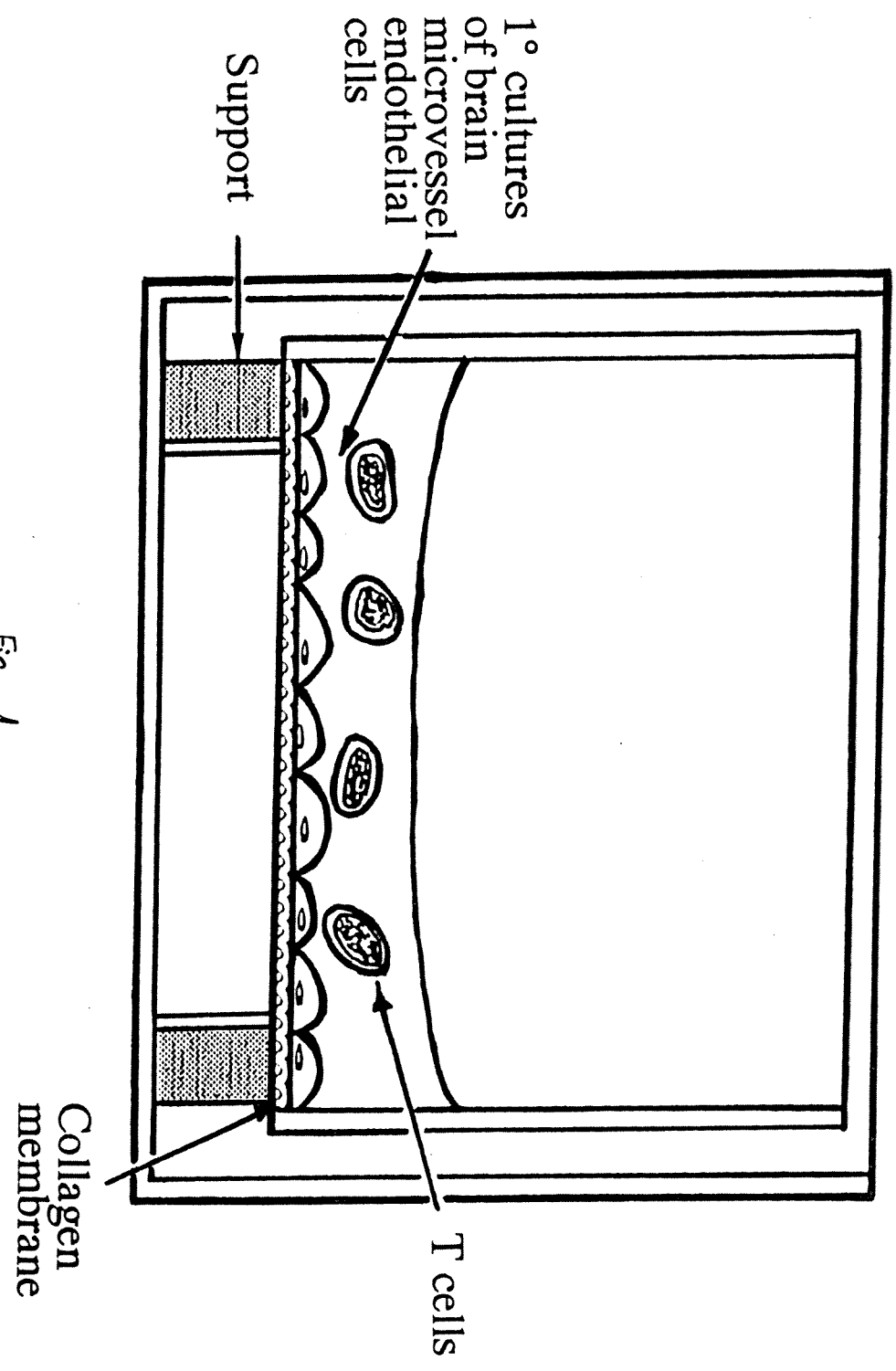


Fig. 1

Figure 2: Primary cultures of HBMEC grown on plastic wells (a) or collagen membranes (b) and maintained under standard culture conditions form highly organized, confluent, contact inhibiting monolayers composed of elongated endothelial cells. Bars = 20  $\mu\text{m}$ .

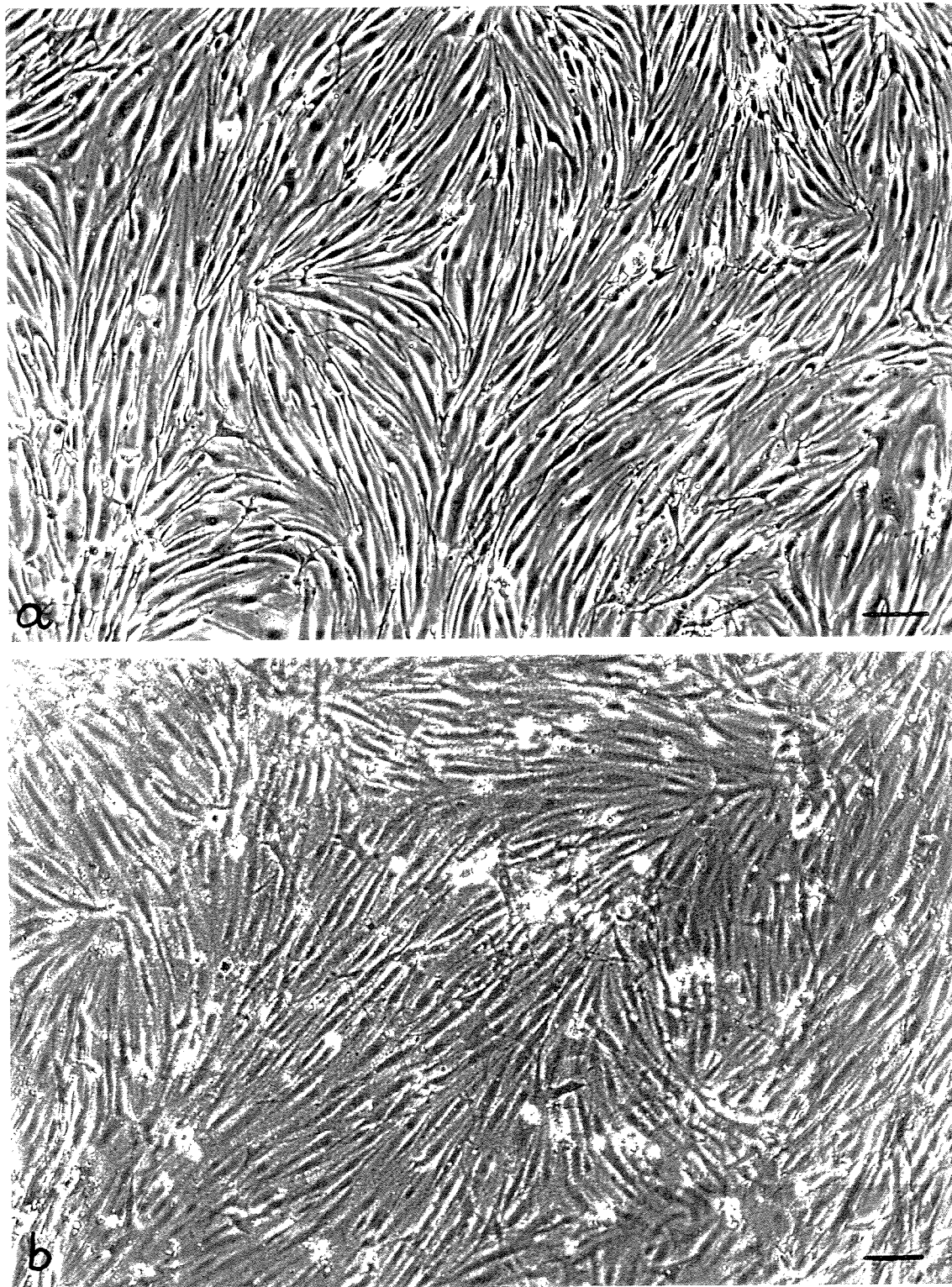


Fig. 2

Figure 3: Intense, predominantly perinuclear cytoplasmic staining of cultured HBMEC for FVIII:Ag with the immunoperoxidase reaction (a). Lectin binding by HBMEC is indicated by their positive immunoperoxidase staining for UEA I (b). Bars = 20  $\mu\text{m}$ .

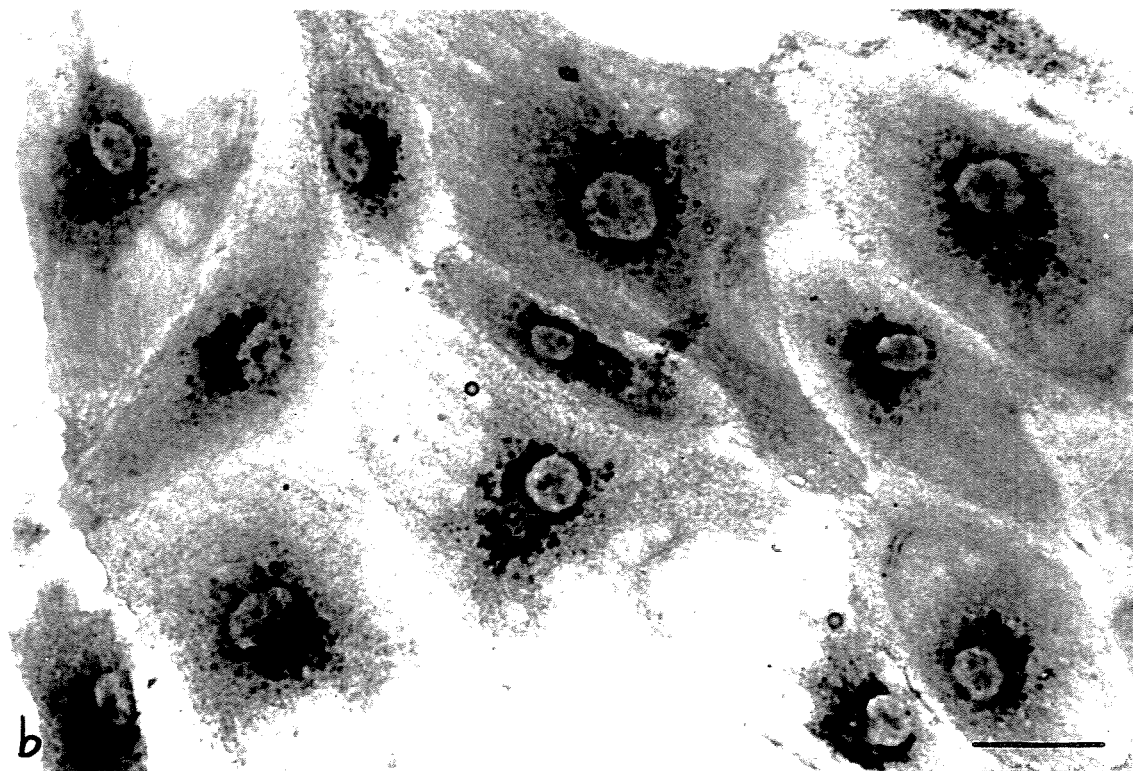
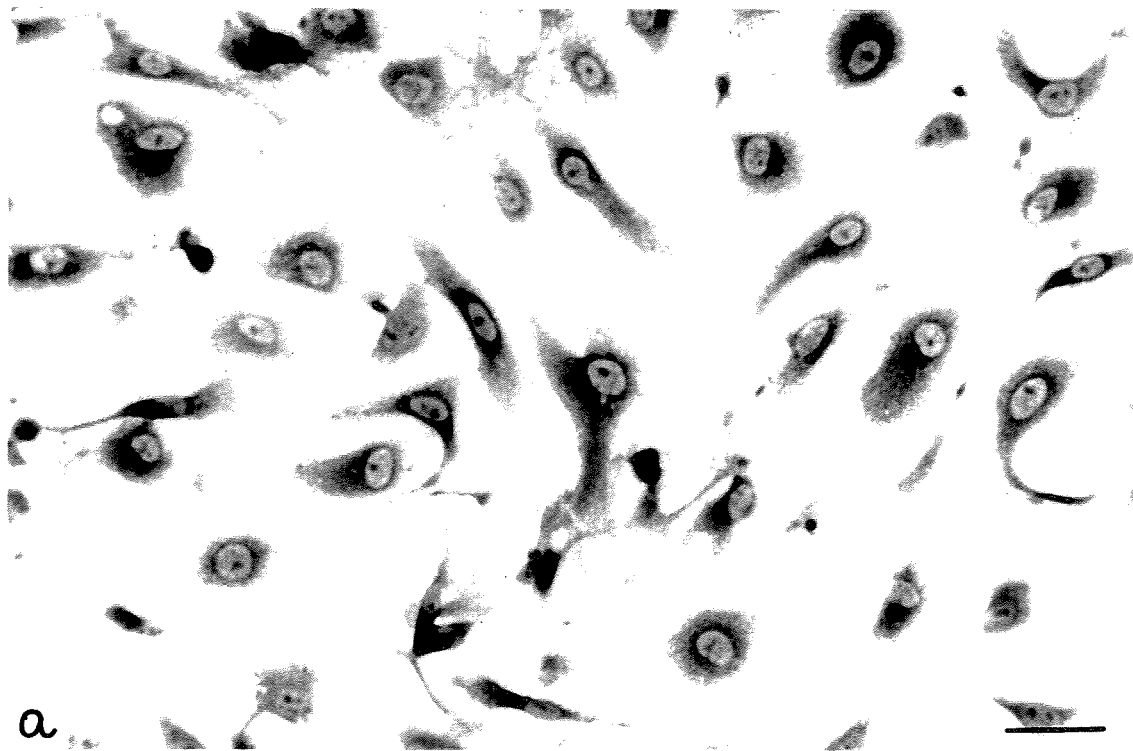


Fig. 3

Figure 4: Confluent monolayers of HBMEC (EC) grown on collagen membrane (C). Elongated cells with focally evident finger-like cytoplasmic projections form a continuous cell layer firmly attached to the substrate. Bars = 2  $\mu\text{m}$ .

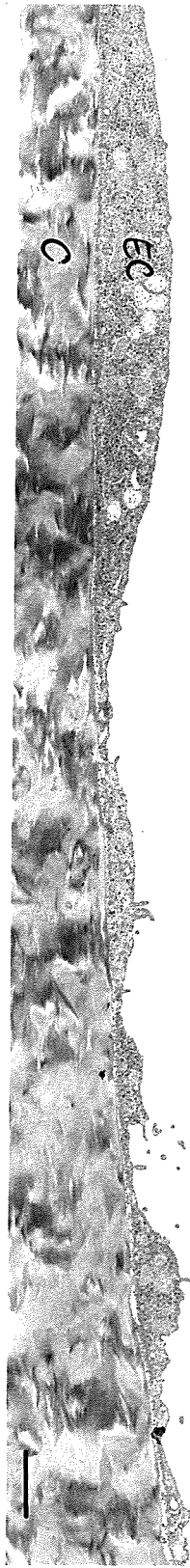


Fig. 4

Figure 5: Primary cultures of HBMEC (EC) cultivated on collagen membranes (C) (a - d). Intercellular contacts vary in length and complexity. Tight junctional complexes (arrows) with pentalaminar configuration are present in areas of cell to cell contact. Bars = 0.2  $\mu\text{m}$ .

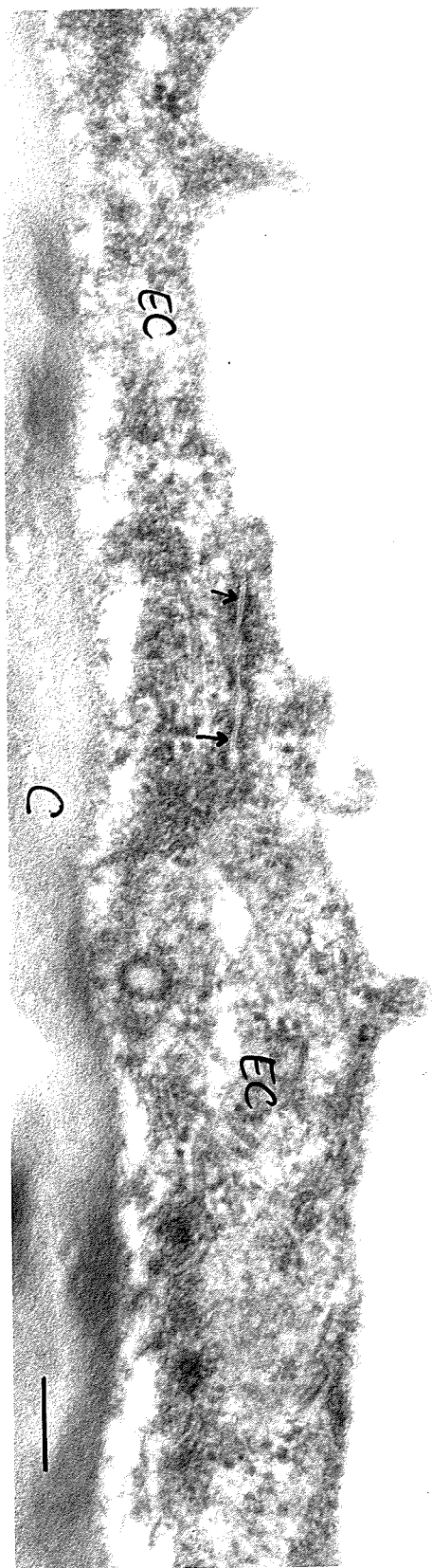


Fig. 5a

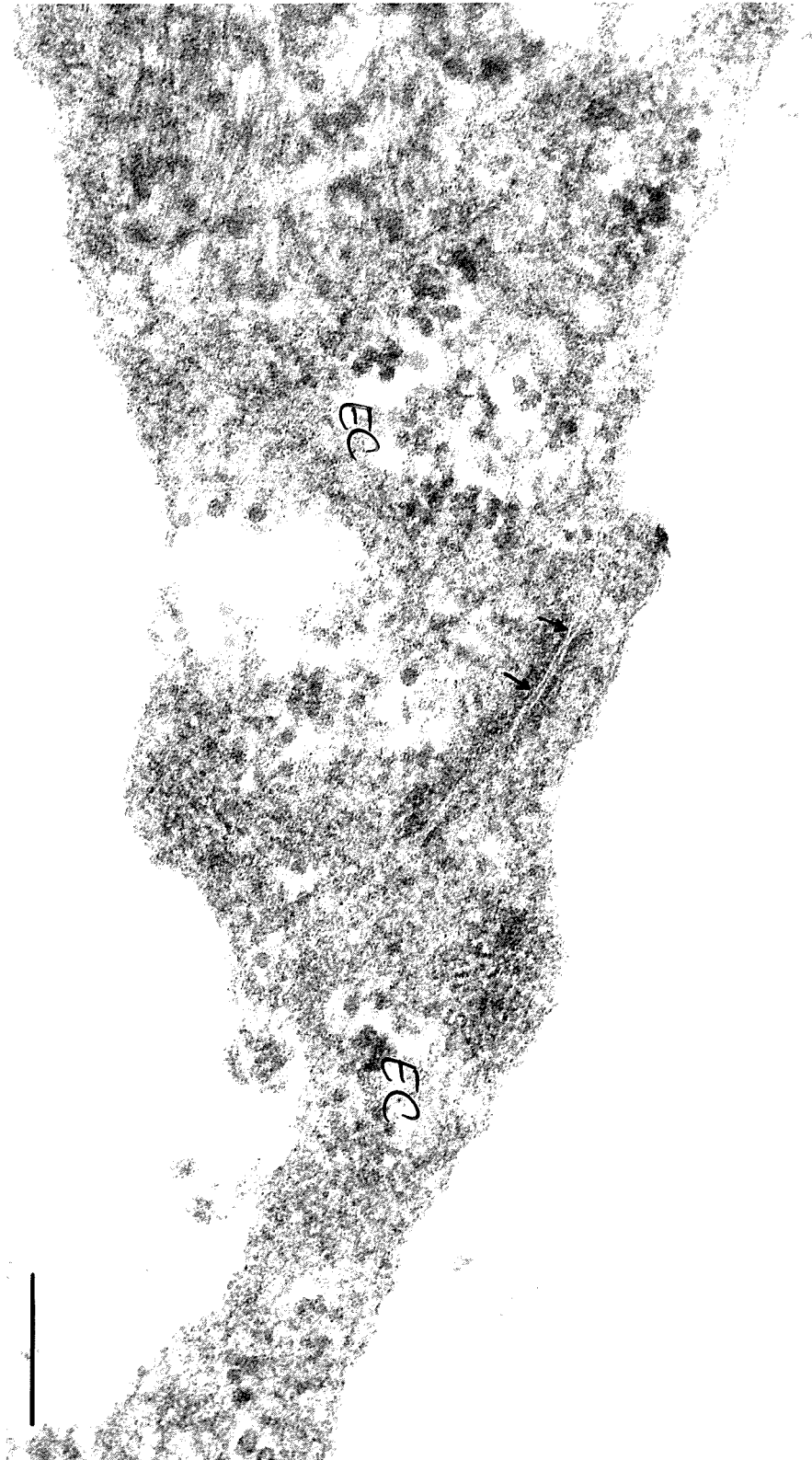


Fig. 5 b

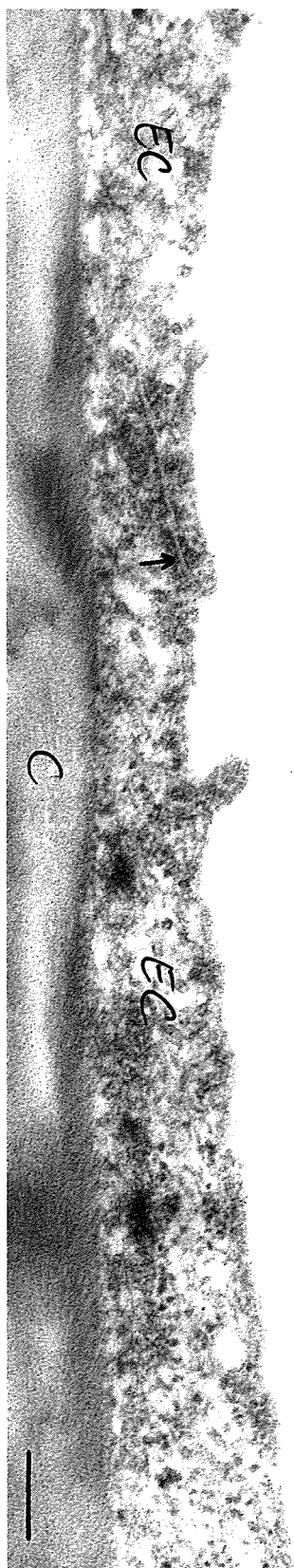


Fig. 5C



Fig. 5d

**Figure 6:** The cytoplasm of cerebral microvessel endothelial cells (EC) contains prominent rough endoplasmic reticulum (small arrows), small to large mitochondria (arrowheads), and a variable number of small and large vesicles (V) in juxtannuclear position. Small amounts of amorphous material are present, otherwise, the vacuoles are clear and bound by a single limiting membrane. The endoplasmic reticulum is closely associated with the vesicular profiles. EC were grown on collagen membranes (a) or plastic wells (b). Weibel-Palade bodies are not present. C = collagen membrane; N = nucleus. Bars = 1  $\mu\text{m}$ .

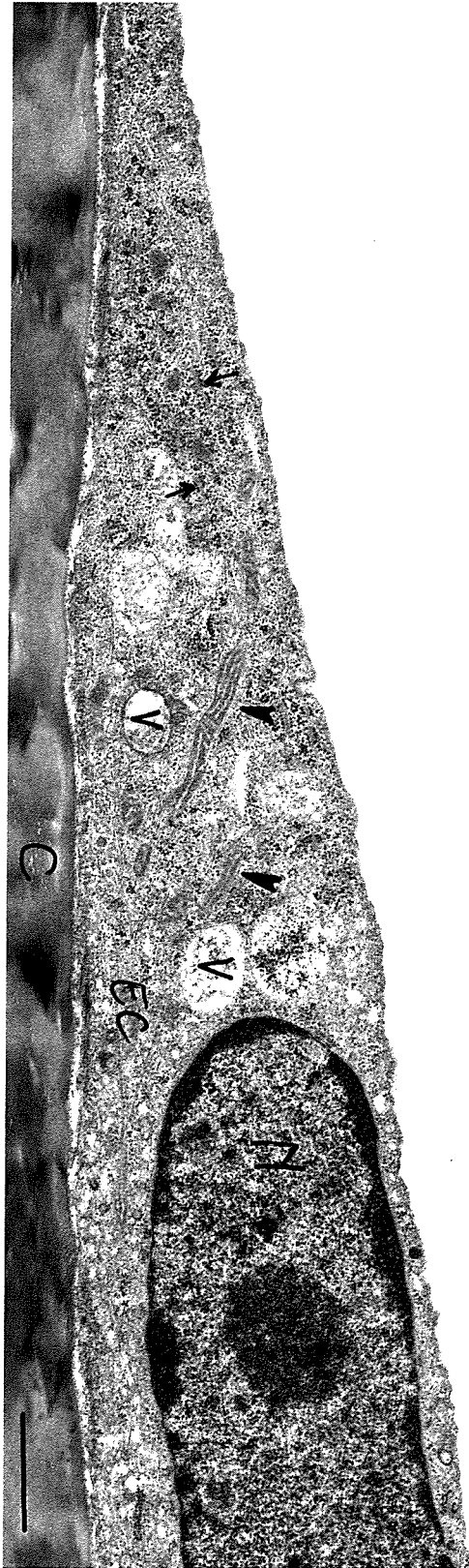


Fig. 6 a

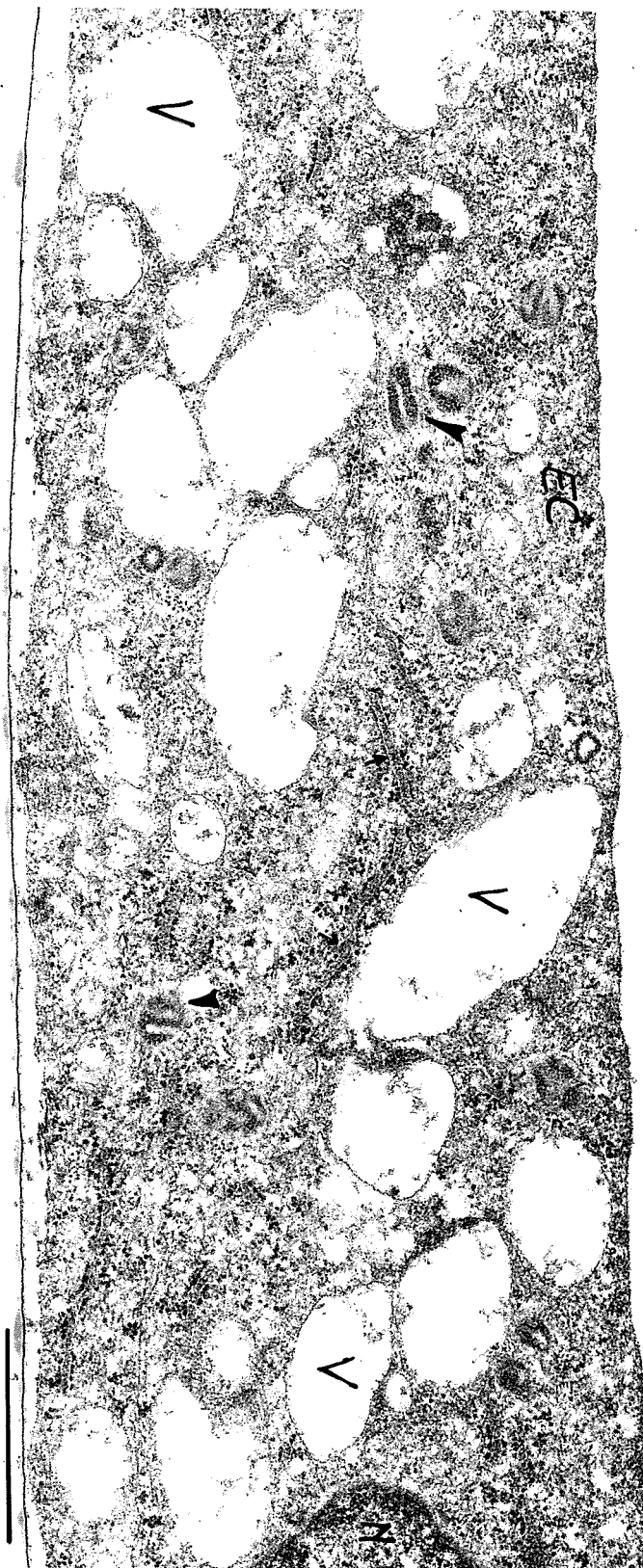


Fig. 6b

Figure 7: Immunogold staining of intact endothelial monolayers for FVIII:Ag. (A) Five-nm gold particles form dense aggregates within several cytoplasmic vesicles (large arrowheads). Other vesicles contain scant particles (small arrowheads), whereas still others are not stained. Labeled vesicles are located close to the Golgi apparatus (B) and the endoplasmic reticulum (A). (C) Occasionally, a few gold particles localize within cisternae of endoplasmic reticulum (arrowhead) next to a labeled vesicle. (D) Staining is absent in control cultures incubated with carrier buffer instead of primary antibody. N, nucleus; G, Golgi. Bars = 1  $\mu$ m.

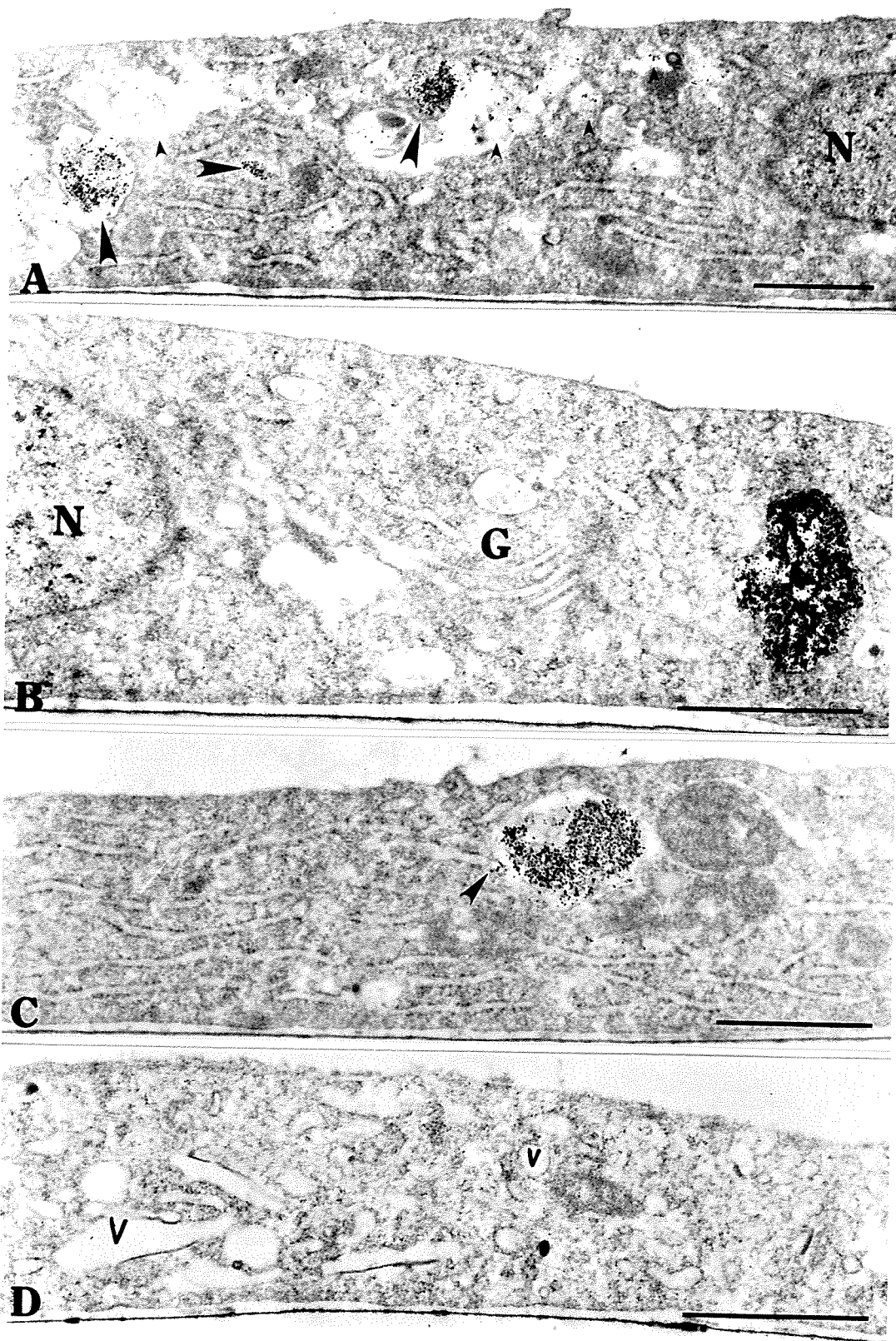


Fig. 7

Figure 8: Time course of Ia antigen induction on human cerebral endothelium. Confluent HBMEC cultures were incubated with 200 units/ml IFN- $\gamma$  for 0.5 to 4 days and then stained with the immunogold technique for the immunohistochemical demonstration of Ia antigen. Results are expressed as percentage of labeled cells in treated cultures. Untreated cells were not labeled. Bars represent the mean  $\pm$  SEM of duplicate wells of two separate experiments.

**Fig. 8** Time course of Ia Ag induction on HBMEC by IFN- $\gamma$

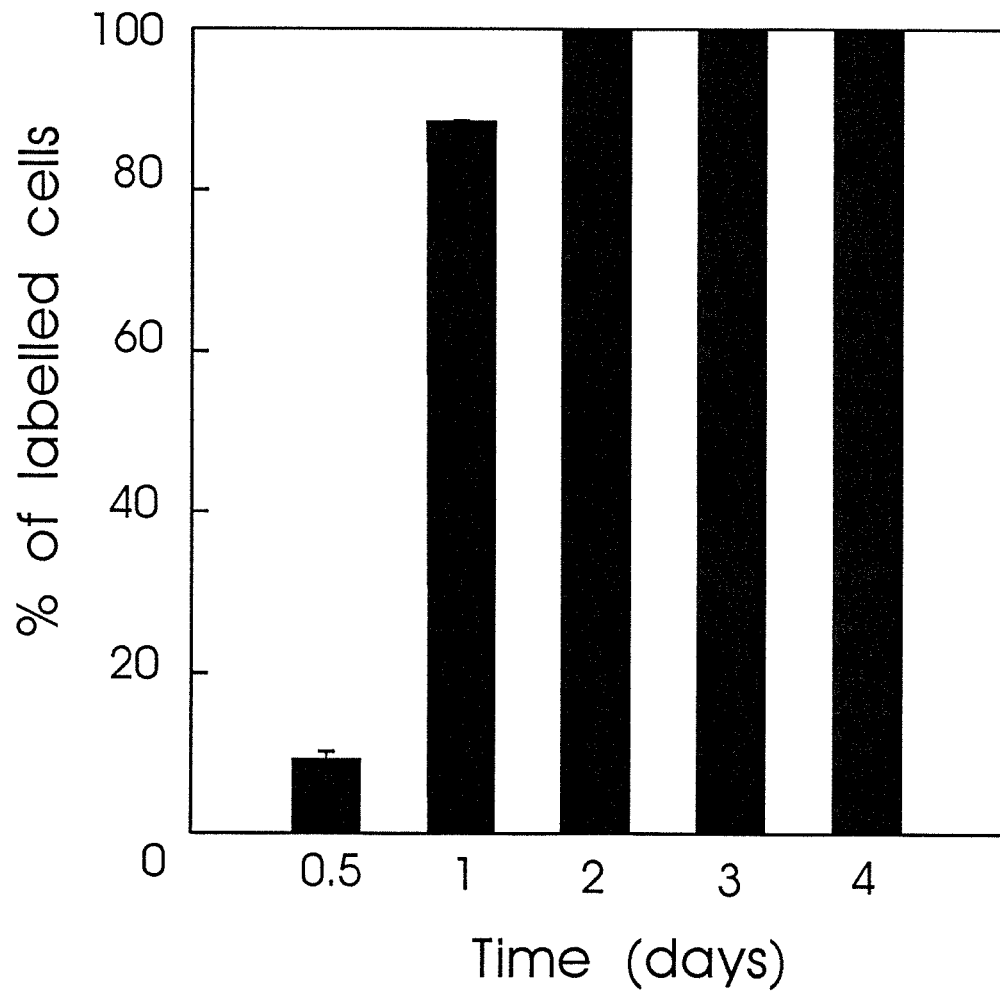


Figure 9: Dose response of Ia antigen induction by IFN- $\gamma$  on HBMEC. Confluent monolayers were incubated for 4 days with 10 to 200 units/ml IFN- $\gamma$  and then immunostained for the demonstration of Ia antigen. Results are expressed as percentage of labeled cells in treated and untreated cultures. Bars represent the mean  $\pm$  SEM of duplicate wells of three separate experiments.

**Fig. 9 Dose-response of Ia Ag induction by IFN- $\gamma$  on HBMEC**

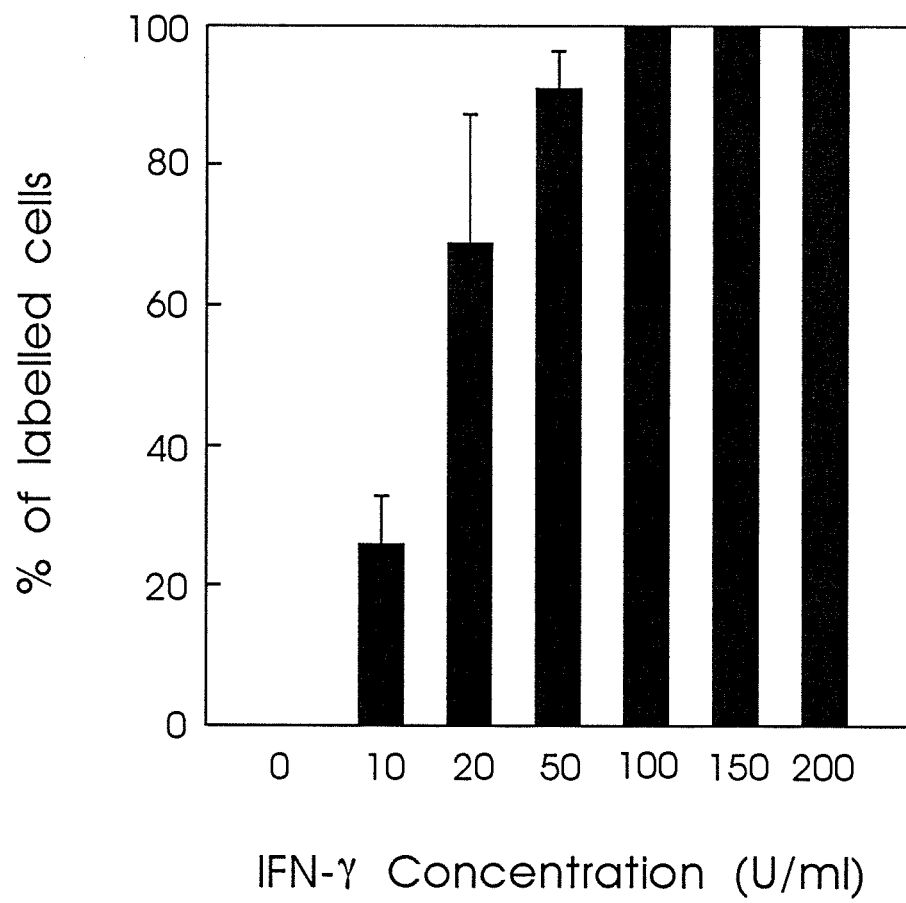


Figure 10: Ia antigen expression by HBMEC detected by immunogold silver staining. A, endothelial cells incubated with 200 units/ml IFN- $\gamma$  for 4 days demonstrating intense granular surface staining for Ia antigen. B, control untreated monolayers not expressing Ia antigen. C, endothelial cells treated with 200 units/ml IFN- $\gamma$  for 24 hours exhibiting less dense labeling. Individual cell variation in staining intensity is apparent in A and C. In D, cultures coincubated with anti-IFN- $\gamma$  antibody failed to label with the immunogold reagent. Bars = 20  $\mu$ m.

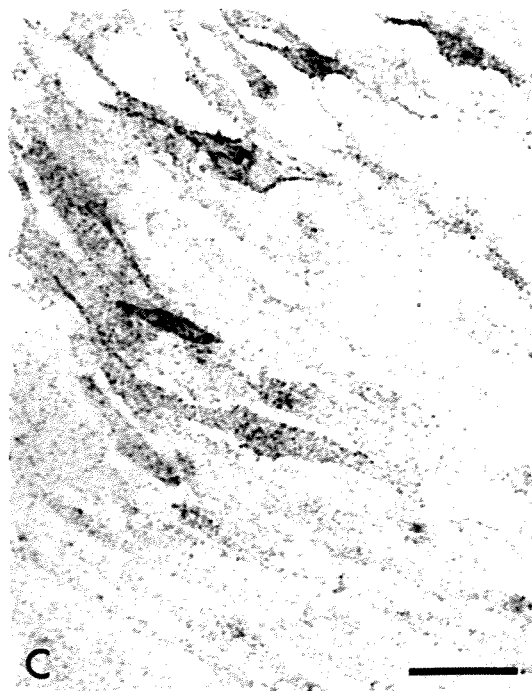


Fig. 10

Figure 11: Immunogold staining of HBMEC for the demonstration of Ia antigen. A, endothelial cells incubated with 200 units/ml IFN- $\gamma$  for 4 days. Five-nanometer gold particles focally decorate the apical surface of endothelial cells (arrowheads) with a tendency to localize close to fingerlike cytoplasmic folds. The basal cell surface is not labeled. B, staining is absent in untreated cells. Bars = 0.5  $\mu\text{m}$ .

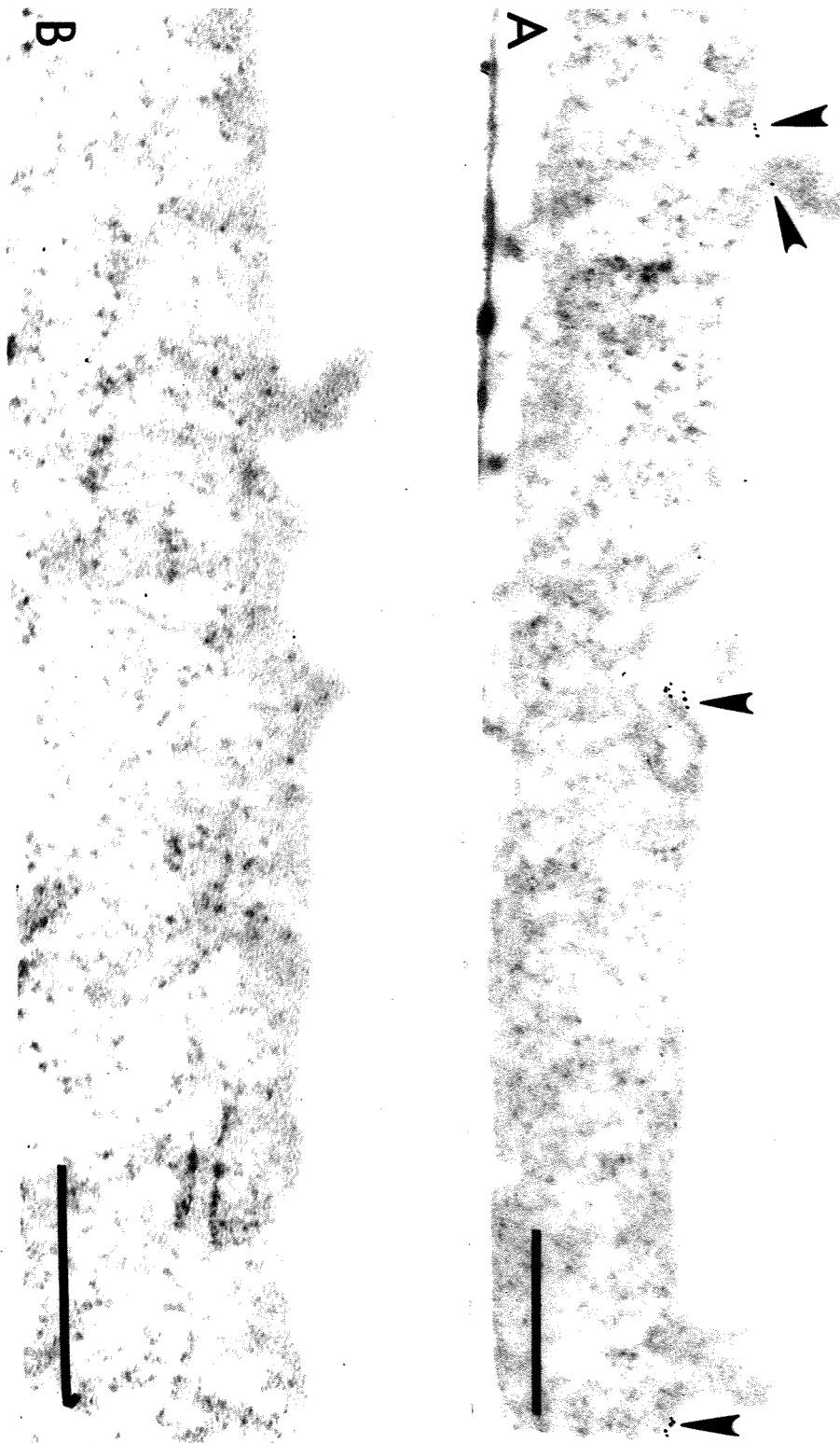


Fig. 11

Figure 12: Ia antigen expression by HBMEC detected by immunogold silver staining. a) endothelial cells incubated with 6,000 units/ml IFN- $\beta$  for 4 days failed to express of Ia Ag as indicated by the negative staining of EC. b) In cultures coincubated with IFN- $\gamma$  (100 units/ml) and IFN- $\beta$  (500 units/ml) expression of Ia Ag is limited to a small number of endothelial cells displaying positive surface labeling with immunogold silver staining (arrows). Bars = 20  $\mu$ m.

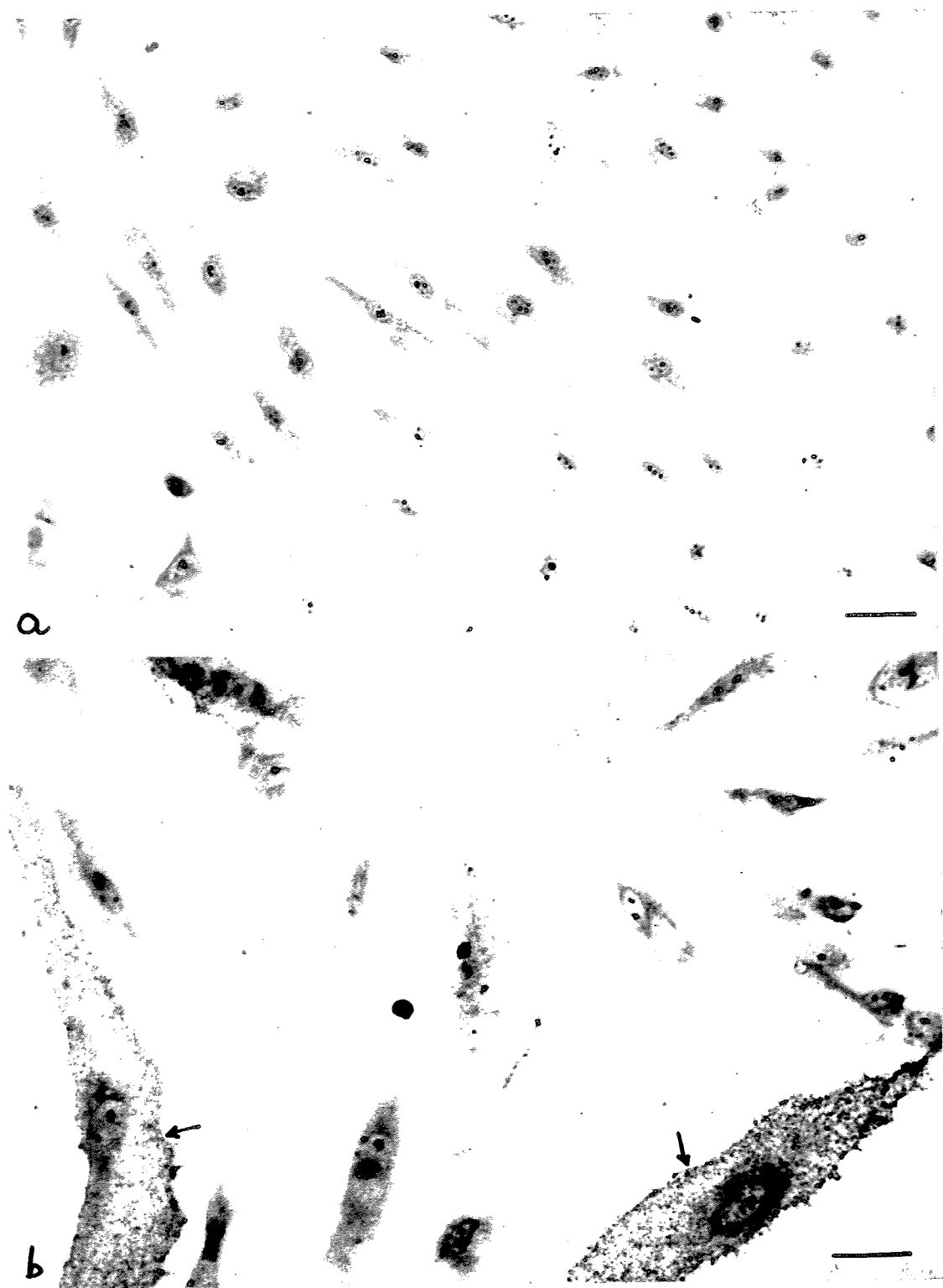


Fig. 12

Figure 13: Dose response of Ia Ag expression by HBMEC treated with IFN- $\gamma$  and/or IFN- $\beta$ . Confluent monolayers were examined untreated, or following treatment with IFN- $\beta$  (6,000 units/ml) or IFN- $\gamma$  (100 units/ml) or with a combination of IFN- $\gamma$  (100 units/ml) and  $\beta$  (100 to 6,000 units/ml) for 4 days. At the end of the incubation period, monolayers were stained with the immunogold silver staining technique for the surface detection of Ia Ag. Results are expressed as percentage of labeled cells in treated and untreated cultures. Bars represent the mean  $\pm$  SEM of triplicate wells of three separate experiments.

**Fig. 13 Dose-response of Ia Ag expression by HBMEC treated with IFN- $\gamma$  and/or IFN- $\beta$**

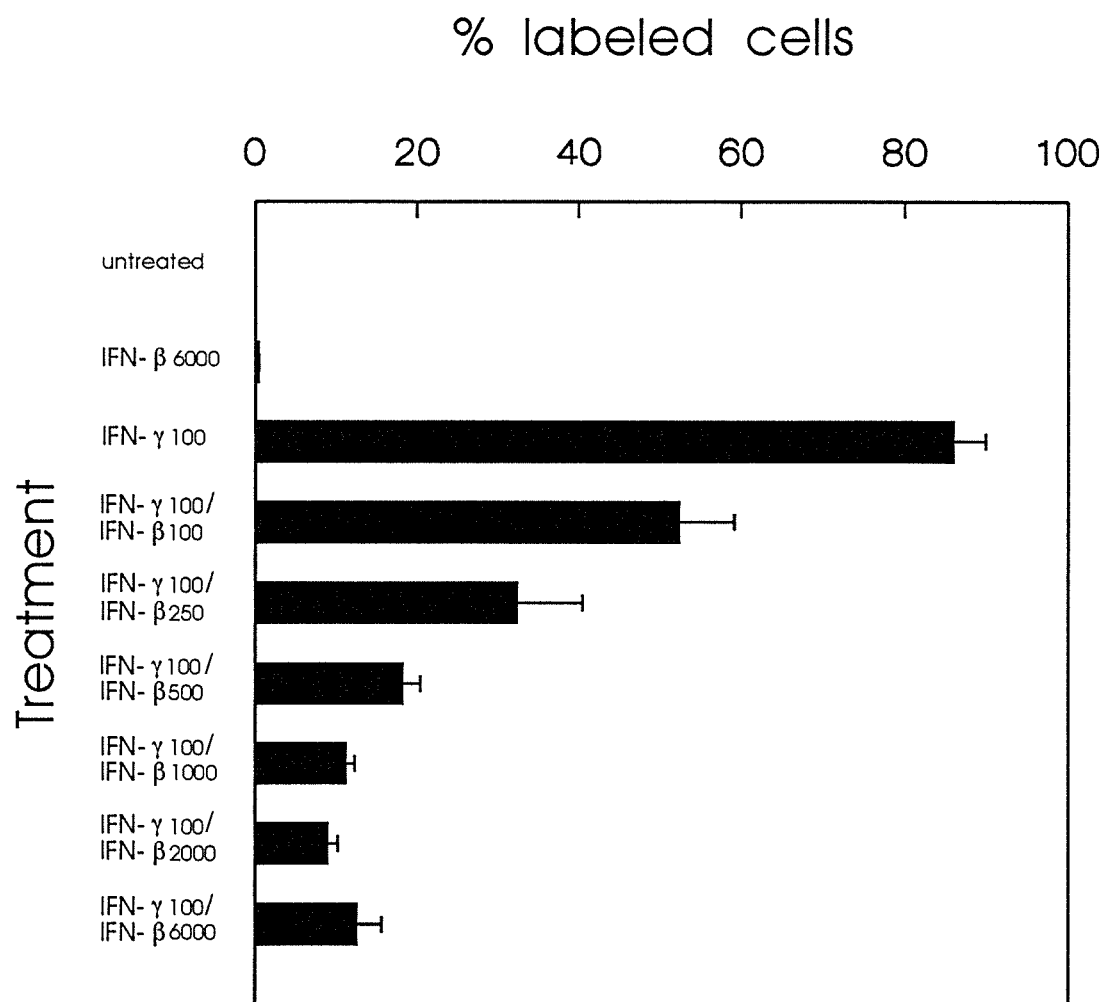


Figure 14: Effects of different treatments of IFN- $\gamma$  and  $\beta$  on Ia Ag expression by HBMEC. Confluent monolayers were left untreated, or treated with IFN- $\beta$  (6,000 units/ml) or IFN- $\gamma$  (100 units/ml) or a combination of IFN- $\gamma$  (100 units/ml) and  $\beta$  (6,000 units/ml) for 4 days, or treated with IFN- $\gamma$  or IFN- $\beta$  alone for 2 days, followed by a combination of IFN- $\gamma$  and  $\beta$  for another 4 days [IFN- $\gamma$ (2) or IFN- $\beta$ (2)/IFN- $\beta$ + $\gamma$ (4)], or with a combination of IFN- $\beta$  (6,000 units/ml) and  $\gamma$  (100 units/ml) for 2 days, followed by IFN- $\gamma$  alone for another 4 days [IFN- $\beta$ + $\gamma$  (2)/IFN- $\gamma$  (4)] and then immunostained for the demonstration of Ia Ag. Results are expressed as percentage of labeled cells in treated and untreated cultures. Bars represent the mean  $\pm$  SEM of triplicate wells of two separate experiments.

**Fig. 14** Effects of different treatments of IFN- $\gamma$  and  $\beta$  on Ia Ag expression by HBMEC

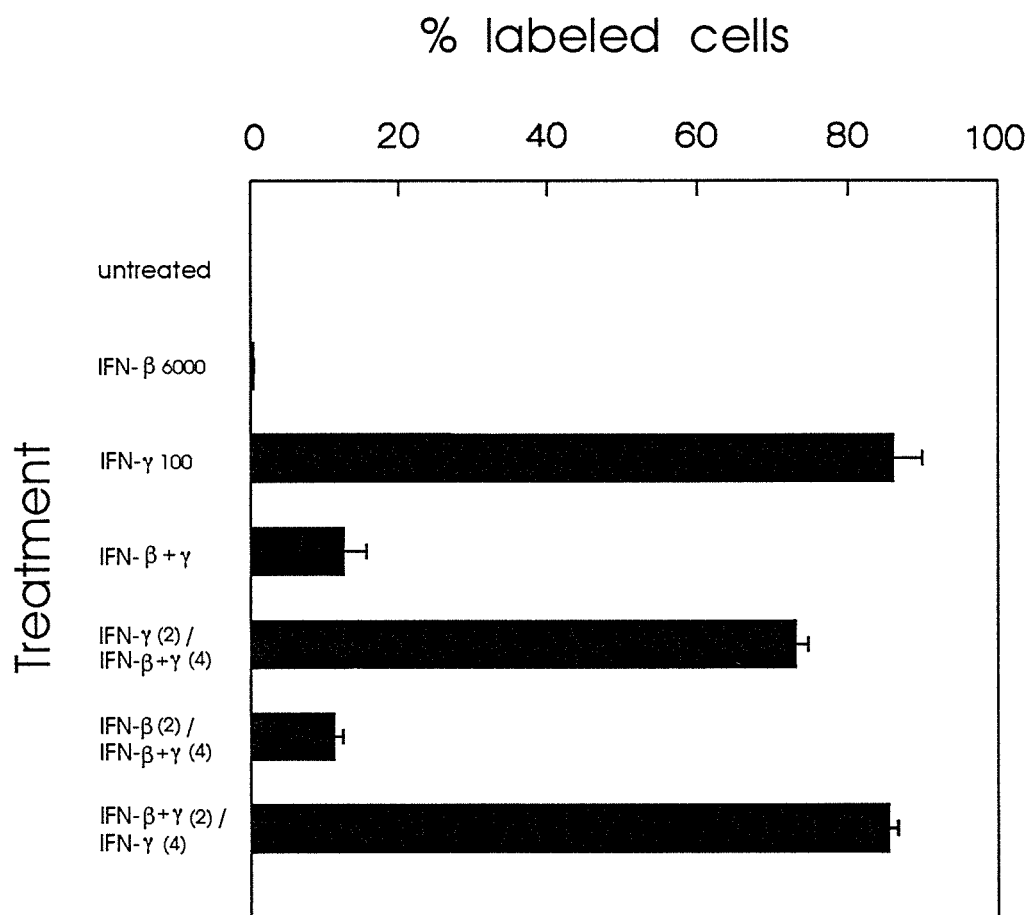


Figure 15: Quantitation by ELISA of Ia Ag expression by HBMEC treated with IFN- $\gamma$  and/or IFN- $\beta$ . Confluent monolayers of HBMEC were left untreated, or treated with IFN- $\gamma$  (100 units/ml), or IFN- $\beta$  (6,000 units/ml), or with a combination of IFN- $\gamma$  (100 units/ml) and  $\beta$  (100 to 6,000 units/ml) for 4 days, or with IFN- $\beta$  or  $\gamma$  alone for 2 days, followed by a combined treatment with IFN- $\beta$  and  $\gamma$  for another 4 days ( $\beta$ 2/ $\gamma$ 2 +  $\beta$  $\gamma$ 4). Values represent mean  $\pm$  SEM of triplicate wells.

Ia Ag expression was measured in triplicate wells of confluent HBMEC cultures.

**Fig. 15** Quantitation by ELISA of Ia Ag expression by HBMEC treated with IFN- $\gamma$  and/or IFN- $\beta$

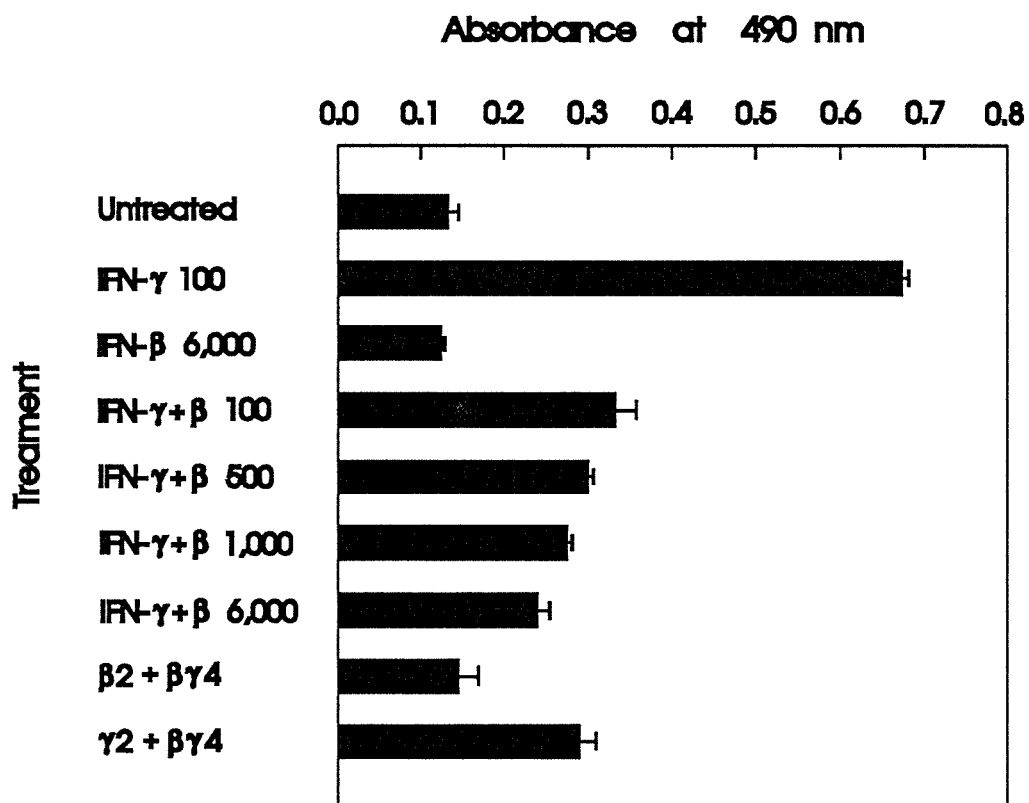


Figure 16: A, HBMEC maintained under standard culture conditions formed highly organized, confluent, contact inhibiting monolayers composed of elongated cells. B, endothelial cells incubated with IFN- $\gamma$  (200 units/ml) for 4 days have become spindle shaped, overlap, and focally arrange themselves into whorls. Bars = 10  $\mu\text{m}$ .

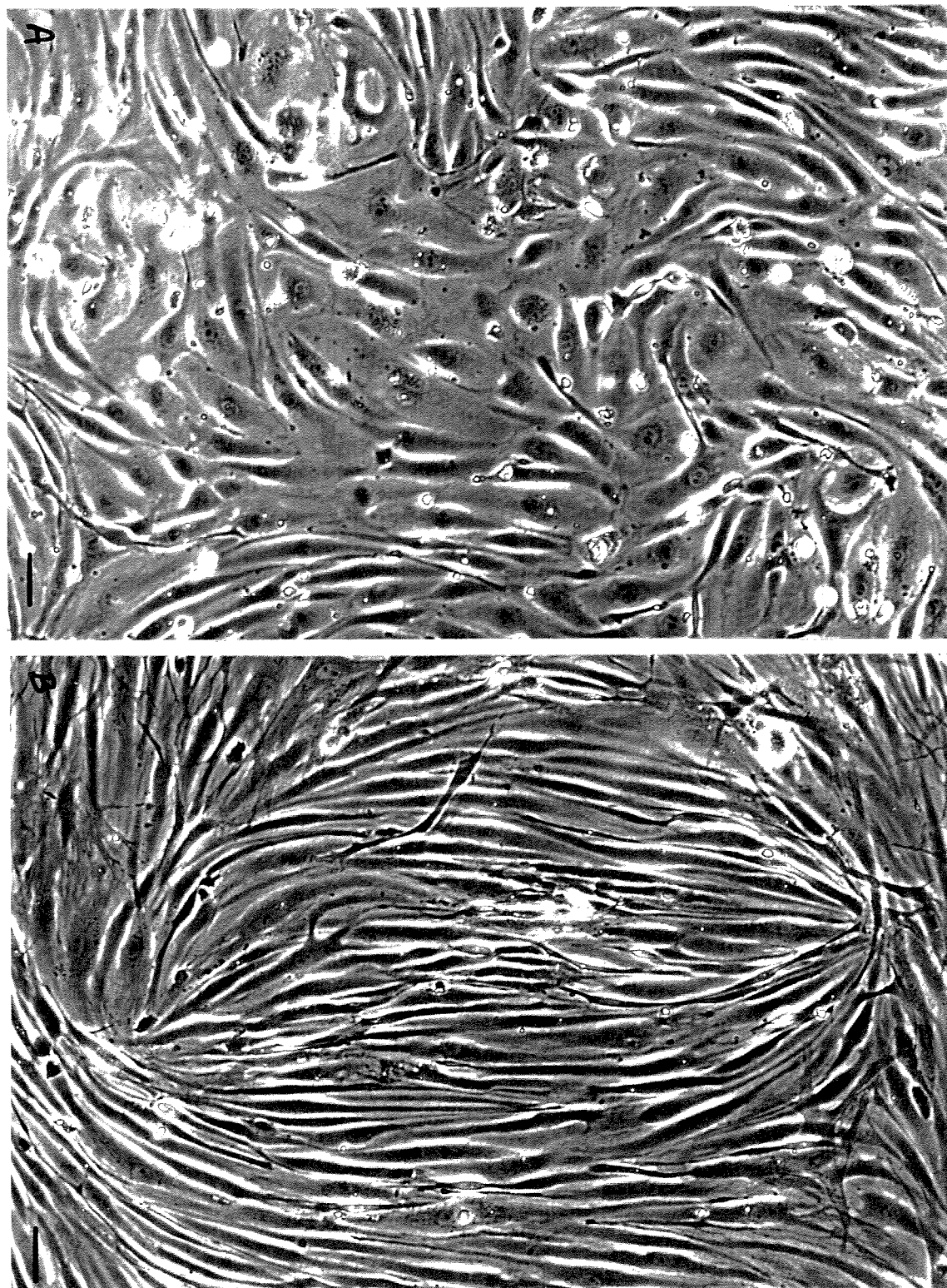


Fig. 16

Figure 17: Scanning electron micrograph of HBMEC grown in the absence (A) or presence (B) of IFN- $\gamma$  in the culture media. A, endothelial cells closely packed without apparent intercellular spaces. Marginal folds (arrows) are present in areas of cell-cell contact. In B, incubation with IFN- $\gamma$  (200 units/ml) for 3 days induces marked attenuation of cell cytoplasm and disorganization of the monolayer due to the tendency of endothelial cell processes to extend over and under adjacent cells. Bars = 20  $\mu\text{m}$ .

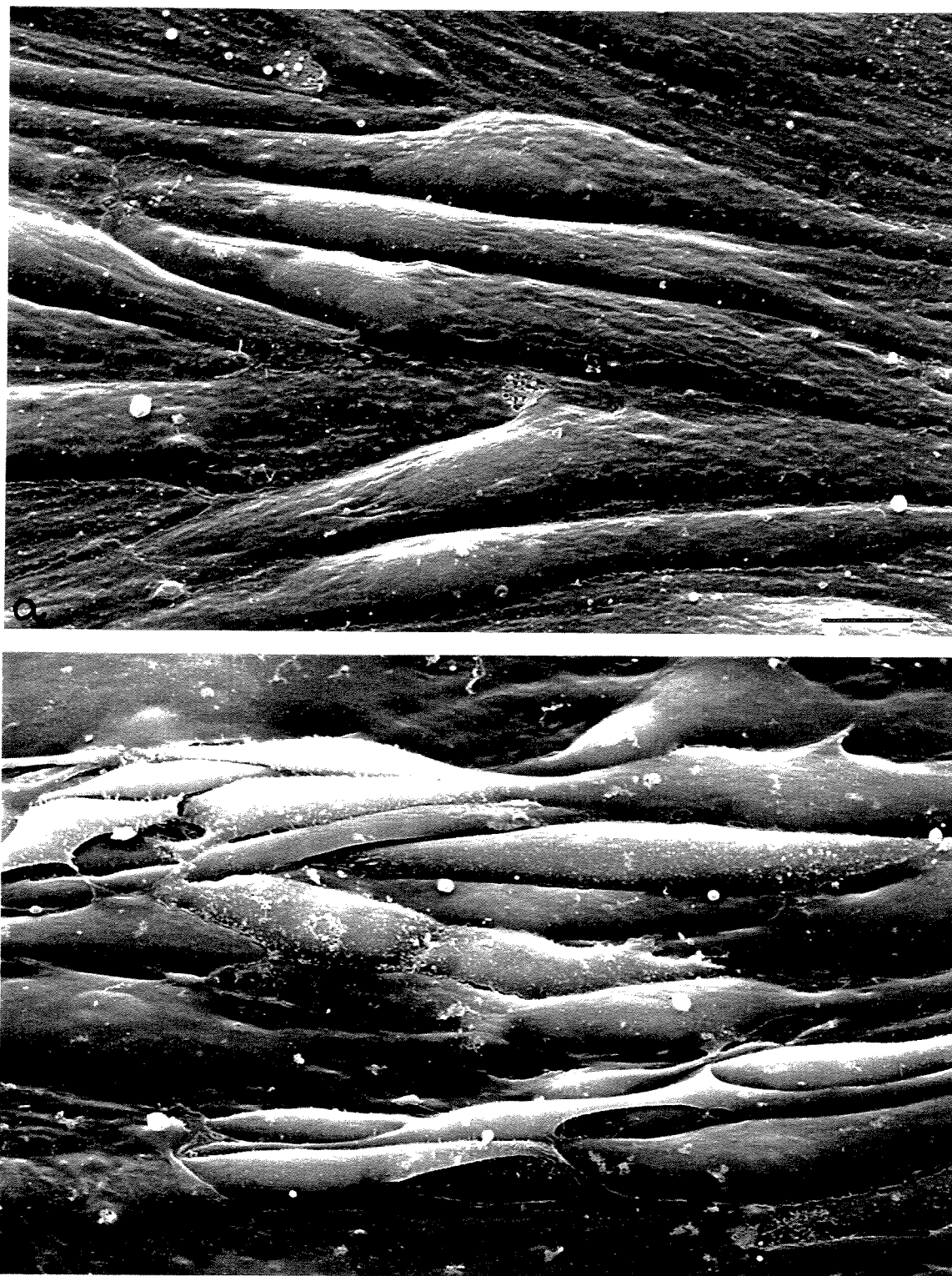


Fig. 17

Figure 18: Effects of IFN- $\gamma$  and  $\beta$  upon the growth of primary cultures of HBMEC. Cells were left untreated or treated from day 1 with IFN- $\gamma$  (150 units/ml) or IFN- $\beta$  (1,000 units/ml) alone, or with a combination of IFN- $\gamma$  and  $\beta$  (100 units/ml and 1,000 units/ml, respectively). Bars represent the mean  $\pm$  SEM of triplicate wells.

**Fig. 18** Effects of IFN- $\gamma$  and  $\beta$  upon the growth of primary cultures of HBMEC

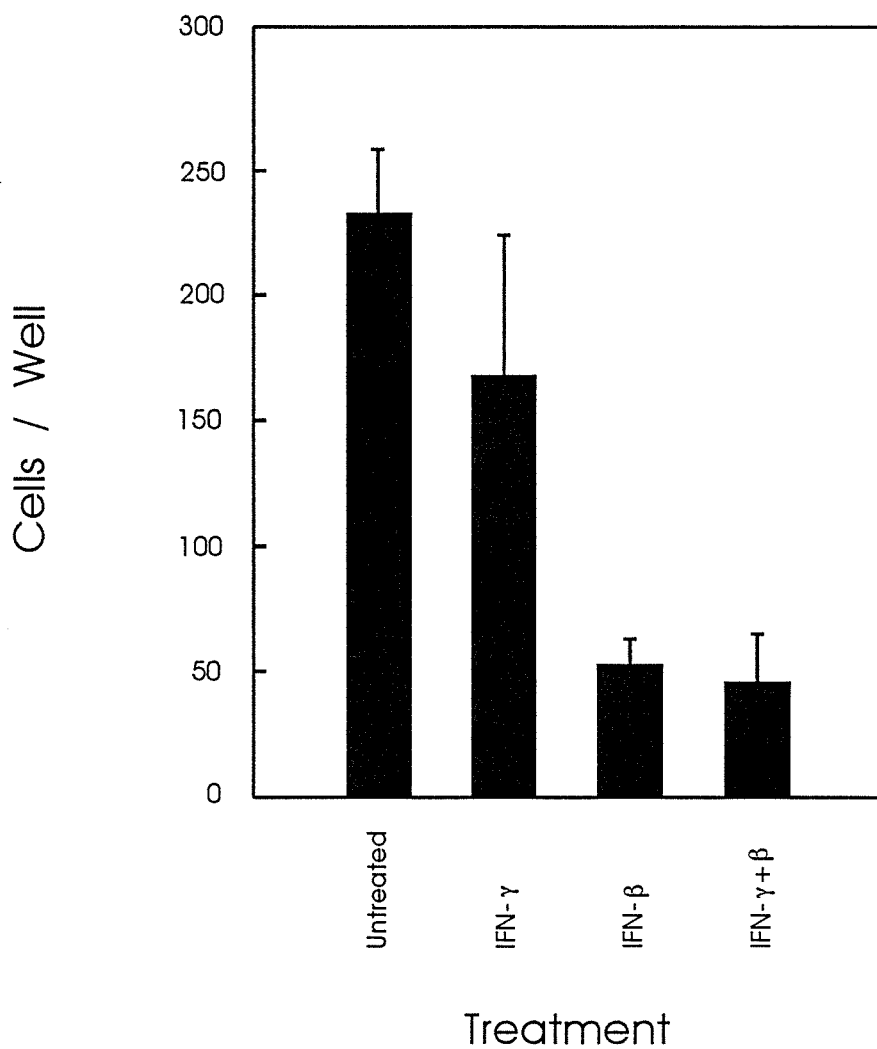


Figure 19: Scanning electron micrograph of HBMEC grown in the presence of IFN- $\beta$  alone (a) or IFN- $\beta$  and  $\gamma$  (b) in the culture media. a) endothelial cells are morphologically identical to untreated cultures, they are closely packed without apparent intercellular spaces. Marginal folds (arrows) are present in areas of cell-cell contact. In b) incubation with a combination of IFN- $\beta$  and  $\gamma$  (6,000 units/ml and 200 units/ml, respectively) prevents the occurrence of the IFN- $\gamma$  induced changes in cell morphology and organization of the monolayers. Arrows point to marginal folds in areas of cell-cell contact. Bars = 50  $\mu\text{m}$ .



Fig. 19 a



Fig. 19 b

Figure 20: Permeability of untreated (A and B) and IFN- $\gamma$ -treated (C - F) confluent HBMEC monolayers to HRP. A, under standard culture conditions, tight junctions at intercellular contacts (between arrowheads) impede the passage of HRP. B, HRP penetrates a short segment of an intercellular cleft from the basal cell surface, forming small deposits at the basal aspect of the cleft (arrowheads) and stopping at a junctional complex (arrow). The remaining interendothelial cleft is free of HRP. Untreated Cultures. In C, following 4 days' incubation with IFN- $\gamma$  (200 units/ml), heavy deposits of HRP are seen under the basal cell surface, and the tracer permeates the entire length of a long intercellular cleft. The proximal portion of the cleft is focally dilated (\*). There is no increase in the pinocytotic activity of the endothelium. D, in monolayers treated with IFN- $\gamma$ , HRP penetrates the intercellular clefts and forms extensive deposits between the layers of overlapping EC. Bars = 0.5  $\mu$ m. E, F, Permeable interendothelial clefts of IFN- $\gamma$  treated monolayers exhibit HRP deposits throughout their length. Bars = 0.5  $\mu$ m.

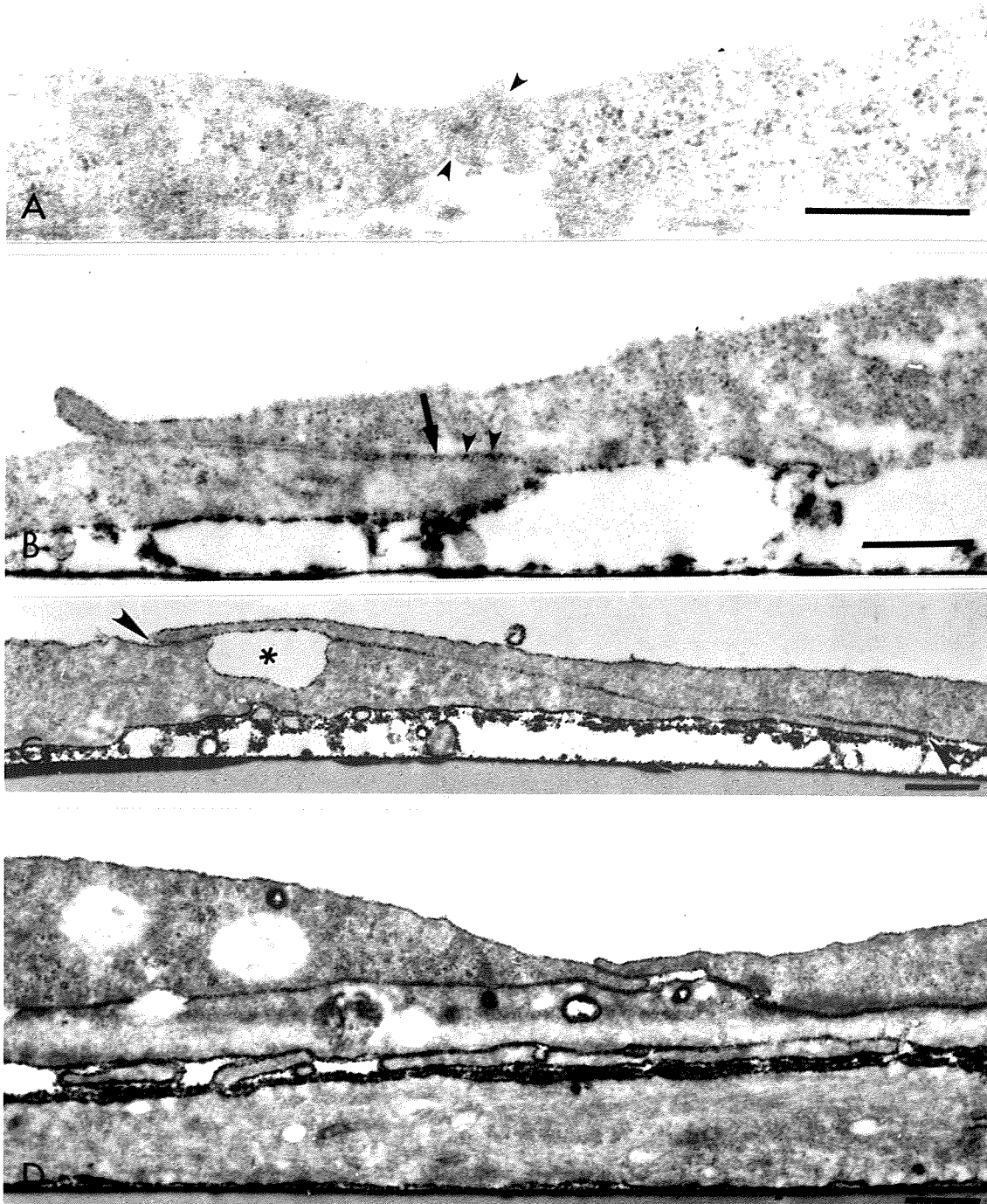


Fig. 20



Fig. 20 E



Fig. 20 F

Figure 21: Expression of IL-2R on resting T cells and anti-CD3 stimulated ( $\alpha$ -CD3) lymphocytes. Approximately 2 fold increase in IL-2R expression is observed when lymphocytes are stimulated with  $\alpha$ -CD3 mAb for 3 days at 37 °C.

**Fig. 21 Expression of IL-2R on Resting and Anti-CD3 stimulated lymphocytes**

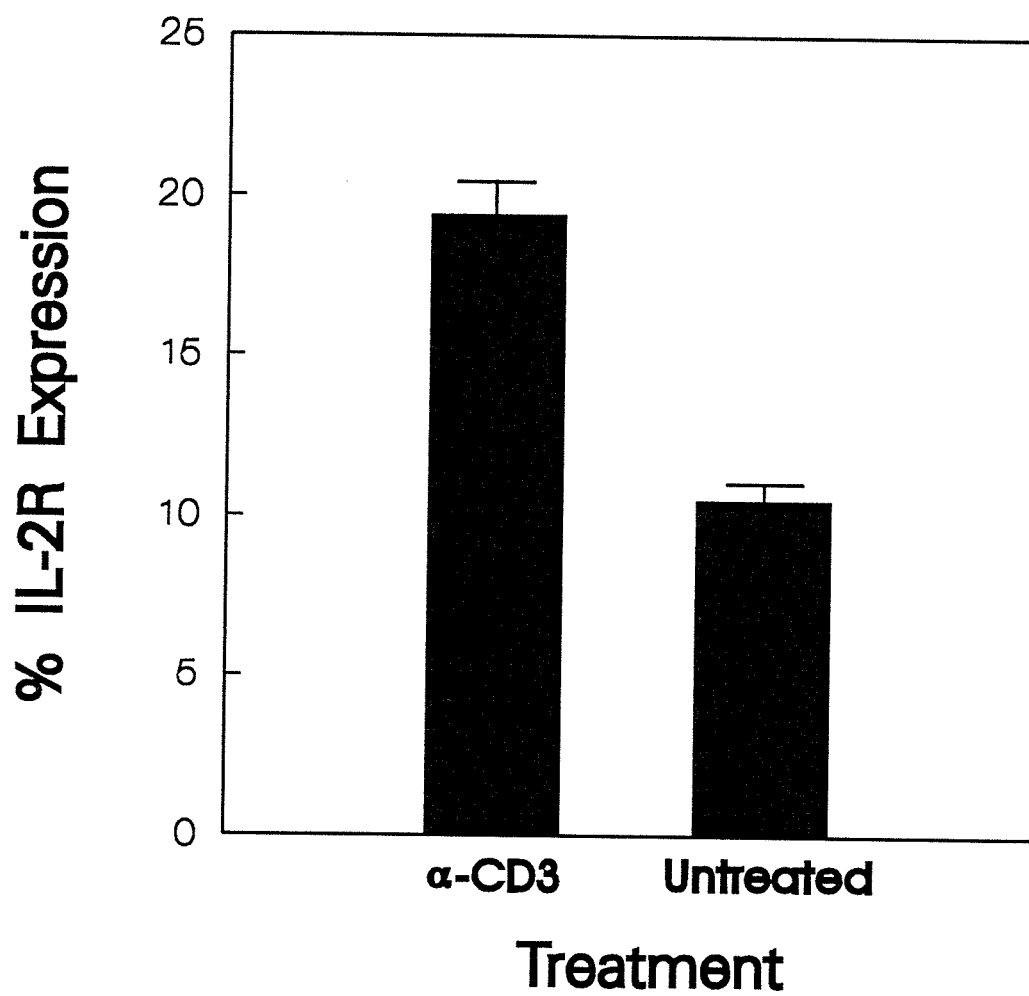


Figure 22: Adhesion of resting T lymphocytes to untreated confluent HBMEC monolayers. At the end of the incubation period, EC cultures with adherent lymphocytes were fixed and stained with the immunoperoxidase technique for leukocyte common antigen (LCA). Small number of LCA positive lymphocytes (L, arrowhead) adhere to the untreated endothelial cells (ec). Bar = 10  $\mu\text{m}$ .

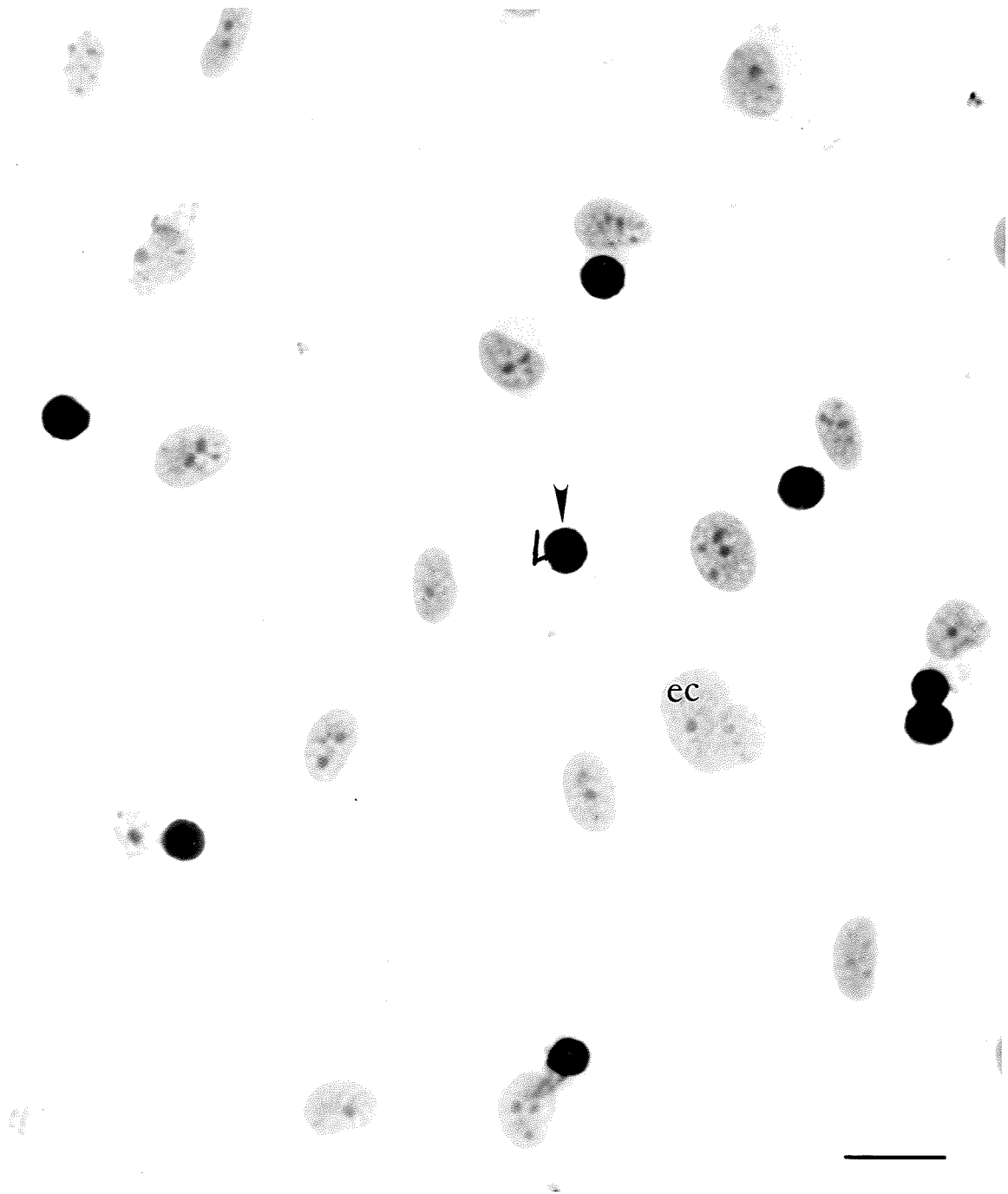


Fig. 22

Figure 23: Adhesion of resting T lymphocytes to IFN- $\gamma$  (150 units/ml) treated HBMEC as demonstrated by immunoperoxidase staining for leukocyte common antigen (LCA). Large numbers of LCA positive lymphocytes (L, arrowhead) adhere to the IFN- $\gamma$  treated endothelial cells (ec). Bar = 10  $\mu$ m.



Fig. 23

Figure 24: Adhesion of resting T lymphocytes to IFN- $\beta$  (2,000 units/ml) treated HBMEC as demonstrated by immunoperoxidase staining for leukocyte common antigen (LCA). A small number of LCA positive lymphocytes (L, arrowhead) adhere to IFN- $\beta$  treated endothelial cells (ec). Bar = 10  $\mu$ m.

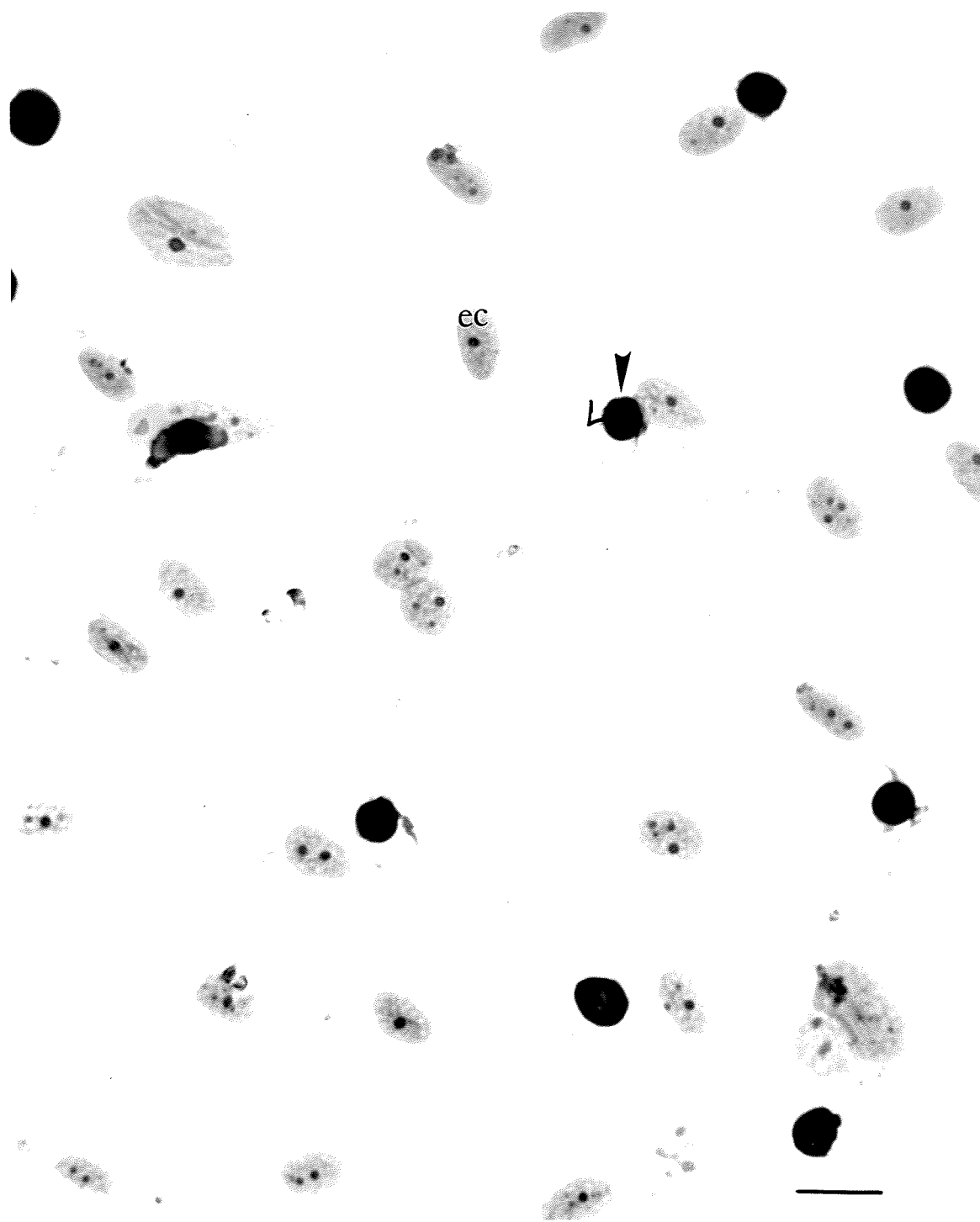


Fig. 24

Figure 25: Adhesion of resting lymphocytes to untreated and cytokine-treated HBMEC. Confluent monolayers of EC were left untreated or treated with IFN- $\gamma$  (150 units/ml) or IFN- $\beta$  (2,000 units/ml), or with a combination of IFN- $\gamma$  (150 units/ml) and  $\beta$  (2,000 units/ml) or IFN- $\gamma$  (150 units/ml) and anti-IFN- $\gamma$  antibody ( $\alpha\gamma$  - 10  $\mu\text{g/ml}$ ) for 3 days prior to incubation with resting T cells. For the mAb blocking studies, cultures were treated with IFN- $\gamma$  for 3 days, followed by 2 hr incubation with anti-human HLA-DR mAb ( $\alpha\text{Ia}$ ) prior to incubation with resting T lymphocytes (T). Bars represent the mean  $\pm$  SEM of triplicate wells of two separate experiments.

**Fig. 25 Adhesion of resting Lymphocytes to untreated and cytokine-treated HBMEC**

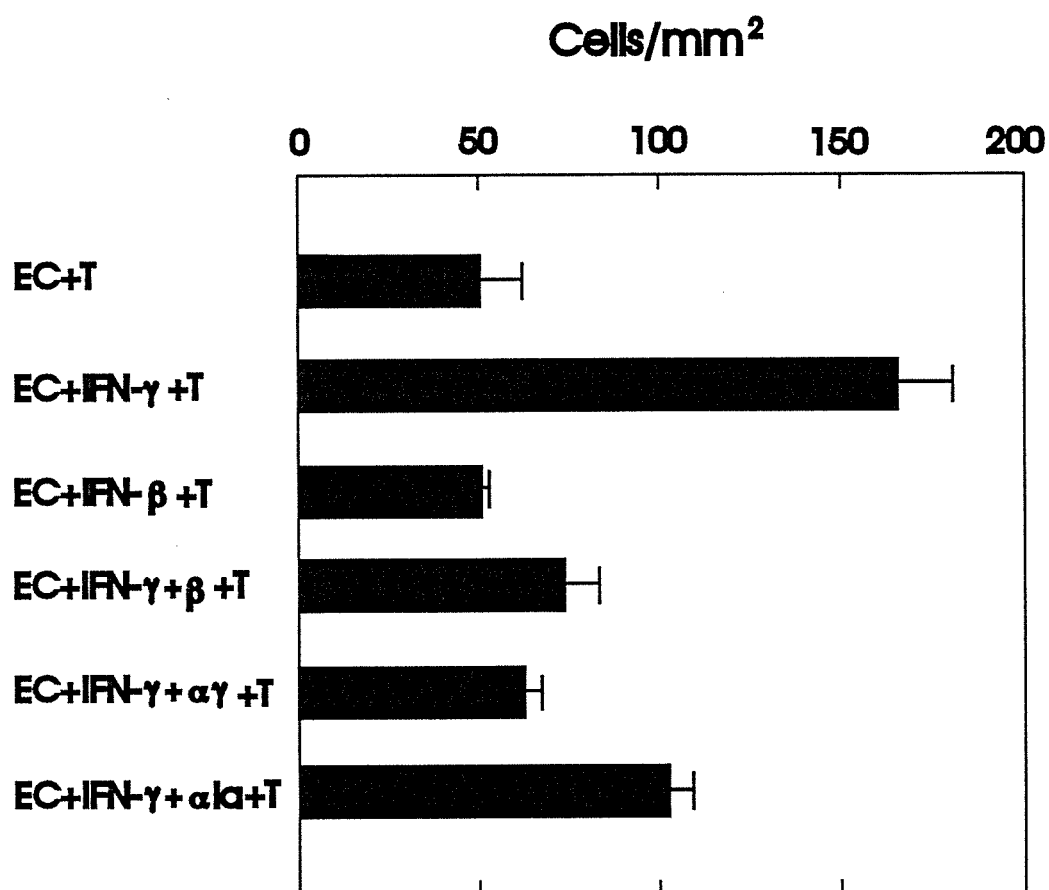


Figure 26: Scanning electron micrograph demonstrating the adhesion of resting T lymphocytes to untreated HBMEC. a) Lymphocytes (L) first adhere to the endothelium (EC) by extending pseudopodia that contact the endothelial surface (arrowhead). Marginal folds (arrow) are present in areas of cell-cell contact. Bar = 20  $\mu\text{m}$ . b) Lymphocytes eventually position themselves between adjacent EC (bar = 4.5  $\mu\text{m}$ ), and c) begin migrating across the monolayer (bar = 1.8  $\mu\text{m}$ ). d) Lymphocytes were infrequently seen penetrating the apical EC plasma membrane (arrowheads) and moving through the endothelial cytoplasm (bar = 4.36  $\mu\text{m}$ ).



Fig. 26 a

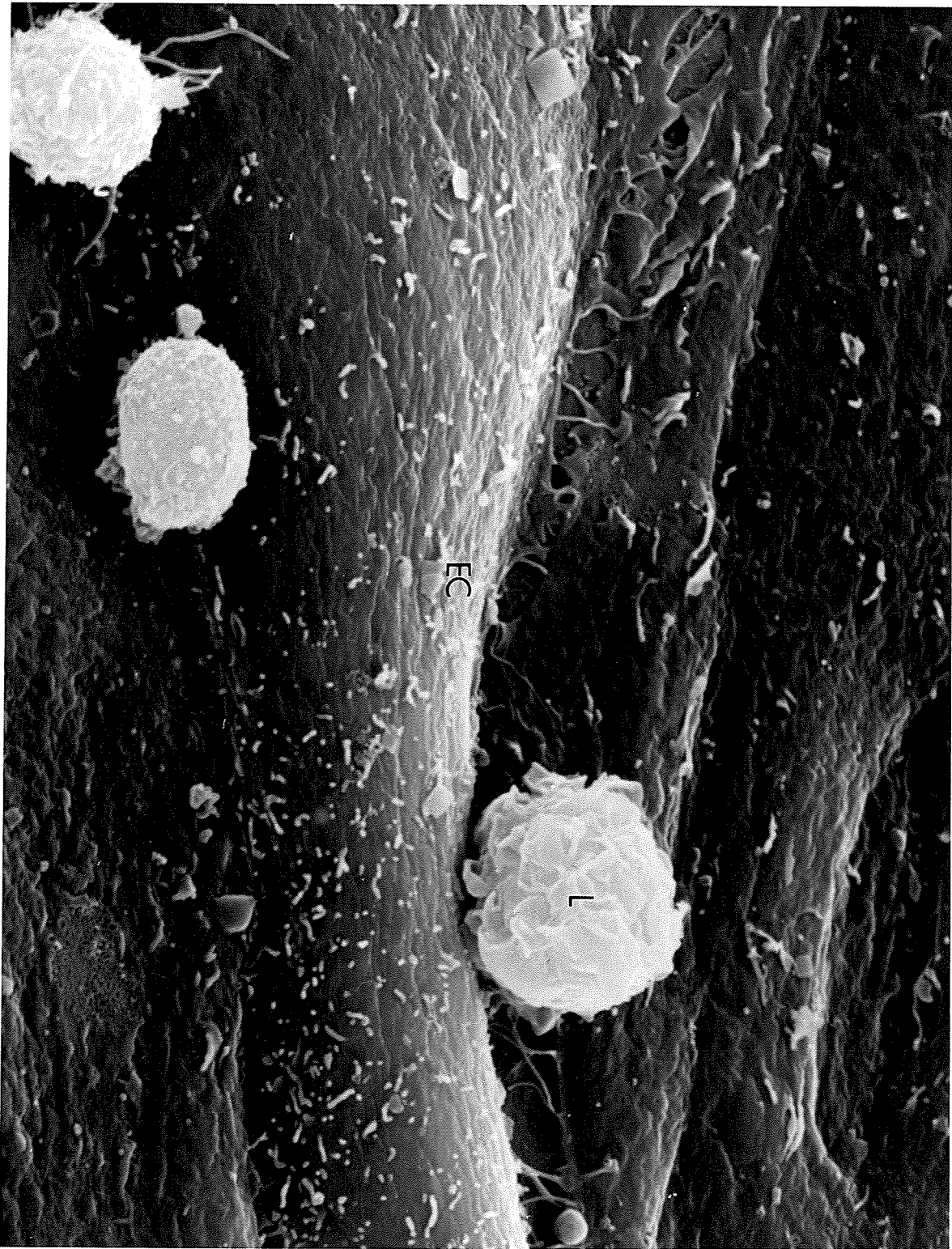


Fig. 266



Fig. 26 C

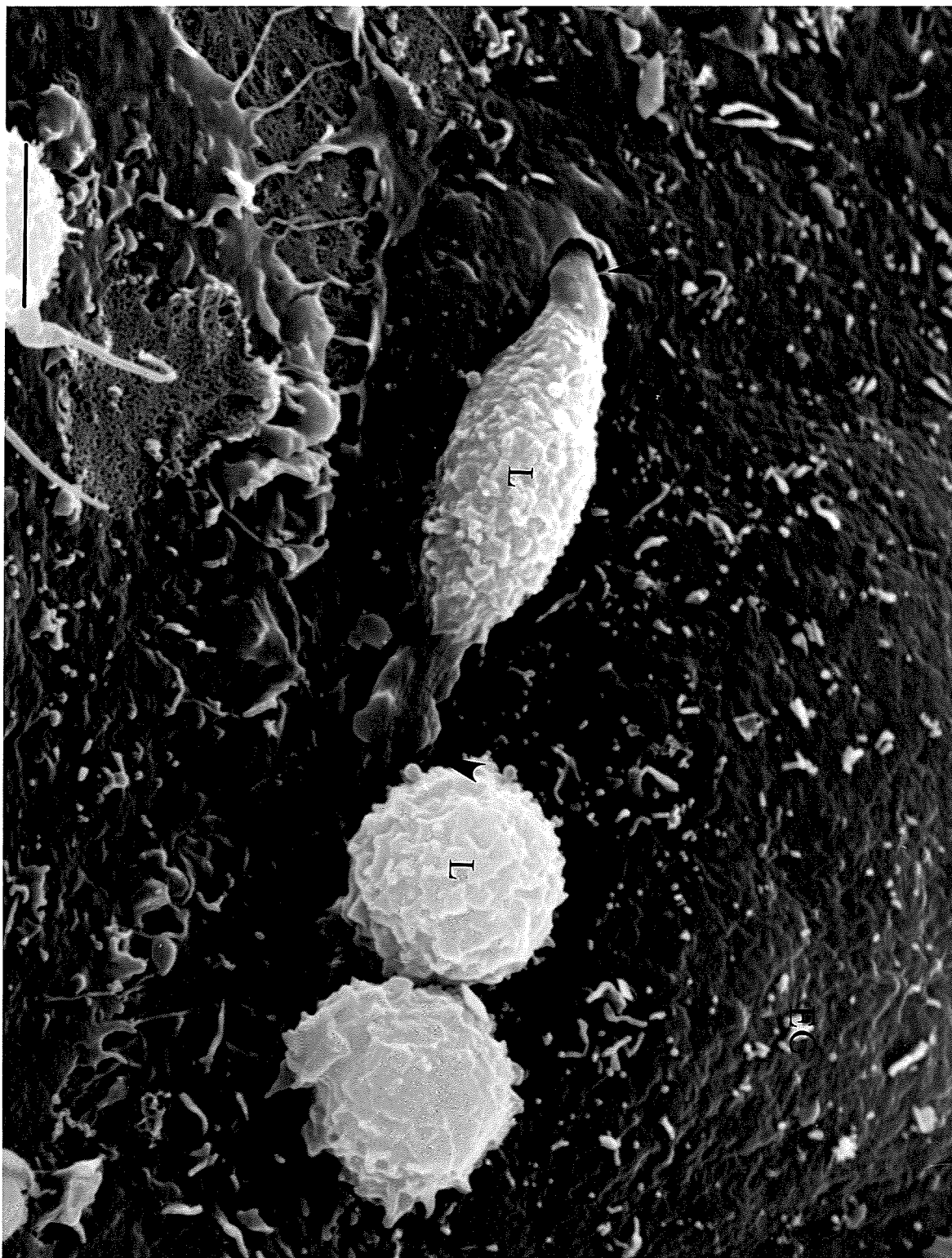


Fig. 26 d

Figure 27: Scanning electron micrograph of the adhesion of resting T lymphocytes to IFN- $\gamma$  (150 units/ml) treated HBMEC. IFN- $\gamma$  treatment of the endothelial cells (EC) induces reorganization of the monolayer and a tendency of EC processes to overlap (arrow). a) Large numbers of lymphocytes (L) establish contact with the endothelium via pseudopodia (arrowheads). Bar = 50  $\mu\text{m}$ . b) Lymphocytes (L), singly or in small aggregates (arrowheads), align themselves along the borders between adjacent EC in preparation for crossing the monolayers. Bar = 20  $\mu\text{m}$ .



Fig. 27a



Fig. 27b

Figure 28: Adhesion of anti-CD3 stimulated T lymphocytes to untreated HBMEC as demonstrated by immunoperoxidase staining for leukocyte common antigen (LCA). Significant numbers of LCA positive activated lymphocytes (L) adhere to untreated endothelial cells (EC). Activated T cells are larger than resting lymphocytes and display irregular, folded, cell membranes. Bar = 10  $\mu$ m.

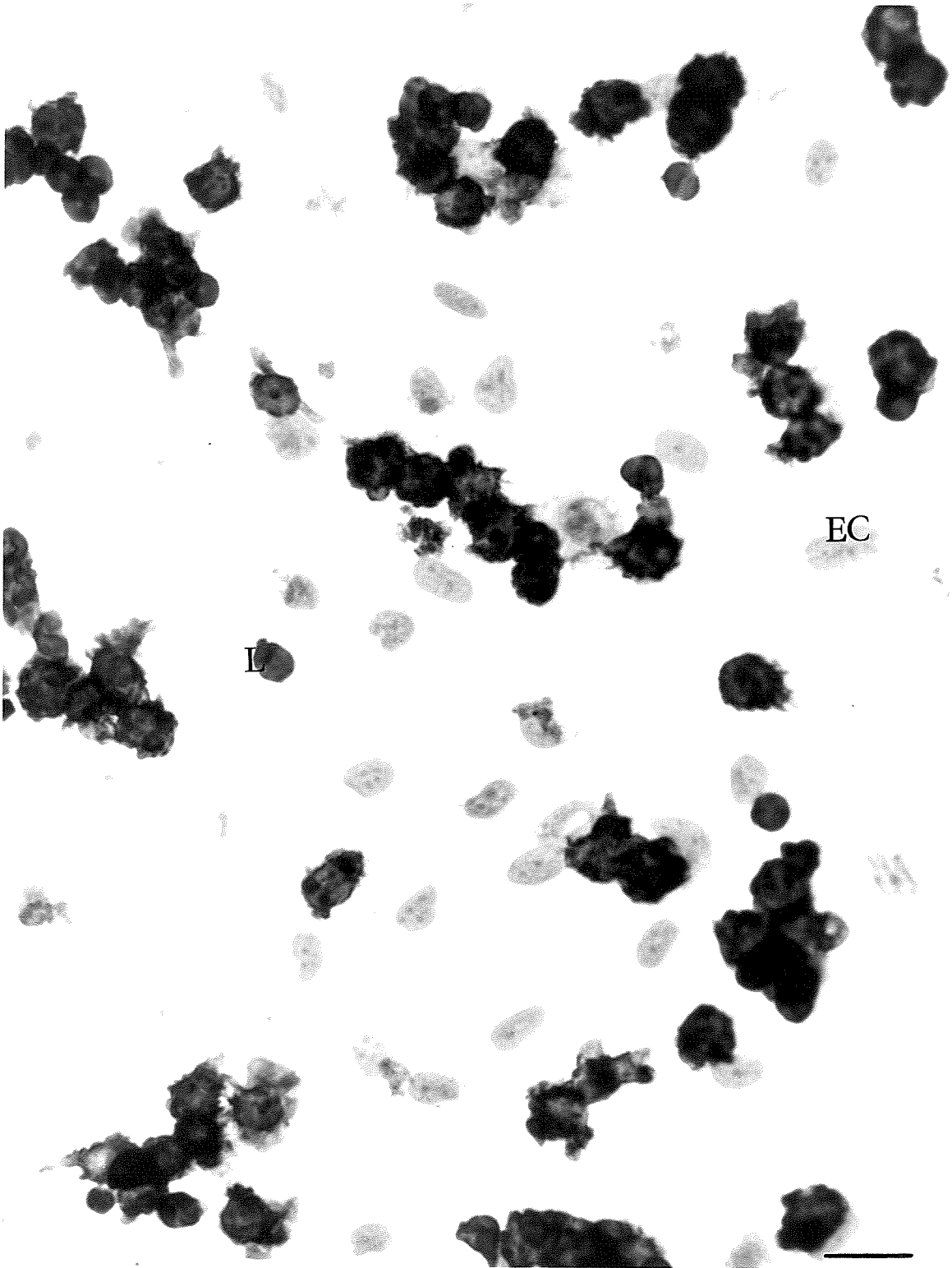


Fig. 28

Figure 29: Adhesion of anti-CD3 stimulated T lymphocytes to IFN- $\gamma$  (150 units/ml) treated HBMEC as demonstrated by immunoperoxidase staining for leukocyte common antigen (LCA). Large numbers of LCA positive activated lymphocytes (L) adhere to endothelial cells (EC). Focally, lymphocytes begin to migrate across the monolayer by extending pseudopodia between EC (arrowheads). Bar = 10  $\mu$ m.

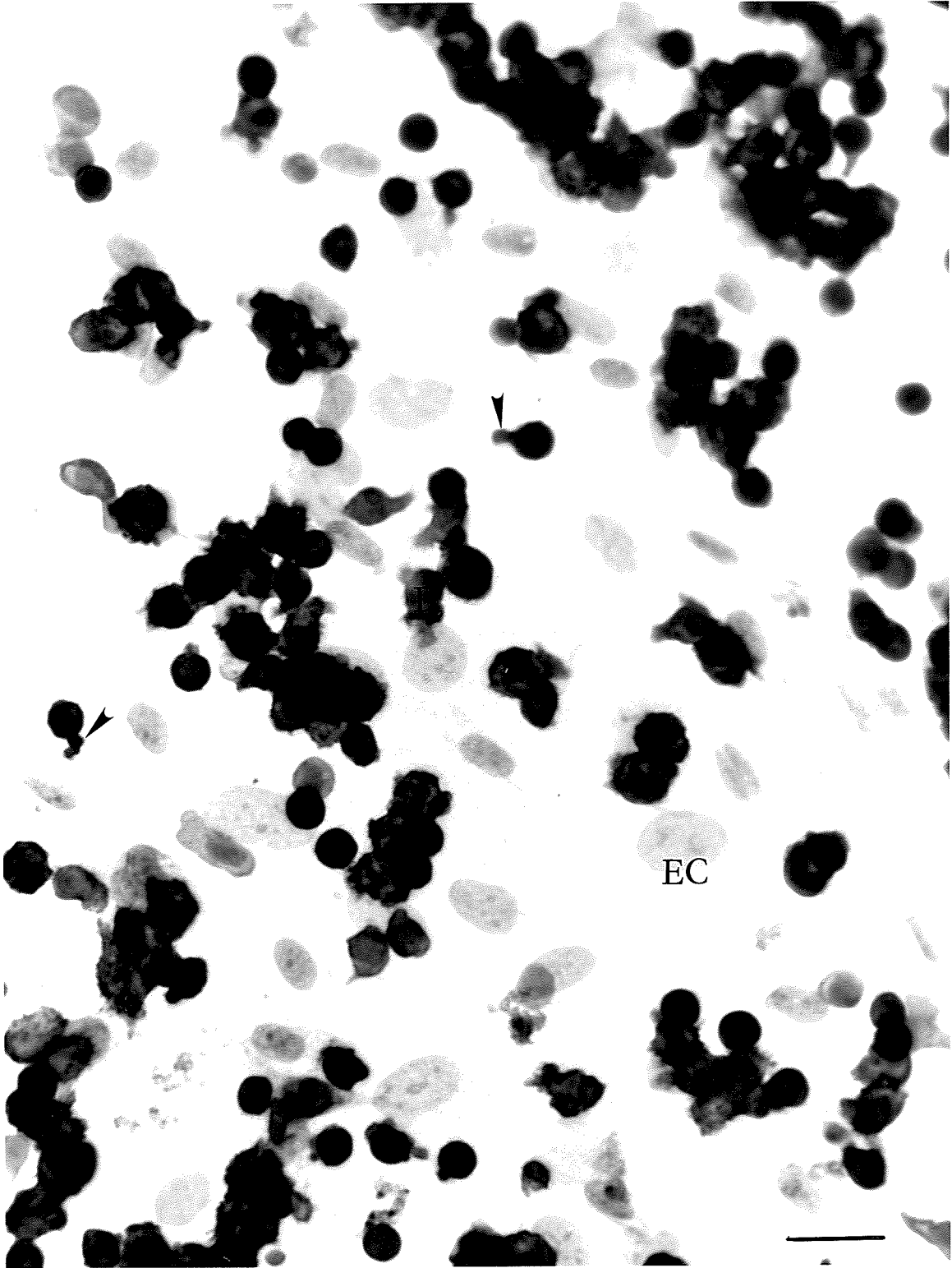


Fig. 29

Figure 30: Adhesion of anti-CD3 stimulated T lymphocytes (L) to IFN- $\gamma$  (150 units/ml) and  $\beta$  (2,000 units/ml) treated HBMEC as demonstrated by immunoperoxidase staining for leukocyte common antigen (LCA). Leucocyte-EC adhesion is comparable to that observed between anti-CD3 stimulated T cells and untreated EC. Bar = 10  $\mu$ m.

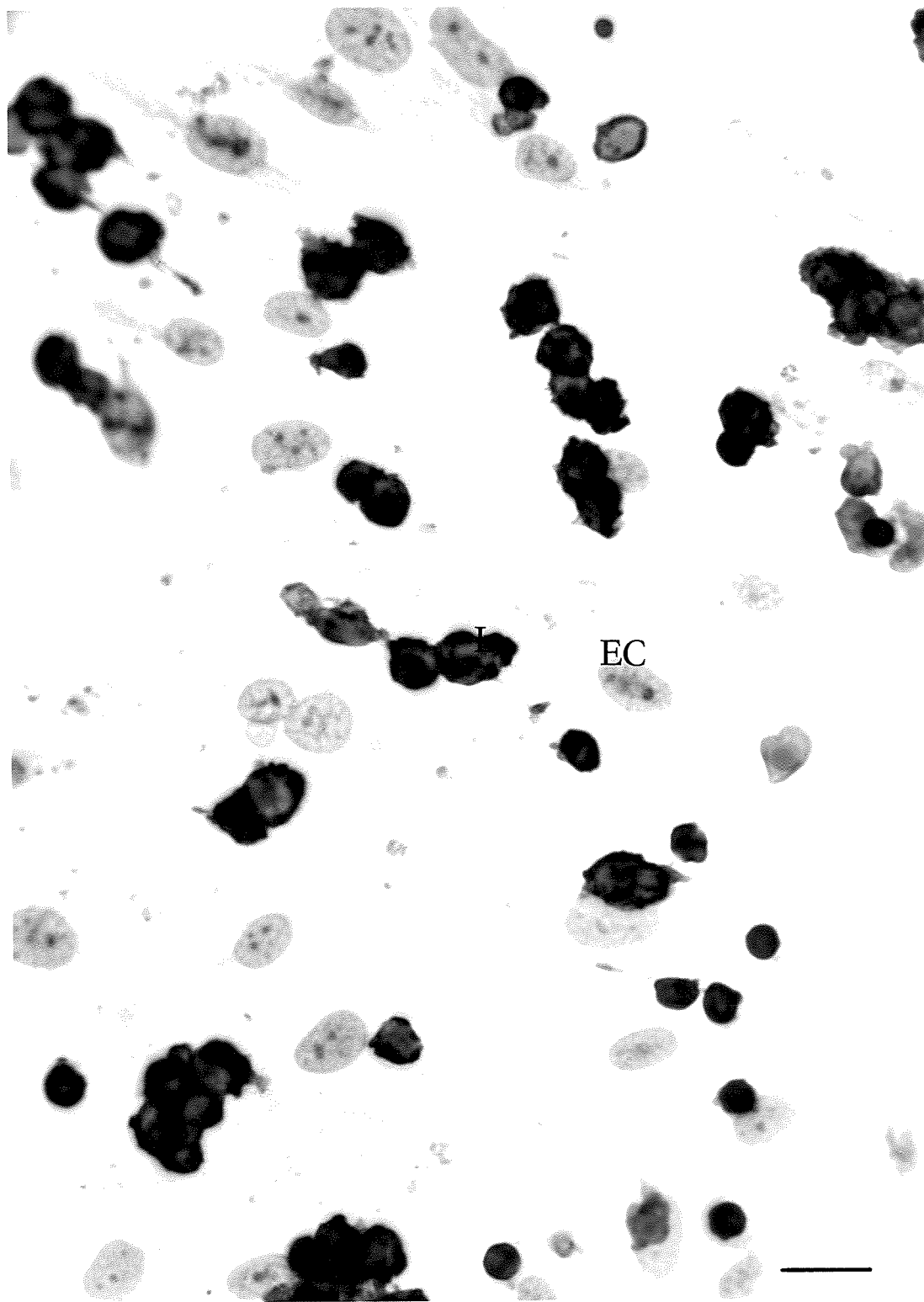


Fig. 30

Figure 31: Adhesion of anti-CD3 activated lymphocytes to untreated and cytokine-treated HBMEC. Confluent monolayers of EC were left untreated or treated with IFN- $\gamma$  (150 units/ml) or IFN- $\beta$  (2,000 units/ml), or with a combination of IFN- $\gamma$  (150 units/ml) and  $\beta$  (2,000 units/ml) or IFN- $\gamma$  (150 units/ml) and anti-IFN- $\gamma$  antibody ( $\alpha\gamma$  - 10  $\mu\text{g/ml}$ ) for 3 days prior to incubation with activated T cells. For the mAb blocking studies, cultures were treated with IFN- $\gamma$  for 3 days, followed by 2 hr incubation with anti-human HLA-DR mAb ( $\alpha\text{Ia}$ ) prior to incubation with activated T lymphocytes (Tcd3). Bars represent the mean  $\pm$  SEM of triplicate wells of two separate experiments.

**Fig. 31 Adhesion of anti-CD3 activated lymphocytes to untreated and cytokine-treated HBMEC**

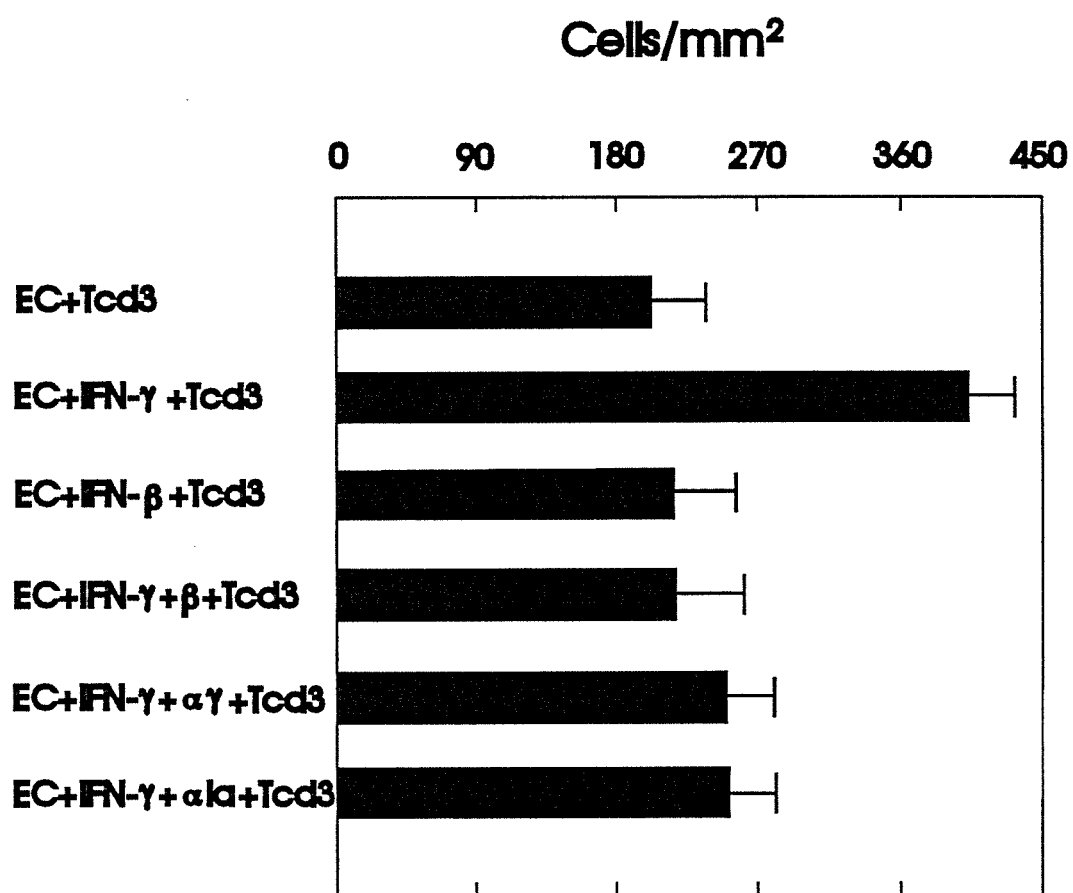


Figure 32: Scanning electron micrograph of the adhesion of activated T lymphocytes to untreated (a) and IFN- $\gamma$  (150 units/ml) treated HBMEC (b, c). IFN- $\gamma$  treatment of endothelial cells (EC) induces overlapping of EC processes (\* in b). Activated lymphocytes (L) adhere to the endothelium (EC) in large numbers, and they appear enlarged and exhibit a ruffled cell membrane with numerous folds in comparison to the resting lymphocytes (r) (arrowheads). Activated lymphocytes establish close contact with EC by means of cytoplasmic projections (small arrows) and usually position themselves along the borders between adjacent EC in both untreated and IFN- $\gamma$  treated EC. Protuberances on the apical surface of the endothelium, having the size and shape of an activated T cell, indicate movement through the EC cytoplasm (large arrows) (a - c). Bars = 50  $\mu\text{m}$  (a ,b) and 19  $\mu\text{m}$  (c).



Fig. 32a

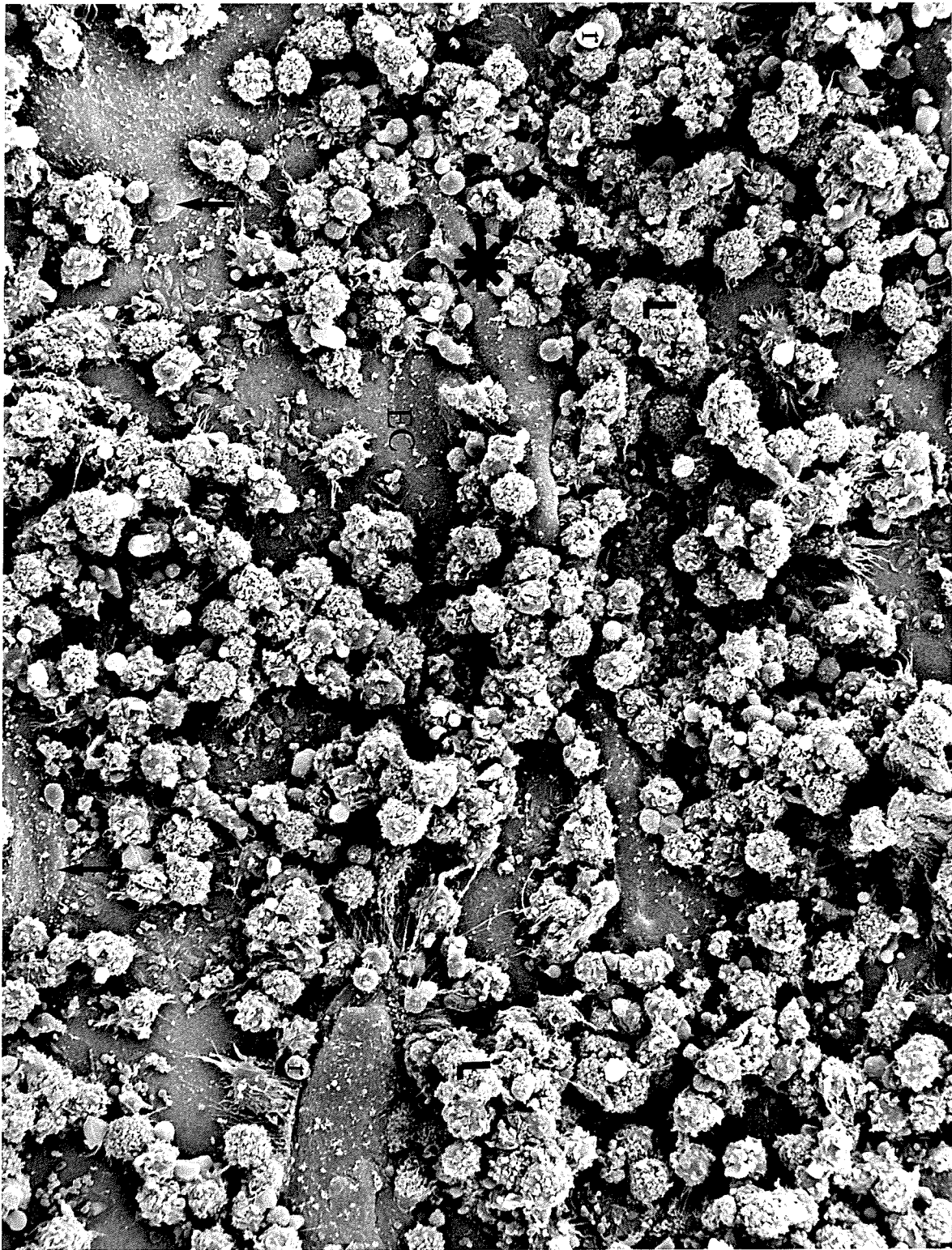


Fig. 32 b

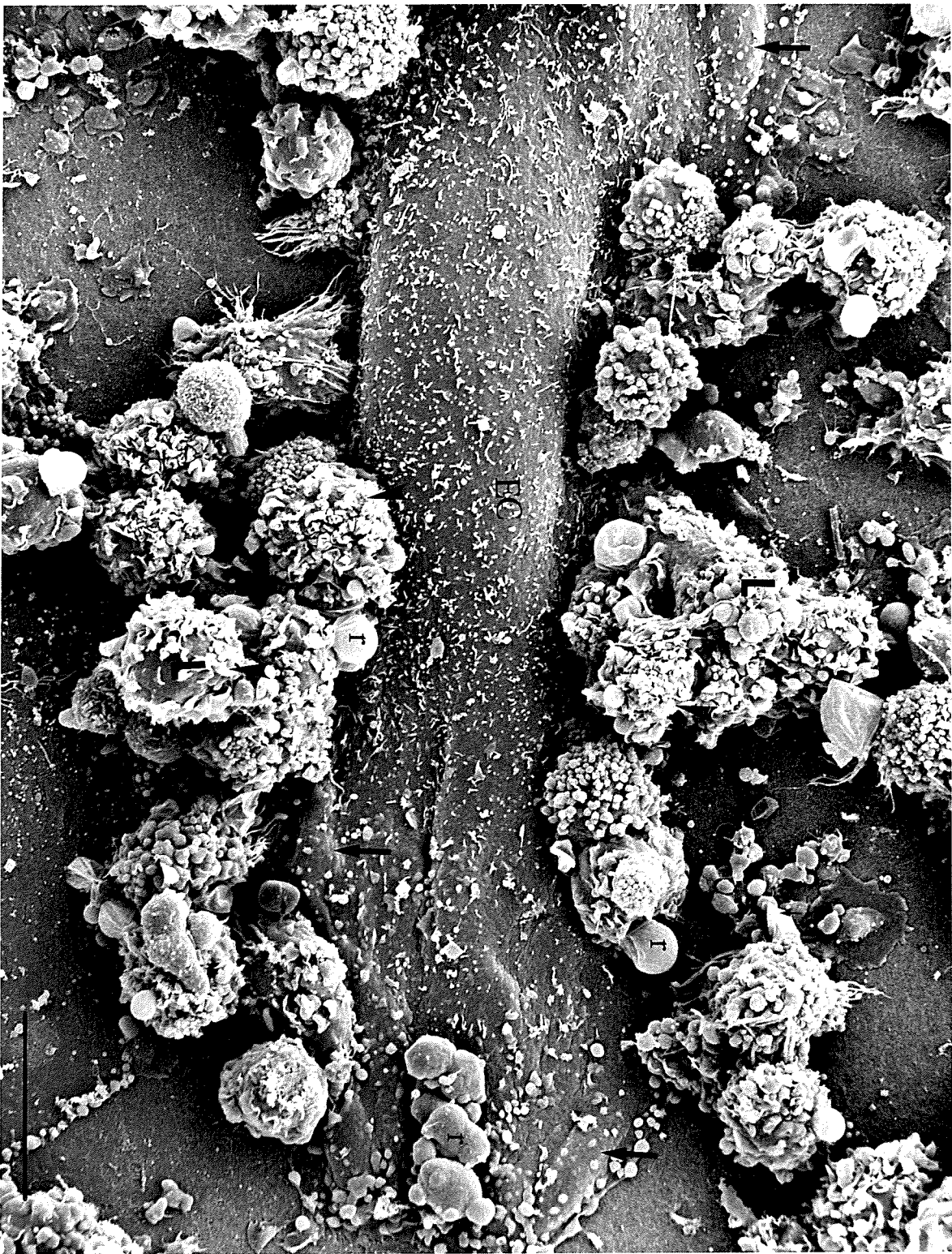


Fig. 32c

Figure 33: Adhesion anti-CD3 activated lymphocytes to untreated HBMEC. Activated lymphocytes (L) display abundant cytoplasm, increased numbers of mitochondria (m) and variable numbers of cytoplasmic vacuoles (V) containing amorphous, flocculent material. Several points of close cell to cell contact between endothelium (EC) and processes of adherent lymphocytes are present (arrows). C, collagen membrane. Bar = 1  $\mu\text{m}$ .

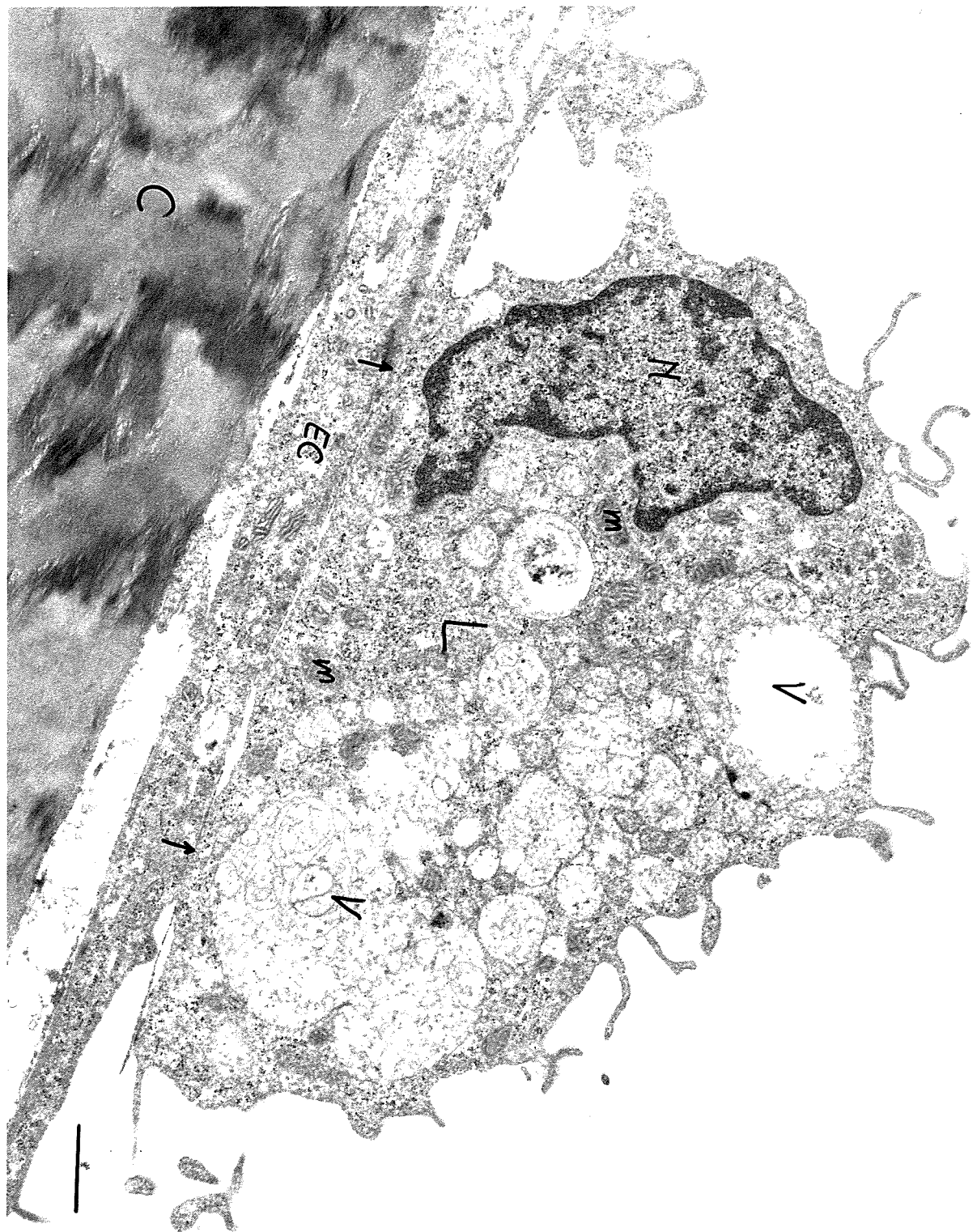


Fig. 33

Figure 34: Adhesion of anti-CD3 stimulated T cells to untreated HBMEC. The cell surface of activated T lymphocytes (L) is extremely irregular due to the presence of numerous thin, finger-like cytoplasmic processes (arrows). Variable numbers of cytoplasmic vacuoles (V) containing amorphous, flocculent material are present in the lymphocyte cytoplasm. EC, endothelial cell; N, nucleus; C, collagen membrane. Bar = 1  $\mu$ m.

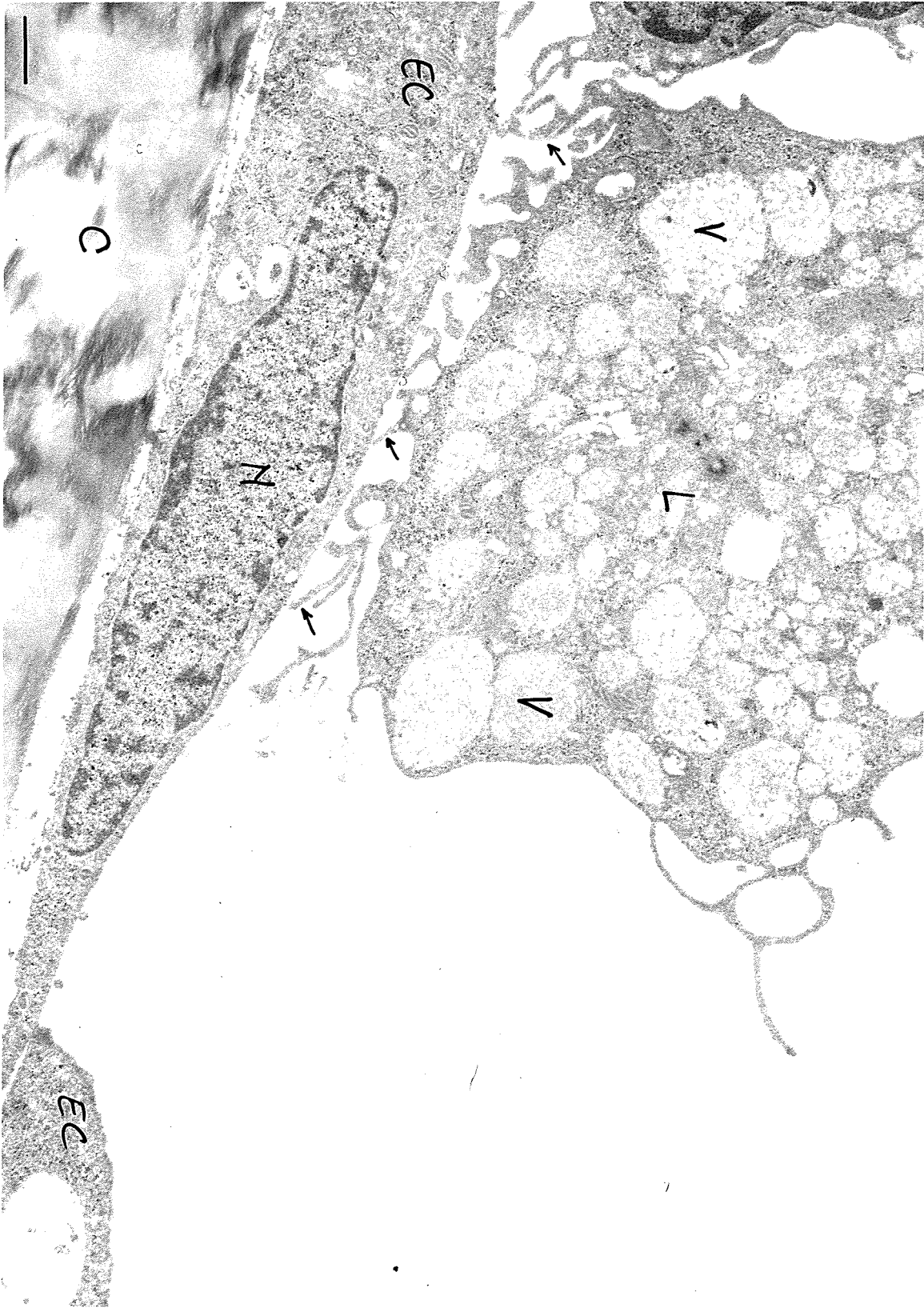


Fig. 34

Figure 35: Adhesion of resting lymphocytes (L) to IFN- $\gamma$  (150 units/ml) and anti-human HLA-DR mAb treated HBMEC as demonstrated by immunoperoxidase staining for leukocyte common antigen (LCA). Few LCA positive lymphocytes adhere to endothelial cells (EC). Bar = 10  $\mu$ m.

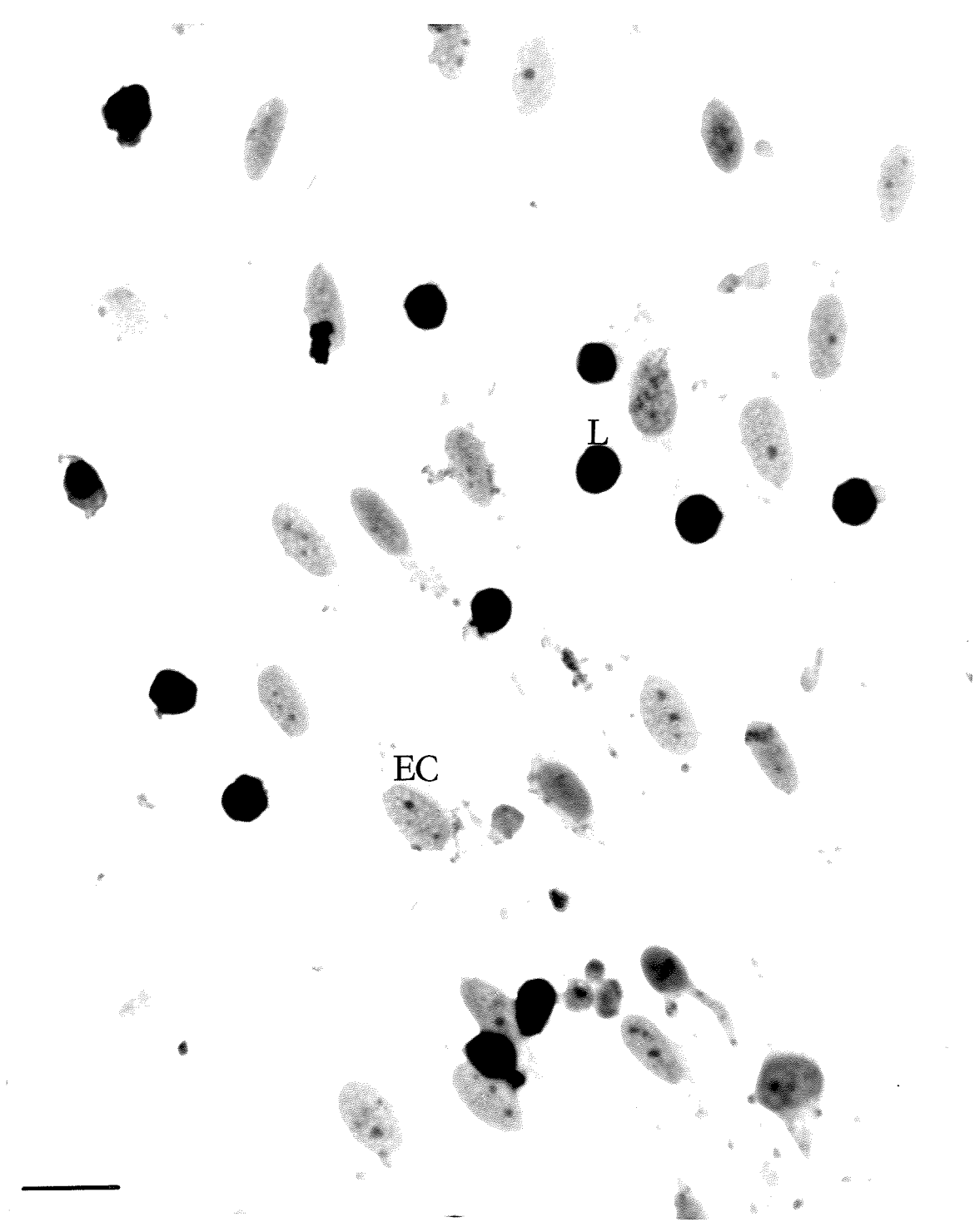


Fig. 35

Figure 36: Adhesion of anti-CD3 stimulated lymphocytes (L) to IFN- $\gamma$  (150 units/ml) and anti-human HLA-DR mAb treated HBMEC as demonstrated by immunoperoxidase staining for leukocyte common antigen (LCA). The number of lymphocytes adhering to endothelial cells (EC) is comparable to that observed in the absence of pretreatment with mAb. Bar = 10  $\mu$ m.

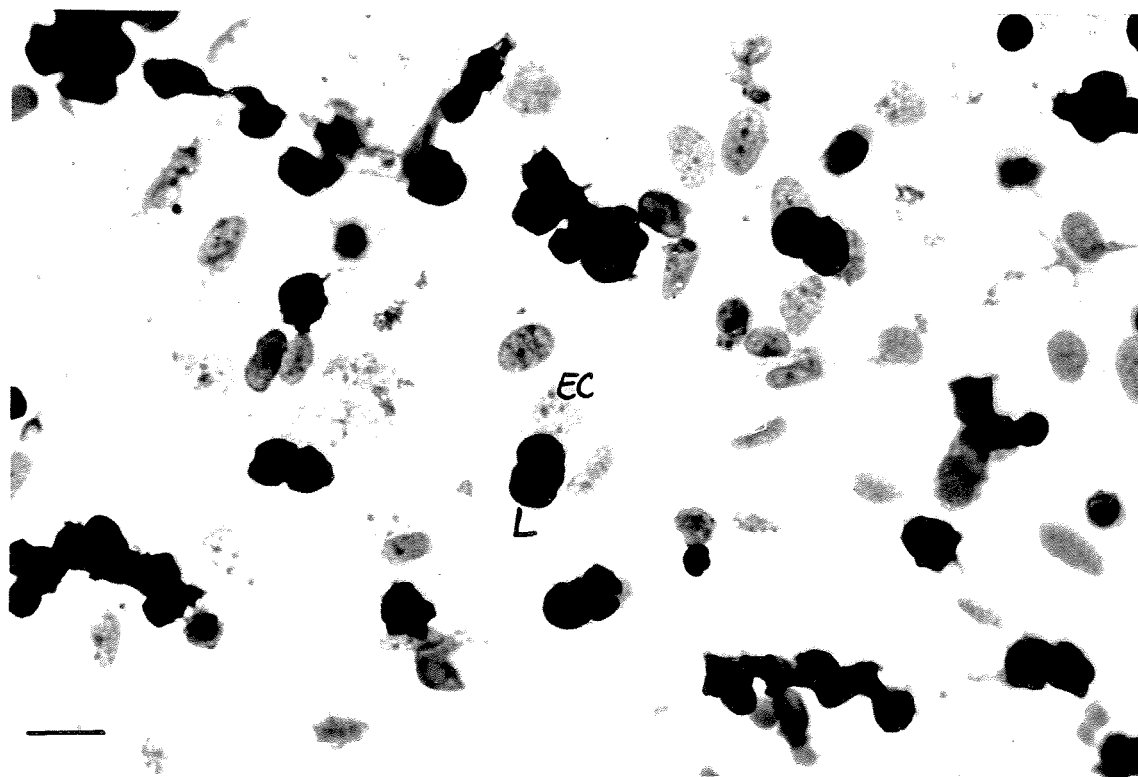


Fig. 36

Figure 37: a) Transendothelial migration of resting T lymphocytes (arrow) across untreated HBMEC (EC) monolayers is minimal. C, collagen membrane. b) Significant increase in migration of lymphocytes (arrows) was observed in HBMEC pretreated with IFN- $\gamma$  (150 units/ml) for 3 days. c) Coincubation of EC with IFN- $\gamma$  (150 units/ml) and  $\beta$  (2,000 units/ml) for 3 days, significantly suppresses the IFN- $\gamma$ -enhanced migration (arrow). Bars = 10  $\mu\text{m}$  (a-c).

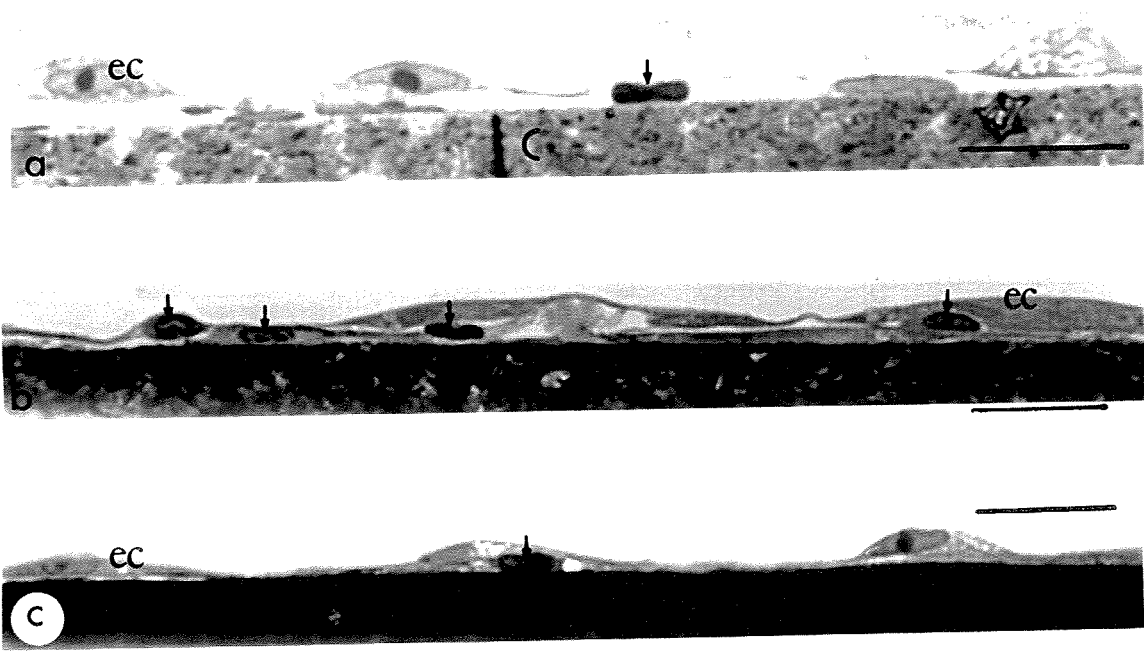


Fig. 37

Figure 38: Migration of resting and anti-CD3 stimulated T lymphocytes across untreated and IFN- $\gamma$  and/or IFN- $\beta$  treated HBMEC. Confluent monolayers of EC were left untreated or treated with IFN- $\gamma$  (150 units/ml) or IFN- $\beta$  (2,000 units/ml), or with a combination of IFN- $\gamma$  (150 units/ml) and  $\beta$  (2,000 units/ml) for 3 days prior to incubation with resting (T) or anti-CD3 stimulated lymphocytes (Tcd3) for 3 hours. For the blocking studies, EC were treated for 3 days with IFN- $\gamma$  (150 units/ml), followed by 2 hours of incubation with anti-human HLA-DR ( $\alpha$ Ia) mAb before incubating with T or Tcd3 for 3 hours. Bars represent the mean  $\pm$  SEM of 200 different levels.

**Fig. 38 Migration of resting and anti-CD3 activated T cells across untreated and IFN- $\gamma$  and/or IFN- $\beta$  treated HBMEC**

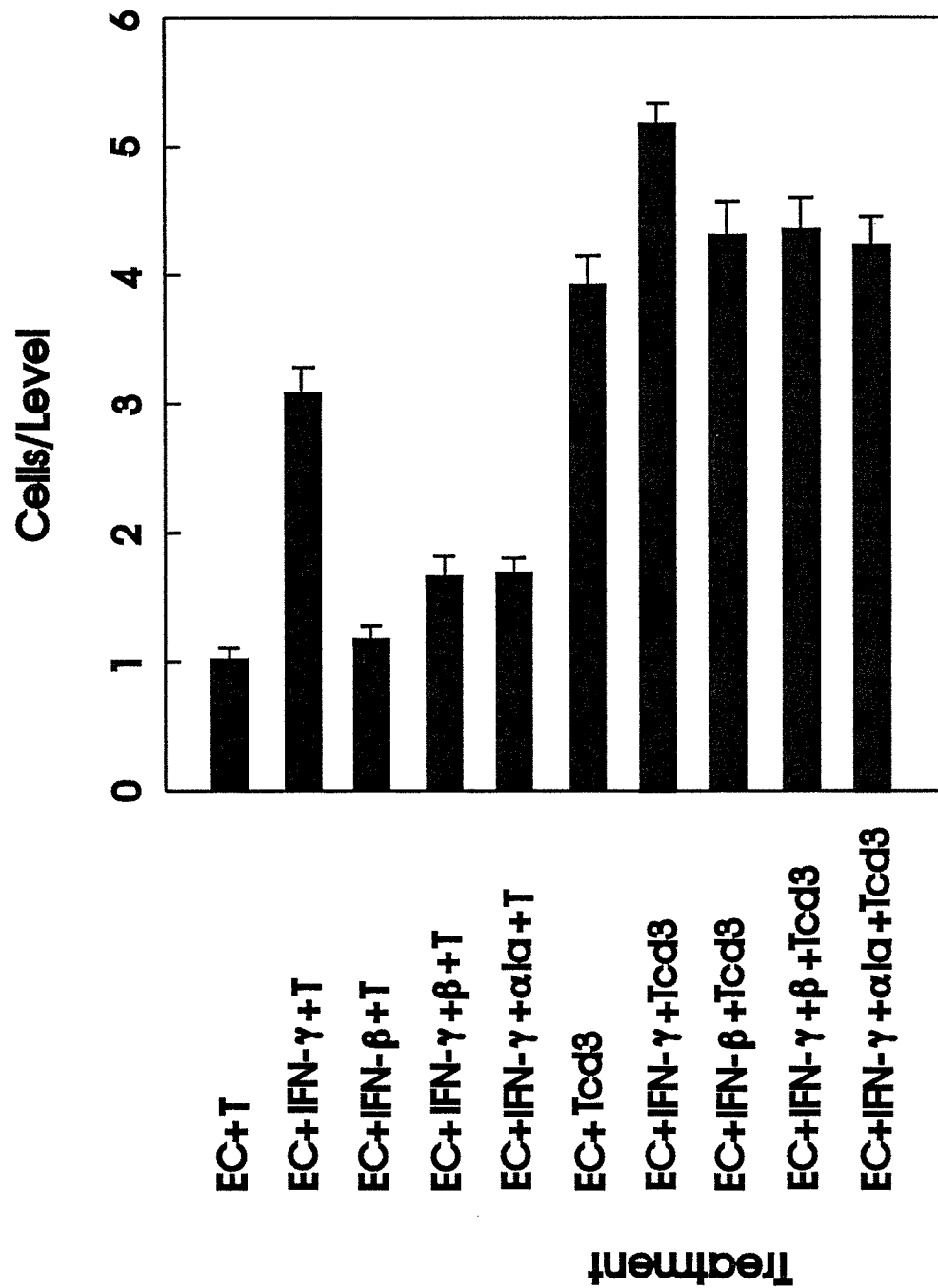


Figure 39: Migration of resting T lymphocytes across untreated HBMEC monolayers (a - d). a) A lymphocyte (L) initiates its migration across the endothelial cell (EC) monolayers by directing cytoplasmic processes between two adjacent EC. N, nucleus; C, collagen membrane. Bar = 1  $\mu\text{m}$ . b and c) Part of the cytoplasm and nucleus moves between two adjacent EC. The cell membranes of the T cell and EC are closely apposed. Bars= 2  $\mu\text{m}$  for (b) and 1  $\mu\text{m}$  for (c). d) At the end of the migration period, the lymphocytes position themselves between the overlying EC and underlying collagen membrane and become elongated and flattened. The processes of the overlying EC have been resealed (arrow). Bar = 1  $\mu\text{m}$ .

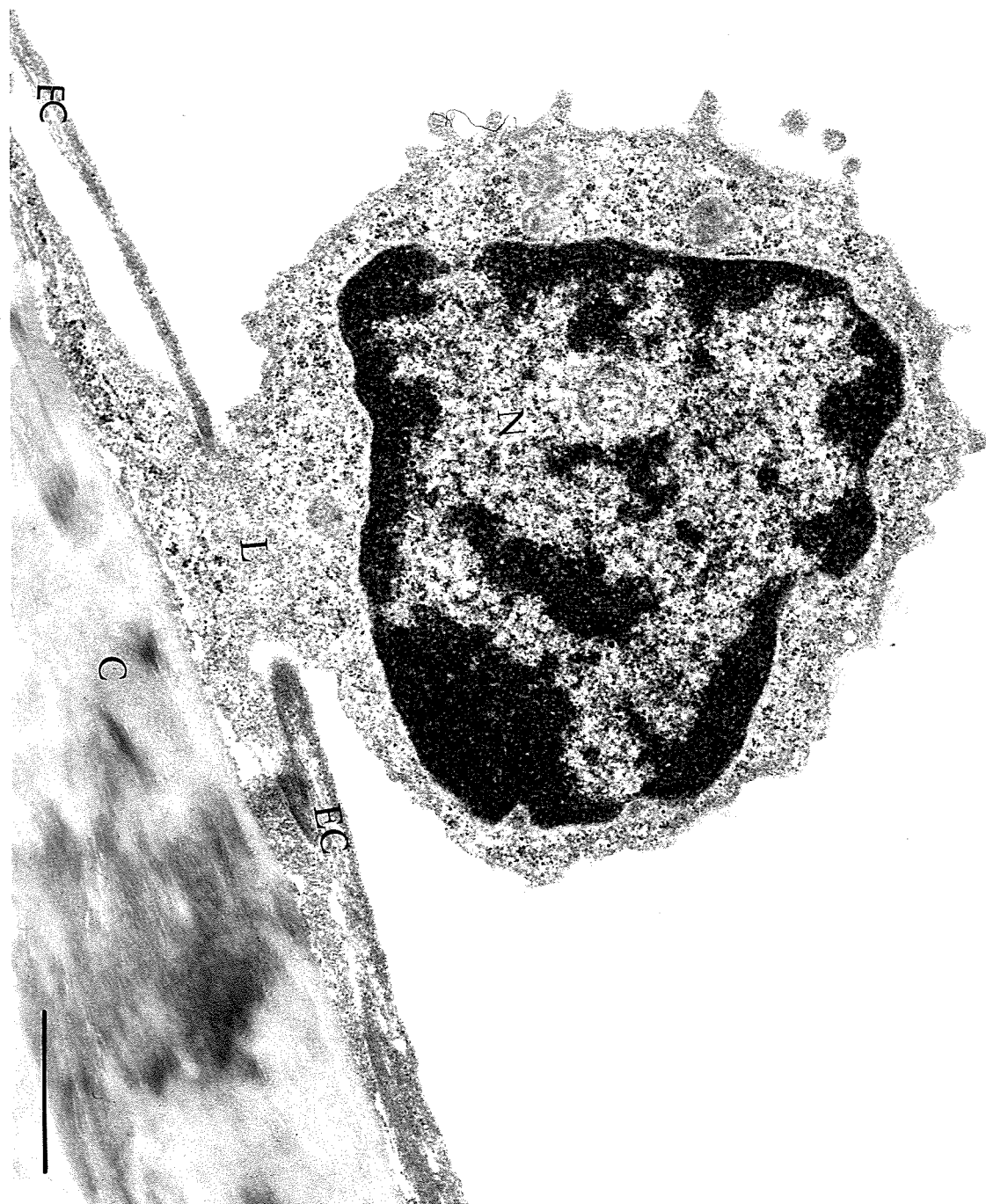


Fig. 39 a



Fig. 39 b



Fig. 39C

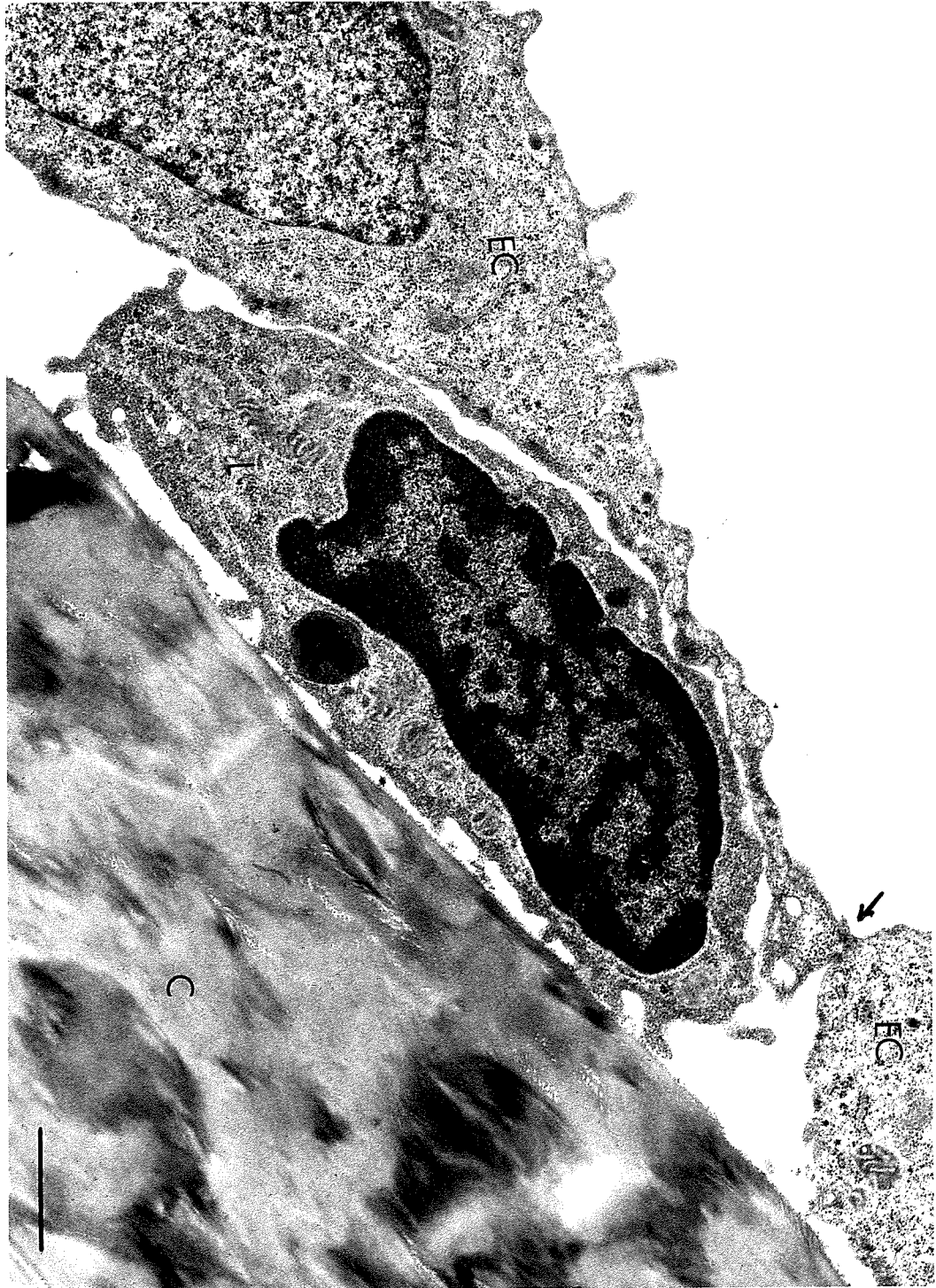


Fig. 39 d

Figure 40: Transendothelial migration of a resting lymphocyte (L) across untreated HBMEC (EC). This lymphocyte is considered moving through rather than between adjacent EC because the EC cytoplasm surrounds the lymphocyte. C, collagen membrane. Bar = 1  $\mu\text{m}$ .



Fig. 40

Figure 41: The integrity of the EC monolayers is reestablished once resting lymphocytes (L) have completed their migration across the IFN- $\gamma$  (150 units/ml, 3 days) treated EC (a, b). Bars = 2  $\mu$ m.

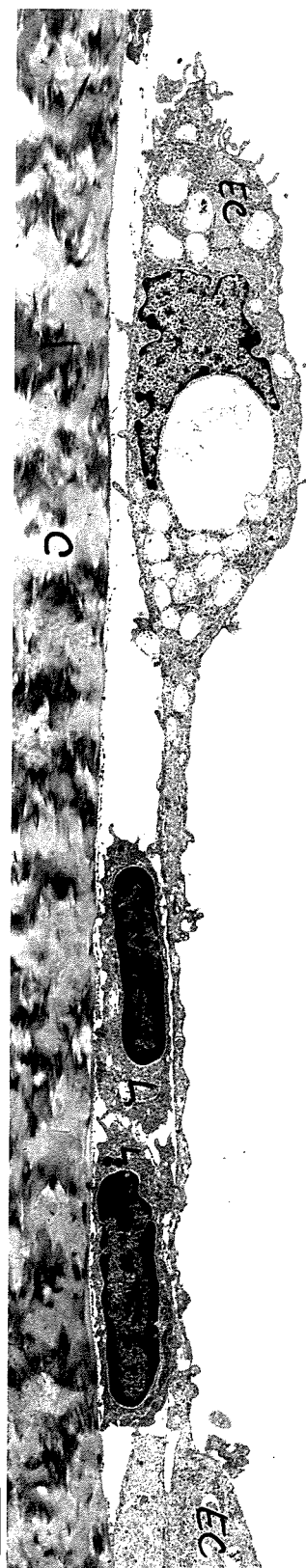


Fig. 41 a

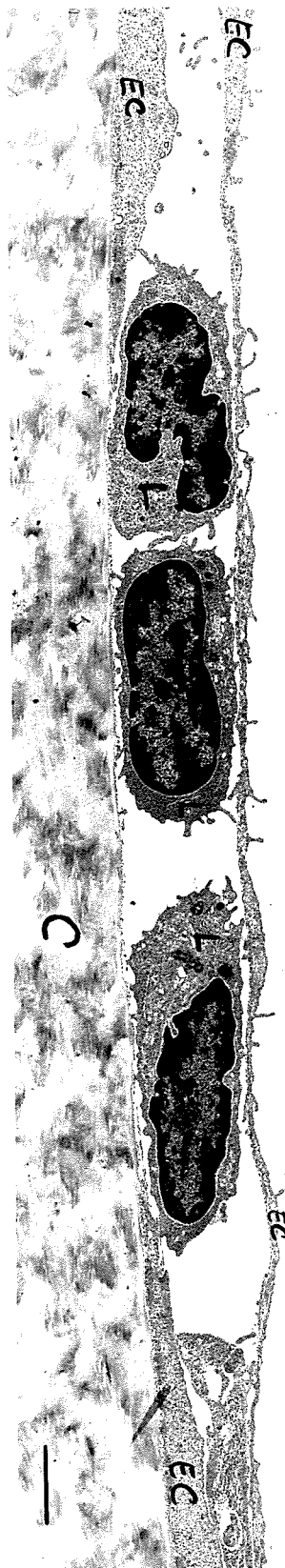


Fig. 41 b

Figure 42: Nonspecific activation of T lymphocytes enhances their migration across untreated HBMEC monolayers. Migrated T cells (arrows) remain between EC and collagen membranes (C). Bar = 10  $\mu\text{m}$ .

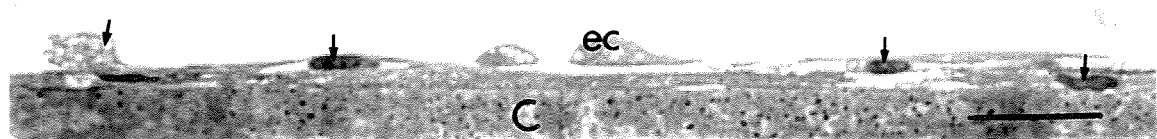


Fig. 42

Figure 43: Migration of activated lymphocytes across untreated (a) and IFN- $\gamma$  treated HBMEC (b). a) An activated T lymphocyte (L) begins to migrate between adjacent endothelial cells (EC). Close contact between EC and the lymphocyte is maintained (arrows). C, collagen membrane. b) At the end of the migration period, monolayers resume their continuity over the migrated lymphocytes (L). EC, endothelial cells; C, collagen membrane. Bars = 2  $\mu\text{m}$ .

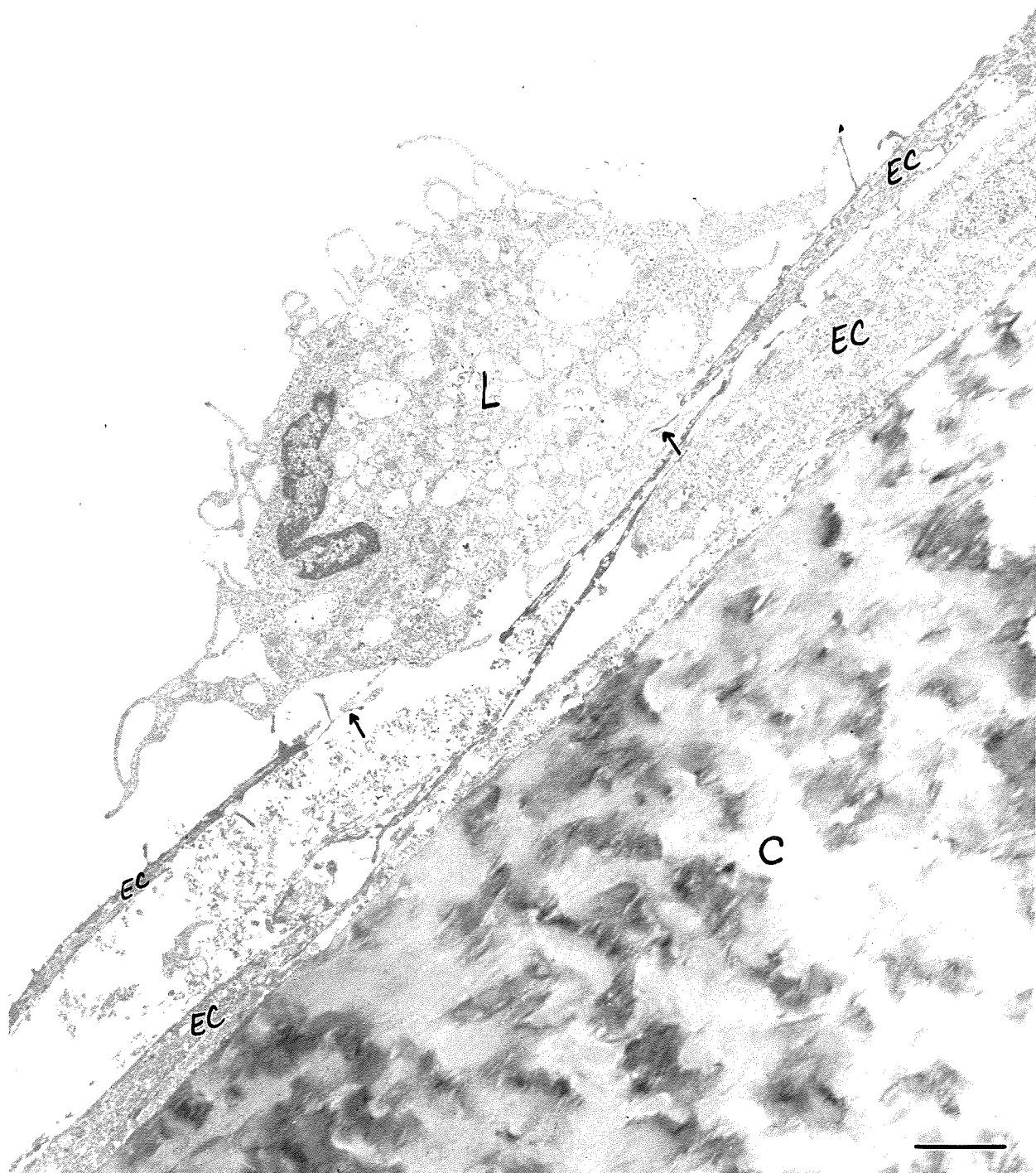


Fig. 43 a

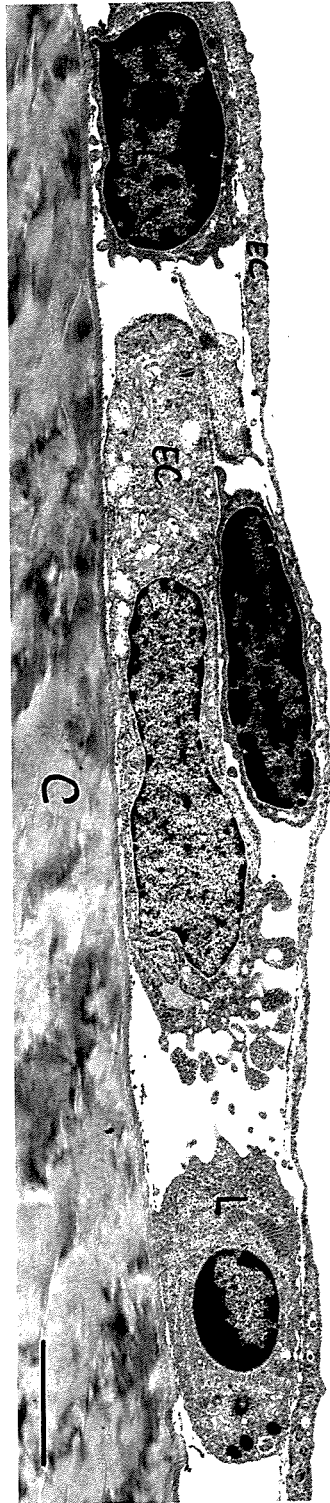


Fig. 43 b

Figure 44: Migration of anti-CD3 stimulated lymphocytes across IFN- $\gamma$  treated HBMEC. The lymphocytes (L) that have completed their migration across EC of the top layer, proceeded to migrate across the next layer of EC. Bar = 2  $\mu\text{m}$ .

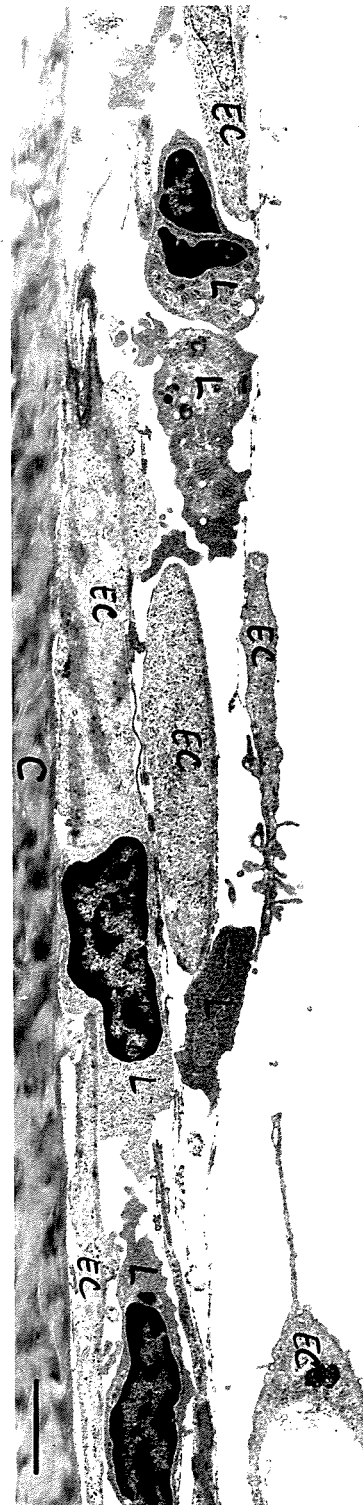


Fig. 44

Figure 45: Effect of (A)  $\text{Ca}^{2+}$  ionophore, (B) EGTA, and (C) IFN- $\gamma$  on the release of FVIII:Ag from human brain microvessel endothelial cells. After a 10 min incubation with 10  $\mu\text{M}$   $\text{Ca}^{2+}$  ionophore (A), the cytoplasmic vesicles are depleted of FVIII:Ag, as indicated by their lack of staining. N, nucleus. (B) After 10 min treatment with 1 mM EGTA, most of the vesicles contain gold particles in small aggregates. N, nucleus. (C) Incubation with 200 U/ml IFN- $\gamma$  for 24 hours is associated with variable staining of a large number of vesicles. Bars: A = 1  $\mu\text{m}$ ; B,C = 1.5  $\mu\text{m}$ .

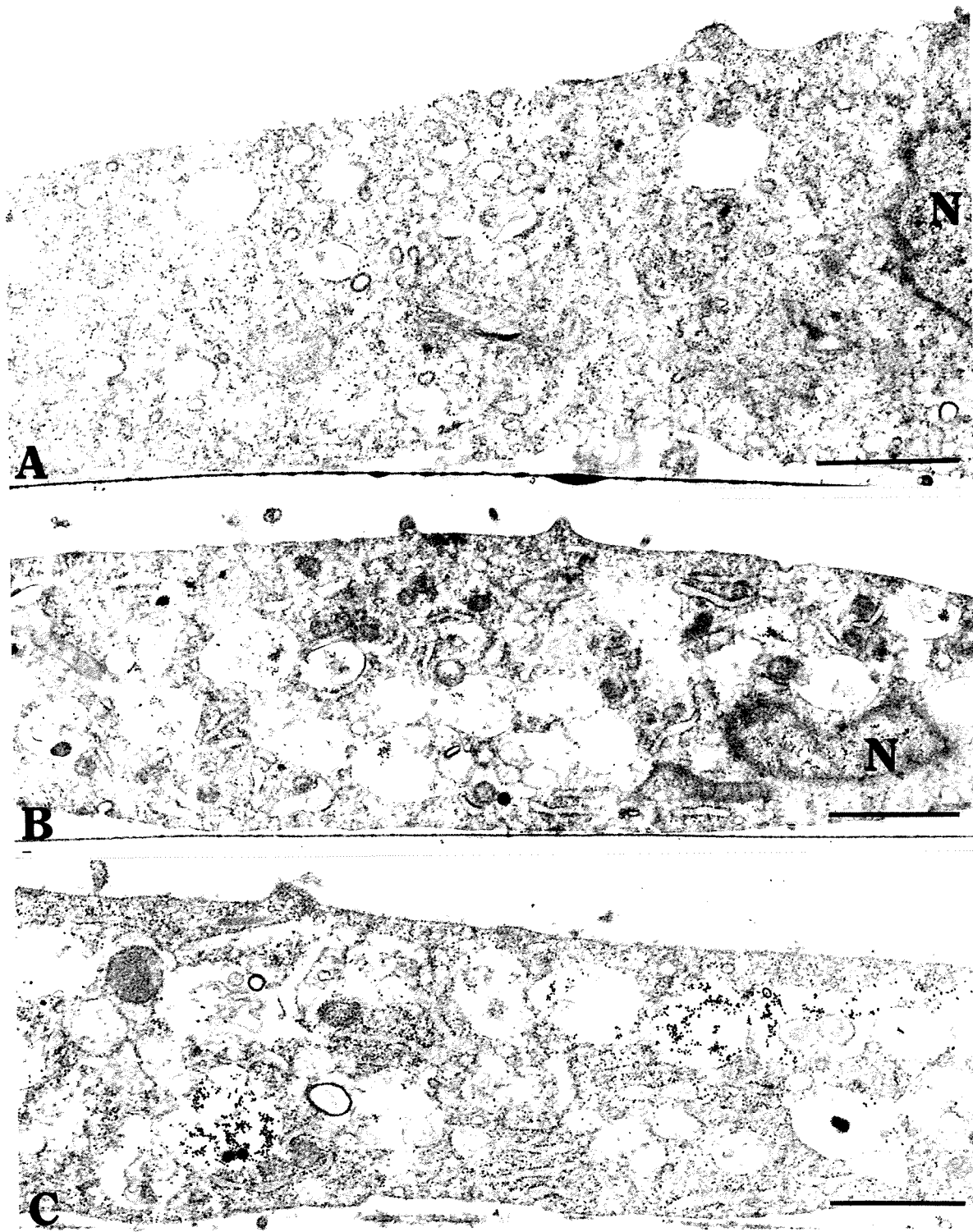
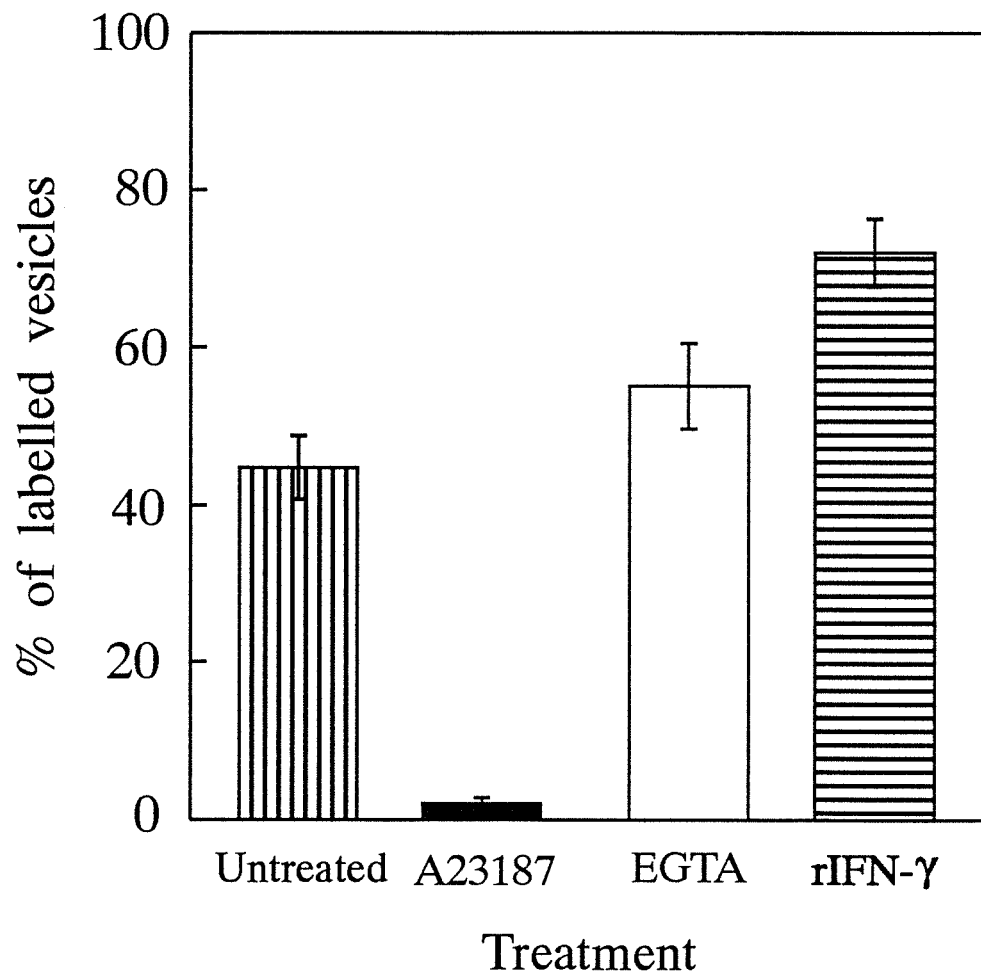


Fig. 45

Figure 46: Percentage of immunostained vesicles in untreated and treated cultures. There is a slight increase in the number of labeled vesicles after incubation with EGTA (55%) vs the untreated cultures (45%),  $p = 0.21$ . The number of stained vesicles increased significantly after pre-incubation with IFN- $\gamma$  (72%),  $p = 0.000$ . Staining was largely abolished after treatment with  $\text{Ca}^{2+}$  ionophore. Bars represent the mean  $\pm$  SEM.

**Fig. 46** Immunocytochemical Localization of Factor VIII/Von Willebrand Antigen in Human Brain Microvessel Endothelial Cells



## REFERENCES

1. Cohnheim J. Lectures on general pathology: A handbook for Practitioners and Students. Section 1 - The pathology of the circulation. The New Sydenham Society, London, England 1889: 242 - 382
2. Gallin J.I., Goldstein I.M., Snyderman R. Inflammation: Overview. In Gallin J.I., Goldstein I.M., and Snyderman R. (eds). Inflammation: Basic Principles and Clinical Correlates. Raven Press, Ltd. New York 1992: 1 - 4
3. Weissman G. Inflammation: Historical Perspective. In Gallin J.I., Goldstein I.M., and Snyderman R. (eds). Inflammation: Basic Principles and Clinical Correlates. Raven Press, Ltd. New York 1992: 5 - 9
4. Clark E.R., Clark E.L. Observations on changes in blood vascular endothelium in the living animal. *Am. J. Anat.* 1935, 57: 385 - 438
5. Swerlick R.A., Lawley T.J. Role of microvascular EC in inflammation. *J. Invest. Dermatol.* 1993, 100: 111S - 115S
6. Lorant D.E., Patel K.D., McIntyre T.M., McIver R.P., Prescott S.M., Zimmerman G.E. Coexpression of GMP-140 and PAF by Endothelium stimulated by histamine or thrombin: A juxtacrine system for adhesion and activation of neutrophils. *J. Cell. Biol.* Oct. 1991, 115: 223 - 234
7. Dorovini-Zis K., Bowman P.D., Prameya R. Adhesion and Migration of human polymorphonuclear leukocytes across cultured bovine brain microvessel EC. *J. Neuropath. Exp. Neurol.* March 1992, 51: 194 - 205
8. Hartung H.P., Jung S., Stoll G., Zielasek J., Schmidt B., Archelos J.J., Toyka K.V. Inflammatory mediators in demyelinating disorders of the CNS and PNS. *J. Neuroimmunol.* 1992, 40: 197 - 210
9. Gamble J.R., Harlan J.M., Klebanoff S.J., Vadas M.A. Stimulation of the adherence of neutrophils to umbilical vein endothelium by human recombinant tumor necrosis factor. *Proc. Natl. Acad. Sci. U.S.A.* 1985, 82: 8667 - 8671
10. Bevilacqua M.P., Pober J.S., Wheeler M.E., Cotran R.S., Gimbrone M.A. Jr. Interleukin-1 acts on cultured human vascular endothelium to increase the adhesion of polymorphonuclear leukocytes, monocytes, and related leukocyte cell lines. *J. Clin. Invest.* 1985, 76: 2003 - 2011
11. Pober J.S., Gimbrone M.A. Jr., Lapierre I.A., Mendrick D.L., Fiers W., Rithlein R., Springer T.A. Overlapping patterns of activation of human EC by interleukin-1, tumor necrosis factor, and immune interferon. *J. Immunol.* 1986, 137: 1893 - 1896
12. Hartung H.P., Schafer B., Heininger K., Toyka K.V. Recombinant interleukin-1 $\beta$  stimulates eicosanoid production in rat primary culture astrocytes. *Brain Res.* 1989,

- 489: 113 - 119
13. Hartung H.P., Heininger K. Non-specific mechanisms of inflammation and tissue damage in MS. *Res. Immunol.* 1989, 140: 226 -233
  14. Wekerle H., Engelhardt B., Risau W., Meyermann R. Interaction of T lymphocytes with Cerebral EC in vitro. *Brain Pathology* 1991, 1: 107 - 114
  15. Panitch H.S., Hirsch R.K., Schindler J., Johnson K.P. Treatment of multiple sclerosis with gamma interferon: exacerbation associated with activation of the immune system. *Neurology* 1987, 37: 1097 - 1102
  16. Page C., Rose M., Yacoub M., Pigott R. Antigenic Heterogeneity of Vascular Endothelium. *Am. J. Path.* 1992, 141: 673 - 683
  17. Plendl J, Sinowatz F., Auerbach R. Heterogeneity of the vascular endothelium. *Anat. Histol. Embryol.* 1992, 21: 256 - 262
  18. Fajardo L.F. The complexity of EC. *Am. J. Clin. Path.* 1989, 92: 241 - 250
  19. Zetter B.R. Endothelial heterogeneity: influence of vessel size, organ localization and species specificity on the properties of cultured EC. In Una S Ryan (ed) *EC II*. CRC Press, Inc. Florida 1988: 63 - 79
  20. Isaacs A. and Lindenmann J. Virus interference. I The interferon. *Proc. R. Soc. London B. Biol. Sci.* 1957, 147: 258 - 267
  21. Sen G.C. and Lengyel P. The Interferon System. A bird's eye view of its biochemistry. *J. Biol. Chem.* 1992, 267: 5017 - 5020
  22. Pober J.S., Gimbrone M.A. Jr, Cotran R.S., Reiss C.S., Burakoff S.J., Fiers W., Ault K.A. Ia expression by vascular endothelium is inducible by activated T cells and by human  $\gamma$  interferon. *J. Exp. Med.* 1983, 157: 1339 - 1353
  23. Yu C.L., Haskard D.O., Cavender D., Johnson A.R., Ziff M. Human gamma interferon increases the binding of T lymphocytes to EC. *Clin. Exp. Immunol.* 1985, 62: 554 - 560
  24. Oppenheimer-Marks N., Ziff M. Migration of lymphocytes through EC monolayers: Augmentation by Interferon- $\gamma$ . *Cell. Immunol.* 1988, 114: 307 - 323
  25. Barna B.P., Chou S.M., Jacobs B., Yen-Lieberman B., Ransohoff R.M. Interferon beta impairs induction of HLA-DR antigen expression in cultured adult human astrocytes. *J. Neuroimmunol.* 1989, 23: 45 - 53
  26. Joseph J., Knobler R.L., D'Imperio C., Lublin F.D. Down - regulation of interferon gamma induced class II expression on human glioma cells by recombinant interferon beta: effects of dosage treatment schedule. *J. Neuroimmunol.* 1988, 20: 39 - 44
  27. Inaba K., Kitaura M., Kato T., Watanabe Y., Kawade Y., Muramatsu S. Contrasting effect of alpha/beta and gamma interferons on expression of macrophage Ia Ags. *J. Exp. Med.* 1986, 163: 1030 - 1035

28. Panitch H.S., Folus J.S., Johnson K.P. Beta interferon prevents HLA Class II antigen induction by gamma interferon in MS. *Neurology* 1989, 39 (Suppl 1): 171
29. Trent J.M., Olson S and Cawn R.M. Chromosomal localization of human leucocyte, fibroblast, and immune interferon genes by means of in situ hybridization. *Proc. Natl. Acad. Sci. USA* 1982, 79: 7809 - 7813
30. Morris A.G., Lin Y.L., Askonas B.A. Immune interferon release when a cloned cytotoxic T cell line meets its correct influenza infected target cell. *Nature* 1982, 295: 150 - 152
31. Klein J.R., Raulet D.H., Pasternack M.S., Bevan M.J. Cytotoxic T lymphocytes produce immune interferon in response to antigen or mitogen. *J. Exp. Med.* 1982, 155: 1198 - 1203
32. Trinchieri G., Matsumoto-Kobayashi M., Clark S.V., Sheera J., London L., Perussia B. Response of resting human peripheral blood natural killer cells to interleukin-2. *J. Exp. Med.* 1984, 160: 1147 - 1169
33. Munakata T., Semba U., Shibaya Y., Kuwano K., Akagi M., Arai S. Induction of interferon- $\gamma$  production by human natural killer cells stimulated by hydrogen peroxide. *J. Immunol.* 1985, 134: 2449 - 2455
34. Taniguchi T. Regulation of Interferon- $\beta$  gene: Structure and Function of cis-elements and trans-acting factors. *J. Int. Res.* 1989, 9: 633 - 640
35. Lengyel P. Biochemistry of interferons and their actions. *Annu. Rev. Biochem.* 1982, 51: 251 - 282
36. Pestka S., Langer A.J., Zoon K., Samuel C. Interferons and their actions. *Annu. Rev. Biochem.* 1987, 56: 727 - 777
37. Fleischmann W.R. Jr., Schwarz L.A. Demonstration of potentiation of the antiviral and antitumor actions of interferon. *Methods Enzymol.* 1981, 79: 432 - 440
38. Panitch H.S., Folus J.S., Johnson K.P. Recombinant beta interferon inhibits gamma interferon production in multiple sclerosis. *Ann. Neurol.* 1987, 22: 139
39. Noronha A., Toscas A., Jensen M.A. IFN- $\beta$  down-regulates IFN- $\gamma$  production by activated T cells in MS. *Neurology* 1991, 41(Suppl.1): 219
40. Ling P.D., Warren M.K., Vogel S.N. Antagonistic effect of IFN- $\beta$  on the IFN- $\gamma$  induced expression of Ia Ag in murine macrophages. *J. Immunol.* 1985, 135: 1857 - 1863
41. Ransohoff R.M., Devajyothi C., Estes M.L., Babcock G., Rudick R.A., Frohman E.M., Barna B.P. IFN- $\beta$  specifically inhibits interferon-induced class II major histocompatibility complex gene transcription in a human astrocytoma cell line. *J. Neuroimmunol.* 1991, 33: 103 - 112
42. Noronha A., Toscas A., Jensen M.A. Interferon beta augments suppressor cell function

- in Multiple Sclerosis. *Ann. Neurol.* 1990, 27: 207 - 210
43. Janeway C.A. Jr. How the Immune System Recognizes Invaders. *Scientific American* 1993, 269: 73 - 79
  44. Benacerraf B., Dausset J., Snell G.D. The Nobel lectures in Immunology. *Scand. J. Immunol.* 1992, 36: 145 - 157
  45. Unanue E.R., Allen P.M. The basis for the immunoregulatory role of macrophages and other accessory cells. *Science* 1987, 236: 551 - 557
  46. Hirschberg H., Braathen L.R., Thorsby E. Antigen presentation by vascular EC and epidermal Langerhans cells. The role of HLA-DR. *Immunol. Rev.* 1982, 66: 57 - 77
  47. Brown J.H., Jardetzky T.S., Gorga J.C., Stern L.J., Urban R.G., Strominger J.L., Wiley D.C. Three - dimensional structure of the human class II histocompatibility antigen HLA-DR1. *Nature* 1993, 364: 33 - 39
  48. Germain R.N. Antigen processing and presentation. *AIDS Research and Human Retrovirus* 1992, 8: 769 - 776
  49. Erlich P., Morgenroth J. In: The collected papers of Paul Erlich. Edited by Himmelweit F., Marquardt M., Dale H.D.E. 1900. Pergamon, London.
  50. Nepom G.T., Hansen J.A., Nepom B.S. The molecular basis of HLA class II associations with rheumatoid arthritis. *J. Clin. Immunol.* 1987, 7: 1 - 7
  51. Nepom G.T., Erlich H. MHC class-II molecules and autoimmunity. *Annu. Rev. Immunol.* 1991, 9: 493 - 525
  52. Smilek D.E., Lock C.B., McDevitt H.O. Antigen recognition and peptide-mediated immunotherapy in autoimmune disease. *Immunol. Rev.* 1990, 118: 37 - 71
  53. Awata T., Kuzuya T., Matsuda A., Iwamoto Y., Kanazawa Y. Genetic analysis of HLA class II alleles and susceptibility to type 1 (Insulin-dependent) diabetes mellitus in Japanese subjects. *Diabetologia* 1992, 35: 419 - 424
  54. Stastny P. Association of the B cell alloantigen DRw4 with rheumatoid arthritis. *N. Eng. J. Med.* 1978, 298: 869 - 871
  55. Roudier J., Rhodes G., Petersen J., Vaughan J.H., Carson D.A. The Epstein-Barr virus glycoprotein gp 110, a molecular link between HLA DR4, HLA DR1, and rheumatoid arthritis. *Scand. J. Immunol.* 1988, 27: 367 - 371
  56. Carlsson B., Wallin J., Pirskanen R., Matell G., Smith C.I. Different HLA-DR-DQ associations in subgroups of idiopathic myasthenia gravis. *Immunogenetics* 1990, 31: 285 - 290
  57. Spurkland A., Gilhus N.E., Ronningen K.S., Aarli J.A., Vartdal F. Myasthenia gravis patients with thymus hyperplasia and myasthenia gravis patients with thymoma display different HLA associations. *Tissue Antigens* 1991, 37: 90 - 93

58. Haegert D.G., Michaud M., Francis G.S. Multiple sclerosis in French Canadians: Evidence for HLA class II susceptibility and resistance genes. *Can. J. Neurol. Sci.* 1990, 17: 382 - 386
59. Spurkland A., Ronningen K.S., Vandvik B., Thorsby E., Vartdal F. HLA-DQ A1 and HLA-DQB1 genes may jointly determine susceptibility to develop multiple sclerosis. *Human Immunology* 1991, 30: 69 - 75
60. Tomimoto H., Akiguchi I., Akiyama H., Kimura J., Yanagihara T. T cell infiltration and expression of MHC class II antigen by macrophages and microglia in a heterogenous group in Leukoencephalopathy. *Am. J. Path.* 1993, 143: 579 - 586
61. Yokoyama H., Takaeda M., Wada T., Ogi M., Tomosugi N., Takabatake T., Abe T., Yoshimura M., Kida H., Kobayashi K. Intraglomerular expression of MHC class II and Ki-67 antigens and serum  $\gamma$ -interferon levels in IgA Nephropathy. *Nephron* 1992, 62: 169 - 175
62. Helbig H., Gurley R.C., Reichl R.J., Mahdi R., Nussenblatt R.B., Palestine A.G. Induction of MHC class II antigen in cultured bovine ciliary epithelial cells. *Graefes Arch. Clin. Exp. Ophthalmol.* 1990, 228: 556 - 561
63. Sinha A.A., Lopez M.T., McDevitt H.O. Autoimmune disease: The failure of self-tolerance. *Science* 1990, 248: 1380 - 1388
64. Ferry B., Halttunen J., Leszczynski D., Schellekens H., Meide P.H., Hayry P. Impact of class II major histocompatibility complex antigen expression on the immunogenic potential of isolated rat vascular EC. *Transplantation* 1987, 44: 499 - 503
65. Vass K., Lassmann H., Wekerle H., Wisniewski H.M. The distribution of Ia-antigen in the lesion of rat acute experimental allergic encephalomyelitis. *Acta Neuropathol.* 1986, 70: 149 - 160
66. Sobel R.A., Blanchette B.W., Bhan A.K., Colvin R.B. The immunopathology of experimental allergic encephalomyelitis. II EC Ia increases prior to inflammatory cell inflammation. *J. Immunol.* 1984, 132: 2402 - 2407
67. Lampson L.A. Molecular bases of the immune response to neural behaviors. *Trends Neurosci.* 1987, 10: 211 - 216
68. Traugott U., Scheinberg L.C., Raine C.S. On the presence of Ia-positive EC and astrocytes in multiple sclerosis lesions and its relevance to antigen presentation. *J. Neuroimmunol.* 1985, 8: 1 - 14
69. Pardridge W.M., Yang J., Buciak J., Tourtellotte W.W. Human Brain Microvascular DR-Antigen. *J. Neurosci. Res.* 1989, 23: 337 - 341
70. Male D.K., Pryce G., Hughes C.C.W. Antigen presentation in brain: MHC induction on brain endothelium and astrocytes compared. *Immunology* 1987, 60: 453 - 459
71. Berrih S., Arenzana-Seisdedos F., Cohen S., Devos R., Charron D., Virelizier J.L. Interferon- $\gamma$  modulates HLA class II antigen expression on cultured human thymic epithelial cells. *J. Immunol.* 1985, 135: 1165 - 1171

72. Skoskiewicz M.J., Colvin R.B., Schneeberger E.E., Russel P.S. Widespread and selective induction of major histocompatibility complex-determined antigens in vivo by  $\gamma$ -interferon. *J. Exp. Med.* 1985, 162: 1645 - 1664
73. Martin M., Schwinzer R., Schellekens H., Resch K. Glomerular mesangial cells in local inflammation. Induction of the expression of MHC class II antigens by IFN- $\gamma$ . *J. Immunol.* 1989, 142: 1887 - 1894
74. Steeg P.S., Moore R.N., Johnson H.M., Oppenheim J.J. Regulation of murine macrophage Ia Ag expression by a lymphokine with immune interferon activity. *J. Exp. Med.* 1982, 156: 1780 - 1793
75. Fertsch-Ruggio D., Schoenberg D.R., Vogel S.N. Induction of macrophage Ia Ag by rIFN- $\gamma$  and down-regulation by IFN- $\alpha/\beta$  and dexamethasone are regulated transcriptionally. *J. Immunol.* 1988, 141: 1582 - 1589
76. Wong G.H.W., Clark-Lewis I., McKimm-Breschkin J.L., Schrader J.W. Interferon- $\gamma$ -like molecule induces Ia Ags on cultured mast cell progenitors. *Proc. Natl. Acad. Sci. USA* 1982, 79: 6989 - 6993
77. Morel P.A., Manolagas S.C., Provvedini D.M., Wegmann D.R., Chiller J.M. Interferon- $\gamma$ -induced Ia expression in WEHI-3 cells is enhanced by the presence of 1, 25-dihydroxyvitamin D<sub>3</sub>. *J. Immunol.* 1986, 136: 2181 - 2186
78. Basham T.Y., Merigan T.C. Recombinant Interferon- $\gamma$  increases HLA-DR synthesis and expression. *J. Immunol.* 1983, 130: 1492 - 1494
79. Kelley V.E., Fiers W., Strom T.B. Cloned human interferon-gamma, but not interferon-beta or -alpha, induces expression of HLA-DR determinants by fetal monocytes and myeloid leukemic cell lines. *J. Immunol.* 1984, 132: 240 - 245
80. Collins T., Korman A.J., Wake C.T., Boss J.M., Kappes D.J., Fiers W., Ault K.A., Gimbrone M.A., Strominger J.L., Pober J.S. Immune interferon activates multiple class II major histocompatibility complex genes and the associated invariant chain gene in human EC and dermal fibroblasts. *Proc. Natl. Acad. Sci. USA* 1984, 81: 4917 - 4921
81. Mantegazza R., Hughes S.M., Mitchell D., Travis M., Blau H.M., Steinman L. Modulation of MHC class II antigen expression in human myoblasts after treatment with IFN- $\gamma$ . *Neurology* 1991, 41: 1128 - 1132
82. Michaelis D., Goebels N., Hohlfeld R. Constitutive and cytokine-induced expression of human leukocyte antigens and cell adhesion molecules by human myotubes. *Am. J. Path.* 1993, 143: 1142 - 1149
83. Doukas J., Pober J.S. Lymphocyte-mediated activation of cultured EC (EC). CD4<sup>+</sup> T cells inhibit EC class II MHC and intercellular adhesion molecule-1 expression. *J. Immunol.* 1990, 145: 1088 - 1098
84. Ruszczak Z., Detmar M., Imcke E., Orfanos C.E. Effects of rIFN Alpha, Beta, Gamma on the morphology, proliferation, and cell surface antigen expression of human dermal

- microvascular EC in vitro. *J. Invest. Dermatol.* 1990, 95: 693 - 699
85. Botazzo G.F., Pujol-Borrell R., Hanafusa T., Feldman M. Role of aberrant HLA-DR expression and antigen presentation in the induction of endocrine autoimmunity. *Lancet* 1983, 2: 1115 - 1118
  86. Unanue E.R. Antigen-presenting function of the macrophage. *Annu. Rev. Immunol.* 1984, 2: 395 - 428
  87. de Waal R.M.W., Bogman M.J.J., Maass C.N., Cornelissen L.M.H., Tax W.J.M., Koene R.A.P. Variable expression of Ia Ags on the vascular endothelium of mouse skin allografts. *Nature* 1983, 303: 426 - 429
  88. McFarlin D.E., McFarland H.F. Multiple Sclerosis. *N. Engl. J. Med.* 1982, 307: 1246 - 1251
  89. Oger J., Roos R., Antel J.P. Immunology of multiple sclerosis. In: Antel J.P., ed. *Neurologic clinics*. Philadelphia: WB Saunders, 1983: 655 - 679
  90. Waksman B.H., Reynolds W.E. Multiple sclerosis as a disease of immune regulation. *Proc. Soc. Exp. Biol. Med.* 1984, 175: 282 - 294
  91. Neighbour P.A., Miller A.E., Bloom B.R. Interferon responses of leucocytes in multiple sclerosis. *Neurology* 1981, 31: 561 - 566
  92. Vervliet G., Claeys H., Van Haver H., Carton H., Vermynen C., Meulepas E., Billiau A. Interferon production and natural killer cell (NK) activity in leucocyte cultures from multiple sclerosis patients. *J. Neurol. Sci.* 1983, 60: 137 - 150
  93. Hirsch R.L., Panitch H.S., Johnson K.P. Lymphocytes from multiple sclerosis patients produce elevated levels of gamma interferon in vitro. *J. Clin. Immunol.* 1985, 5: 386 - 389
  94. Goust J.M., Verselis S.J., Shums A. Interferon gamma and interleukin 2 (IL2) production in MS. *Abstract. Neurology* 1987, 37 (Suppl. 1): 289
  95. Sheremata W.A., Bohn R.N., Resnick L., Berger J.R., Sazant A. Cerebrospinal fluid gamma interferon is increased in active multiple sclerosis. *Ann. Neurol.* 1987, 22: 153
  96. Aguet M. High-affinity binding of <sup>125</sup>I-labeled mouse interferon to a specific cell surface receptor. *Nature* 1980, 284: 459 - 461
  97. Branca A.A., Baglioni C. Evidence that type I and type II interferons have different receptors. *Nature* 1981, 294: 768 - 770
  98. Sarkar F.H., Gupta S.L. Receptors for human  $\gamma$  interferon: binding and cross-linking of <sup>125</sup>I-labeled human recombinant  $\gamma$  interferon to receptors on WISH cells. *Proc. Natl. Acad. Sci. USA* 1984, 81: 5160 - 5164
  99. Littman S.J., Faltynek C.K., Baglioni C. Binding of human recombinant <sup>125</sup>I-interferon- $\gamma$  to receptors on human cells. *J. Biol. Chem.* 1985, 260: 1191 - 1195

100. Rashidbaigi A., Kung H., Pestka S. Characterization of receptors for immune interferon in U937 cells with <sup>32</sup>P-labeled human recombinant immune interferon. *J. Biol. Chem.* 1985, 260: 8514 - 8519
101. Anderson P., Yip Y.K., Vilcek J. Specific binding of <sup>125</sup>I-human interferon- $\gamma$  to high affinity receptors on human fibroblasts. *J. Biol. Chem.* 1982, 257: 11301 - 11304
102. Branca A.A., Faltynek C.R., D'Alessandro S.B., Baglioni C. Interaction of interferon with cellular receptors. Internalization and degradation of cell-bound interferon. *J. Biol. Chem.* 1982, 257: 13291 - 13296
103. Hannigan G.E., Gewert D.R., Williams B.R.G. Characterization and regulation of  $\alpha$ -interferon receptor expression in interferon-sensitive and -resistant human lymphoblastoid cells. *J. Biol. Chem.* 1984, 259: 9456 - 9460
104. Thompson M.R., Zhang Z., Fournier A., Tan Y.H. Characterization of human  $\beta$ -interferon-binding sites on human cells. *J. Biol. Chem.* 1985, 260: 563 - 567
105. Lapierre L.A., Fiers W., Pober JS. Three distinct classes of regulatory cytokines control EC MHC antigen expression. *J. Exp. Med.* 1988, 167: 794 - 804
106. Swerlick R.A., Garcia-Gonzalez E., Kubota Y., Xu Y., Lawley T.J. Studies of the modulation of MHC antigen and cell adhesion molecule expression on human dermal microvascular EC. *J. Invest. Dermatol.* 1991, 97: 190 - 196
107. Dorovini-Zis K., Prameya R., Bowman P.D. Culture and characterization of microvascular EC derived from human brain. *Lab. Invest.* 1991, 64: 425 - 436
108. Rapoport S.I. *Blood-brain barrier in Physiology and Medicine.* Raven Press, 1976
109. Brightman M.W. Morphology of blood-brain interfaces. In Bito L.Z., Davson H., Fenstermacher J.D. (eds). *The ocular and cerebrospinal fluids.* *Exp. Eye Res. (suppl.)* 1977, 25: 1 - 25
110. Leibowitz S., Hughes R.A.C. *Immunology of the Nervous System.* Edward Arnold, London, 1983
111. Nagy Z., Pappius H.M., Mathieson G., Huttner I. Opening of tight junctions in cerebral endothelium. 1. Effect of hyperosmolar mannitol infused through the internal carotid artery. *J. Comp. Neurol.* 1979, 185: 569 - 578
112. Brightman M.W., Hori M., Rapoport S.I., Reese T.S., Westergaard E. Osmotic opening of tight junctions in cerebral endothelium. *J. Comp. Neurol.* 1973, 152: 317 - 326
113. Dorovini-Zis K., Sato M., Goping G., Rapoport S.I., Brightman M.W. Ionic lanthanum passage across cerebral endothelium exposed to hyperosmotic arabinose. *Acta Neuropath. (Berl)* 1983, 60: 49 - 60
114. Nakagawa Y., Cervos-Navarro J., Artigas J. Tracer study on a paracellular route in Experimental Hydrocephalus. *Acta Neuropath. (Berl)* 1985, 65: 247 - 254

115. Beggs J.L., Waggener J.D. Transendothelial vesicular transport of protein following compression injury to the spinal cord. *Lab. Invest.* 1976, 34: 428 - 439
116. Petito C.K., Schaefer J.A., Plum F. Ultrastructural characteristics of the brain and blood-brain barrier in experimental seizures. *Brain Res.* 1977, 127: 251 - 267
117. Petito C.K. Early and late mechanisms of increased vascular permeability following experimental cerebral infarction. *J. Neuropath. Exp. Neurol.* 1979, 38: 222 - 234
118. Nag S., Robertson D.M., Dinsdale H.B. Cerebral cortical changes in acute experimental hypertension. *Lab. Invest.* 1977, 36: 150 - 161
119. Juhler M., Barry D.I., Offner H., Konat G., Klinken L, Paulson O.B. Blood-brain and blood-spinal cord barrier permeability during the course of experimental allergic encephalomyelitis in the rat. *Brain Res.* 1984, 302: 347 - 355
120. Vulpe M., Hawkins A., Rozdilsky B. Permeability of cerebral blood vessels in EAE as studied by radioactive iodinated bovine albumin. *Neurology* 1960, 10: 171 - 177
121. Kristensson K., Wisniewski H.M. Chronic relapsing experimental allergic encephalomyelitis: Studies in vascular permeability changes. *Acta Neuropathol.* 1977, 39: 189 - 194
122. Kato S., Nakamura H. Ultrastructural and ultracytochemical studies on the blood-brain barrier in chronic relapsing experimental allergic encephalomyelitis. *Acta Neuropathol.* 1989, 77: 455 - 464
123. Lossinsky A.S., Badmajew V., Robson J.A., Moretz R.C., Wisniewski H.M. Sites of egress of inflammatory cells and horseradish peroxidase transport across the blood-brain barrier in a murine model of chronic relapsing experimental allergic encephalomyelitis. *Acta Neuropathol.* 1989, 78: 359 - 371
124. Simmons R.D., Buzbee T.M., Linthicum D.C., Mandy W.J., Chen G., Wang C. Simultaneous visualization of vascular permeability change and leukocyte egress in the central nervous system during autoimmune encephalomyelitis. *Acta Neuropathol.* 1987, 74: 191 - 193
125. McDonald W.I., Barnes D. Lessons from magnetic resonance imaging in multiple sclerosis. *Trends Neurosci.* 1989, 12: 376 - 379
126. Stolpen A.H., Guinan E.C., Fiers W., Pober J.S. Recombinant Tumor Necrosis Factor and Immune Interferon act singly and in combination to reorganize human vascular EC monolayers. *Am. J. Path.* 1986, 123: 16 - 24
127. Huynh H.K., Dorovini-Zis K. Effects of Interferon - gamma on primary cultures of human brain microvessel EC. *Am. J. Path.* 1993, 142: 1265 - 1278
128. Burke-Gaffney A., Keenan A.K. Modulation of human EC permeability by combinations of the cytokines interleukin-1  $\alpha/\beta$ , tumor necrosis factor- $\alpha$  and interferon- $\gamma$ . *Immunopharmacology* 1993, 25: 1- 9
129. Martin S., Maruta K., Burkart V., Gillis S., Kolb H. IL-1 and IFN- $\gamma$  increase vascular

- permeability. *Immunology* 1988, 64: 301 - 305
130. Damle N.K., Doyle L.V. Ability of human T lymphocytes to adhere to vascular EC and to augment endothelial permeability to macromolecules is linked to their state of post-thymic maturation. *J. Immunol.* 1990, 144: 1233 - 1240
  131. Sibley W.A., Bamford C.R., Clark K. Clinical viral infections and multiple sclerosis. *Lancet* 1985, 1: 1313 - 1315
  132. Johnson K.P., Panitch H.S. Interferon therapy for multiple sclerosis. *Maryland Med. J.* 1992, 41: 601 - 603
  133. Poser C.M. Pathogenesis of multiple sclerosis. *Acta Neuropathol. (Berl.)* 1986, 71: 1 - 10
  134. Masuyama J., Minato N., Kano S. Mechanisms of lymphocyte adhesion to human vascular EC in culture. T lymphocyte adhesion to EC through endothelial HLA-DR antigens induced by gamma interferon. *J. Clin. Invest.* 1986, 77: 1596 - 1605
  135. Goodall C.A., Curtis A.S.G., Lang S.C. Modulation of adhesion of lymphocytes to murine brain EC in vitro: relation to class II major histocompatibility complex expression. *J. Neuroimmunol.* 1992, 37: 9 - 22
  136. McCarron R.M., Wang L., Cowan E.P., Spatz M. Class II MHC antigen expression by cultured human cerebral vascular EC. *Brain Res.* 1991, 566: 325 - 328
  137. McCarron R.M., Spatz M., Kempinski O., Hogan R.N., Muehl L., McFarlin D.E. Interaction between myelin basic protein sensitized T lymphocytes and murine cerebral vascular EC. *J. Immunol.* 1986, 137: 3428 - 3435
  138. Traugott U., Raine C.S. Evidence for antigen presentation in situ by EC and astrocytes. *J. Neurol. Sci.* 1985, 69: 365 - 370
  139. Sobel R.A., Natale J.M., Schneeberger E.E. The immunopathology of acute experimental allergic encephalomyelitis. *J. Neuropath. Exp. Neurol.* 1987, 46: 239 - 249
  140. Craggs R.I., Webster H. deF. Ia Ags in the normal rat nervous system and in lesions of experimental allergic encephalomyelitis. *Acta Neuropath. (Berl)* 1985, 68: 263 - 272
  141. Sakai K., Tabira T., Endoh M., Steinman L. Ia expression in chronic relapsing experimental allergic encephalomyelitis induced by long-term cultured T cell lines in mice. *Lab. Invest.* 1986, 54: 345 - 352
  142. Male D., Pryce G. Kinetics of MHC gene expression and mRNA synthesis in brain endothelium. *Immunology* 1988, 63: 37 - 42
  143. Rosa F., Hatat D., Abadie A., Wallach D., Revel M., Fellows M. Human interferons enhance HLA-DR mRNA. *EMBO J.* 1983, 2: 1585 - 1589
  144. Pober J.S., Collins T., Gimbrone M.A. Jr., Libby P., Reiss C.S. Inducible expression of class II major histocompatibility complex antigens and the immunogenicity of

- vascular endothelium. *Transplant* 1986, 41: 141 - 146
145. Thornhill M.H., Williams D.M., Speight P.M. Enhanced adhesion of autologous lymphocytes to gamma-interferon-treated human EC in vitro. *Br. J. Exp. Path.* 1989, 70: 59 - 64
  146. Royer H.D., Campen T.J., Ramarli D., Chang H.C., Acuto O., Reinherz E.L. Molecular aspects of human T-lymphocyte antigen recognition. *Transplantation* 1985, 39: 571 - 582
  147. Doyle C., Strominger J.L. Interaction between CD4 and class II MHC molecules mediates cell adhesion. *Nature* 1987, 330: 256 - 259
  148. Steinman L., Solomon D., Lim M., Zamvil S., Sriram S. Prevention of experimental allergic encephalitis with in vivo administration of anti Ia antibody. Decreased accumulation of radiolabeled lymph node cells in the central nervous system. *J. Neuroimmunol.* 1983, 5: 91 - 97
  149. Astrom K.E., Webster H. deF., Arnason B.G. The initial lesion in experimental allergic neuritis. A phase and electron microscopic study. *J. Exp. Med.* 1968, 128: 469 - 495
  150. Haskard D., Cavender D., Ziff M. Phorbol ester-stimulated T lymphocytes show enhanced adhesion to human EC monolayers. *J. Immunol.* 1986, 137: 1429 - 1434
  151. Oppenheimer-Marks N., Davis L.S., Lipsky P.E. Human T lymphocyte adhesion to EC and transendothelial migration. Alteration of receptor use relates to the activation status of both the T cell and the EC. *J. Immunol.* 1990, 145: 140 - 148
  152. Oppenheimer-Marks N., Davis L.S., Bogue D.T., Ramberg J., Lipsky P.E. Differential utilization of ICAM-1 and VCAM-1 during the adhesion and transendothelial migration of human T lymphocytes. *J. Immunol.* 1991, 147: 2913 - 2921
  153. Kavanaugh A.F., Lightfoot E., Lipsky P.E., Oppenheimer-Marks N. Role of CD11/CD18 in adhesion and transendothelial migration of T cells. Analysis utilizing CD18-deficient T cell clones. *J. Immunol.* 1991, 146: 4149 - 4156
  154. Male D., Pryce G., Hughes C., Lantos P. Lymphocyte migration into brain modelled in vitro: Control by lymphocyte activation, cytokines, and antigen. *Cell. Immunol.* 1990, 127: 1 - 11
  155. Male D., Pryce G., Rahman J. Comparison of the immunological properties of rat cerebral and aortic endothelium. *J. Neuroimmunol.* 1990, 30: 161 - 168
  156. Wang Y.F., Calder V.L., Greenwood J., Lightman S.L. Lymphocyte adhesion to cultured EC of the blood-retinal barrier. *J. Neuroimmunol.* 1993, 48: 161 - 168
  157. Damle N.K., Doyle L.V., Bender J.R., Bradley E.C. Interleukin-2 activated human lymphocytes exhibit enhanced adhesion to normal vascular EC and cause their lysis. *J. Immunol.* 1987, 138: 1779 - 1785
  158. Pankonin G., Reipert B., Ager A. Interactions between interleukin-2-activated

- lymphocytes and vascular endothelium: binding to and migration across specialized and non-specialized endothelia. *Immunol.* 1992, 77: 51 - 60
159. Dustin M.L., Springer T.A. T cell receptor cross-linking transiently stimulates adhesiveness through LFA-1. *Nature* 1989, 341: 619 - 624
  160. Tsukada N., Matsuda M., Miyagi K., Yanagisawa N. Adhesion of cerebral EC to lymphocytes from patients with multiple sclerosis. *Autoimmunity* 1993, 14: 329 - 333
  161. Hickey W.F., Hsu B.L., Kimura H. T-lymphocyte entry into the Central Nervous System. *J. Neurosci. Res.* 1991, 28: 254 - 260
  162. Springer T.A. Adhesion receptors of the immune system. *Nature* 1990, 346: 425 - 434
  163. Parrott D.M.V., Wilkinson P.C. Lymphocyte locomotion and migration. *Prog. Allergy* 1981, 28: 193 - 284
  164. Traugott U., Stone S.H., Raine C.S. Experimental allergic encephalomyelitis. Migration of early T cells from the circulation into the central nervous system. *J. Neurol. Sci.* 1978, 36: 55 - 61
  165. Traugott U., Stone S.H., Raine C.S. Chronic relapsing experimental allergic encephalomyelitis. *J. Neurol. Sci.* 1979, 41: 17 - 29
  166. Kateley J.R., Bazzell S.J. Immunological dysfunctions in multiple sclerosis. I. Diminution of "active" thymus-derived lymphocytes and presence of immunomodulating serum factors. *Clin. Exp. Immunol.* 1979, 35: 218 - 226
  167. Traugott U., Scheinberg L.C., Raine C.S. Multiple sclerosis: Circulating antigen-reactive lymphocytes. *Ann. Neurol.* 1979, 6: 425 - 429
  168. Kam-Hansen S. Reduced number of active T cells in cerebrospinal fluid in multiple sclerosis. *Neurology* 1979, 29: 897 - 899
  169. Schluesener H.J., Sobel R.A., Weiner H.L. Demyelinating experimental allergic encephalomyelitis (EAE) in the rat: treatment with a monoclonal antibody against activated T cells. *J. Neuroimmunol.* 1988, 18: 341 - 351
  170. Greenwood J., Calder V.L. Lymphocyte migration through cultured EC monolayers derived from the blood-retinal barrier. *Immunology* 1993, 80: 401 - 406
  171. Jaffe E.A. Synthesis of von Willebrand factor by EC. In Una S. Ryan, ed. *EC. Vol. I.* Boca Raton, FL: CRC Press, 1988: 119 - 126
  172. Rand J.H., Gordon R.E., Sussman I.I., Chu S.V., Solomon V. Electron microscopic localization of factor-VIII-related antigen in adult human blood vessels. *Blood* 1982, 60: 627 - 634
  173. Sakariassen K.S., Bolhuis P.A., Sixma J.J. Human blood platelet adhesion to artery subendothelium is mediated by Factor VIII-von Willebrand factor bound to the subendothelium. *Nature* 1979, 279: 636 - 638

174. Reinders H.J., DeGroot P.G., Gonsalves M.D., Zandbergen J., Loesberg C., Van Mourik J.A. Isolation of a storage and secretory organelle containing von Willebrand protein from cultured human EC. *Biochimica et Biophysica Acta* 1984, 804: 361 - 369
175. Wagner D.D., Olmsted J.B., Marder V.J. Immunolocalization of von Willebrand protein in Weibel-Palade bodies of human EC. *J. Cell. Biol.* 1982, 95: 355 - 360
176. Warhol M.J., Sweet J.M. The ultrastructural localization of von Willebrand factor in EC. *Am. J. Pathol.* 1984, 117: 310 - 315
177. Weibel E.R., Palade G.E. New cytoplasmic components in arterial endothelia. *J. Cell. Biol.* 1964, 23: 101 - 112
178. DeBault L.E., Henriquez E., Hart M.N., Cancilla P.A. Cerebral microvessels and derived cells in tissue culture: II. Establishment, identification and preliminary characterization of an EC line. *In Vitro* 1981, 17: 480 - 494
179. Bowman P.D., Betz A.L., Ar D., Wolinsky J.S., Penney J.B., Shivers R.R., Goldstein G.W. Primary culture of capillary endothelium from rat brain. *In Vitro* 1981, 17: 353 - 362
180. Diglio C., Grammas P., Giacomelli F., Wiener J. Primary culture of rat cerebral microvascular EC. *Lab. Invest.* 1982, 46: 554 - 563
181. Spatz M., Bembry J., Dodson R.F., Hervonen H., Murray M.R. EC cultures derived from isolated cerebral microvessels. *Brain Res.* 1980, 191: 577 - 582
182. Tannenbaum S.H., Gralnick H.R.  $\gamma$ -Interferon modulates von Willebrand factor release by cultured human EC. *Blood* 1990, 75: 2177 - 2184
183. Bowman P.D., Betz A.L., Ar D., Wolinsky J.S., Shivers R.R., Goldstein G.W. Primary culture of capillary endothelium from rat brain. *In Vitro Cell Dev. Biol.* 1981, 17: 353 - 362
184. McLean I.W., Nakane P.K. Periodate-Lysine-Paraformaldehyde fixative: A new fixative for immunoelectron microscopy. *J. Histochem. Cytochem.* 1974, 22: 1077 - 1083
185. Schroeter D., Spiess E., Paweletz N., Benke R. A procedure for rupture-free preparation of confluent grown monolayer cells for scanning electron microscopy. *J. Electron Microsc. Tech.* 1984, 1: 219 - 225
186. Dorovini-Zis K., Bowman P.D., Betz A.L., Goldstein G.W. Hyperosmotic urea reversibly opens the tight junctions between brain capillary EC in cell culture. *J. Neuropath. Exp. Neurol.* 1987, 46: 130 - 140
187. Julius M.H., Simpson E., Hertenberg L.A. A rapid method for the isolation of functional thymus-derived murine lymphocytes. *Eur. J. Immunol.* 1973, 3: 645 - 649
188. Hormia M., Lehto V.P., Virtanen I. Identification of UEA I binding surface

- glycoproteins of cultured human EC. *Cell Biol. Int. Rep.* 1983, 7: 467 - 475
189. Weber T., Seitz R.J., Liebert U.G., Gallasch E., Wechsler W. Affinity cytochemistry of vascular endothelia in brain tumors by biotinylated *Ulex europaeus* type I lectin (UEA I). *Acta Neuropathol.* 1985, 67: 128 - 135
  190. Sobel R.A., Ames M.B. Major histocompatibility complex molecule expression in the human central nervous system: immunohistochemical analysis of 40 patients. *J. Neuropath. Exp. Neurol.* 1988, 47: 19 - 28
  191. Lampson L.A., Hickey W.F. Monoclonal antibody analysis of MHC expression in human brain biopsies: tissue ranging from "histologically normal" to that showing different levels of glial tumor involvement. *J. Immunol.* 1986, 136: 4054 - 4062
  192. Frank E., Pulver M., de Tribolet N. Expression of Class II Major Histocompatibility antigens on reactive astrocytes and EC within the gliosis surrounding metastases and abscesses. *J. Neuroimmunol.* 1986, 12: 29 - 36
  193. Pober J.S., Gimbrone M.A. Jr. Expression of Ia-like antigens by human vascular EC is inducible in vitro: Demonstration by monoclonal antibody binding and immunoprecipitation. *Proc. Natl. Acad. Sci. USA* 1982, 79: 6641 - 6645
  194. Wagner C.R., Vetto R.M., Burger D.R. Expression of I-region-associated antigen (Ia) and interleukin 1 by subcultured human EC. *Cell. Immunol.* 1985, 93: 91 - 104
  195. Reddy P.G., Graham G.M., Datta S., Guarini L., Moulton T.A., Jiang H., Gottesman M.M., Ferrone S., Fisher P.B. Effect of recombinant fibroblast interferon and recombinant immune interferon on growth and the antigenic phenotype of multidrug-resistant human glioblastoma multiforme cells. *J. Natl. Cancer Inst.* 1991, 83: 1307 - 1315
  196. Wilcox C.E., Baker D., Butter C., Willoughby D.A., Turk J.L. Differential expression of guinea pig class II major histocompatibility complex antigens on vascular EC in vitro and in experimental allergic encephalomyelitis. *Cell. Immunol.* 1989, 120: 82 - 91
  197. Beilke M.A., Riding In D., Hamilton R., Stone G.A., Jordan E.K., Brashears G., Nusbaum W., Huddleston D., Gibbs C.J. Jr, Gravell M. HLA-DR expression in macaque neuroEC in vitro and during SIV encephalitis. *J. Neuroimmunol.* 1991, 33: 129 - 143
  198. Amaldi I., Reith W., Berte C., Mach B. Induction of HLA class II genes by IFN gamma is transcriptional and requires a trans acting protein. *J. Immunol.* 1989, 142: 999 - 1004
  199. Traugott U. Multiple sclerosis: relevance of class I and class II MHC-expressing cells to lesion development. *J. Neuroimmunol.* 1987, 16: 283 - 302
  200. Steinman L., Waldor M.K., Zamvil S.S., Lim M., Herzenberg L, McDevitt H.O., Mitchell D., Sriram S. Therapy of autoimmune disease with antibody to immune response gene products or to T-cell surface markers. *Ann. N.Y. Acad. Sci.* 1986, 475: 274 - 284

201. Heyns A du P., Eldor A., Vlodavsky I., Kaiser N., Fridman R., Panet A. The antiproliferative effect of interferon and the mitogenic activity of growth factors are independent cell cycle events. *Exp. Cell. Res.* 1985, 161: 297 - 306
202. Friesel R., Komoriya A., Maciag T. Inhibition of EC proliferation by gamma Interferon. *J. Cell. Biol.* 1987, 104: 689 - 696
203. Saegusa Y., Ziff M., Welkovich L., Cavender D. Effect of inflammatory cytokines on human EC proliferation. *J. Cell. Physiol.* 1990, 142: 488 - 495
204. Maheshwari R.K., Srikantan V., Bhartiya D., Kleinman H.K., Grant D.S. Differential effects of interferon gamma and alpha on in vitro model of angiogenesis. *J. Cell. Physiol.* 1991, 146: 164 - 169
205. Tsuruoka N., Sugiyama M., Tawaragi Y., Tsujimoto M., Nishihara T., Goto T., Sato N. Inhibition of *in vitro* angiogenesis by lymphotoxin and interferon- $\gamma$ . *Biochem. Biophys. Res. Commun.* 1988, 155: 429 - 435
206. Numa Y., Kawamoto K., Sakai N., Matsumura H. Flow cytometric analysis of antineoplastic effects of interferon- $\alpha$ ,  $\beta$  and  $\gamma$  labeled with fluorescein isothiocyanate on cultured brain tumors. *J. Neuro-Oncology* 1991, 11: 225 - 234
207. Palmer H., Libby P. Interferon- $\beta$ . A potential autocrine regulator of human vascular smooth muscle cell growth. *Lab. Invest.* 1992, 66: 715 - 721
208. Brett J., Gerlach H., Nawroth P., Steinberg S., Godman G., Stern D. Tumor necrosis factor/cachectin increases permeability of EC monolayers by a mechanism involving regulatory G proteins. *J. Exp. Med.* 1989, 169: 1977 - 1991
209. Hirano A., Dembitzer H.M., Becker N.H., Levine S., Zimmerman H.M. Fine structural alterations of the blood-brain barrier in experimental allergic encephalomyelitis. *J. Neuropath. Exp. Neurol.* 1970, 29: 432 - 440
210. Kristensson K., Wisniewski H.M. Chronic relapsing experimental allergic encephalomyelitis. Studies in vascular permeability changes. *Acta Neuropath.* 1977, 39: 189 - 194
211. Claudio L., Kress Y., Factor J., Brosnan C.F. Mechanisms of edema formation in experimental autoimmune encephalomyelitis. *Am. J. Path.* 1990, 137: 1033 - 1045
212. Pryce G., Male D., Sedgwick J. Antigen presentation in brain: brain EC are poor stimulators of T - cell proliferation. *Immunology* 1989, 66: 207 - 212
213. St. Louis J.D., Lederer J.A., Lichtman A.H. Costimulator deficient antigen presentation by an EC line induces a nonproliferative T cell activation response without anergy. *J. Exp. Med.* 1993, 178: 1597 - 1605
214. Boussiotis V.A., Freeman G.J., Gray G., Gribben J., Nadler L.M. B7 but not Intercellular adhesion molecule-1 costimulation prevents the induction of human alloantigen-specific tolerance. *J. Exp. Med.* 1993, 178: 1753 - 1763
215. Wu Y., Guo Y., Liu Y. A major costimulatory molecule on antigen-presenting cells,

- CTLA4 ligand A, is distinct from B7. *J. Exp. Med.* 1993, 178: 1789 - 1793
216. Lin H., Bolling S.F., Linsley P.S., Wei R., Gordon D., Thompson C.B., Turka L.A. Long-term acceptance of major histocompatibility complex mismatched cardiac allografts induced by CTLA4Ig plus donor-specific transfusion. *J. Exp. Med.* 1993, 178: 1801 - 1806
  217. Borst J., Alexander S., Elder J., Terhorst C. The T3 complex on human T lymphocytes involves four structurally distinct glycoproteins. *J. Biol. Chem.* 1983, 258: 5135 - 5141
  218. Van Wauwe J.P., de Mey J.R., Goossens J.G. OKT3: A monoclonal anti-human T lymphocyte antibody with potent mitogenic properties. *J. Immunol.* 1980, 124: 2708 - 2713
  219. Chang T.W., Kung P.C., Gingras S.P., Goldstein S. Does OKT3 monoclonal antibody react with an antigen-recognition structure on human T cells? *Proc. Natl. Acad. Sci. USA* 1981, 78: 1805 - 1808
  220. Imboden J.B., Stobo J.D. Transmembrane signalling by the T-cell antigen receptor. *J. Exp. Med.* 1985, 161: 446 - 456
  221. Imboden J.B., Weiss A., Stobo J.D. Transmembrane signalling by the T3-antigen receptor complex. *Immunol. Today* 1985, 6: 328 - 331
  222. Hara T., Fu S.M. Human T-cell activation. I. Monocyte-independent activation and proliferation induced by anti-T3 monoclonal antibodies in the presence of tumor promoter 12-O-tetradecanoyl Phorbol-13-acetate. *J. Exp. Med.* 1985, 161: 641 - 656
  223. Ledbetter J.A., Parsons M., Martin P.J., Hansen J.A., Rabinovitch P.S., June C.H. Antibody binding to CD5 (Tp67) and Tp44 T-cell surface molecules: effects on cyclic nucleotides, cytoplasmic free calcium, and cAMP-mediated suppression. *J. Immunol.* 1986, 137: 3299 - 3305
  224. Novak T.J., Rothenberg E.V. cAMP inhibits induction of interleukin-2 but not of interleukin-4 in T cells. *Proc. Natl. Acad. Sci. USA* 1990, 87: 9353 - 9357
  225. Anastassiou E.D., Paliogianni F., Balow J.P., Yamada H., Boumpas D.T. Prostaglandin E2 and other cyclic AMP-elevating agents modulate IL-2 and IL-2R $\alpha$  gene expression at multiple levels. *J. Immunol.* 1992, 148: 2845 - 2852
  226. Keren D.F. *Flow cytometry in clinical diagnosis.* American Society of Clinical Pathologists Press, Chicago, 1989
  227. Platts K.E., Lawry J., Hancock B.W., Rees R.C. Phenotypic and cell cycle analysis of human peripheral blood mononuclear cells activated with Interleukin-2 and/or OKT3. *Exp. Cell Res.* 1993, 208: 154 - 160
  228. Tsoukas C.D., Landgraf B., Bentin J., Valentine M., Lotz M., Vaughan J.H., Carson D.A. Activation of resting T lymphocytes by anti-CD3 (T3) antibodies in the absence of monocytes. *J. Immunol.* 1985, 135: 1719 - 1723

229. Hughes C.C.W., Male D.K., Lantos P.L. Adhesion of lymphocytes to cerebral microvascular cells: effects of Interferon- $\gamma$ , tumor necrosis factor and interleukin-1. *Immunology* 1988, 64: 677 - 681
230. Liversidge J., Sewell H.F., Forrester J.V. Interactions between lymphocytes and cells of the blood-retina barrier: mechanisms of T lymphocyte adhesion to human retinal capillary EC and retinal pigment epithelial cells in vitro. *Immunol.* 1990, 71: 390 - 396
231. Curtis A.S.G. The H-2 histocompatibility system and lymphocyte adhesion. Interaction modulation factor involvement. *J. Immunogenet.* 1979, 6: 155 - 166
232. Curtis A.S.G., Rooney P. H-2 restriction of contact inhibition of epithelial cells. *Nature* 1979, 281: 222 - 223
233. Thornhill M.H., Speight P.M., Williams D.M. A monoclonal antibody to CD4 inhibits interferon-gamma (IFN- $\gamma$ ) enhanced adhesion of autologous lymphocytes to EC. *J. Pathol.* 1987, 151: 26A
234. Sriram S., Topham D.J., Carroll L. Haplotype-specific suppression of experimental allergic encephalomyelitis with anti-Ia antibodies. *J. Immunol.* 1987, 139: 1485 - 1489
235. Sriram S., Carroll L. Haplotype-specific inhibition of homing of radiolabeled lymphocytes in Experimental Allergic Encephalomyelitis following treatment with Anti-Ia Antibodies. *Cell. Immunol.* 1991, 135: 222 - 231
236. McCarron R.M., Wang L., Racke M.K., McFarlin D.E., Spatz M. Cytokine-regulated adhesion between encephalitogenic T lymphocytes and cerebrovascular EC. *J. Neuroimmunol.* 1993, 43: 23 - 30
237. Cavender D.E., Haskard D.O., Joseph B., Ziff M. Interleukin-1 increases the binding of human B and T lymphocytes to EC monolayers. *J. Immunol.* 1986, 136: 203 - 207
238. Haskard D.O., Cavender D.E., Fleck R.M., Sontheimer R., Ziff M. Human dermal microvascular EC behave like umbilical vein EC in T cell adhesion studies. *J. Invest. Dermatol.* 1987, 88: 340 - 344
239. Wong D., Dorovini-Zis K. Upregulation of intercellular adhesion molecule-1 (ICAM-1) expression in primary cultures of human brain microvessel EC by cytokines and lipopolysaccharide. *J. Neuroimmunol.* 1992, 39: 11 - 22
240. Haskard D., Cavender D., Beatty P., Springer T., Ziff M. T lymphocyte adhesion to EC: Mechanisms demonstrated by anti-LFA-1 monoclonal antibodies. *J. Immunol.* 1986, 137: 2901 - 2906
241. van Kooyk Y., Weder P., Hogervorst F., Verhoeven A.J., van Seventer G., te Velde A.A., Borst J., Keizer G.D., Figdor C.G. Activation of LFA-1 through a Ca<sup>2+</sup>-dependent epitope stimulates lymphocyte adhesion. *J. Cell. Biol.* 1991, 112: 345 - 354
242. van Kooyk Y., van de Wiel-van Kemenade E., Weder P., Huijbens R.J.F., Figdor C.G. Lymphocyte function-associated antigen 1 dominates very late antigen-4 in binding of

- activated T cells to endothelium. *J. Exp. Med.* 1993, 177: 185 - 190
243. Dustin M.L., Springer T.A. Lymphocyte function-associated antigen-1 (LFA-1) Interaction with Intercellular Adhesion Molecule-1 (ICAM-1) is one of at least three mechanisms for lymphocyte adhesion to cultured EC. *J. Cell. Biol.* 1988, 107: 321 - 331
244. Shimizu Y., Newman W., Gopal T.V., Horgan K.J., Graber N., Beall L.D., van Seventer G.A., Shaw S. Four molecular pathways of T cell adhesion to EC: Roles of LFA-1, VCAM-1, and ELAM-1 and changes in pathway hierarchy under different activation conditions. *J. Cell. Biol.* 1991, 113: 1203 - 1212
245. Elices M.J., Osborn L., Takada Y., Crouse C., Luhowskyj S., Hemler M.E., Lobb R.R. VCAM-1 on activated endothelium interacts with the leukocyte integrin VLA-4 at a site distinct from the VLA-4/fibronectin binding site. *Cell* 1990, 60: 577 - 584
246. Osborn L., Hession C., Tizard R., Vassallo C., Luhowskyj S., Chi-Rosso G., Lobb R.R. Direct expression cloning of vascular cell adhesion molecule-1 (VCAM-1), a cytokine-induced endothelial protein that binds to lymphocytes. *Cell* 1989, 59: 1203 - 1211
247. Wellicome S.M., Thornhill M.H., Pitzalis C., Thomas D.S., Lanchbury J.S.S., Panayi G.S., Haskard D.O. A monoclonal antibody that detects a novel antigen on EC that is induced by tumor necrosis factor, IL-1 or lipopolysaccharide. *J. Immunol.* 1990, 144: 2558 - 2565
248. Rice G.E., Munro J.M., Bevilacqua M.P. Inducible cell adhesion molecule 110 (INCAM-110) is an endothelial receptor for lymphocytes: a CD11/CD18-independent adhesion mechanism. *J. Exp. Med.* 1990, 171: 1369 - 1374
249. Wong D., Dorovini-Zis K. Expression of VCAM-1 and E-selectin by human brain microvessel EC in vivo and in vitro. *Can. J. Neurol. Sci.* 1993, 20: S104
250. Pryce G., Male D.K., Sarkar C. Control of lymphocyte migration into brain: selective interactions of lymphocyte subpopulations with brain endothelium. *Immunol.* 1991, 72: 393 - 398
251. Male D., Pryce G., Linke A., Rahman J. Lymphocyte migration into the CNS modelled in vitro. *J. Neuroimmunol.* 1992, 40: 167 - 172
252. Haskard D.O., Strobel S., Thornhill M., Pitzalis C., Levinsky R.J. Mechanisms of lymphocyte adhesion to EC: studies using an LFA-1-deficient cell line. *Immunol.* 1989, 66: 111 - 116
153. Naparstek Y., Cohen I.R., Fuks Z., Vlodaysky I. Activated T lymphocytes produce a matrix degrading heparan sulphate endoglycosidase. *Nature* 1984, 310: 241 - 244
254. Lider O., Baharav E., Mekori Y.A., Miller T., Naparstek Y., Vlodaysky I., Cohen I.R. Suppression of experimental autoimmune diseases and prolongation of allograft survival by treatment of animals with low doses heparins. *J. Clin. Invest.* 1989, 83: 752 - 756

255. Muller W.A., Weigl S.A., Deng X., Phillips D.M. PECAM-1 is required for transendothelial migration of leukocytes. *J. Exp. Med.* 1993, 178: 449 - 460
256. Newman P.J., Berndt M.C., Gorski J., White II G.C., Lyman S., Paddock C., Muller W.A. PECAM-1 (CD31) cloning and relation to adhesion molecules of the immunoglobulin gene superfamily. *Science (Wash. D.C.)* 1990, 247: 1219 - 1222
257. Muller W.A., Ratti C.M., McDonnell S.L., Cohn Z.A. A human EC-restricted, externally disposed plasmalemmal protein enriched in intercellular junctions. *J. Exp. Med.* 1989, 170: 399 - 414
258. Ohto H., Maeda H., Shibata Y., Chen R.F., Ozaki Y., Higashihara M., Takeuchi A., Tohyama H. A novel leukocyte differentiation antigen: two monoclonal antibodies TM2 and TM3 define a 120-kd molecule present on neutrophils, monocytes, platelets, and activated lymphoblasts. *Blood* 1985, 66: 873 - 881
259. Goyert S.M., Ferrero E.M., Seremetics S.V., Winchester R.J., Silver J., Mattison A.C. Biochemistry and expression of myelomonocytic antigens. *J. Immunol.* 1986, 137: 3909 - 3914
260. Stockinger H., Gadd S.J., Eher R., Majdic O., Schreiber W., Kasinrek W., Strass B., Schnabl E., Knapp W. Molecular characterization and functional analysis of the leukocyte surface protein CD 31. *J. Immunol.* 1990, 145: 3889 - 3897
261. Perkett E.A., Disabato G., Brigham K.L., Meyrick B. Lymphocyte and granulocyte migration across the endothelial layer of bovine pulmonary artery intimal explants towards lymphocyte conditioned medium. *Tissue and Cell* 1986, 18: 839 - 852
262. Bowman P.D., du Bois M., Dorovini-Zis K., Shivers R.R. Microvascular EC from brain. In H.M. Piper, ed. *Cell culture techniques in heart and vessel research.* Springer-Verlag, NY, 1990: 140 - 157
263. Buzney S.M., Massicotte S.J. Retinal vessels: proliferation of endothelium in vitro. *Invest. Ophthalmol. Visual. Sci.* 1979, 18: 1191 - 1195
264. Phillips P., Kumar P., Kumar S., Waghe M. Isolation and characterization of EC from rat and cow brain white matter. *J. Anat.* 1979, 129: 261 - 272
265. Hirano A., Ghatak N.R., Becker N.H., Zimmerman H.M. A comparison of the fine structure of small blood vessels in intracranial and retroperitoneal malignant lymphomas. *Acta. Neuropath.* 1974, 27: 93 - 104
266. Hirano A., Matsui T. Vascular structures in brain tumors. *Human Path.* 1975, 6: 611 - 621
267. Herrlinger H., Anzil A.P., Blinzinger K., Kronschi D. Endothelial microtubular bodies in human brain capillaries and venules. *J. Anat.* 1974, 118: 205 - 209
268. Kumar P., Kumar S., Marsden H.B., Lynch P.G., Earnshaw E. Weibel-Palade bodies in EC as a marker for angiogenesis in brain tumors. *Cancer Res.* 1980, 40: 2010 - 2019
269. Pavelka M. Functional morphology of the Golgi apparatus. *Advances in anatomy,*

- embryology and cell biology 1987, 106: 1 - 94
270. Griffiths G., Pfeiffer S., Simons K., Matlin K. Exit of newly synthesized membrane proteins from the trans cisterna of the Golgi complex to the plasma membrane. *J. Cell. Biol.* 1985, 101: 949 - 964
  271. Handin R.I., Wagner D.D. The molecular and cellular biology of von Willebrand factor. *Prog. Hemostasis Thromb.* 1989, 9: 233 - 259
  272. Loesberg C., Gonsalves M.D., Zandbergen J., Willems C., Van Aken W.G., Stel H.V., Van Mourik J.A., DeGroot P.G. The effect of calcium on the secretion of factor-VIII-related antigen by cultured human EC. *Biochim. Biophys. Acta* 1983, 763: 160 - 168
  273. Sporn L.A., Marder V.J., Wagner D.D. Inducible secretion of large, biologically potent von Willebrand factor multimers. *Cell* 1986, 46: 185 - 190
  274. Sporn L.A., Marder V.J., Wagner D.D. Differing polarity of the constitutive and regulated secretory pathways for von Willebrand factor in EC. *J. Cell. Biol.* 1989, 108: 1283 - 1289
  275. Sinha S., Wagner D.D. Intact microtubules are necessary for complete processing, storage and regulated secretion of von Willebrand factor by EC. *Eur. J. Cell. Biol.* 1987, 43: 377 - 383
  276. Edgell C-JS., Haizlip J.E., Bagnell C.R., Packerham J.P., Harrison P., Wilbourn B., Madden V.J. Endothelium specific Weibel-Palade bodies in a continuous human cell line, EA. hy 926. *In Vitro Cell Dev. Biol.* 1990, 26: 1167 - 1172
  277. Renkonen R., Mennander A., Ustinov J., Mattila P. Activation of protein kinase C is crucial in the regulation of ICAM-1 expression on EC by interferon- $\gamma$ . *Internat. Immunol.* 1990, 2: 719 - 724
  278. Mason D.W., Charleton H.M., Jones A.J., Lavy C.B.D., Puklavek M., Simmonds S.J. The fate of allogeneic and xenogeneic neuronal tissue transplanted into the third ventricle of rodents. *Neuroscience* 1986, 19: 685 - 694
  279. Cross A.H., Cannella B., Brosnan C.F., Raine C.S. Homing to Central Nervous System vasculature by antigen-specific lymphocytes. I. Localization of  $^{14}\text{C}$ -labeled cells during acute, chronic, and relapsing experimental allergic encephalomyelitis. *Lab. Invest.* 1990, 63: 162 - 170
  280. Caspi R.R., Chan C., Fujino Y., Najafian F., Grover S., Hansen C.T., Wilder R.L. Recruitment of antigen-non specific cells plays a pivotal role in the pathogenesis of a T cell-mediated organ-specific autoimmune disease, experimental autoimmune uveoretinitis. *J. Neuroimmunol.* 1993, 47: 177 - 188
  281. The IFN- $\beta$  Multiple Sclerosis Study Group. Interferon beta-1b is effective in relapsing-remitting multiple sclerosis. I. Clinical results of a multicenter, randomized, double-blind, placebo-controlled trial. *Neurology* 1993, 43: 655 - 661